CPUC-1003

Blade Supplemental Report (Vol. 3: Post-SS-25 Leak Events)

I.19-06-016

ALJs: Hecht/Poirier

Date Admitted: 3/24/2021

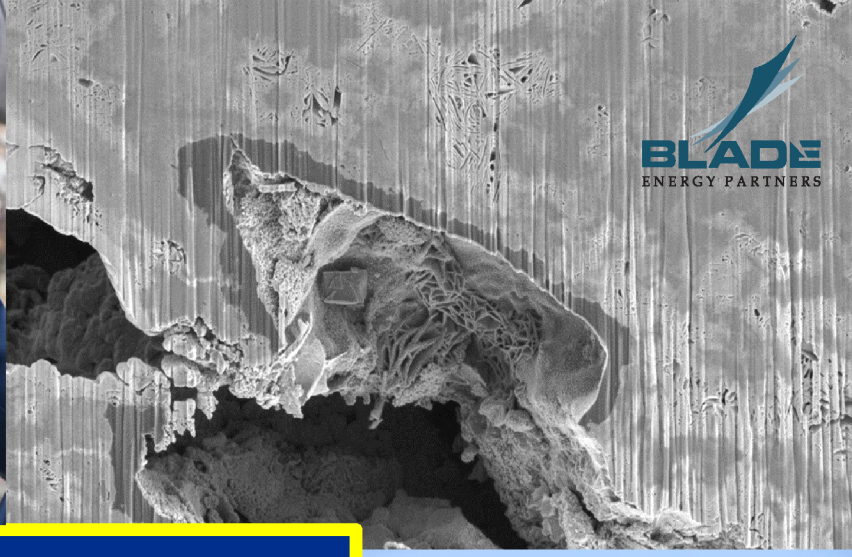

BLADE ENERGY PARTNERS

Root Cause Analysis of the Uncontrolled Hydrocarbon Release from Aliso Canyon SS-25

SUPPLEMENTARY REPORTS

May 31, 2019

VOLUME 3: POST-SS-25 LEAK EVENTS

This RCA work necessitated a substantial amount of testing, analyses, and modeling. The integrated work is reflected in the overall RCA report. Additionally, all the technical details and discussions are provided in supplementary reports—the source documents for the RCA report—in four volumes. This is Volume 3.

MAIN REPORT

Root Cause Analysis of the Uncontrolled Hydrocarbon Release from Aliso Canyon SS-25

SUPPLEMENTARY REPORTS

Volume 1: Approach

Volume 2: SS-25 Well Failure Causes

Volume 3: Post-SS-25 Leak Events

SS-25 Nodal Analysis with Uncontrolled Leak Estimation

Aliso Canyon Injection Network Deliverability Analysis Prior to Uncontrolled Leak

Analysis of the Post-Failure Gas Pathway and Temperature Anomalies at the SS-25 Site

SS-25 Transient Well Kill Analysis

Volume 4: Aliso Canyon Casing Integrity

SS-25 RCA Supplementary Report

SS-25 Well Nodal-Analysis with Uncontrolled Leak Estimation

Purpose:
Report on the post-leak analysis of Well SS-25 using a well nodal-analysis model to explain measured data during the event.

Date:
May 31, 2019

BLADE ENERGY PARTNERS

2600 Network Boulevard, Suite 550
Frisco, Texas 75034

+1 972-712-8407 (phone)
+1 972-712-8408 (fax)

16285 Park Ten Place, Suite 600
Houston, Texas 77084

1-800-319-2940 (toll free)
+1 281-206-2000 (phone)
+1 281-206-2005 (fax)

www.blade-energy.com

Abstract

The gas storage well Standard Sesnon 25 (SS-25) in the Aliso Canyon Gas Storage Field located in Los Angeles County, California started leaking gas in October 2015. A relief well was drilled, and SS-25 was brought under control. The leak stopped in February 2016.

In January 2016, as part of their investigation of the leak, the California Public Utilities Commission (CPUC) and the Division of Oil, Gas, and Geothermal Resources (DOGGR) selected and gave provisional authority to Blade Energy Partners (Blade) to perform an independent Root Cause Analysis (RCA). The Blade Team and parties under Blade's direction were responsible for directing the work of subcontractors who performed the extraction of the SS-25's wellhead, tubing, and casings and the preservation and protection of associated evidence. Blade's RCA Reports, including this report, document and describe the key activities undertaken in support of the RCA effort.

Blade built a nodal-analysis well model to determine the state of the wellbore and of the leaked flow for SS-25—it was important to understand the well flow in order to analyze the root cause of the leak event. This study used daily measured wellhead pressures for the tubing, production casing, and surface casing for determining:

- The total leak volume from the moment the injection was shut off until the well was killed. The SS-25 leak emitted a best estimate of 120,000 metric tons of methane. The upper limit based on new pipe was 131,000 metric tons of methane, and the lower limit based on badly corroded pipe was 102,000 metric tons of methane.
- The state of the tubulars to match measured pressures. Key findings include:
  - The production casing must have been failed when pressure was first measured after the injection had been shut off.
  - The surface casing must have had holes open to leak gas at the time of the first measured pressure after injection shutoff. The holes open to flow would have decreased with the first kill attempt when the kill fluid froze, would have increased after the glycol treatment to remove the frozen kill fluid, and would have increased again at the kill attempt when the *conventional* uncontrolled leak began.
  - The surface casing pressure was indicative of holes in the surface casing and did not always support a casing shoe leak other than during the uncertainty of the frozen plugs in the tubing and casing.

The following are additional important determinations:

- The inflow performance model for the well was significantly better than the model used during kill operations. The model presented as used during kill operations was not representative of past well tests.
- The precise time of origin of the leak during injection was not observable from measured data. The gas injection network could have provided volumes of gas significantly greater than those allocated to the well without noticeable changes in the injection header pressures or nearby SS-5 observation well pressures. Because pressures were measured at the wellhead weekly, a leak could have initiated unnoticed anytime during the week.

- A leak during injection could have had a significant positive Joule-Thomson effect that could have led to brittle fracturing of the pipe metal, while a leak during withdrawal would have not experienced the same extreme cooling effect.
- A leak during injection or during withdrawal could have resulted in temperatures low enough to potentially explain the fluid freezing during the kill attempt that plugged the tubing. The tubing plugged quickly and was indicative of ice and not hydrates; conditions for hydrate formation lasted in the tubulars afterwards and until the treatment to remove the plug.

The well nodal-analysis model in this study is being used post-mortem, but this type of model can be also used during a well's life for continuous well or reservoir surveillance. If a model had been available and used at the time the leak was first noticed, the reported speculation that the leak rate was abating would have been shown not to be true.

Table of Contents

List of Figures

List of Tables

1 Introduction

The primary objective of this study was to discern the state of well SS-25 by studying the flow occurrences from shortly before and during the leak via a nodal-analysis well model. A well-built nodal-analysis model gives insight to all pertinent, known, measured, and documented occurrences over time, and it also aids in discerning the well's conditions during the leak.

Blade built the well model using Petroleum Experts' PROSPER. It is an industry standard application, vetted and used extensively by large and small oil companies. The SS-25 well modeling, used data provided by SoCalGas from the original completion of the well to the leak. This work used and analyzed data collected by Blade Energy Partners (Blade) during the on-site root cause investigation.

The modeling included the following:

1. Estimation of the leak potential during injection before the leak was first noticed. There were no measurements at the wellhead during the week before the leak. This study postulates how a leak could have begun during injection, dispersed underground, and leaked out the hillside. (Other complementary Blade work documented in the supplementary reports corroborates these findings.)
2. Estimation of the gas flow rate escaping from the well when the leak was first noticed, October 23, 2015, until the well was killed, February 11, 2016. The leak rate continued at a declining rate as the reservoir pressure declined. The leak rate declined faster with withdrawal from other wells to draw down the field as a whole.

Modeling required gathering and defining the most pertinent, stable data each day to estimate the rates, pressures, and temperature. Blade reviewed all data to build a representative well model.

The steps to build the nodal-analysis well model were the following:

1. Build an Equation of State (EoS) model with recent compositional analysis considering that:
   - The EoS implementation gave better physical property estimates with temperature modeling than a simple black-oil correlation.
   - The modeling assumed constant composition throughout the time of the leak.
   - The gas injected was sales gas—it always has to meet specific composition constraints.
   - The injection/withdrawal cycle had been in operation for enough years that residual oil in the formation negligibly affected the composition.
2. Build an outflow deliverability model with the following characteristics:
   - Well schematics for the tubing, production casing, and surface casing.
   - Geothermal gradient measurements before, during, and after the leak. The leak caused the ground to be colder in the upper 1,000 ft, thereby leading to lower temperatures in the tubulars and changing the gas physical properties.
   - Piping measurements to indicate its state at the time of the leak. The well had been in service for many years, and the state of the piping had changed from what it was when installed. Corrosion and scaling cause surface roughness, which increases frictional pressure at high rates and has minimal impact at typical operating rates.

3. Build an inflow deliverability model to:

    a. Estimate the reservoir pressure, permeability-thickness, and skin from production well tests—these tests included the static pressure, flowing pressure, and flow rate. Field operations had occurred for many years, and the cyclical nature of injection and withdrawal had been well established to trend the average reservoir pressure when the well tests were performed. The permeability should have stayed the same. There was no evidence that the leak exposed new pay-thickness. The skin showed no evidence of change in time, and this is reasonable because only clean sales gas had been injected.

    b. Determine the decline of drainage area reservoir pressure during the leak. The well withdrew more gas than what had been injected, and therefore the gas leaked was gas injected into other wells. Also, during the leak, the entire field had been drawn down via other wells to decrease the gas available to leak, which made the reservoir pressure decline faster.

This modeling assumed pseudo-steady-state and solved for a daily rate at stable conditions. This modeling cannot model the rate transients during the kill attempts. The elapsed time of the kill attempts was minimal relative to the total time of the leak. Therefore, the total volume estimated was not significantly affected by not modeling the transients of the kill attempts. Rather, the concern was about how the kill attempts may have changed the nodal model state, such as the back-pressure in the well—this affects the rate prediction.

This study relied extensively on the data measured and provided by SoCalGas and data acquired, under Blade's supervision, after the well was killed. Often, assumptions were inferred to construct a workable theory that matched the data. This spawned additional objectives to validate the assumptions, and these other studies are reported in other Blade supplementary reports. The assumptions investigated by these other studies intended to:

- Understand if the better deliverability of Blade's Inflow Performance Relationship (IPR) compared to the IPR model used during the kill operations, caused issues with the kill operations. This is discussed in the supplementary report titled: *SS-25 Transient Well Kill Analysis* [1].
- Understand if to achieve the cold temperatures that rapidly froze the fluids pumped into the well during the first kill:
    - The leak began during the injection phase or after the injection was shut in.
    - The volume of leak needed to maintain the cold temperatures.
    - The leak could have been dispersed in the ground to delay its path into the atmosphere.

    Analyzing this required reservoir and well temperature modeling. This is discussed in the supplementary report titled: *Analysis of the Post-Failure Gas Pathway and Temperature Anomalies at the SS-25 Site* [2].
- Understand if the leak rates during the injection could have been greater than the injection rates allocated for the well. That is, if gas could have been diverted in the injection network. Determining this required building an integrated network model that included the injection pipelines, injection manifolds, and injection wellhead conditions. This is discussed in the supplementary report titled: *Aliso Canyon Injection Network Deliverability Analysis Prior to Uncontrolled Leak* [3].

1.1 Abbreviations and Acronyms

Term	Definition
A-annulus	7 in. × 2 7/8 in. annulus
AOF	Absolute Open Flow
B-annulus	11 3/4 in. × 7 in. annulus
BHP	Bottomhole Pressure (presumed at mid-point of perforations)
Blade	Blade Energy Partners
CHP	Casing Head Pressure
CPUC	California Public Utilities Commission
DOGGR	Division of Oil, Gas, and Geothermal Resources
DS	Down Stream
ELF	Elf Acquitaine was a French Oil Company—Elf is now a brand of Total
EoS	Equation of State
FWHP	Flowing Wellhead Pressure
GAP	General Allocation Program (Petroleum Experts software)
GTC	General Terms and Conditions
HPT	High Precision Temperature
IPM	Integrated Production Modeling
IPR	Inflow Performance Relationship
LPIP	Leak Point Inlet Pressure
LPIT	Leak Point Inlet Temperature
LPOT	Leak Point Outlet Temperature
MD	Measured Depth
MMscf/D	Million Standard Cubic Feet per Day
PPT	Plug-point
PROSPER	PROduction and Systems PERformance (Petroleum Experts software)
P-Res	Reservoir Pressure
PVT	Pressure Volume Temperature
RCA	Root Cause Analysis
scf	Standard Cubic Feet
SIWHP	Shut In Wellhead Pressure
SoCalGas	Southern California Gas Company
SS	Standard Sesnon
SSSV	Sub Surface Safety Valve
THP	Tubing Head Pressure
TVD	True Vertical Depth
WD	Withdrawal
WHP	Wellhead Pressure

2 Leak Background

The following are the background conditions for the SS-25 leak analysis:

1. The pressure at the injection plant compressor increased to maintain a total injection rate as the reservoir pressure increased, and from the compressor pressure and rate, it was possible to ascertain a field average reservoir pressure. During the eight months of injection, the injection pressure at SS-25 would have continued to increase, and line pressures were near their highest at the time of the leak. The pressures became great enough to initiate a leak on a weakened pipe.
2. The well's injection pressure was such that the injected rate was limited to a few MMscf/D (as this was not a high-priority injection well). Individual well injection rates were allocated rather than measured. The injection pattern for the field was set by chokes at the well injection manifolds. Wellhead injection chokes were set at a fixed opening and not adjusted individually during injection, although they may have been closed for well work. The allocation was based on injection compressor measurements, well choke settings, and well tests.
3. The well would have had a lower back pressure when the leak initiated, and the injection could have then increased from a 3–4 MMscf/D to 70 MMscf/D. Other than the pressures for the injection header downstream of the compressor, there was no continuous pressure monitoring in the field. The wellhead pressures were monitored on a weekly basis. Therefore, this increase in gas rate would have been noticed only by the pressure measured weekly at the wellhead.
4. The well leak occurred at 892 ft MD as confirmed by the production casing recovered from the well. This is consistent with other Blade analyses.
5. The well leak began during injection, and the early stages of the leak had likely spread into the underground fracture matrix. Injection conditions could yield extreme cooling of the casing and ground; withdrawal conditions were cool but not as extreme. The leak size and timing could not be determined from wellbore modeling because there were no well pressure measurements for the week prior to the injection shut-in. The leak magnitude was limited based on the observation well SS-5. A very large leak would have caused significant withdrawal from the formation and led to a significant decline in drainage area reservoir pressure; SS-5's daily pressure measurements did not show this decline. However, other methodologies have been used to identify the size and time.
6. The well leak was suspected by SoCalGas, and the injection to the well was shut down. The well would have continued to leak with the withdrawal of gas from the formation. Per the wellbore modeling, sometime on the day the injection was shut in, prior to shut in, the axial rupture became the parted failed production casing. Modeling of the wellbore with daily pressure measurements supported that the casing failed prior to the first kill attempt.
7. The well leak was affected by the first kill attempt—the freezing of the kill fluid partially blocked the leak pathways. The path for the leaked gas was up the production casing annulus, out the failed casing, into the surface casing annulus, and out the multiple holes in the surface casing. The holes coincided with zones where the formation was highly fractured. The temperature in the fractures was cold enough for ice to form. Hydrate formation conditions also existed in these fractures, and it is possible that some gas was trapped as gas hydrates. The formation rock matrix was such that hydrates in the rock matrix were not likely to occur. Surface, or airborne, measurements of the leak would have been measuring less than the actual leak rate because of the dispersed and delayed nature of gas flowing through the fractures in the ground.

3 Wellbore Nodal Model

Figure 1 shows SS-25's basic wellbore schematic from SS-25 Well Documentation [4]. A Camco Sub Surface Safety Valve (SSSV) was originally installed. The SSSV was problematic and posed a greater risk because of the workovers that were needed to maintain it. The SSSV was removed, and this left open ports in the tubing at 8,451 ft MD; consequently, the tubing and the production casing annulus were in communication.

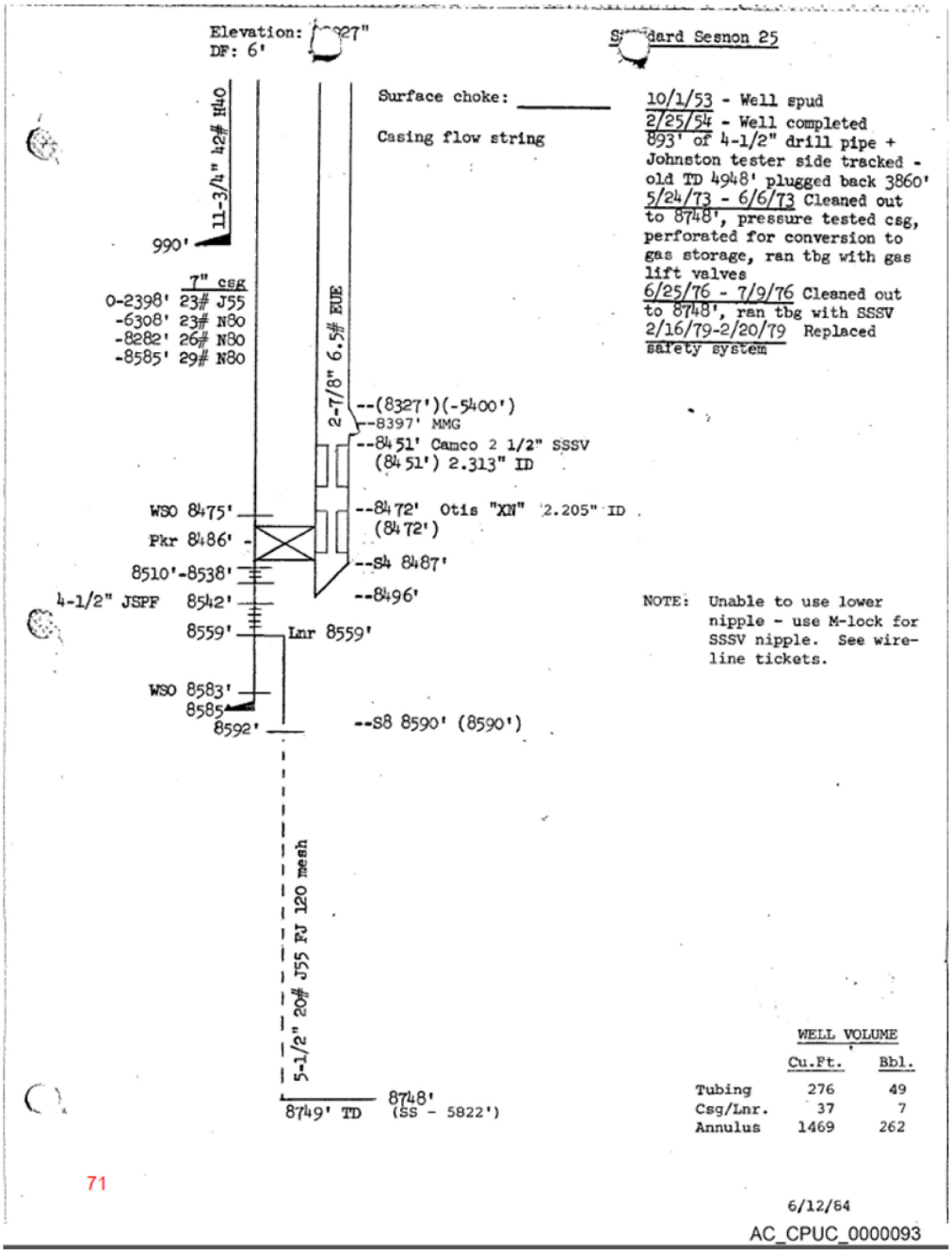

Figure 1: SS-25 Wellbore Diagram

During injection and withdrawal, the flow could have been simultaneously through the tubing and production casing annulus, through the tubing, or only through the production casing annulus. The tubing had been shut in at the surface during injection and withdrawal, and as a result, the flow was through the production casing annulus while the tubing held static gas under pressure. During injection, the flow path was down through the 7 in. × 2 7/8 in. annulus, through the ports in the tubing, down through the tubing past the packer, and through the perforated casing into the formation. The holes were restrictions that caused a small additional pressure loss. During withdrawal, the flow path was reversed.

SS-25 was not the first well in the field to have a leak. Leaks in other wells had occurred at the wellhead and along the production casing, and these leaks had been successfully repaired. In this instance, the leak was in the production casing at 892 ft MD instead of the wellhead, which means that the gas leaked from the well either through a corroded surface casing, through the casing shoe at 990 ft MD, or down past the shoe. Sufficient holes were found in the surface casing to handle all of the leaked gas. Testing showed no probable leak in the shoe, but the conditions were such that some gas could have flowed down past the shoe.

The well nodal-analysis model was solved in two sequential steps:

1. The flow was modeled up to the production casing leak point during injection and injection shutoff (withdrawal leak). This modeling used the tubing and production casing head pressures, reservoir pressure, and temperature to predict the flow rate, pressure, and temperature at the leak point.
2. The flow was modeled from the production casing leak point as predicted by the previous step and then leaked out the surface casing holes. This modeling used the surface casing head pressures to match and validate the surface casing holes and potential flow past the shoe.

The analysis began with the tubing and production casing head pressures and accurately predicted the surface casing head pressures. The same model fit all points in time, giving credence to its predictions of rates.

3.1 Storage Gas Pressure Volume Temperature Model

In February 2016 Blade collected gas samples and measured the gas composition. This study used the average of all measured gas compositions for the Equation of State model (EoS). Table 1 summarizes the results from the file [5]—a facsimile from SoCalGas.

Table 1: Aliso Canyon Gas Composition Analysis

Gas	Average	Sample	Sample	Sample	Sample	Sample	Sample	Sample	Sample
H2	0.000	0.000	0.000	0.000	0.000	0.000	0.000	0.006	0.006
N2	0.323	0.332	0.336	0.332	0.331	0.316	0.322	0.322	0.315
CO2	0.855	0.994	0.996	0.993	0.730	0.723	0.725	0.936	0.937
C1	94.805	94.897	94.876	94.892	94.670	94.710	94.755	94.755	94.788
C2	3.394	3.411	3.436	3.424	3.144	3.117	3.113	3.650	3.625
C3	0.373	0.278	0.266	0.267	0.566	0.570	0.557	0.246	0.252
iC4	0.049	0.028	0.028	0.028	0.087	0.087	0.088	0.025	0.025
nC4	0.066	0.032	0.033	0.032	0.133	0.134	0.128	0.027	0.028
iC5	0.021	0.009	0.008	0.009	0.045	0.046	0.043	0.008	0.008
nC5	0.018	0.005	0.006	0.007	0.041	0.042	0.037	0.007	0.005
C6	0.095	0.015	0.016	0.017	0.254	0.256	0.234	0.019	0.012

Gas	Sample	Sample	Sample	Sample	Sample	Sample	Sample	Sample	Sample
H2	0.006	0.000	0.000	0.000	0.000	0.000	0.000	0.000	0.000
N2	0.307	0.336	0.338	0.339	0.352	0.353	0.281	0.288	0.283
CO2	0.939	0.823	0.817	0.818	0.842	0.846	0.815	0.805	0.806
C1	94.782	94.664	94.682	94.691	95.095	95.096	94.750	94.772	94.802
C2	3.635	3.223	3.232	3.214	2.898	2.914	3.906	3.891	3.861
C3	0.250	0.524	0.529	0.526	0.464	0.457	0.198	0.196	0.199
iC4	0.026	0.075	0.074	0.074	0.068	0.068	0.017	0.018	0.017
nC4	0.027	0.109	0.106	0.106	0.091	0.090	0.017	0.017	0.017
iC5	0.010	0.034	0.031	0.033	0.033	0.033	0.005	0.004	0.004
nC5	0.006	0.030	0.026	0.028	0.029	0.029	0.003	0.003	0.003
C6	0.014	0.182	0.166	0.171	0.129	0.116	0.009	0.007	0.007

The average composition was used for the PROSPER Pressure Volume Temperature (PVT) model using a Peng-Robinson EoS. Given the primary composition of methane and ethane and low values of nitrogen and carbon dioxide, the predictions were quite accurate.

3.2 Data for Well Outflow Model

A well outflow-inflow model was built using PROSPER. The outflow model began with the wellbore schematic and fluid properties previously discussed, and sequentially added into well model the following data:

1. Deviation survey
2. Geothermal gradient
3. Piping properties
4. Thermal properties

3.2.1 Outflow Model Deviation Survey

SoCalGas provided a complete deviation survey [6], which was filtered by PROSPER to create the best representation from wellhead to mid-point of perforations in twenty points or less. Additionally, the deviation survey was extrapolated to match the depth of the geothermal gradient. Table 2 gives the filtered deviation survey from the SoCalGas survey.

Table 2: SS-25 Deviation Survey for Well Model

	True Vertical Depth (ft TVD)	Measured Depth (ft MD)
1	0	0.00
2	230	229.99
3	240	239.99
4	3,880	3,879.75
5	4,080	4,079.02
6	4,560	4,556.60
7	4,960	4,955.95
8	7,710	7,705.13
9	7,740	7,735.11
10	7,780	7,775.07
11	7,950	7,944.74
12	8,110	8,103.34
13	8,370	8,359.89
14	8,378	8,367.77
15	8,535	8,522.41
16	8,716	8,700.69

3.2.2 Outflow Model Geothermal Gradient

The geothermal gradient was deduced from temperature surveys in the well. In-situ, at-rest temperatures were required; that is, the formation temperatures were not disturbed by any drilling, injection, or withdrawal temperature transients. Data quality was critical and depended on how the temperature survey was conducted; the thermal mass of the carrier could have affected measurements if time had not been taken to stabilize at a depth. Table 3 shows the geothermal gradient used in the model along with geothermal gradients measured at various points in time. The geothermal gradient used in PROSPER is shown as a hollow black line with markers.

Table 3: SS-25 Geothermal Gradients for Well Model

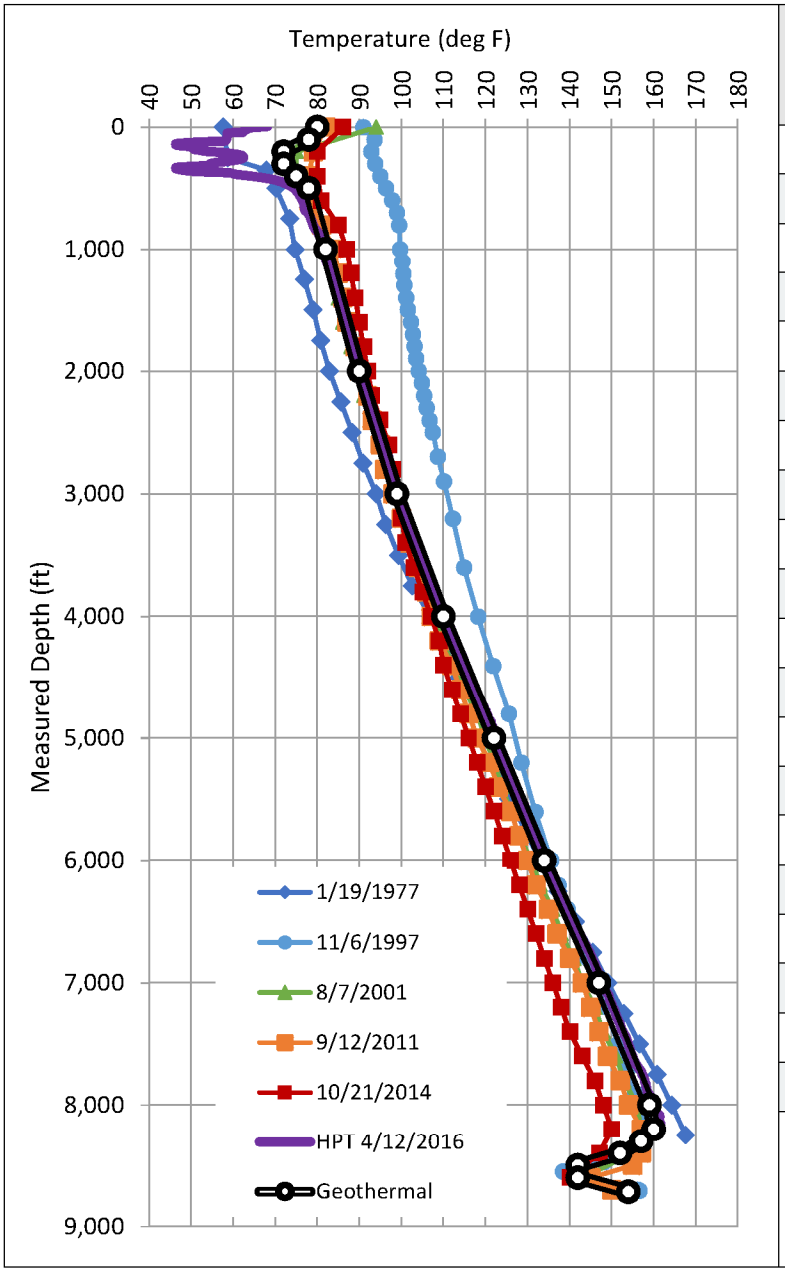

	Measured Depth (ft MD)	Formation Temperature (°F)
1	0	80
2	100	78
3	200	72
4	300	72
5	400	75
6	500	78
7	1,000	83
8	2,000	91
9	3,000	99
10	4,000	110
11	5,000	122
12	6,000	134
13	7,000	147
14	8,000	159
15	8,200	160
16	8,300	157
17	8,400	152
18	8,500	142
19	8,600	142
20	8,716	154

The geothermal gradient showed the presence of:

- Cooling at the surface, because of the mountains—a common occurrence.
- Surface changes—they vary by the time of year and were more pronounced due to the presence of mountains.
- Cooling in the reservoir resulting from years of injection of a cooler gas and its withdrawal.

The gradient used was measured in April 2016 by High Precision Temperature (HPT), months after the well had been killed. This methodology was more accurate overall than the other methods used previously. The measurements were taken following a prolonged period of no flow in the well; the well temperatures would have stabilized by then. Blade managed the HPT survey [7], which was compared with surveys that SoCalGas was conducting regularly as given in the file [8]. The HPT survey shows abnormal cooling near the surface, a result of the leak, and was local to around the wellbore; several older surveys were charted and used to define the shallow geothermal temperatures.

3.2.3 Outflow Model Piping Roughness

The well model for the production casing annulus required the piping roughness of the outside of the tubing and the inside of the casing. At high rates, as when well control was lost, the roughness dramatically increased the friction pressure drop and thereby affected the estimated rates. Given the age and history of the well, new pipe roughness is questionable. It is not possible to separate the roughness of the outflow model from the unknowns of the inflow model by using surface-only measurements without matching downhole measurements. Besides, the flow rates during the well tests were too low for friction to be dominant and for an accurate determination of the pipe roughness. The roughness could have increased over time from corrosion and/or scaling. Roughness could have also resulted from the scraping and cleaning of the well when it was first converted from a production to an injection well. The roughness from the top to the bottom of the well could not be measured; therefore, the roughness had to be inferred.

Metal loss logs were useful to infer roughness. Figure 2 shows the metal loss data reported [9].

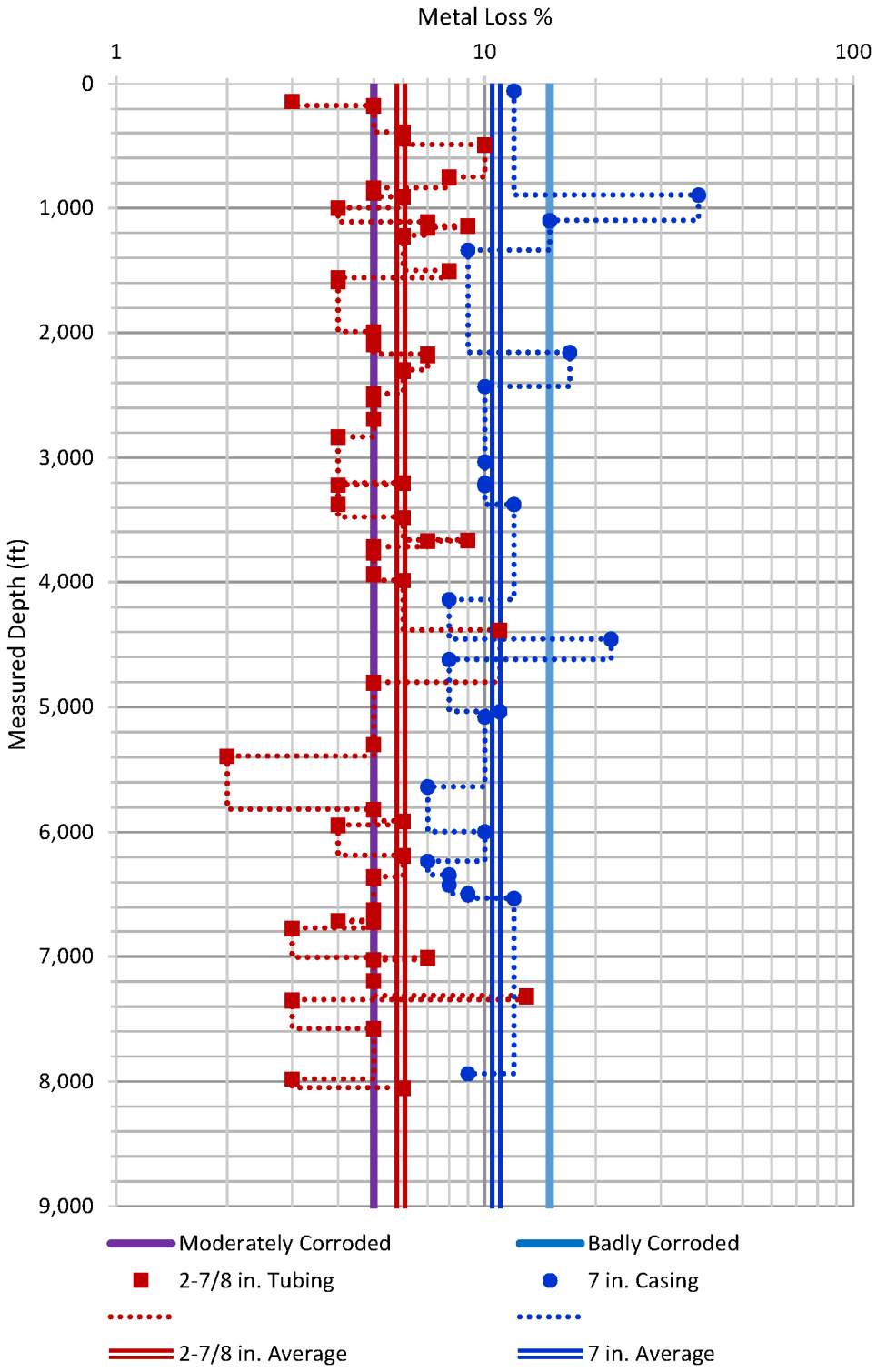

Figure 2: SS-25 Tubing and Production Casing Metal Loss Log

When SS-25 was completed, the roughness of the carbon-steel tubing and casing could reasonably be assumed as 0.001 in. (which was a reasonable new pipe value at the time of completion). Corrosion over time caused greater roughness. The production casing that was pulled from the well showed that the majority of the metal loss was on the outside diameter and affected the surface casing annulus significantly more than the production casing annulus. The average metal loss in the tubing was a slightly more than moderate degree of corrosion.

Figure 3 shows the general pipe roughness for varying degrees of corrosion.

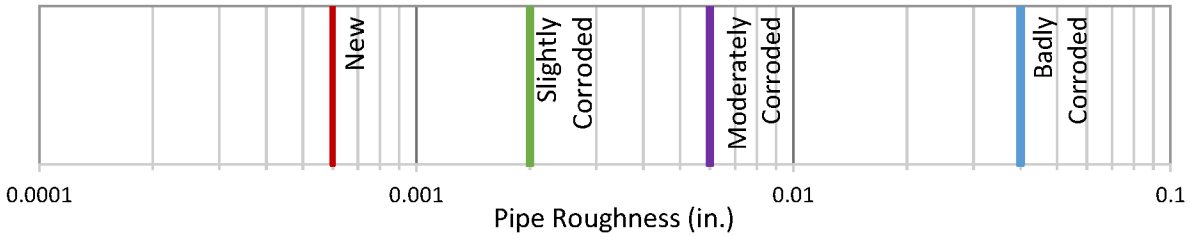

Figure 3: Pipe Roughness Vs. Corrosion for Carbon-Steel

Inside casing roughness and outside pipe roughness were presumed to be equal along the entire length of the piping and were based on the metal loss logs in Figure 2 and the correlation between corrosion and roughness in Figure 3. The roughness factor was best-estimated to be 20% greater than the minimum roughness for a moderately corroded (0.006 in.) pipe, that is, 0.0072 in.; this corresponds to used, cleaned pipe, which has a typical roughness of 0.006–0.008 in.

Roughness factor can affect the leak rates significantly. Figure 4 shows the pressure drop in the production casing annulus caused by pipe roughness as a function of rate (estimated by PROSPER).

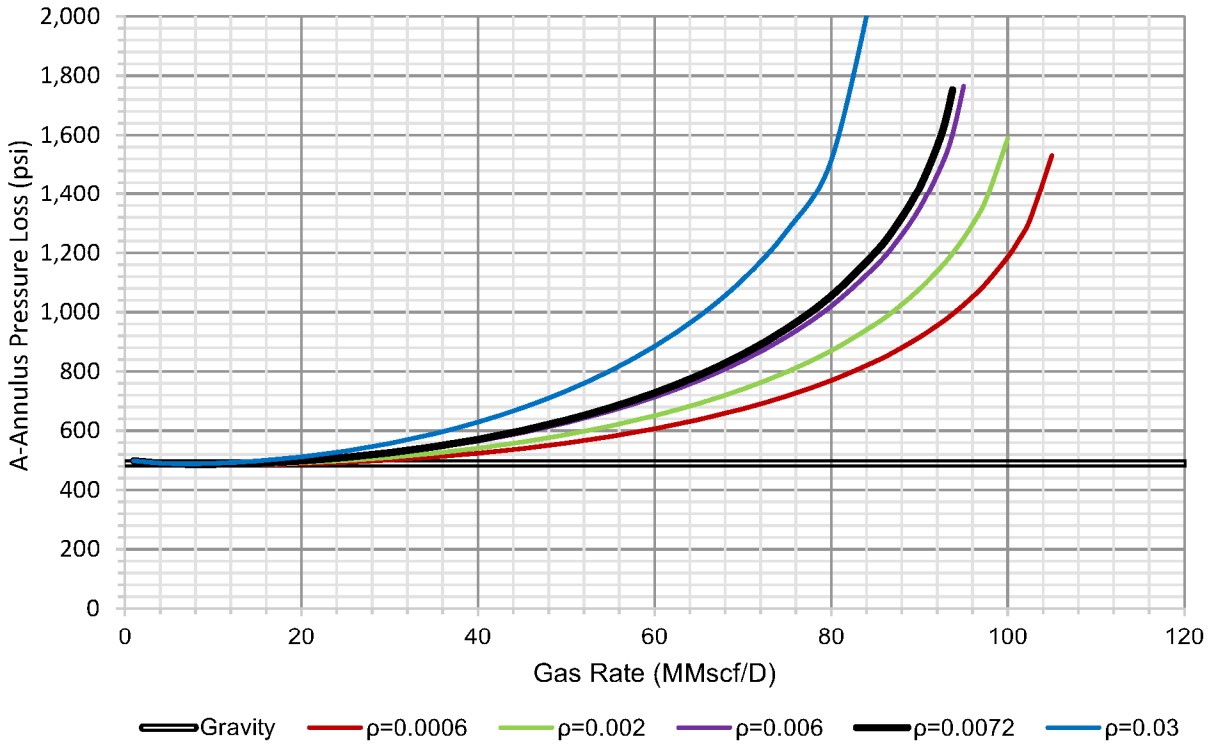

Figure 4: SS-25 A-Annulus Pressure Loss with Pipe Roughness

For three years prior to the leak, withdrawal allocations ranged from 3 to 15 MMscf/D, and injection allocations ranged from 2 to 7 MMscf/D. Over this flow range, Figure 4 shows the change in flow from roughness was negligible. For the modeled value of 0.0072 in., the effect from pipe roughness up to 30 MMscf/D was also negligible.

In 1954, SS-25 was completed as an oil and gas production well. In 1973, a workover was conducted on the well to convert it to a gas storage well, and this included using a casing scraper. In 1976, another workover was conducted where the casing was cleaned using a mill and scraper. In 1979, the well was worked over again for the removal of a safety valve, listed as removed in 1980. No further work was done on the well until the leak occurred.

It is presumed that when the well was being converted to an injection well, the scraping and milling removed any scaling that may have been present. Also, no scaling was assumed upon injection because the injection gas was sales-quality natural gas. Upon flow-back, the natural gas could pick up water and oil from the reservoir, and this may have possibly scaled with decreasing amounts over time as the original reservoir was flushed by sales gas.

Pipe roughness was an unknown and depended on corrosion and scale. At the extreme, when the well was leaking with the wellhead at atmospheric back-pressure, the extra roughness caused significant extra pressure drop that lowered the flowing gas rate. Because of the uncertainty, sensitivities with respect to pipe roughness were investigated when estimating leak rates. The final best-estimate roughness value was the one that could have best matched the pressures over the entire leak-path and leak-time.

3.2.4 Outflow Model Heat Transfer Coefficient

For the heat transfer model, the well model used PROSPER's Improved Approximation—it uses a specified heat transfer coefficient versus depth and the geothermal gradient to estimate heat-loss and gain to and from the formation. Table 4 lists suggestions from PROSPER's documentation for heat transfer coefficients.

Table 4: Heat Transfer Coefficients Recommended for PROSPER Model

Dry and Wet Gas	1 to 3 BTU/(hr-ft^2-°F)
Retrograde Condensate	5 to 7 BTU/(hr-ft^2-°F)
Oil and Water	8 to 10 BTU/(hr-ft^2-°F)

This study investigated the coefficient when predicting leak rates, and the results at the leak point showed no significant effect on the rate, while the temperature prediction was 5°F different from the lowest to the highest rule of thumb value. The higher coefficient allowed the earth to better warm the gas cooled by Joule-Thomson cooling during the leak. The uncertainty in the heat transfer coefficient caused uncertainty in the temperature estimate but little uncertainty in the rate estimate. The rule-of-thumb is that when there is flow in tubing with a no-flow annulus, the annulus reduces the overall coefficient. Since there was flow in the annulus, the high-side value was assumed, and the heat transfer coefficient was set at 3 BTU/(hr-ft^2-°F). The temperature surveys were performed during the leak, and the model with this coefficient matched these temperatures within 2°F at the leak point.

3.3 Data for Well Inflow Model

From reviewing the records, it is not clear what gas flow rate was used by the well-control company and SoCalGas in the planning of the kill operations for SS-25. SoCalGas responded to a DOGGR District Information Request, which asked for information related to the kill attempt modeling, by sending an IPR curve for approximately 30 MMscf/D [10]. Figure 5 shows the IPR.

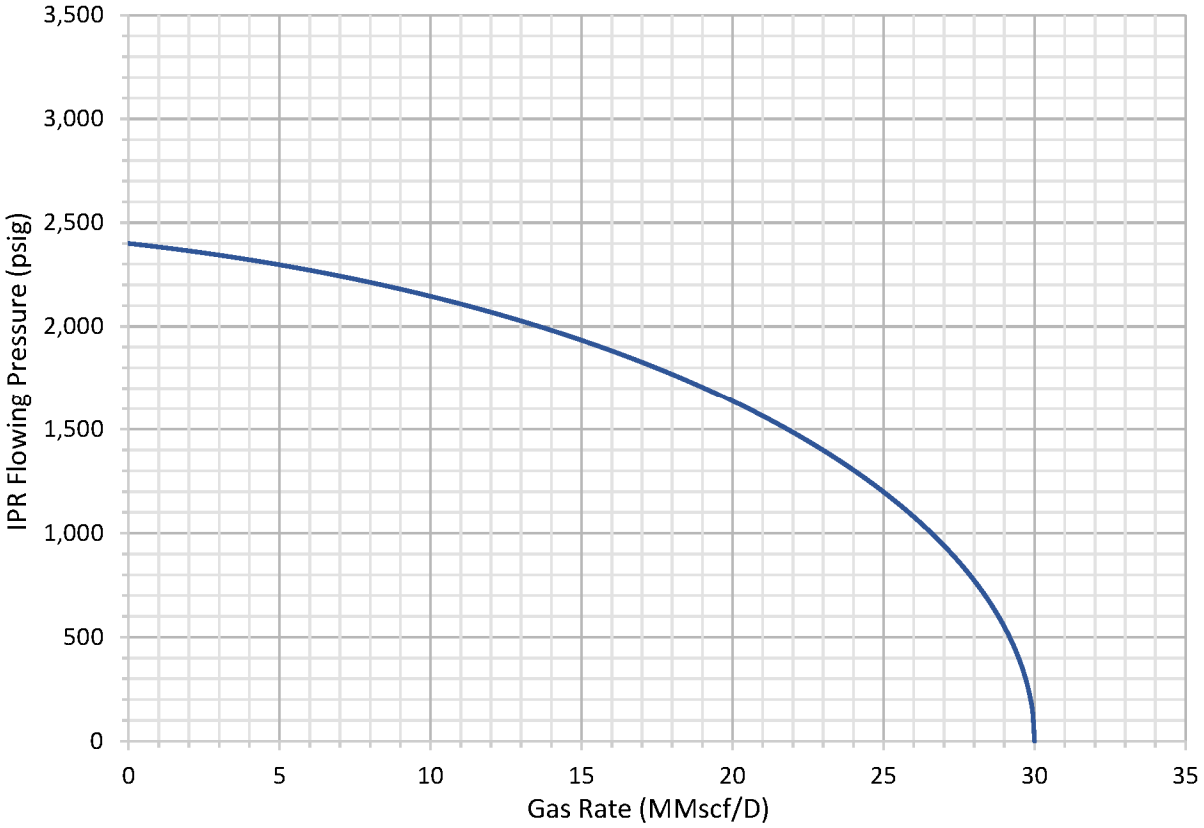

Figure 5: SS-25 Inflow Performance Relationship from SoCalGas

The following exceptions to this IPR immediately come forth after reviewing all data:

- The reservoir pressure was too low during the times of the kill attempts. There had been injection from February to October 2015, and the reservoir pressure shown was more akin to the pressure before the storage began. Given the time of year, it was unlikely for the reservoir pressure to ever be as Figure 5.
- The reservoir's deliverability, or permeability-thickness, was too low, which limited the absolute-openhole flow potential, i.e., the flow rate when the IPR flowing pressure equals 0 psig.

The true well deliverability was greater than the IPR provided by SoCalGas to DOGGR, and this may have been an issue in designing the kills, if modeling was conducted. Since the reservoir pressure and permeability-thickness were both better, the actual IPR would have been far better. This study presented an IPR that would have been more representative of SS-25 gas deliverability during the past 40 years. The IPR model was developed by matching the combined outflow-inflow well model to available well tests that had surface measurements. The IPR provided by SoCalGas to DOGGR underestimated deliverability.

3.3.1 Inflow Model Base Properties

Table 5 shows the properties set for the inflow model based on data provided by SoCalGas:

Table 5: SS-25 Inflow Properties for PROSPER Model

Reservoir thickness, net	45 ft
Perforation interval, net	45 ft
Wellbore radius (drilled hole size—not casing O.D.)	0.4167 ft
Reservoir porosity	0.20 fraction
Connate water saturation	0.20 fraction

The following properties were not preset for the inflow model:

- The reservoir pressure—it varied with time depending on injection or withdrawal.
- The reservoir permeability—it was fit via well tests (The fit property is dependent on the set properties.) and was an effective permeability matched to deliverability. The analysis determined the permeability-thickness, and then permeability was calculated by using the given reservoir thickness.

3.3.2 Inflow Model Reservoir Pressure

Table 6 lists SS-25's static pressure measurements reported by SoCalGas [11]. (Static pressure measurements near the time of the leak were unavailable.)

Table 6: SS-25 Static Pressure Measurements

Date	WHP (psig)	BHP (psig)	Depth (ft MD)
October 21, 2014	2,561	3,119	8,720
October 02, 2013	2,640	3,200	8,647
May 29, 2012	2,576	3,158	8,630
September 12, 2011	2,450	2,966	8,730
December 14, 2010	2,410	2,930	8,698
October 05, 2009	2,738	3,303	8,470
December 05, 2007	2,650	3,112	8,470
July 22, 2006	2,336	2,844	8,463
August 10, 2005	2,637	3,197	8,694

Details of how the static pressure measurements were determined were unavailable; therefore, the numbers could not be validated. Since the permeability of the formation was good, the pressure in the formation should have equilibrated quickly. The analysis of the static pressure measurements should have been straightforward and meaningful.

For the static measurements, the estimate of reservoir pressure ranged from 3,100 to 3,300 psig in the October timeframe. Given that gas storage cycled similarly on a yearly basis, and there was questionable justification to consider 2015 any different, the expected value of the reservoir pressure should have ranged from 3,100 to 3,300 psig.

The PROSPER modeling required the average pressure in the drainage/injection volume of the well and not the average pressure of the entire reservoir. It is certainly possible that the drainage volume during withdrawal was greater than the volume during injection. That is, this well withdrew gas injected by other wells. Pressure differences created by differing injection and withdrawal schemes of multiple wells quickly stabilize, which is because the 80 md formation permeability was quite good and the reservoir continuity between the wells was good. The actual reservoir drainage volume and average pressure for the IPR model are unknown, but the pressure could be reasonably estimated by a neighboring observation well.

In lieu of static pressure measurements around the time of the leak, this study used the monitoring well, SS-5, located near SS-25. Calculating downhole pressures from the measured surface pressures gave an approximate estimate of SS-25's drainage area reservoir pressure. Figure 6 shows the SS-5 bottomhole pressure estimates prior to and during the leak. The reservoir pressure increased as injection continued through July, August, and September, until the leak in October 2015. The pressures in 2015 were consistent with the previous yearly pressures measured during the month of October for SS-25. An appropriate value to use for the SS-25 reservoir pressure at the initial time of the leak would have been 3,200 psig.

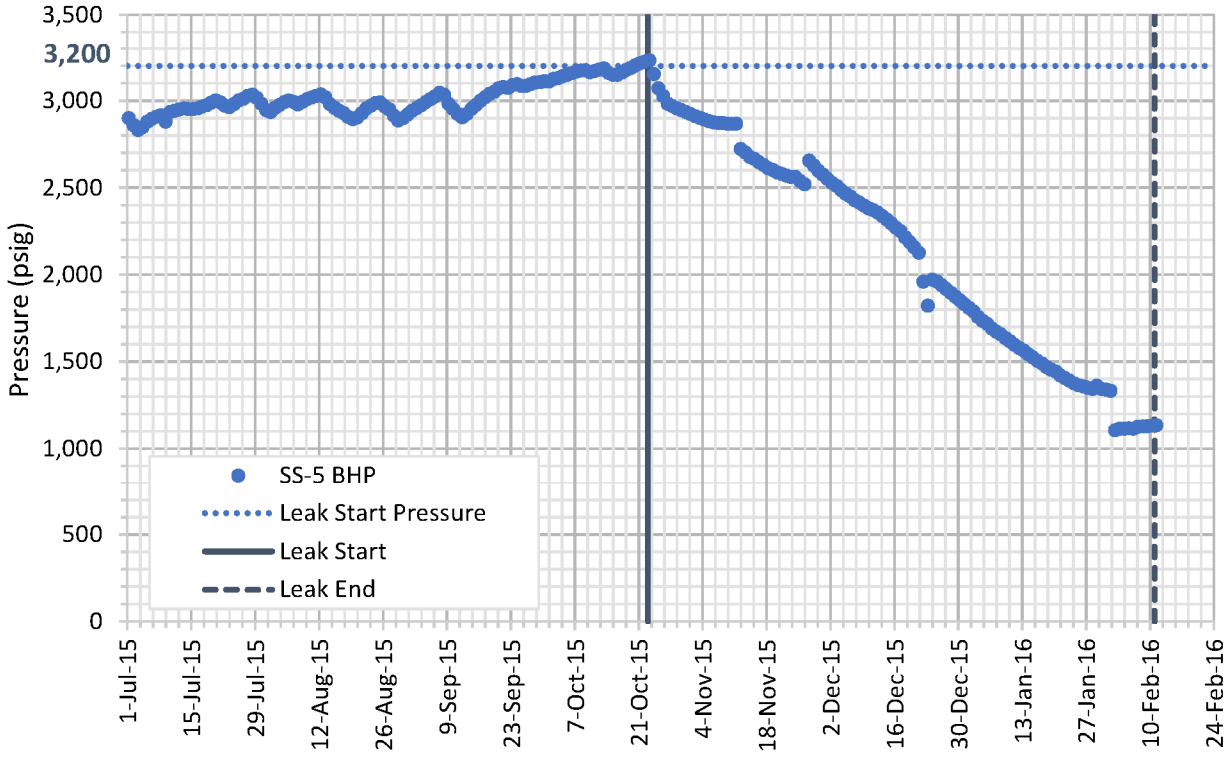

Figure 6: SS-5 Bottomhole Pressure from Surface Pressure

3.3.3 Inflow Model Permeability

The next concern was to determine permeability from the well deliverability. Table 7 gives the withdrawal well tests exactly as provided by SoCalGas in [12].

Table 7: SS-25 Withdrawal Well Tests Since 1978

DATE	WD Mode (T/C/D)	SIWHP (psig)	FWHP (psig)	DS (psig)	Choke Size (in.)	RATE (MMscf/D)
09/08/1978	C	2,760	2,720	490	0.62	11
09/19/1978	C	2,790	2,630	490	0.62	25
09/22/1978	C	2,820	2,605	525	0.63	28
09/26/1978	C	2,840	2,635	500	0.72	33
09/29/1978	C	2,805	2,520	505	0.79	37
10/02/1978	C	2,825	2,445	525	0.86	44
10/07/1978	C	2,790	2,295	540	0.95	53
10/13/1978	C	2,890	2,300	575	1.05	62
10/21/1978	C	2,930	2,105	510	1.17	74
10/28/1978	C	3,030	1,890	565	1.30	82
12/08/1981	C	2,600	590	590	0.00	71
01/13/1982	C	1,780	1,075	550	1.25	40
01/29/1982	C	1,360	720	525	1.35	30
02/05/1982	C	1,380	540	520		26
02/08/1982	C	1,430	530			23
03/03/1982	C	1,610	540	520	0.00	47
03/17/1982	C	1,580	600	555		48
10/15/1982	C	2,900	2,300	500	1.25	82
01/04/1984	C	2,090	1,320	490	1.25	50
01/24/1984	C	1,530	950	500	1.35	29
02/09/1984	C	1,430	900	480	1.40	32
02/17/1984	C	1,320	750	560	1.50	33
02/01/1985	C	1,300	890	580	1.30	30
02/25/1985	C	1,340	1,080	490	0.00	38
12/12/1995	C	2,520			1.00	49
12/26/1995	C	1,980	1,550	500	1.00	45
01/20/1996	C	1,640	1,060	510	1.00	35
01/30/1996	C	1,320	950	500	1.00	28
10/02/1997	C	2,280	2,090	480	0.90	55
01/06/1998	C	1,320	950	510	1.10	23
02/27/1998	C	870	540	500	1.40	20
03/04/1998	C	890	520	480	1.40	20
10/13/1999	C	2,590	2,220	500	0.90	48
01/31/2001	C	1,280	715	500	1.30	25
12/14/2006	C	2,367	544	544		50
12/06/2011	T	2,629	1,080	545	0.98	24
01/12/2013	T	2,233	2,155		0.97	30
01/28/2013	T	1,965	1,527	500	1.00	39
01/29/2014	T	1,305	510	480	0.98	4

When observing the flow rates in Table 7, it is apparent that the kill-planning IPR yielding an Absolute Open Flow (AOF) of 30 MMscf/D was not a realistic number. If only considering the most recent well test, the AOF was more realistic. Unfortunately, the table does not show the quality of the tests, and this study showed that the most recent well test was a bad test and should have been repeated.

When matching the withdrawal well tests, only the permeability and static skin were varied. Since the well tests were surface measurements with no downhole measurements, estimating the permeability was a combined outflow and inflow exercise—the outflow could not be separated from the inflow. Care had to be taken because issues with the outflow model could have led to errors in the permeability and skin.

The inflow model used in PROSPER was a Darcy flow-based model that estimated the non-Darcy flow factor for turbulent flow in the perforations. There was turbulence when well control was lost, and accounting for the turbulence was critical to predict surface rates and temperatures. There were no step-rate tests to estimate the turbulence coefficients, and therefore the PROSPER estimates were used.

3.4 Well Outflow-Inflow Combined Model

The outflow model parameter that had the largest degree of uncertainty to be determined was Pipe Roughness—estimated from withdrawal well tests.

The inflow model parameters that had the largest degree of uncertainty to be determined were:

- Reservoir pressure—estimated from an offset monitoring well.
- Permeability—estimated from withdrawal well tests and backed by cores.
- Skin—estimated from withdrawal well tests.
- Perforation turbulence—calculated by PROSPER.

To separate outflow from inflow was unfeasible because the matching of the withdrawal well tests was from surface measurements with no downhole measurements. Inaccuracies in the outflow model would have yielded inaccuracies in matched properties for the inflow model. Without both surface and downhole measurements, there were too many degrees of freedom, and therefore a best-fit, averaged model was derived from the tests. Uncertainty in the tubing-casing state would have yielded an uncertainty in the estimation of the leak-flow rate when the injection to SS-25 was shut in. Certainty came when the model matched measured data over the entire leak time.

3.4.1 Outflow Model for Surface to Downhole Conditions

The conversion from surface to downhole at the mid-point of perforations (necessary to estimate inflow properties) was affected by the uncertainty in the pipe roughness. The flowing conditions for the withdrawal well tests were such that the frictional pressure loss resulting from the pipe roughness was significant compared to the gravity pressure loss owing to the gas density gradient. The valid well tests were analyzed for 35 years prior to the leak to determine if the tests could be used to ascertain the pipe roughness. Determining the exact pipe roughness was not possible; therefore, ranges of roughness were used with the following categories:

- New, Slightly Corroded, and Badly Corroded—as detailed earlier
- Beyond New—essentially, with no friction loss
- Beyond Badly Corroded—with more friction than reasonably possible

Figure 7 shows that the best-estimate pipe roughness differed from test to test and friction was significant (averaged 45 to 60% of pressure loss in the outflow model).

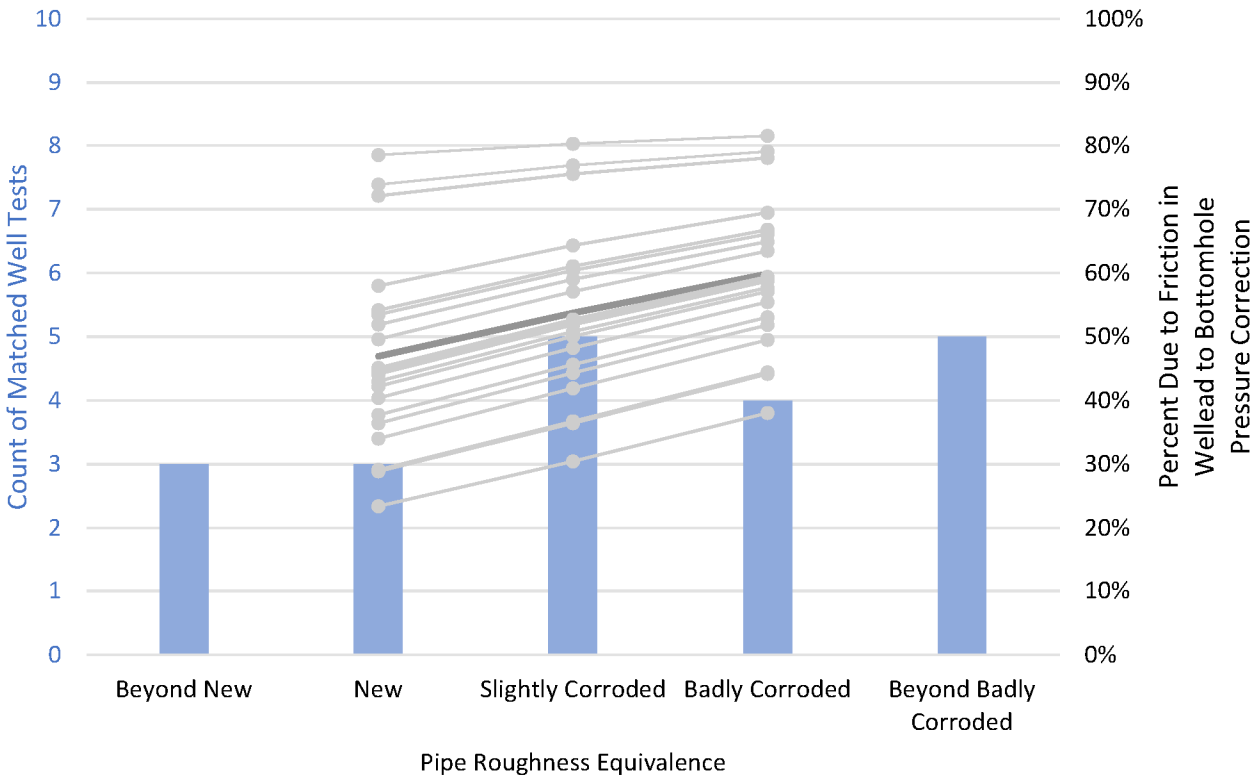

Figure 7: SS-25 Pipe Roughness Study for Well Tests 1980–2015

Because there was sufficient random scatter in the well tests, the best-estimate approach was to assume pipe roughness in the slightly corroded category. The scatter in the well test data assured that there would be uncertainty in determining the mid-point of perforation flowing conditions and, consequently, uncertainty in the analysis of inflow properties. The best estimates were statistically average estimates.

3.4.2 Outflow/Inflow Model Data Matching

This study analyzed the withdrawal well tests from the last 20 years (Table 7) to determine the best estimate of the reservoir permeability and skin. It was presumed that the permeability remained constant in time, and any possible degradation in performance could have been captured by skin. SS-25 was injected with clean sales gas, and the gas itself was not likely to cause skin issues over time.

Figure 8 shows the wells tests on a performance chart. These tests were labeled with dates as listed per SoCalGas [12]. All pressures were converted to bottomhole pressures by using well model to account for the outflow model and focus on the inflow model. The well test itself is marked as a circle with a line connecting back to reservoir pressure at no flow (estimated from provided static shut-in pressure). As expected, the reservoir pressure varied by month of test according to the yearly cycle of demand.

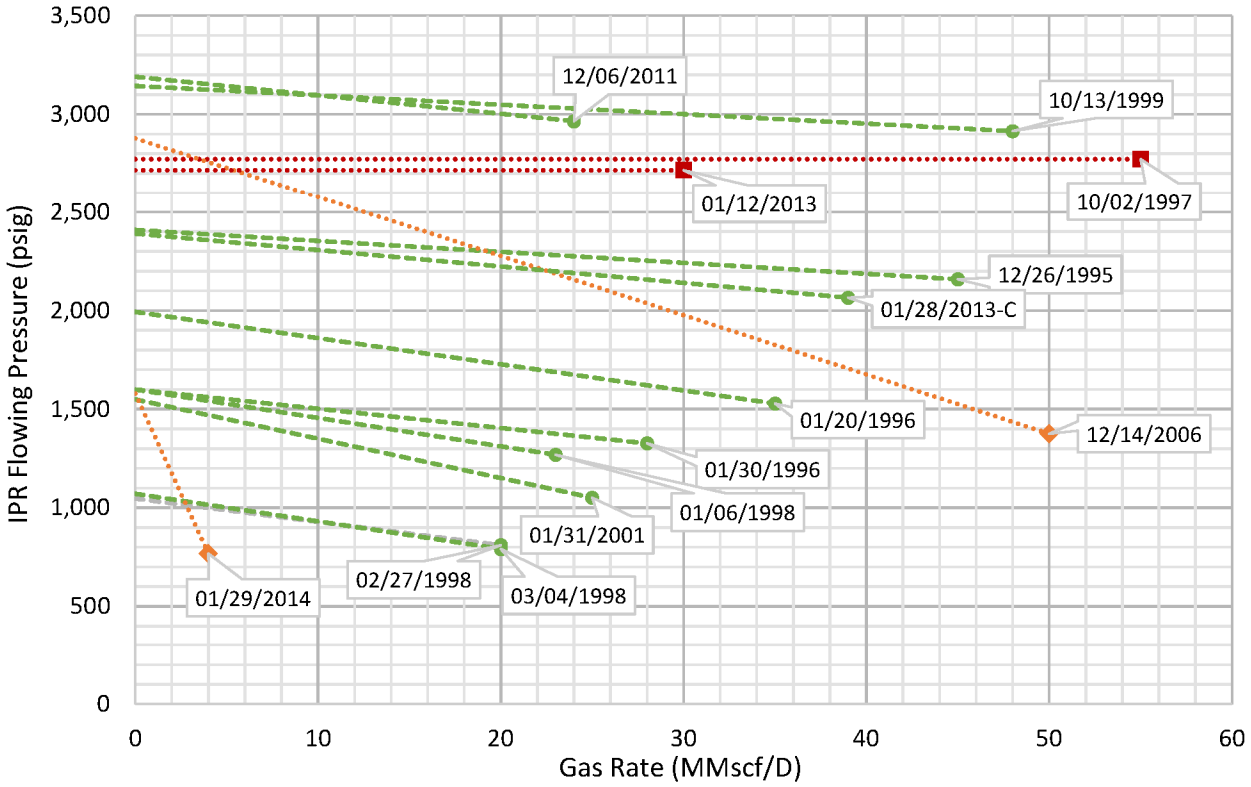

Figure 8: SS-25 Validation of Well Tests 1995–2015

The well tests drawn with a green dashed line follow a consistent trend and are considered valid. The well tests drawn with red and orange dotted lines are questionable; the red-square tests have flowing bottomhole pressures greater than the reservoir pressure, and the orange-diamond tests have excessive drawdowns. The bad test of January 12, 2013, (in red) was properly re-run on January 28, 2013. The well test for January 28, 2013, was modeled as casing flow rather than tubing flow, because the well model indicated that tubing flow alone was not possible. The bad test of January 29, 2014, (in orange) was not re-run, and it was the most recent test prior to the leak. Any adjustments based on the January 29, 2014, test made to a well model would have under-predicted deliverability. This most recent test was inconsistent with the tests of the last 20 years, and another test should have been run.

The valid withdrawal well test matches were analyzed with the following assumptions:

- Permeability was constant over time.
- Skin may have changed over time as a result of the injection and withdrawal operations.
- Reservoir pressures estimated from surface measurements were approximately correct, but the actual pressures may have varied and been greater—it is unknown if the shut-in was long enough to measure the final static pressures.

There have been nine valid well tests over the last 20 years, and they all matched permeability and skin within operational uncertainty. Using the given well test static pressures as reservoir pressures, the estimated skin constantly increased and decreased randomly over time without any operational reason. Assuming uncertainty in estimating reservoir pressures with static pressures allowed for a consistent match. Since it cannot be determined which test is best, it is desirable to have an averaged solution through the valid tests.

The best estimates for all valid tests are:

- Skin: 0
- Reservoir Permeability: 80 md

This best-estimate solution had neither static skin nor permeability and fit most reservoir pressures within 100 psi and all within 200 psi. Six of the well tests estimated a higher reservoir pressure than the static pressure while three of the well tests estimated a lower reservoir pressure than the static pressure. There was no systemic over- or under-estimation in the reservoir pressure. Given its closeness to the static pressure, the modeling differences in the tests were attributed to uncertainty in deriving drainage area reservoir pressures from static wellhead pressures.

Figure 9 shows the best-estimated match of the best flow tests for the last 20 years and the IPR calculated by PROSPER using the best-estimate properties (80 md permeability, no static skin, and the reservoir pressure set per the well test). Blade's IPR estimates for each well test are plotted as solid, thin cyan lines, and the IPR that SoCalGas sent to DOGGR is plotted as a solid, thick blue.

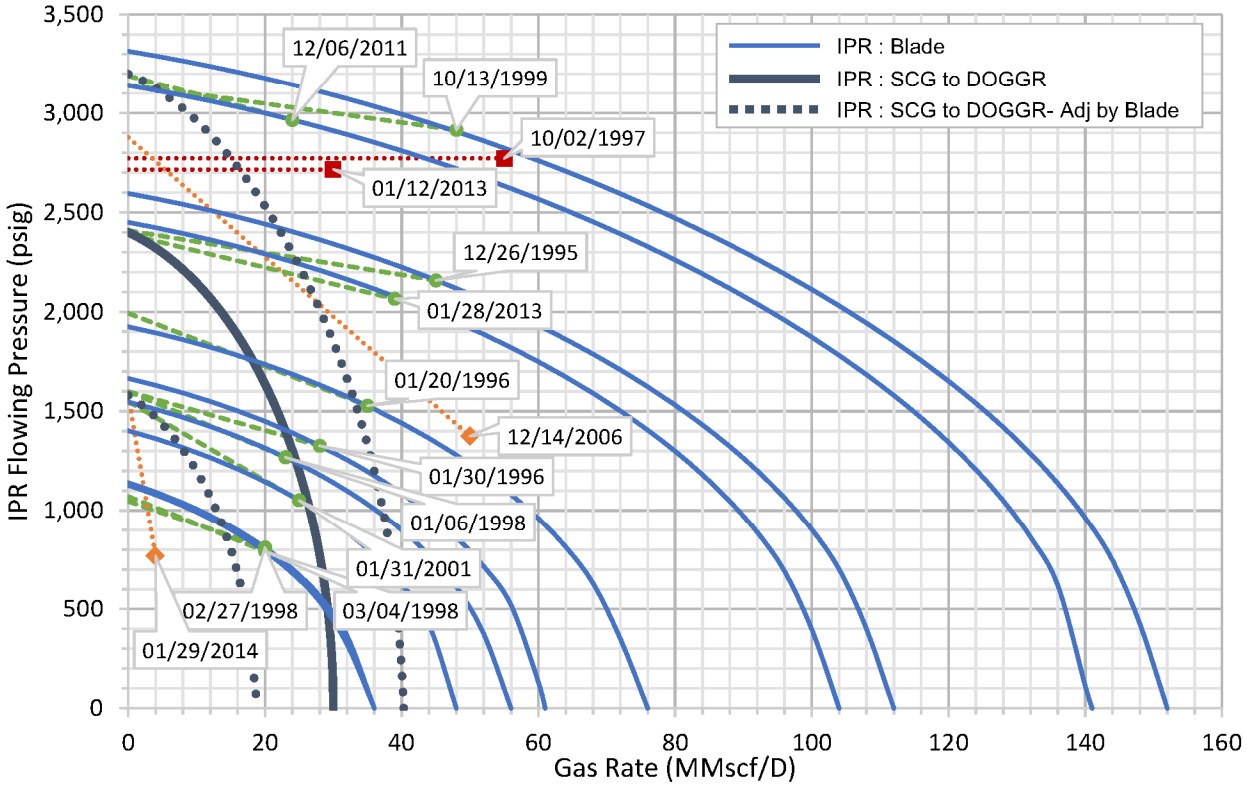

Figure 9: SS-25 Match of Well Tests 1995–2015

The kill-planning IPR followed a trend that did not represent the best-estimate IPR that explains the majority of the valid well tests. The Blade model could be used to match the kill-planning IPR (assumed or derived by the well-control company) by changing the permeability from 80 to 30 md and increasing the gas turbulence to 0.0005 1/(Mscf/D). Increasing the skin alone on the Blade model did not match the IPR data provided by SCG to DOGGR. For the reservoir pressure on the kill-planning IPR, the AOF reported was 30 MMscf/D, but for this condition, Blade's best fit model gave an AOF of 140 MMscf/D. For the reservoir pressure at the time of the leak, adjusting the kill-planning IPR gave 40 MMscf/D. The kill-planning IPR greatly underestimated the well's potential.

3.4.3 Outflow/Inflow Model Reservoir Pressure

The IPR model matched from 20 years of withdrawal well tests had a permeability of 80 md and no static skin. Measured conditions prior to the leak are used to check the model match by:

- Estimating the reservoir pressure from the injection data prior to the leak.
- Comparing the estimated reservoir pressure to that measured by an offset well.

Table 8 shows the monthly injection data and the reservoir pressures estimated by the PROSPER model.

Table 8: SS-25 2015 Monthly Injection Rates and Pressures

Date	Averaged Allocated Injection Rate (MMscf/D)	Averaged Allocated Injection Rate (psig)	Estimated Reservoir Pressure (psig)
March 2015	4.983	2,035	2,380
April 2015	6.749	2,280	2,640
May 2015	5.085	2,415	2,880
June 2015	3.332	2,470	2,990
July 2015	4.393	2,516	3,010
August 2015	5.722	2,490	2,950
September 2015	4.564	2,680	3,210
October 2015	4.062	2,610	3,140

Figure 10 shows a favorable comparison between the reservoir pressures estimated by the PROSPER model and the SS-5 monitoring well pressures.

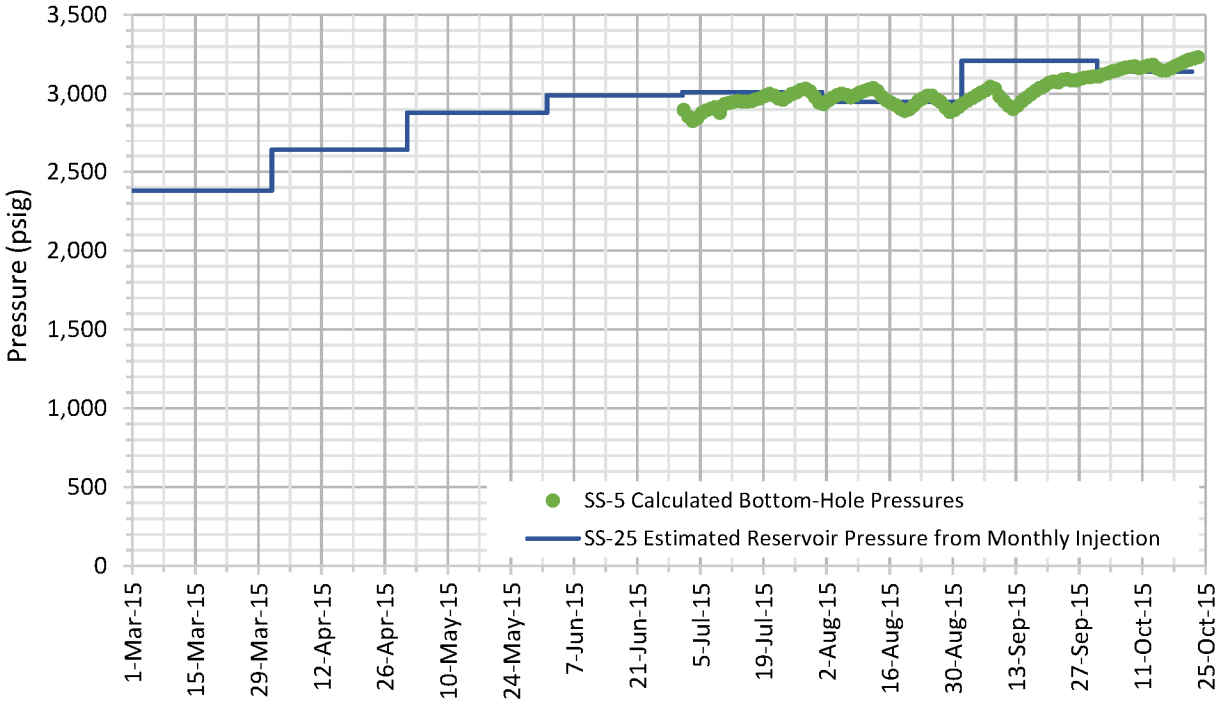

Figure 10: SS-25 Reservoir Pressure Estimates versus SS-5 Measurements

There were also static gradient measurements to compare. Figure 11 shows estimates of the reservoir pressure history using the well model compared to static gradient measurements. The well model's estimation using flowing data compared favorably with the static measured data.

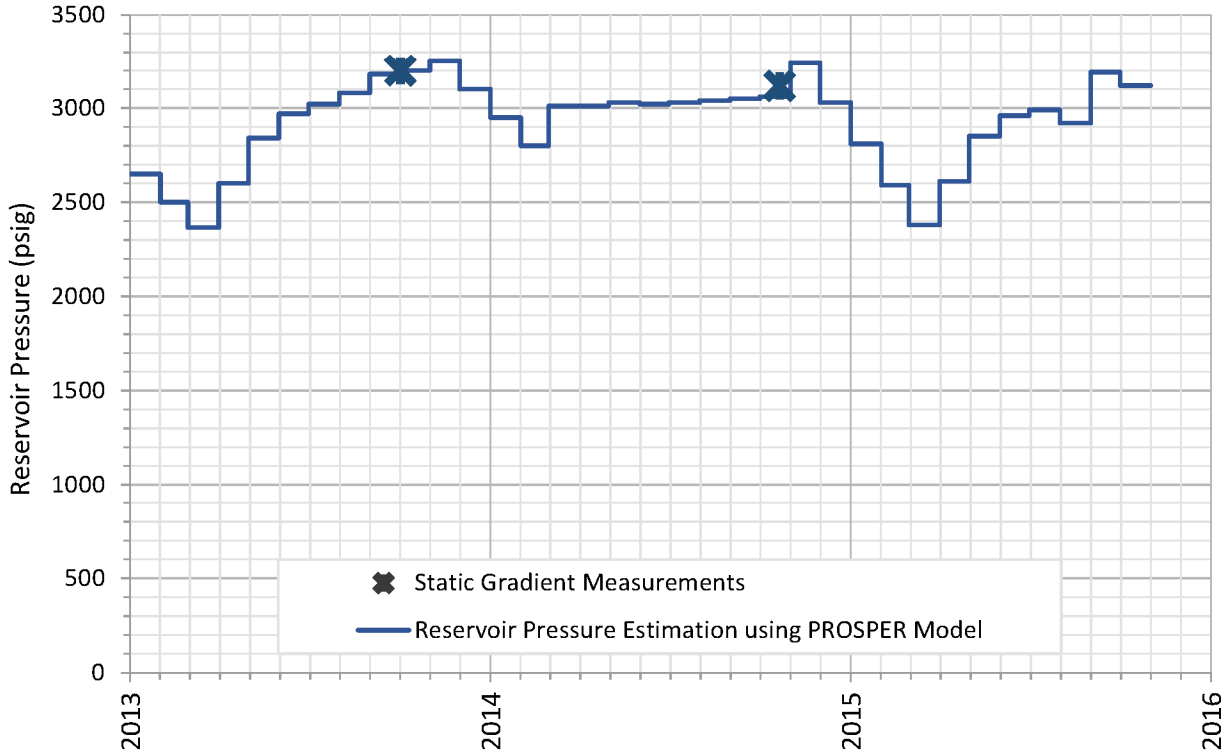

Figure 11: SS-25 Reservoir Pressure Estimates versus SS-25 Static Measurements

SS-25 reservoir pressure estimates in 2015 followed the same trends as the reservoir pressure in the previous two years. That is, there was no change of injection pressuring up the formation over time that should have caused concern. The reservoir pressure at the time of the leak in October 2015 was essentially the same as the reservoir pressure in the two previous years: October 2013 and 2014.

3.4.4 Outflow/Inflow Model Finalized

Figure 12 shows the inflow deliverability curve with the best-estimate properties for the well at the time of injection shut-in—October 23, 2015. This IPR was generated by PROSPER with the Petroleum Experts' IPR model matched to the last 20 years of SS-25 well tests. The temperature drop was from bottomhole isenthalpic expansion as gas entered the wellbore from the reservoir.

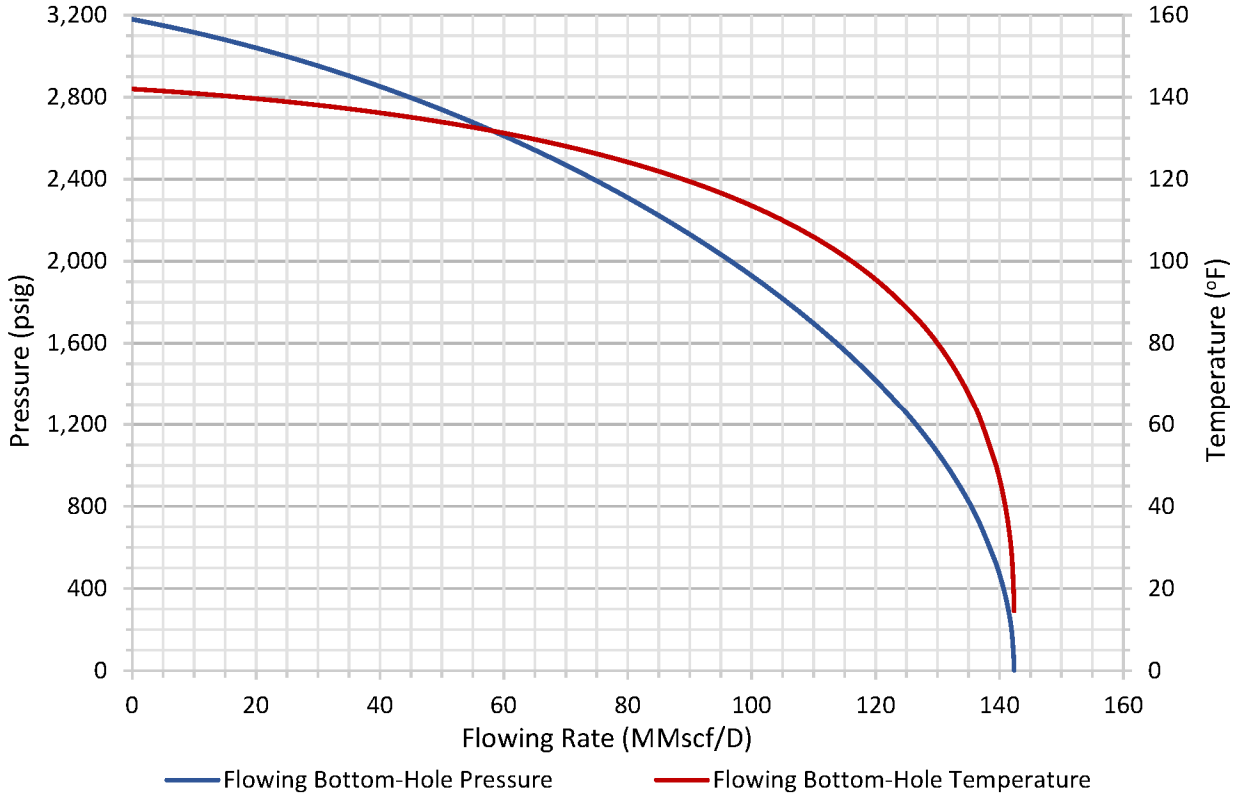

Figure 12: SS-25 Inflow Performance Relationship on October 23, 2015

The model properties are:

- Reservoir pressure: 3,200 psig
- Reservoir permeability: 80 md
- Reservoir thickness, net: 45 ft
- Reservoir porosity: 0.20 fraction
- Connate water saturation: 0.20 fraction
- Perforation interval, net: 45 ft
- Wellbore radius: 0.4167 ft
- Wellbore skin: 0
- Non-Darcy flow factor: 0.0844 1/(MMscf/D)—calculated by PROSPER
- Tubing/Casing roughness: 0.0072 in.

The outflow model properties and the conditions at the leak point control the leak withdrawal flow rate. The outflow model friction coefficient has an effect on rate and wellhead temperature:

- A lower wellbore friction yields lower bottomhole pressure for a higher drawdown, a greater rate, and a lower bottomhole temperature.
- A higher wellbore friction yields a higher bottomhole pressure for a lower drawdown, lower rate, and a greater bottomhole temperature.

Figure 13 shows how the flow rate of the well would have varied according to a tubing and casing roughness constant over the length of the pipe at the time of injection shut-in.

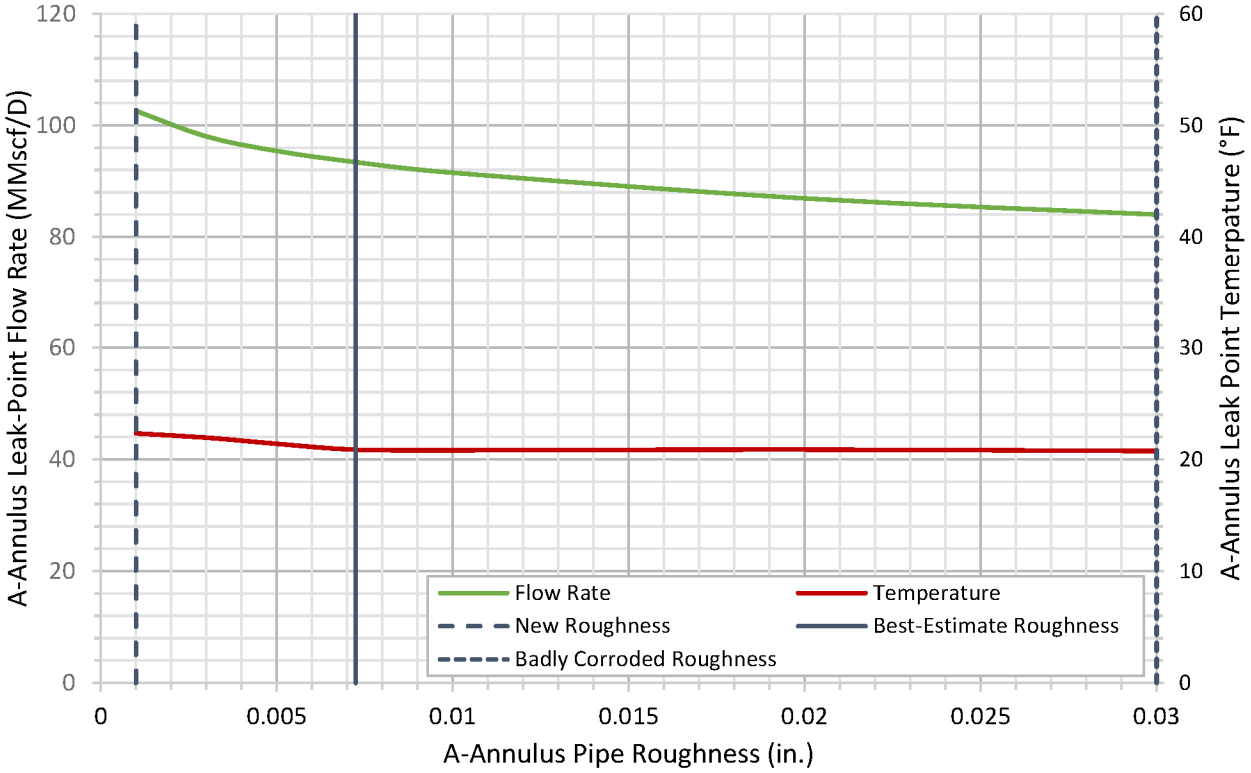

Figure 13: SS-25 Leak Conditions by Pipe Roughness on October 23, 2015

The best-estimate initial rates were:

- 93 MMscf/D at the assumed pipe roughness
- 104 MMscf/D for new pipe roughness
- 84 MMscf/D for badly corroded pipe roughness

Rate estimates vary significantly with pipe roughness, while temperature estimates at the leak point vary with less uncertainty. Uncertainties caused by pipe roughness were considered throughout this study.

4 Leak-Path Modeling

This study analyzed how the well nodal model supported or limited the choices of the leak path. Balancing the tubing, production casing, and surface casing head pressures required the leak path through the production casing to be established by injection shutoff and through the surface casing leak path, which could vary after the shut-in. Precise timing was not possible as pressures were not measured continuously. Once the production casing was pulled and the crack evolution was studied, there was evidence to support a leak leading to a casing failure during injection. To understand the leak path, this study investigated what the well model predicted for a leak during injection and during withdrawal.

4.1 Beginning Leak During Operations

Because no measurements at the wellhead had been recorded the week prior to the injection shut-in, it was not possible to tell exactly when the leak began. Therefore, the goal was to study what evidence the well model gave in corroborating when the leak began. The following conditions are discussed in order:

1. The leak began during injection and injected gas leaked.
2. The leak began post-injection shut-in and withdrawn gas leaked.

4.1.1 Beginning Leak During Injection Operations

At the compressor station, injection pressures and rates were measured on a continual basis. At the injection headers, continuous pressures were measured. At the well manifold, the injection pressure was measured on a weekly basis, and the rate was determined by allocation instead of measurement. A week could have passed with an unnoticed leak of unknown rate. A small leak would take either a portion or all of the injected gas, and the leak could cool down the piping and the formation. The questions to answer are: Had the temperature been low enough to account for the lower ground temperatures and would it have caused issues for the pipe material?

PROSPER was used for the leak calculations by assuming the initial leak in the production casing modeled as a choke. The calculation used an Elf choke model based on Perkin's approach along with discharge coefficients determined by Elf at Tulsa University Artificial Lift Project (for details, consult Petroleum Experts' PROSPER documentation installed with the application). The choke calculation clips temperatures to a minimum of –20°F—well below normal operating conditions.

The reported injection conditions for October 2015 were:

- Surface injection rate: 4 MMscf/D Allocated
- Surface injection pressure: 2,610 psig Measured
- Surface injection temperature: 80°F Estimated

The gas must have leaked first from the production casing and then through the surface casing. The surface casing pressure was unmeasured the entire week prior to the leak. Eventually, the gas would have leaked into a highly fractured formation. If the pressure in the formation outside the casing at the leak point was hydrostatic, the pressure would have been about 400 psig. If the fracture matrix was air-filled, there would have been only a few psi in back pressure. Therefore, understanding the leak required a range of back pressures.

Figure 14 shows the conditions at the choke outlet for the case where all the allocated gas (q=4) leaked or a portion of the gas (q=1) leaked. The choke size reported was the minimum choke size that could have leaked the given gas rate at the given pressure.

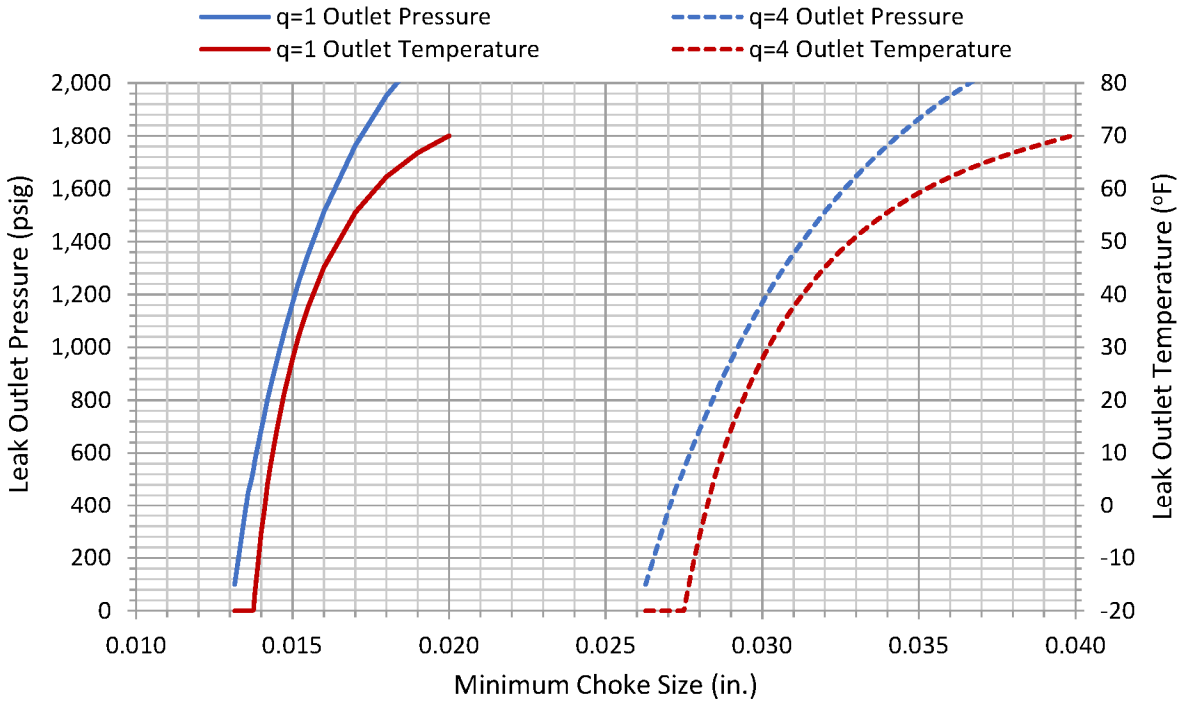

Figure 14: SS-25 Possible Leak Point Conditions During Injection

Both extremes yielded sub-0°F outlet temperatures. If the choke size became larger than shown, more gas than allocated to the well would have leaked and would require a surface network model to study the scenarios during this injection. The important conclusion at this point is that injection could have yielded temperatures below –20°F.

4.1.2 Beginning Leak Post-Injection Shutoff

An alternative theory is that the leak began after the injection had been stopped, and the well would have been withdrawing gas back from the formation. During a withdrawal leak, the temperatures would have been cooled by:

- Joule-Thomson cooling bottomhole as the gas expanded into the wellbore. When a well is flowing at maximum, the bottomhole pressure is low, and there is a large degree of Joule-Thomson cooling from the reservoir into the casing. Typically, a well is not produced with an extreme drawdown, and therefore there is not a significant temperature drop entering the wellbore—the system calculation that estimates rates ignores this effect. But, at uncontrolled withdrawal conditions, it cannot be ignored—the inflow calculation estimates this effect.
- Joule-Thomson cooling in the wellbore. Pipe roughness at high rates yields large pressure drops in the production casing annulus—the gradient calculation estimates this effect.
- Joule-Thomson cooling across the leak. The leak during withdrawal has a lower leak-point inlet pressure, and therefore experiences less cooling across the leak during injection.

Figure 15 shows an example of combining these forms of cooling for conditions at the leak point flowing at 93 MMscf/D (the best-estimate rate at the moment the injection is shut in). This figure shows the cooling could reduce the temperature down to 20°F in the production casing and 10°F in the surface casing.

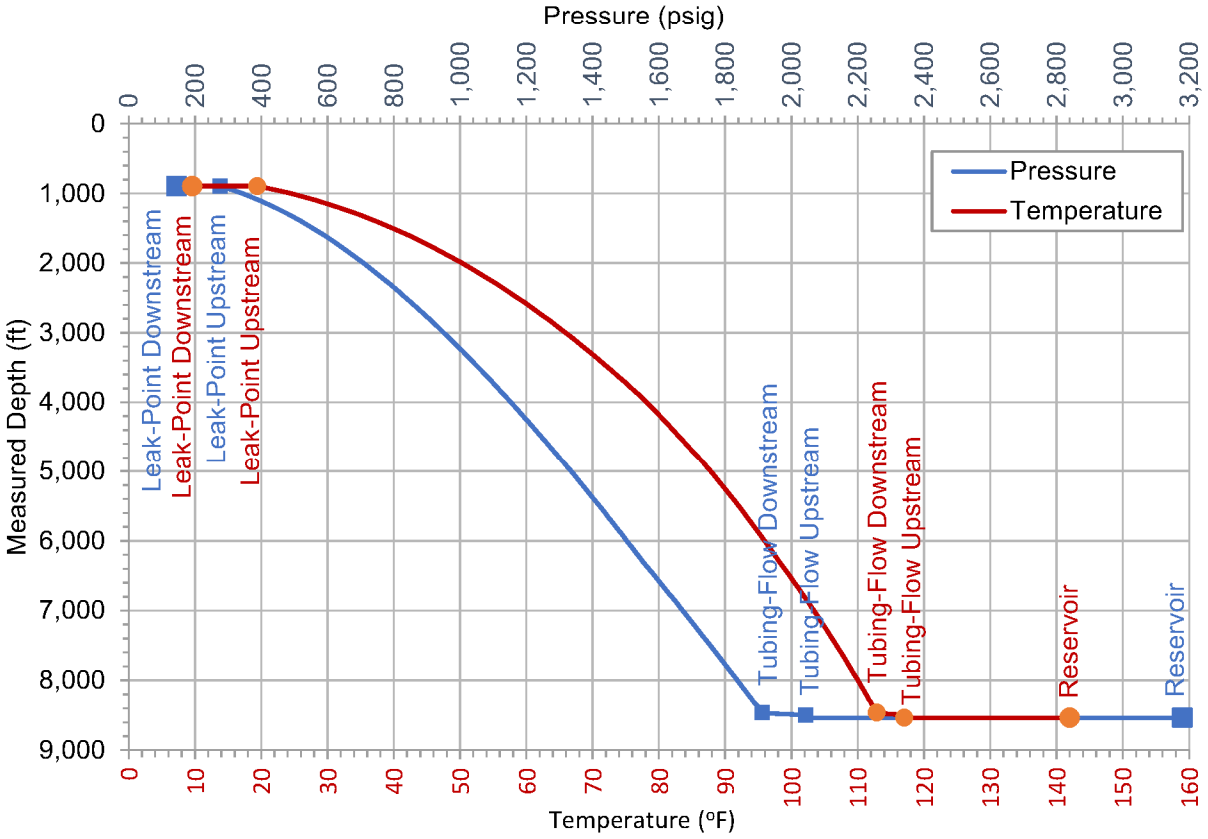

Figure 15: SS-25 A-Annulus Gradient for Leak on October 23, 2015

The temperature was cold enough to form ice or hydrates. The ground did achieve freezing temperatures, which suggests the presence of water that froze and held the temperature. The freezing in the fractures would have also changed the gas flow path, and this would explain reports of the gas rate declining through the surface fractures when the gas was not actually declining as much. The temperature from leaked-withdrawn gas explains the cold ground temperatures—although not cold enough to cause issues to the casing material. The colder temperatures would have only occurred during injection.

Higher pressures at the leak point during withdrawal yield lower rates, and the question becomes, how is the temperature affected? Since there are no continuous pressure measurements, it is not possible to know the pressures during the week before injection was shut in. Higher pressures could have existed before the pressure was measured. The PROSPER model gave insight into possible scenarios.

Figure 16 shows the well model estimations for the temperature, pressure at the inlet of the leak, and the corresponding temperature at the outlet for different back pressures at the leak point.

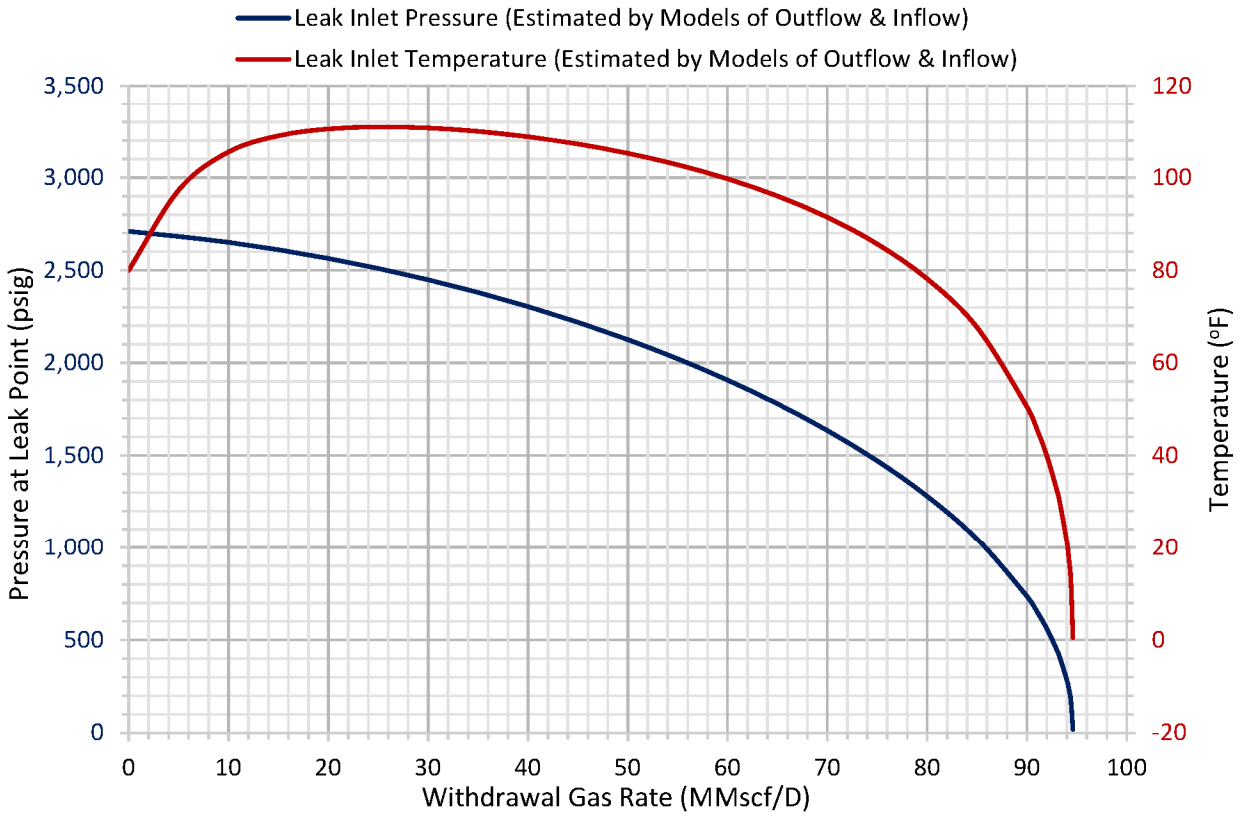

Figure 16: SS-25 Possible Leak Rate Conditions on October 23, 2015

At the highest rate, the gas in the annulus was at its coldest at the leak-point inlet. There was likely no further cooling across the casing axial rupture location; although further cooling could have occurred as the gas exited the surface casing. The post-injection shut-in temperatures were below freezing but were warmer than those temperatures during an injection leak. The coldest temperatures that could have caused issues for the casing would have occurred during injection.

4.2 Hydrates in the Ground and Tubing-casing

Documents provided by SoCalGas mentioned hydrates had formed in the tubing to cause the blockage, but there were no tests proving that it had been hydrates. Hydrates can form at temperatures above the freezing point of water. Whether it is ice or hydrates depends on the temperature and pressure necessary to form ice or hydrates, the temperature and pressure in the wellbore, and the formation kinetics of ice and hydrates. Figure 17 shows the hydrate formation equilibrium conditions for the leaked gas (as predicted by PROSPER).

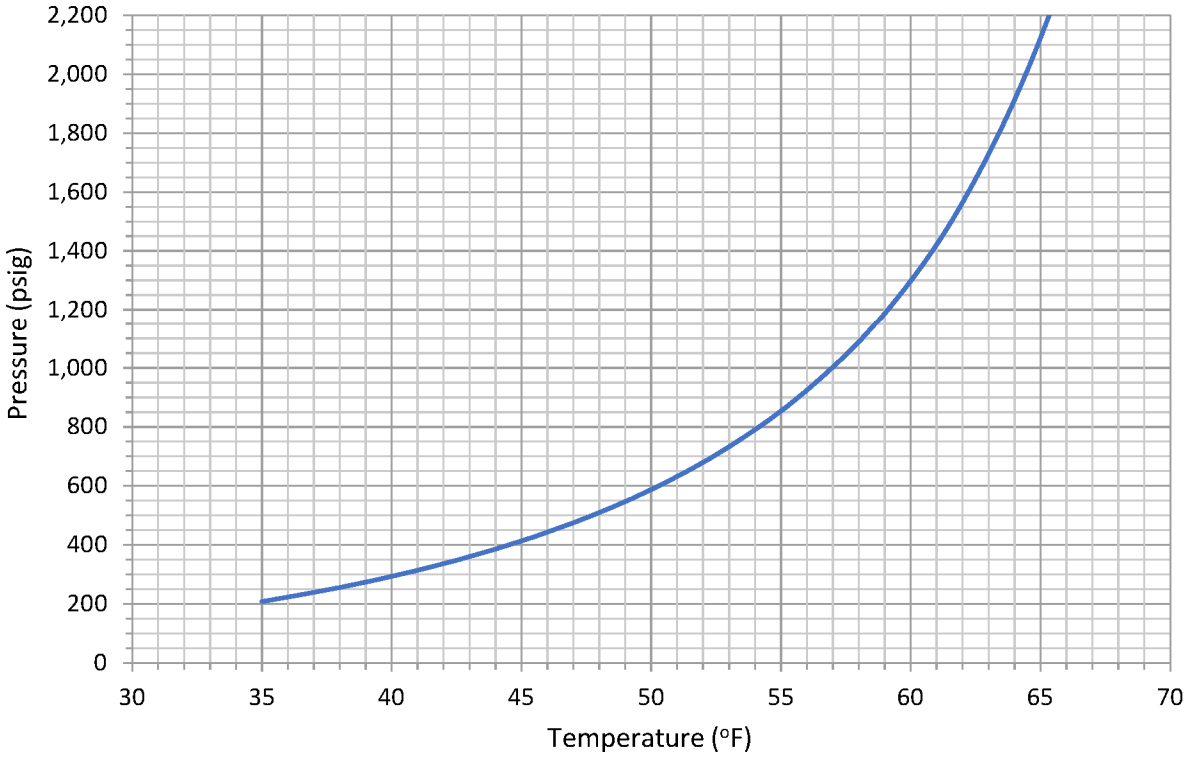

Figure 17: Aliso Canyon Hydrate Formation Conditions

Hydrate formation conditions existed in the wellbore at the point in which the tubing was blocked and until the glycol treatment removed the plug. The back-pressure in the production casing annulus could have gone up to 800 psi while the tubing was plugged. Per Figure 17, if the pressure were 800 psig at the leak outlet, hydrates could have existed (depending on kinetics) at or below 54°F.

Blade met with Dr. E. Dendy Sloan, Professor Emeritus at the Colorado School of Mines, who started the Center for Hydrate Research and is co-author of the book *Clathrate Hydrates of Natural Gas*. Blade presented to Dr. Sloan the SS-25 well and formation properties for his expert opinion on the kinetics of hydrate formation and their ensuing equilibrium conditions. Dr. Sloan stated that the well data presented required a phase change. While the conditions for hydrate formation have been well documented, the kinetics have not. Attempts at forming hydrates in labs under controlled conditions have given inconsistent results. There is no documented occurrence for the flash-forming of hydrates because it takes time for gas and water molecules to arrange themselves into a clathrate structure. The thermodynamic states are known, but the kinetics are not well understood—individual researchers fail to repeat their own kinetics experiments.

The conclusions from and based on the meeting with Dr. Sloan are that:

- Hydrates would not have flash-formed in the tubing, and therefore it must have initially been ice. Hydrates are a clathrate, which means that water molecules must envelop and form a cage around a gas molecule; hydrate formation takes time. The temperature must have been cold enough to quickly form ice.
- The plug in the tubing lasted from October 24 until November 06, 2015, when it was then removed by a glycol treatment. This amount of time was sufficient for hydrates to form in addition to the original ice plug. As the temperature increased above 32°F, the ice would have melted, and the hydrates could have been the remaining plug. The annulus could also have begun as ice and finished as hydrates.
- Hydrate formation conditions existed in the ground surrounding the wellbore. Hydrates could have formed in the fractures but are unlikely to form in the matrix. The hydrate structure needs sufficient space to arrange and form, and fractures provide this space while the matrix pores are too confining.
- Portions of the ground at or below 32°F could also have formed ice.
- Any hydrates or ice that formed could have kept the ground cold for an extended period of time. Both hydrates and ice can explain why the ground stayed colder longer than it should have solely from rock being cooled by gas.

Hydrates take longer to form than it took the initial plug; therefore, the tubing and casing must have initially been cold enough to rapidly form ice. Hydrates could have formed after the ice, and, as the tubulars warmed, the ice could melt and the hydrates remained to keep the tubulars plugged. Estimating temperatures during the leak is important to understand the mechanism of the leak.

4.3 Other Blade Studies to Support Leak-Theory

The wellbore model using PROSPER supported the leak-theory, but the following questions remained:

- How could the leak have cooled the formation and supported occurrences during the kill operation? During injection, the leak required a high enough rate for the ground to stay cold enough while the withdrawal warmed up (relative to injection temperatures), and it was still able to quickly freeze to ice as during the kill operation. Another Blade study developed the theory further, reported in [2]. Reservoir simulation studies were conducted to simulate what could have happened in-situ.
- How large could the leak rate have been at the well for the design of the injection system? Another Blade study developed the theory further and is reported in [3]. A surface injection model per the actual field conditions was built using Petroleum Experts Integrated Production Modeling (IPM) Suite GAP (General Allocation Program) software. GAP is the surface network component while PROSPER is the wellbore model component of the IPM Suite.

Conclusions from these external studies are built into this study's leak theory.

5 Estimation of Leak Potential During Injection

SoCalGas recorded the wellhead pressures weekly prior to the leak and began continuous monitoring measurements after the leak. The leak was noticed on October 23, 2015 but had not been noticed at the previous wellhead pressure measurement on October 15, 2015. Table 9 shows the leak could have begun anytime between these two points.

Table 9: SS-25 Well Pressures at Time of Leak

Date and Time	Injection Status	THP (psig)	A-CHP (psig)	P-Res (per SS-5) (psig)
October 15, 2015 00:00	Active	2,595	2,595	3,150
October 23, 2015 16:00	Suspended	1,700	270	3,180

Injection into SS-25 was determined by allocation based on the total injection network. There were no direct measurements to precisely estimate the rate before the leak was noticed. An integrated network model, documented in another Blade report, was developed using the IPM Suite. There are injection network data and SS-5 observation well pressures to model and understand possible rate scenarios. The following are relevant conclusions from this study:

- The increasing reservoir pressure across the field was balanced by an increasing discharge pressure at the compressor station. The possible volume injected daily was consistent from day to day—there are no reported injection choke changes. It was necessary to study only one of the days to understand the gas leak potential.
- The injection manifold pressure would have dropped insignificantly even if the wellhead injection pressure had dropped significantly. Hence, more gas could have been sent to a leaking well than the amount that would have been noticed at the injection manifold.
- Depending on the extent of the leak, SS-25 could have taken a significant portion of the total field volume injected. But to do so would have required dropping the wellhead pressure low enough that the well itself would have begun to withdraw from the formation. If this flow were significant, it would have been noticed on the SS-5 pressures. There was no significant measured drop in pressure at SS-5, and this limits the possible leak rate.
- SS-25 and SS-25B were at the same injection manifold with each well having its own injection control choke, and the arrangement of these chokes controlled the injection. As the SS-25 wellhead pressure dropped, it took the majority of its gas from the injection network and only slowly took injection gas away from SS-25B. In other words, all gas going to the manifold was not necessarily diverted to the leaking SS-25.

5.1 SS-5 Response to Field Injection and Withdrawal

Figure 18 shows the SS-5 bottomhole pressure measurements with the net daily field volume (produced and injected) around the time the leak was first noticed.

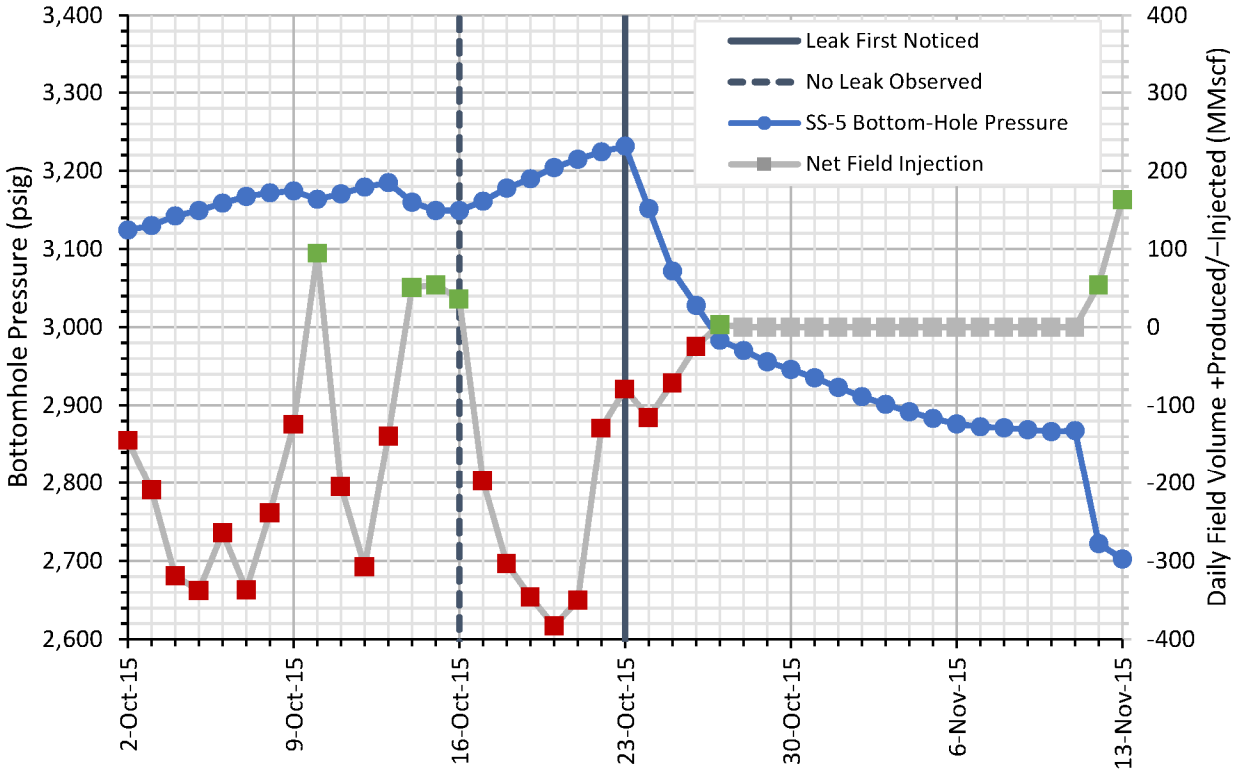

Figure 18: SS-5 Pressure Response to Field Withdrawal

Figure 18 shows that:

- In the time before any leak was possibly observed, the SS-5 pressure increased during a net injection and decreased during a net withdrawal from the field.
- In the days prior to the leak, the field was on net injection with a net volume of 100 to 400 MMscf/D, and the SS-5 bottomhole pressure rose steadily. Given only ~4 MMscf/D was allocated to SS-25, the SS-5 pressure measurement responded to the overall field injection.
- At the time the leak was first observed, the field was on measured net injection of ~100 MMscf/D. After stopping injection, the leak rate withdrawn from the formation by SS-25 was likely ~100 MMscf/D. The SS-5 bottomhole pressure showed a significant drop in pressure at this rate, and, given that the day before there had not been a significant drop, it indicates the leak had that high rate somewhere within that day.

Significant withdrawal by SS-25 was noticed quickly by SS-5. Therefore, the steadily increasing SS-5 pressures indicate that any leak that began during the uncertain week with no SS-25 wellhead measurements could not have been withdrawing significant volumes from the formation. Combined with the injection network model, this limits the rates that could have leaked that week.

5.2 SS-25 Implications from the Injection Network Model

The injection network model showed that an SS-25 leak during injection would have taken in gas from the entire injection network and only slowly would have taken away injection gas from SS-25B. Figure 19 shows the rates that SS-25 and SS-25B would have taken from the injection network as the SS-25 wellhead pressure dropped owing to a leak.

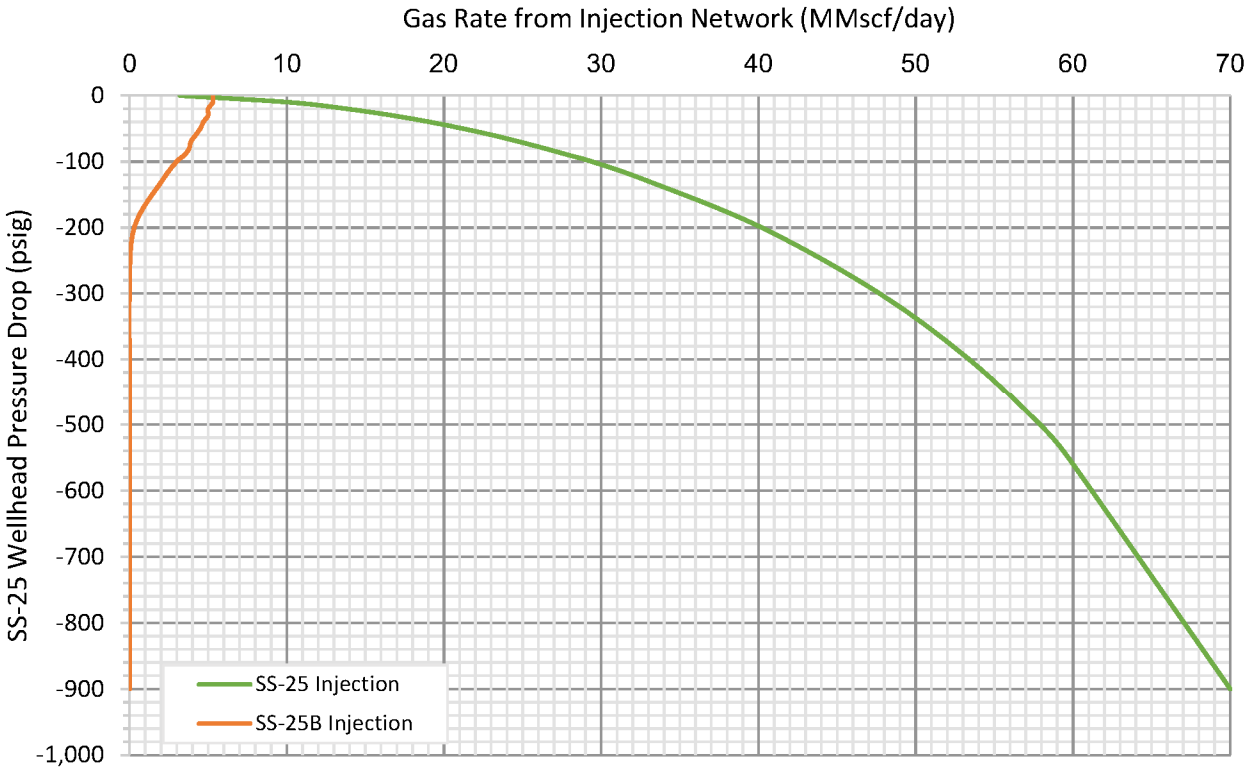

Figure 19: SS-25 and SS-25B Gas from Injection Network

As the leak dropped the wellhead pressure at SS-25, the well did not simply rob SS-25B of its injection gas. Figure 19 shows that SS-25B would have continued to take in injecting gas until a leak in SS-25 caused a 200 psi drop in the wellhead pressure. At this point, SS-25 would have been taking 40 MMscf/D from the gas injection network. It is therefore beneficial to have an integrated network model for the field to understand leak potential.

5.3 SS-25 Combined Well and Injection Network Modeling

Figure 20 shows the balance as the wellhead pressure drops between the rate that could have been injected from the injection model (modeled in GAP) and the rate that would have been withdrawn from the formation (modeled in PROSPER).

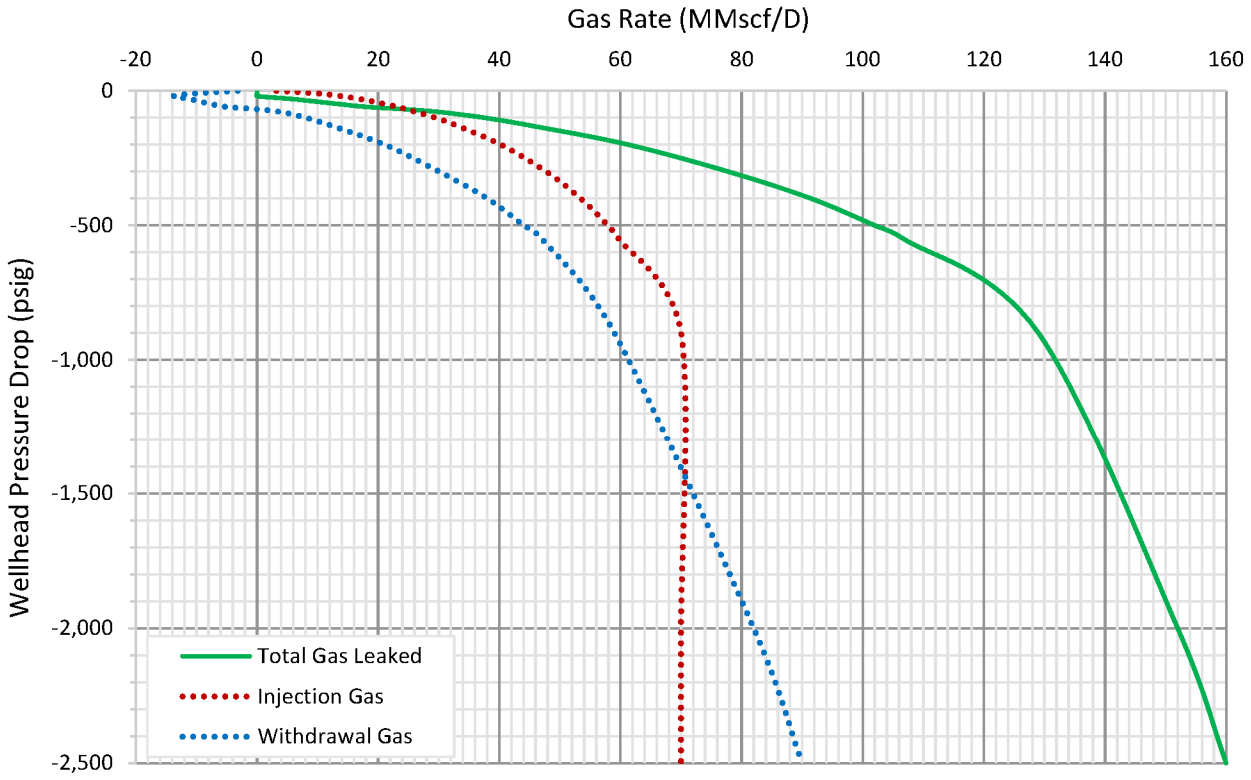

- Total gas leaked = injection gas + withdrawal gas
- If withdrawal gas rate < 0 , gas injected into reservoir
- If withdrawal gas rate > 0, gas withdrawn from reservoir

Figure 20: SS-25 Possible Leak Rates on October 23, 2015

Figure 20 shows that the leak rate could have easily exceeded the allocated rate of 4 to 6 MMscf/D. The actual amount that leaked during injection depended on the evolution of the leak. If the leak was small, a portion would have exited the well through the leak while a portion of the injected gas would have continued to inject into the formation—how the gas prorates between the two paths depends on the leak-hole size. If the leak is large, all injected gas will escape the leak hole and gas will be withdrawn from the formation. From the Figure 20, up to 25 MMscf/D could come from the injection network without any gas produced by the formation. Past this point, the leak would be gas from the injection network plus produced gas. Based on SS-5 observation pressures when ~100 MMscf/D were leaked, produced gas rates greater than 20 MMscf/D are likely to be noticed. At 20 MMscf/D produced from the formation, another 40 MMscf/D would come from the injection network to yield 60 MMscf/D leaked. The maximum leak could have been ~70 MMscf/d from injection and ~90 MMscf/D from withdrawal simultaneously. If the casing failed during injection, it had to part the same day the injection was shut in per the SS-5 daily observation of no decrease in pressure prior to shut-in. No decrease in pressure at SS-5 implies no significant withdrawal from SS-25.

During injection and as the pressure falls at the leak point, the reservoir contributes to the leaking gas and both the pressure and temperature changes in the production casing annulus. Figure 21 shows the evolution at the leak-point inlet in the production casing, and the data show:

- Below ~20 MMscf/D the temperature at the leak point in the production casing annulus will be the temperature of the injection gas.
- From ~20 to ~90 MMscfd/day the withdrawal leak gas from the reservoir increasingly warms the gas.
- Above ~90 MMscfd/day the temperature increase reduces due to Joule-Thomson cooling in the annulus.
- At 70 MMscf/D of injection gas the injection gas choke is at critical flow and provided additional cooling.

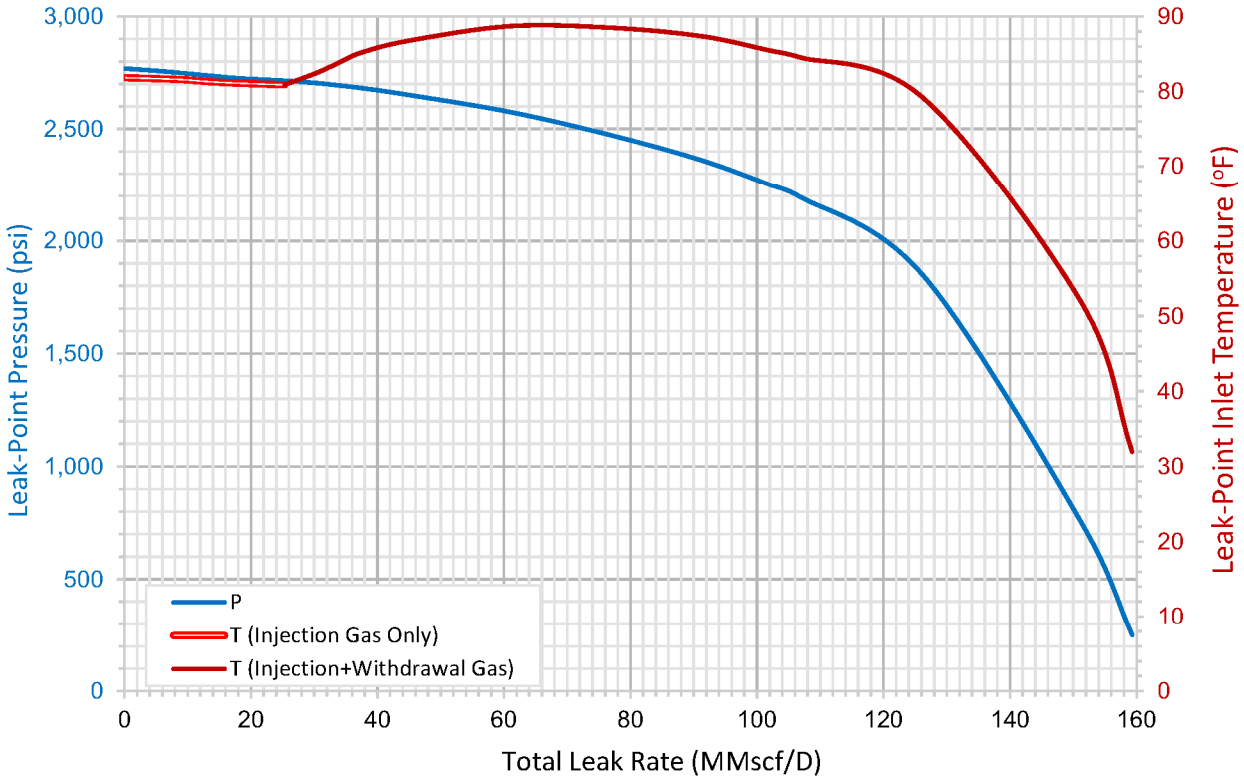

Figure 21: SS-25 Possible Leak-Point Conditions on October 23, 2015

This figure shows the change in pressure and temperature at the leak inlet. It is presumed that the injection gas and withdrawal gas are mixed. The next concern is the pressure and temperature at the leak outlet.

The controlling factor of the leak prior to the injection being shut in is the size and evolution of the leak opening. Figure 22 shows the effective leak opening assuming a circular hole at critical flow with a surface casing pressure of 140 psig as on October 22, 2015.

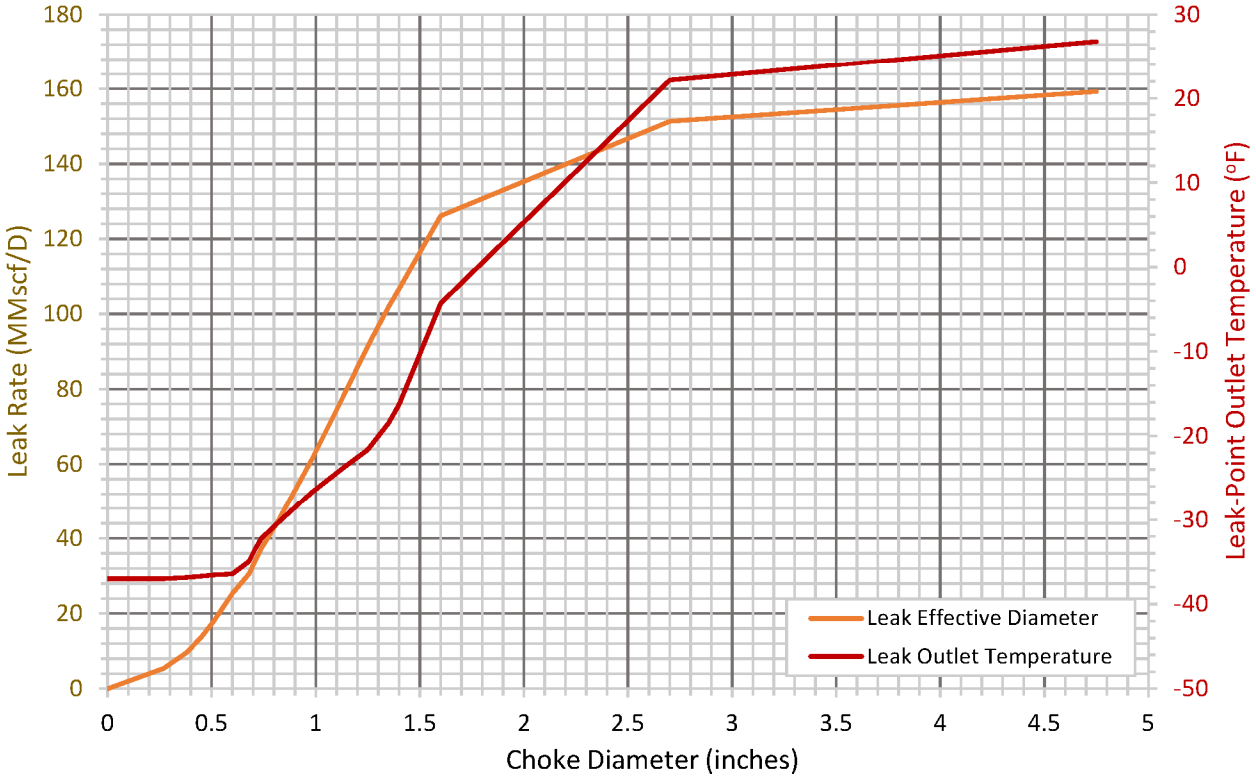

Figure 22: SS-25 Possible Leak Outlet Conditions on October 23, 2015

The leak outlet temperature is stable when all gas leaked is from the injection network (up to 25 MMscf/D). Up to the maximum-likely leak rate during injection of 60 MMscf/D, the leak-hole size would be up to 1.0 in. and the temperature at or below –26°F. Larger openings would have required too much to be withdrawn from the reservoir, and that would have been seen in SS-5 observation pressures. Again, the failure of the production casing had to have happened the same day the injection was shut in.

Note that the time of the day for the measurements is unknown and can be different from day to day. Detecting and monitoring the progression of a leak requires continuous pressure measurements, which were not available. Therefore, it is not feasible to precisely determine the growth of the leak opening from wellbore hydraulics. The data suggest that a small initial opening could cool the metal and allow the fracturing of the casing to a larger opening. Significant cooling of the casing was possible across all reasonable ranges of flow for the leak during injection; no precise set of conditions are required.

6 Estimation of Leak Rates Post-Injection Shutoff

The goal of this section is to estimate gas leak rates post-injection shutoff. SoCalGas recorded the wellhead pressure multiple times a day during the leak. The model used herein to estimate rates is a pseudo-steady-state model. The transients associated with the day-to-day operations or the kill attempts were not investigated. Modeling the transients of the kills was conducted in a Blade study separate from this report. This study chose a single pressure each day when the well was most stable. Once the kills were stopped, the well flow was pseudo-steady-state. This study was able to resolve all stable, measured data assuming that:

- The production casing failed while injecting gas and before injection gas was shut off the afternoon of October 23, 2015.
- The surface casing had sufficient holes to release all gas to the ground after the axial rupture. Casing holes were documented from a surface casing caliper log. Note that a casing shoe leak is not required. The withdrawal gas flowed up the tubing, through the ports above the packer into the 7 in. × 2 7/8 in. annulus, through the parted 7 in. casing into the 11 3/4 in. × 7 in. annulus, and out the holes in the 11 3/4 in. casing (Figure 23).

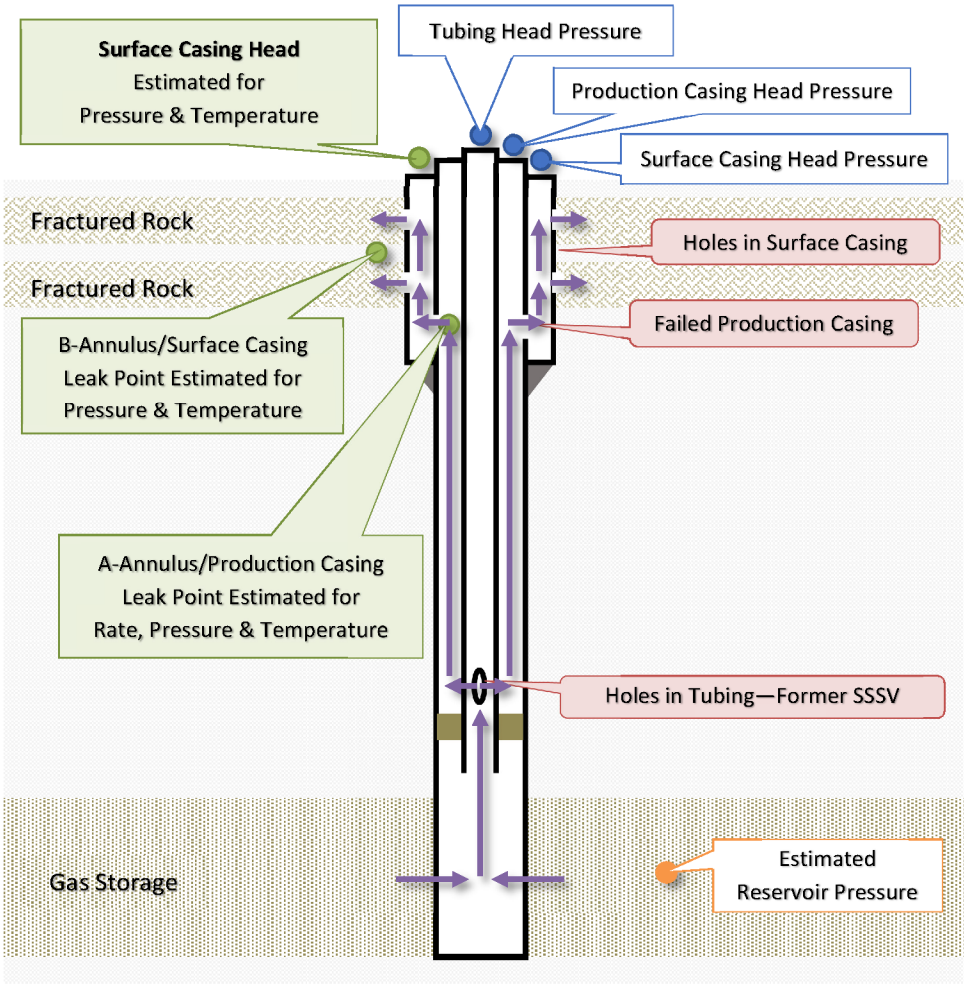

Figure 23: SS-25 Withdrawal Gas Leak Path

The production leak point is where the rate, pressure, and temperature at the inlet of the failed casing were estimated based on the measured tubing head pressure, measured production casing head pressure, and estimated reservoir pressure. The pressure at the surface casing head was estimated using the leak-point conditions and flowing all gas out the surface casing holes. The estimated surface-casing head pressures that matched the measured pressures give support to the proposed model. Modeling a casing shoe to leak required a mismatch in pressures at times when the tubing was not plugged, thereby giving high back pressures. Details of the modeling follow.

6.1 Produced Gas Leak Key Estimation Points

Key points are those estimation points that approximate steady-state conditions primarily before a kill attempt begins. They are the primary study points for rate calculation sensitivity comparisons while all points are considered for the best-estimate rates. Several key points are marked as kill points and maintained consistent with the well kill analyses conducted by Blade. This study inferred SS-25 drainage area reservoir pressures from the SS-5 observation well. Table 10 lists the key estimation points.

Table 10: SS-25 Uncontrolled Flow Key Estimation Points

Kill Point	Date and Time		Elapsed Time (days)	THP (psig)	A-CHP (psig)	P-Res (per SS-5) (psig)
–	October 15, 2015	00:00	–	2,595	–	–
1	October 23, 2015	16:00	00.00	1,700	270	3,180
2	November 13, 2015	11:15	20.80	1,526	253	2,850
3	November 15, 2015	06:00	22.58	1,607	217	2,800
4	November 18, 2015	06:00	25.58	1,597	199	2,770
5	November 24, 2015	06:30	31.60	1,638	199	2,690
6	November 25, 2015	06:30	32.60	1,651	199	2,680
–	November 27, 2015	00:00	34.33	1,600	200	2,660
–	December 08, 2015	00:00	45.33	1,526	200	2,410
–	December 17, 2015	00:00	54.33	1,318	200	2,250
7	December 22, 2015	01:00	59.38	1,215	200	2,080
–	January 10, 2016	00:00	78.33	819	200	1,620
–	January 23, 2016	00:00	91.33	591	200	1,390
–	February 02, 2016	00:00	101.33	583	200	1,320
–	February 11, 2016	00:00	110.33	583	200	1,280

Figure 24 shows the determination of the SS-25 reservoir pressure from the SS-5 bottomhole pressures:

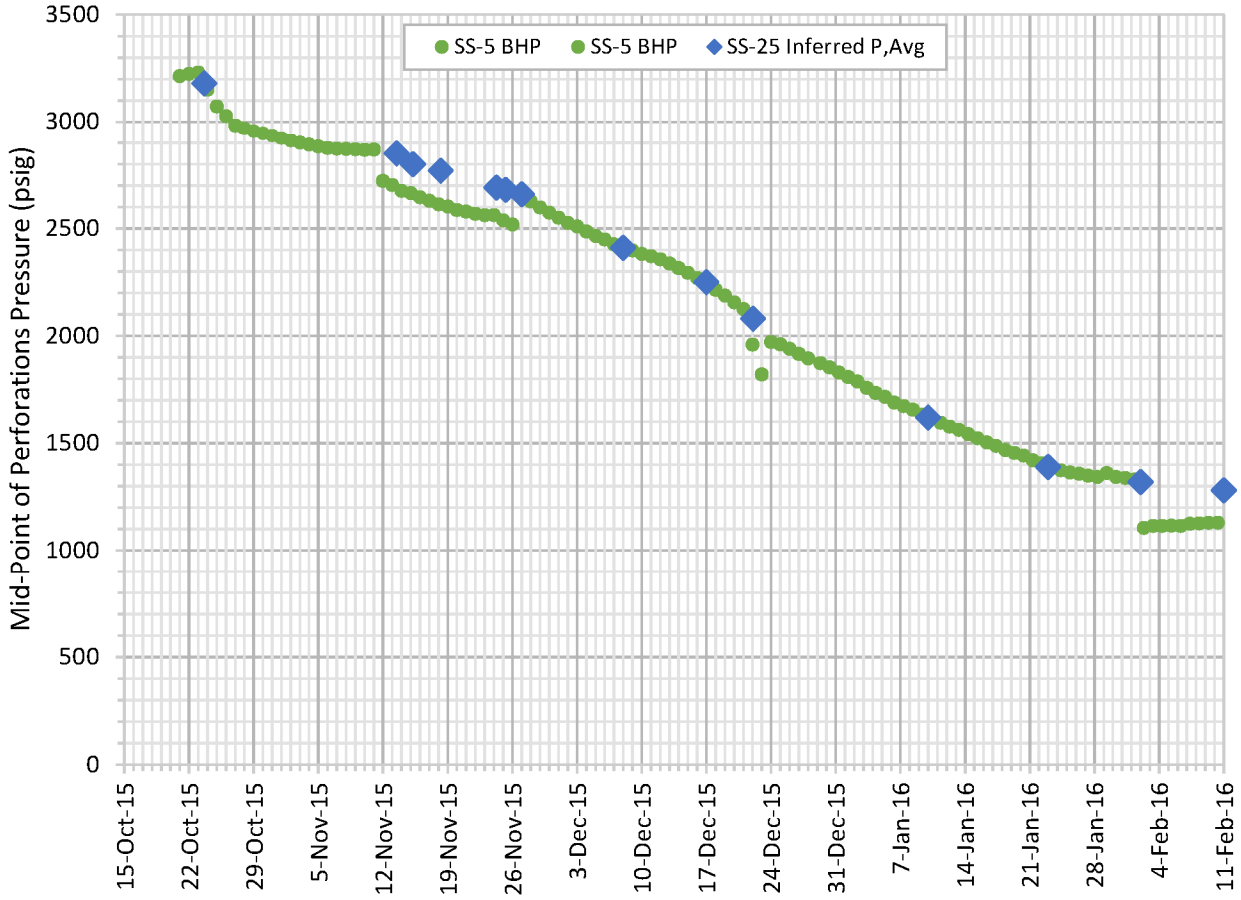

Figure 24: SS-25 Average Reservoir Pressures from SS-5 Pressures

The measured pressure drops at the two date periods in Figure 24 due to gas withdrawal from the SS-5 well. At these times, the reservoir pressure is estimated to follow the overall trend of the data during no withdrawal.

During the kill procedures, the pressures and rates in the tubing and production casing are not stable. This study attempts to determine the rates at times other than during the kill. Figure 25 shows how the tubing and production casing pressures vary during the leak and kills. (Kill attempt #4 occurred on November 18, kill attempt #5 occurred on November 24, and kill attempt #6 occurred on November 25, 2015.)

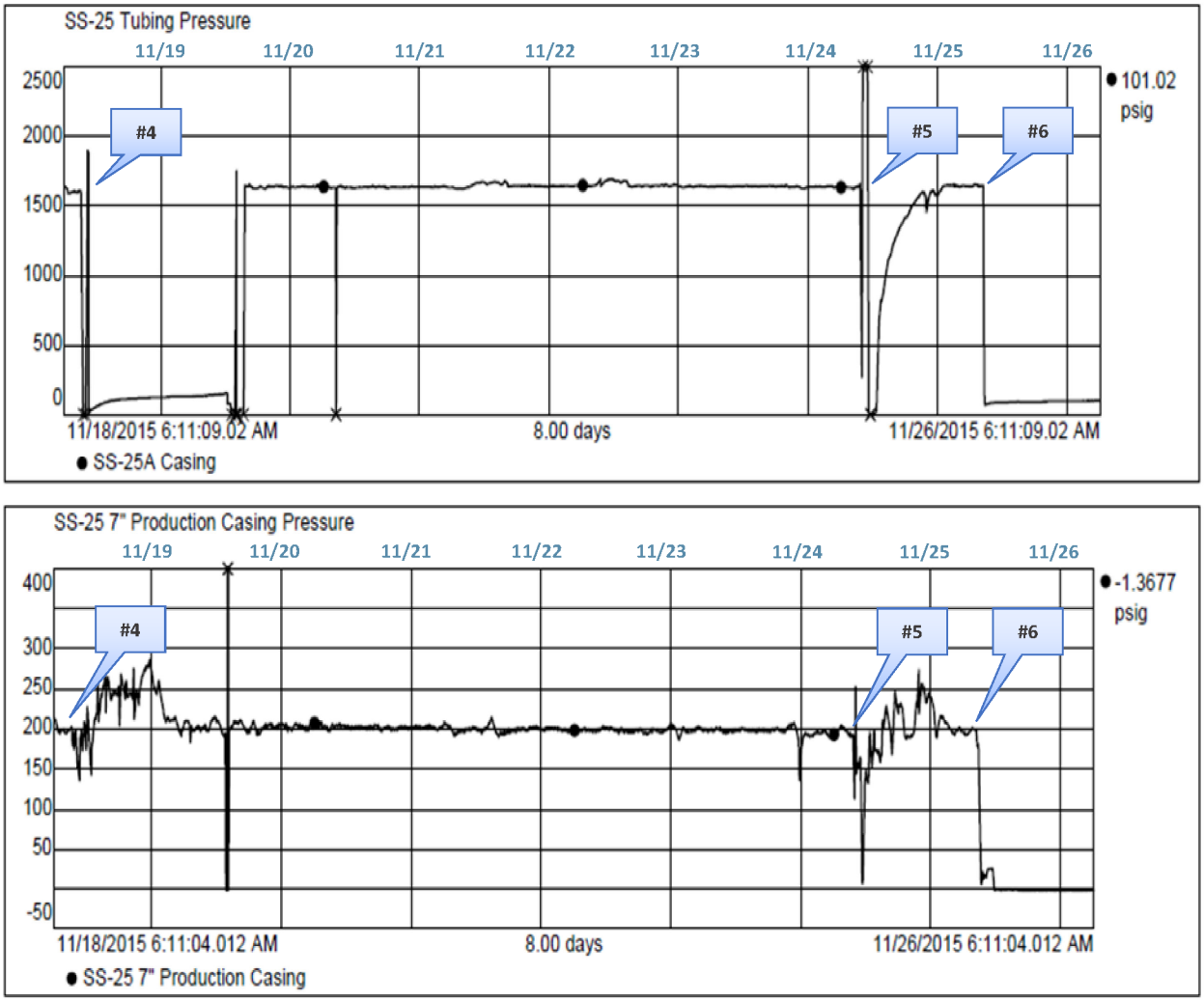

Figure 25: SS-25 Select Pressure Time Strip Chart

The tubing pressure clearly drops during kills #4 and #5, and the corresponding production casing pressures show unstable pressure responses. The lines broke during kill #6, and, as a result, the pressure recordings ceased. The rates presented in this report do not represent what happened during the kills. Between kills, the back pressures in the tubing and production casing are stable. These stable pressures are the ones used to estimate rates. The overall time length of the kills was comparatively short, and it does not significantly affect the estimate of the total volume leaked.

6.2 A-Annulus Leak Point: Best Estimate Formulation

Using the PROSPER model with the measured tubing head, measured casing head, and estimated reservoir pressures, the rates were estimated at the 7 in. × 2 7/8 in. annulus (A-annulus) casing leak-point inlet (Figure 23) before exiting into the 11 3/4 in. × 7 in. annulus (B-annulus) casing. Table 11 summarizes the leak estimates primarily at the key points.

Table 11: SS-25 A-Annulus Leak Inlet Conditions at Key Points

Kill Point	Date	Time	Leak-Point Inlet Pressure (psig)	Leak-Point Inlet Temperature Estimate (°F)	Leak-Point Flow Rate Estimate (MMscf/D)
–	October 15, 2015	00:00	–	–	–
1	October 23, 2015	16:00	276	21	93
2	November 13, 2015	11:15	258	30	82
3	November 15, 2015	06:00	222	29	81
4	November 18, 2015	06:00	204	30	80
5	November 24, 2015	06:30	204	32	77
6	November 25, 2015	06:30	204	32	77
–	November 27, 2015	00:00	205	34	76
–	December 08, 2015	00:00	205	40	68
–	December 17, 2015	00:00	205	48	63
7	December 22, 2015	01:00	205	54	57
–	January 10, 2016	00:00	205	72	42
–	January 23, 2016	00:00	205	81	34
–	February 02, 2016	00:00	205	83	32
–	February 11, 2016	00:00	205	85	31

The best-estimate rates were formulated based on uncertainty analysis at these key-point best estimates. This includes uncertainties in:

- Heat transfer coefficient
- Pipe roughness

The objective was to determine best-estimate values for the inputs that matched the majority of the data the best. An exact determination is not possible with available data. The determination includes, at the A-annulus leak point:

- Flowing conditions from tubing head pressures.
- Flowing conditions from Kill #1 to Kill #2.
- The complete best estimate of flowing conditions.

The best estimates of the leak-point inlet conditions of the production casing are later used to study the leak continuing into the surface casing, out into the ground, and finally into the atmosphere. A third-party took atmospheric measurements during the leak that are used for comparison.

6.2.1 A-Annulus Leak Point: Heat Transfer Coefficient Uncertainty

At conditions just before the first kill attempt, the gas cools from isenthalpic expansion at bottomhole and continues to cool from expansion as it flows up the hole. The overall heat transfer coefficient controls how the gas exchanges heat with the ground. Figure 26 shows the best-estimate temperature profile at the first kill point and a normal withdrawal temperature profile compared to the geothermal gradient.

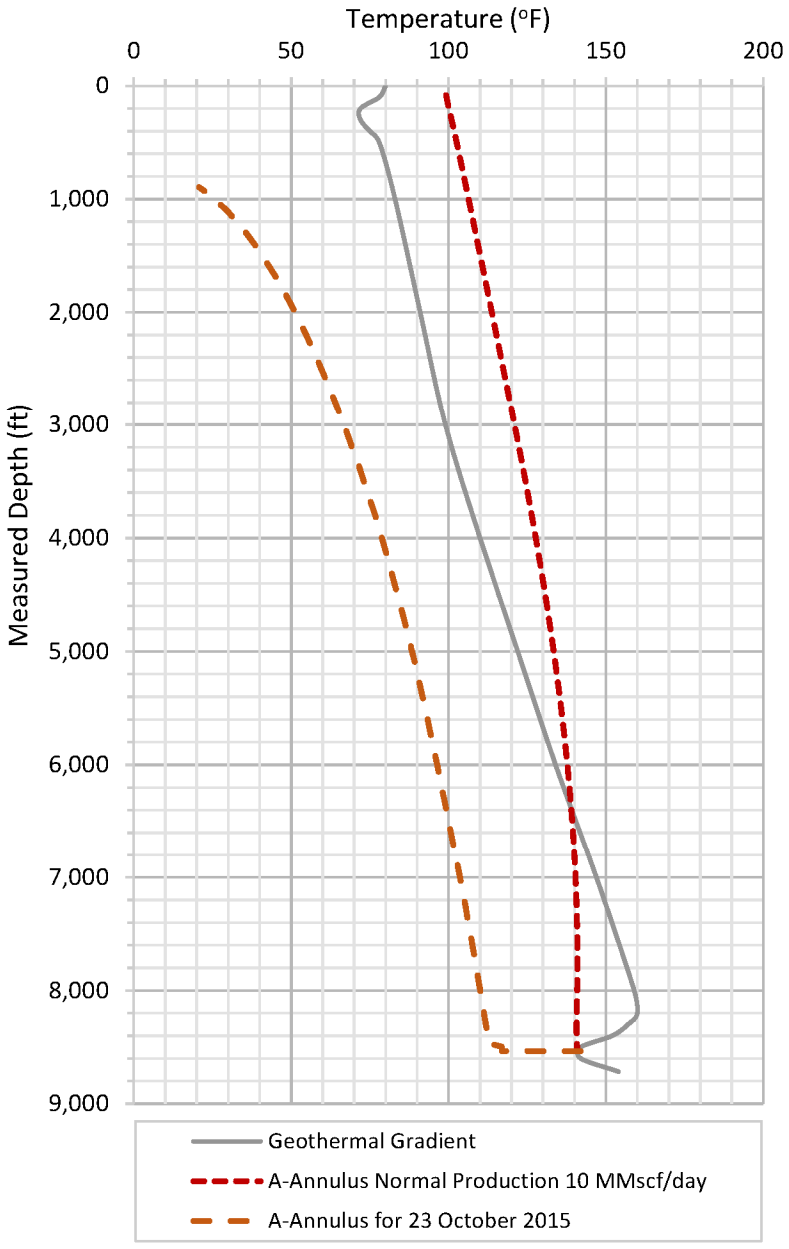

Figure 26: SS-25 Temperature Gradients with Withdrawal

The cooling during the leak has a greater temperature difference from the geothermal gradient than the normal flowing conditions; cold temperatures would not occur during normal flow. The heat transfer coefficient is of greater importance than would be determined during a withdrawal well test.

The heat transfer coefficients for this well are not known, and the rule of thumb for dry and wet gas is to assume 1 to 3 BTU/(hr-ft^2-°F). The well model is such that heat transfer is determined along the wellbore bottom to top, and a constant heat transfer coefficient is used as an average. Table 12 shows how the heat transfer coefficients affect the estimations.

Table 12: SS-25 A-Annulus Leak Inlet Conditions by Heat Transfer Coefficient

Heat Transfer Coefficient Assumed BTU/(hr-ft^2-°F)	Leak-Point Inlet Pressure Measured (psig)	Leak-Point Inlet Temperature Estimated (°F)	Leak-Point Flow Rate Estimated (MMscf/D)
10	276	37	93.0
3	276	21	93.4
1	276	16	93.5
0	276	12	93.6

The likely heat transfer coefficients have minimal effect on the rate estimate but do have an effect on the temperature estimate. The rule of thumb for the coefficient assumes flow up the tubing with an annular buffer in the heat transfer path, but in this case, the gas is flowing up the annulus and has a more direct heat transfer path with the formation; this would result in a heat transfer coefficient on the high side. Therefore, this study assumed a heat transfer coefficient of 3 BTU/(hr-ft^2-°F). This yields slightly lower rates and gives temperature estimates that are on the high side; actual temperatures could be lower.

6.2.2 A-Annulus Leak Point: Pipe Roughness Uncertainty

Previously, this study discussed an appropriate pipe roughness based on corrosion, and, given its importance at leak-rate conditions, it is important to investigate the ramifications of the uncertainty in the pipe roughness. It is normally matched by having wellhead and downhole pressure and temperature measurements and modeling only the outflow. Pipe roughness could not be uniquely matched because only wellhead measurements were available and so the outflow cannot be separated from the inflow. During normal injection and withdrawal, the rates were significantly lower than the well's maximum discharge rate, and at the low rates the friction was not significant compared to gravity. Even if downhole measurements were taken during normal flow, it would still be difficult to solve for pipe roughness because the friction contribution in the annulus was always significantly lower than gravity contribution. The frictional contribution grows at the high leak rates during the leak, and the friction caused by pipe roughness becomes dominant.

It was necessary to consider a range of pipe roughness. The least roughness was when the pipe was new, and the most roughness could have been if the pipe were badly corroded; neither cases were likely to have occurred, but this gave us best-estimate limits. Table 13 lists the rate values for this range of pipe roughness.

Table 13: SS-25 Leak-Rates by Pipe Roughness at Key Points

Kill Point	Date and Time		Elapsed Time (days)	Flow Rate A-Annulus Badly Corroded ρ=0.03[a] (MMscf/D)	Flow Rate A-Annulus Assumed ρ=0.0072 (MMscf/D)	Flow Rate A-Annulus New Pipe ρ=0.001 (MMscf/D)	Flow Rate Via Tubing Head Pressure (MMscf/D)
–	15-Oct-2015	00:00	–	–	–	–	–
1	23-Oct-2015	16:00	0.00	83	93	102	100
2	13-Nov-2015	11:15	20.80	73	82	91	87
3	15-Nov-2015	06:00	22.58	72	81	89	77
4	18-Nov-2015	06:00	25.58	71	80	88	76
5	24-Nov-2015	06:30	31.60	69	77	85	67
6	25-Nov-2015	06:30	32.60	69	77	85	65
–	27-Nov-2015	00:00	34.33	68	76	84	68
–	08-Dec-2015	00:00	45.33	61	68	74	54
–	17-Dec-2015	00:00	54.33	56	63	69	58
7	22-Dec-2015	01:00	59.38	51	57	62	52
–	10-Jan-2016	00:00	78.33	38	42	45	44
–	23-Jan-2016	00:00	91.33	31	34	37	40
–	02-Feb-2016	00:00	101.33	29	32	34	36
–	11-Feb-2016	00:00	110.33	28	31	33	33

[a] ρ = Pipe (tubing and casing) Roughness, inches

The new pipe roughness gave an upper limit estimate of the flow, because after all the years of service of the SS-25 well, it was likely that the roughness was higher and the flow, lower. Likewise, the badly corroded pipe roughness gave a lower-limit estimate of the flow because the piping pulled out after the leak had not been badly corroded. Specifying a roughness for the production casing required a specific roughness in the surface casing to match pressures. The roughness for the limits of the production casing was chosen in such a way that a reasonable roughness was determined for the surface casing. (For example, the production casing annulus was known to be in better condition than the surface casing annulus). The best-estimate-assumed roughness was based on corrosion studies with possible minimal scaling and gave the best-estimate rates.

6.2.3 A-Annulus Leak Point: Flowing Conditions from Tubing Head Pressures

The reported wellhead pressures were used to estimate rates. First, the bottomhole pressures were estimated under the assumptions of a gas gradient in the tubing, and the same temperature gradient was estimated as the gas flowed in the production annulus. Second, using the IPR model, rates were estimated at the assumed reservoir pressures. These rate estimates had an insignificant dependence on the piping roughness because the tubing was static and nearly reached the reservoir. These rate estimates were compared to the annulus estimated rates from new to badly corroded pipe to determine the best fit pipe roughness. Figure 27 charts the rates based on the tubing head pressures and annulus head pressures for the range of piping roughness.

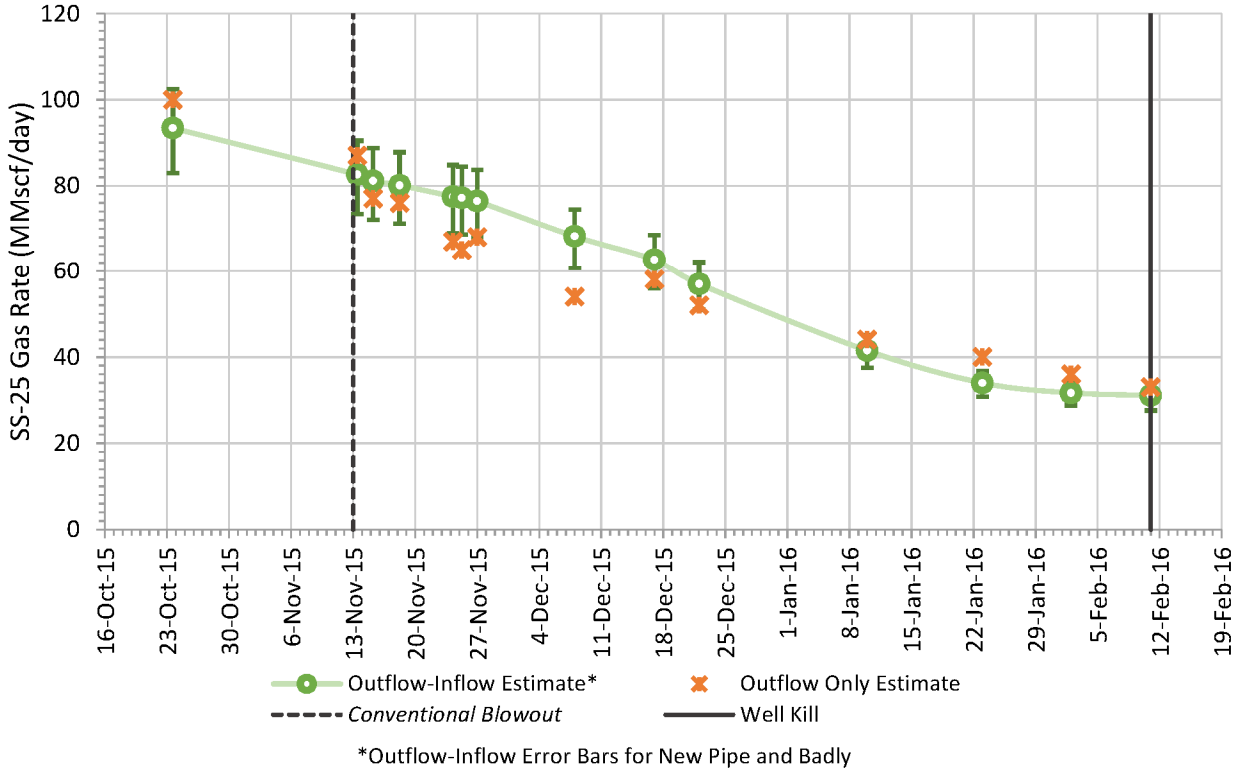

Figure 27: SS-25 Leak-Rates by A-Annulus and by Tubing Conditions

At the higher rates, the pipe roughness was quite relevant, and the range of possible rates was largest. At the lower rates, the pipe roughness was less significant, and the range of possible rates was the smallest of all rate estimates. The tubing-based estimates varied from less than the badly corroded rates to greater than the new pipe rates. The tubing estimates were too varied to yield inferences on the pipe roughness. The assumed roughness was an average comparison case to the tubing-based rate estimates.

6.2.4 A-Annulus Leak Point: Flowing Conditions from Kill #1 to Kill #2

Kill #1 led to a plug in the tubing and an uncertain plug state in the A-annulus, which led to uncertainty in estimating the leak-point rates, pressures, and temperatures. Between Kill #1 on October 23, 2015, and Kill #2 on November 13, 2015, there were full and partial plugs in the tubing and A-annulus that prevented hydraulic communication between the wellhead and the reservoir. On November 13, 2015, the well appeared to blow out in a *conventional* way and rate prediction was more stable. Table 14

summarizes this time period and indicates when the production (A) or surface (B) casing head pressure was used.

Table 14: SS-25 Leak-Point Conditions from Kill #1 to Kill #2

Date	A-CHP (psig)	B-CHP (psig)	Description	Wellhead-Reservoir	P-Res (psig)	A-LPIP (°F)	A-LPIT (°F)	Flow Rate (MMscf/D)
23-Oct-15	270		Discovery	Connected	3,180	276	21	93.4
24-Oct-15	290		Kill #1	Connected	3,152	296	23	92.4
25-Oct-15	401		No work	Connected	3,072	406	34	89.0
26-Oct-15	416		Flowed	Connected	3,028	421	35	87.5
27-Oct-15	308		Flowed	Connected	2,984	313	30	86.7
28-Oct-15	109		Bled—no pressure recharge	No connection	2,970	X	X	X
29-Oct-15	→	770	Bled—pressure recharge/loss	Obscured, yet likely connection	2,956	811	60	80.6
30-Oct-15	→	771	No work	Connected	2,946	815	61	80.2
31-Oct-15	→	727	No work	Connected	2,935	770	59	80.5
01-Nov-15	694		No work	Connected	2,923	699	55	81.2
02-Nov-15	659		No work	Connected	2,911	664	54	81.1
03-Nov-15	645		No work	Connected	2,902	649	53	81.0
04-Nov-15	523		No work	Connected	2,892	528	46	82.0
05-Nov-15	551		No work	Connected	2,883	556	48	81.4
06-Nov-15	305		Glycol down tubing - unplugged	Connected	2,876	310	33	83.2
07-Nov-15	217		No work	Connected	2,873	222	27	83.5
08-Nov-15	212		No work	Connected	2,871	217	26	83.5
09-Nov-15	218		No work	Connected	2,869	223	27	83.4
10-Nov-15	211		No work	Connected	2,867	216	27	83.3
11-Nov-15	227		Flowed	Connected	2,868	232	28	83.2
12-Nov-15	249		No work	Connected	2,865	254	30	82.9
13-Nov-15	229		Kill #2—well blew out in conventional sense	Connected	2,850	234	30	82.6

A-CHP = A-annulus Casing Head Pressure
B-CHP = B-annulus Casing Head Pressure
P-Res = Pressure of reservoir
A-LPIP = A-annulus Leak-Point Inlet Pressure
A-LPIT = A-annulus Leak-Point Inlet Temperature

→ A-annulus likely not in pressure communication with the reservoir; B-annulus pressures used. The field reports indicate that the A-annulus flowed several times with low rates and recharged after being bled down, indicating hydraulic communication to the leak point.

Kill attempt #1 formed plug(s) that prevented further kill attempts, and the plug(s) remained until removal on November 06, 2015. While the plug(s) were in place, the back pressure at the leak point increased. This suggests that the path in which the gas had been flowing was blocked, perhaps initially, by rapid ice formation from the kill fluids. There were reports of ice in the surface fractures, implying that the gas had to find a new flow path that would have a greater back-pressure. If the casings were not partially plugged, there could have been warmer gas around the tubing for nearly two weeks, and this could have melted an ice plug in the tubing. Since the plug remained, it may have required the warm gas to be diverted; or, additional plugging may have occurred from the growth of gas hydrates during the four to five days when the temperature was below freezing and the ice plug remained. The plug(s) that formed during the first kill partially reduced the leak rate, although not as significantly at the surface as reported in on-site logs. The temperature of interest was in the surface casing annulus at the depth of the plug.

6.2.5 A-Annulus Leak Point: Complete Best Estimate of Flowing Conditions

Figure 28 shows the full best-estimate flow rates and temperatures for the whole history of the leak post-injection shutoff. The plugging caused at kill #1 reduced the rate by approximately 10%. The *conventional* uncontrolled leak began at kill #2, and after this time, the rates, pressures, and temperatures followed a predictable trend.

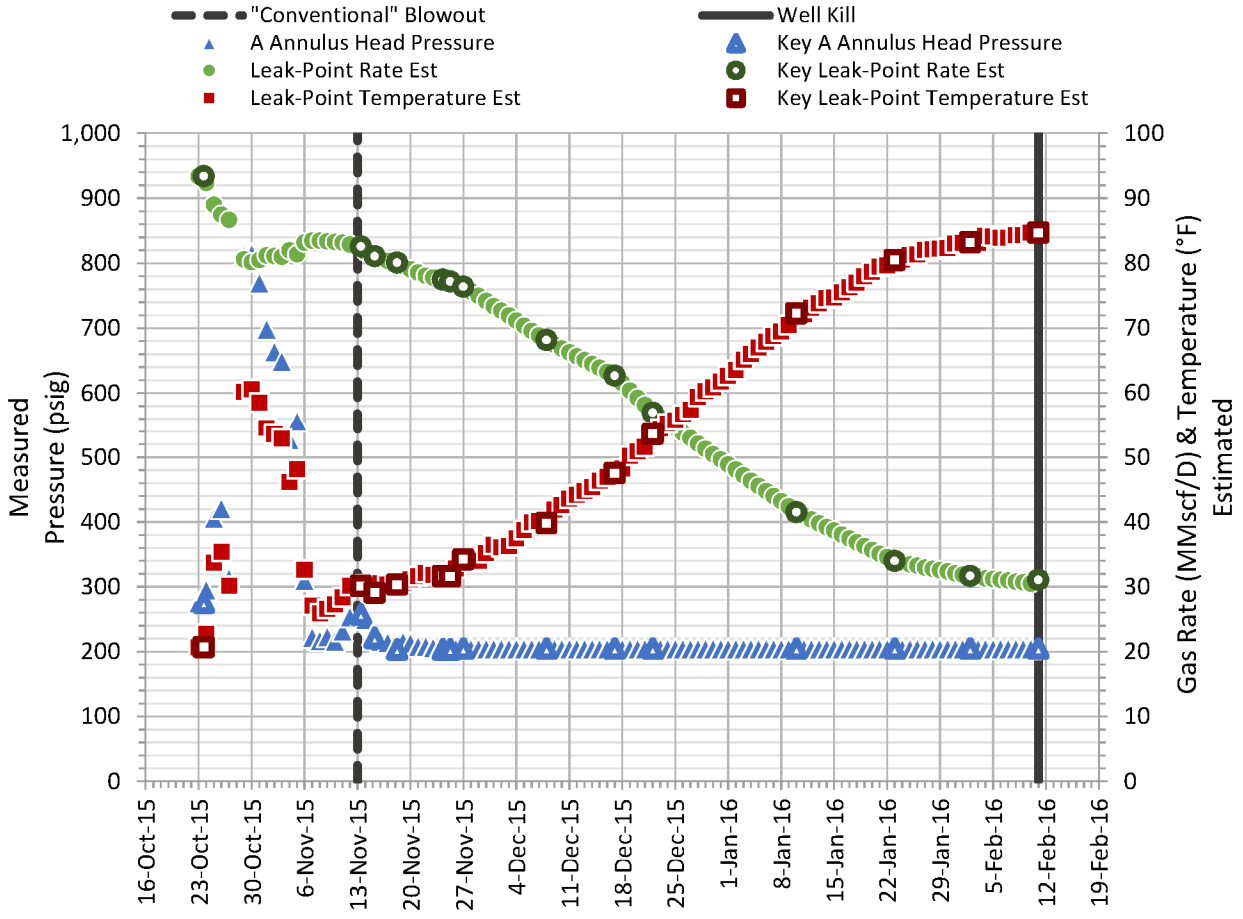

Figure 28: SS-25 A-Annulus Leak Point Flowing Conditions

Figure 29 and Figure 30 show the best-estimate range of flow rates and cumulative volume leaked, respectively. Both figures have sensitivities to pipe roughness for the leak history post-injection shutoff. The pipe was not new, and the new pipe estimate represented an upper limit for the flow. The pipe was not badly corroded either, and this estimate represented a lower limit for the flow.

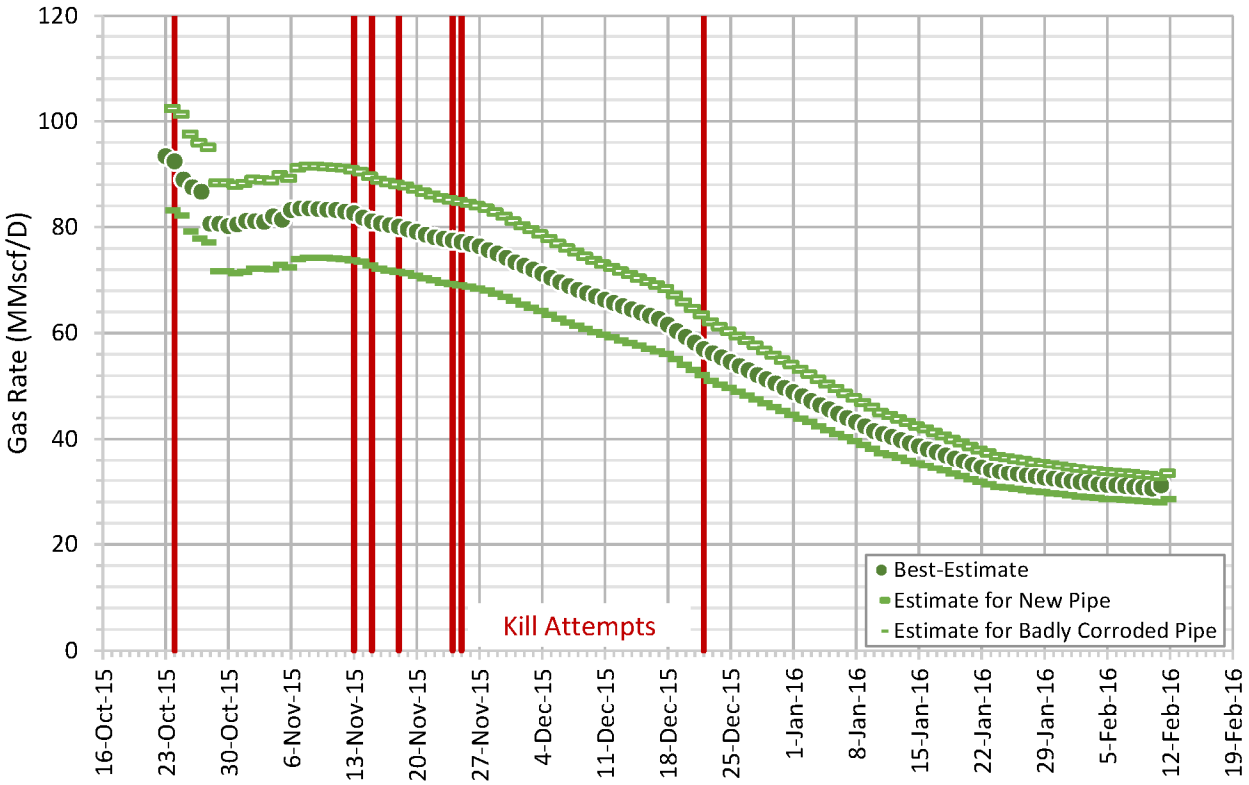

Figure 29: SS-25 Estimated Leak History—Rates

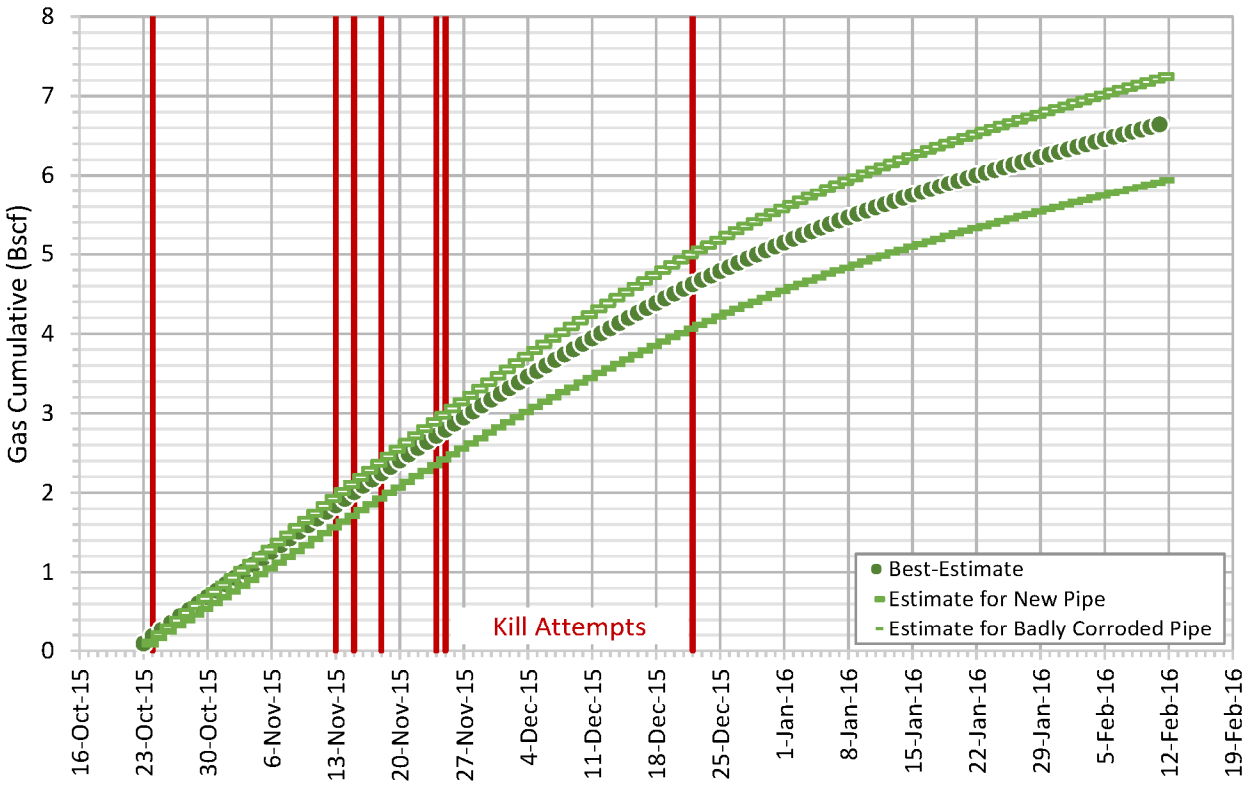

Figure 30: SS-25 Estimated Leak History—Cumulative Volume

The leak cumulative was calculated for each case:

- For the best estimate, the cumulative leak was 6.6 BSCF, and that equates to 120,000 metric tons of CH_4, 11,000 metric tons of other hydrocarbons, and 2,900 metric tons of CO_2.
- If the pipe was new, the cumulative leak was 7.2 BSCF, and that equates to 131,000 metric tons of CH_4, 12,000 metric tons of other hydrocarbons, and 3,200 metric tons of CO_2.
- If the pipe was badly corroded, the cumulative leak was 5.9 BSCF, and that equates to 107,000 metric tons of CH_4, 9,800 metric tons of other hydrocarbons, and 2,600 metric tons of CO_2.

Figure 31 shows the best-estimate rates along with total Aliso Canyon field rates.

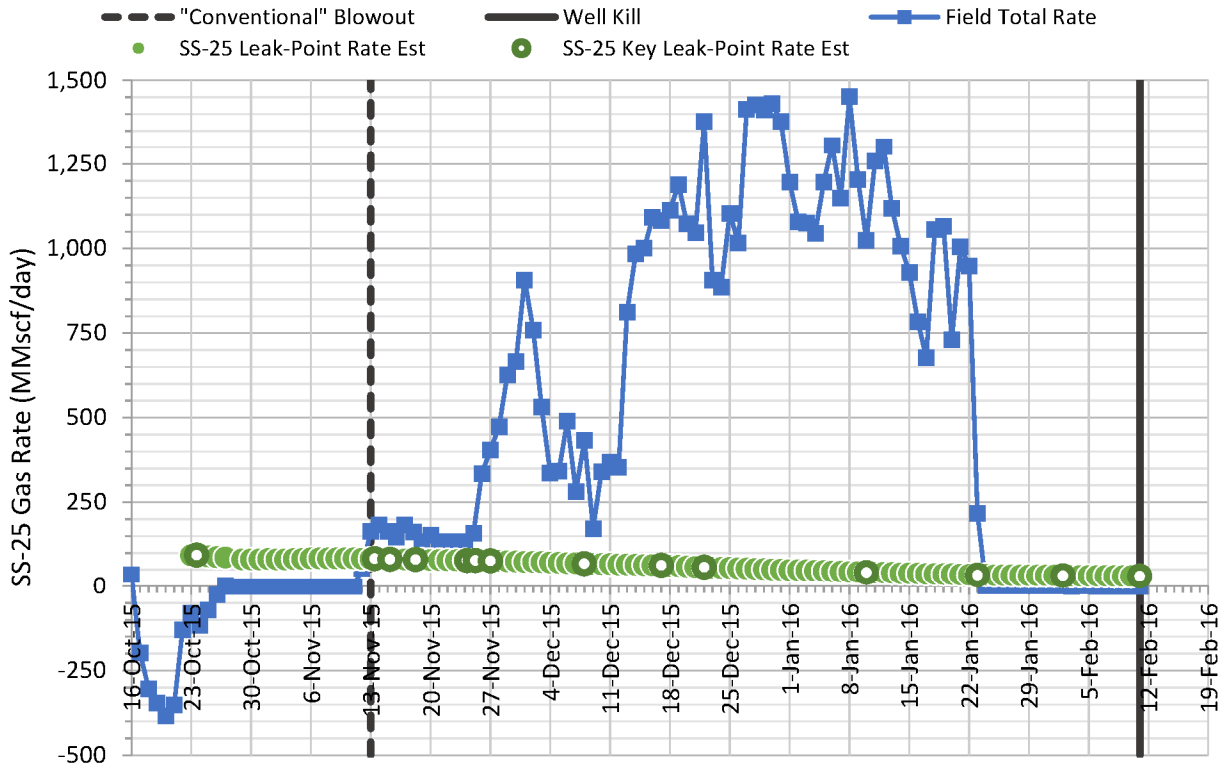

Figure 31: SS-25 Estimated Leak History Compared to Measured Field Gas Rates

More gas leaked than what was injected into the SS-25 well, which implies that the field was well connected, and the well flowed back gas injected through other wells. The decline rate of the SS-25 leak withdrawal followed the total magnitude of withdrawal from the field. That is, when the field rate was the highest, the decline rate of the well was the highest, and when the field was shut in, there was less rate decline for the well.

6.3 B-Annulus Leak Points: Best Estimate of Conditions

The leaked-gas flow continued from the A-annulus leak point out the production casing, parting into the B-annulus of the surface casing, out the surface casing holes, into the ground (Figure 23), and eventually to the atmosphere. After the production casing was pulled from the well, a caliper log was run for the surface casing. The caliper log revealed that the surface casing had a significant number of holes. Initially, two holes were photographed to understand the nature of the holes, and their sizes were estimated. Later, holes up to 190 ft MD were photographed and their sizes estimated. The remainder of the holes were not photographed, and their sizes remained undetermined.

For the gas that flowed to the A-annulus leak point, this study analyzed whether the holes were sufficient to leak all gas or if a casing shoe leak was required. In this analysis, all measured surface tubing pressures, production casing pressures, and surface casing pressures were matched. The matching indicated that the surface casing holes were sufficient and necessary to leak all gas, as there was not enough pressure to leak out the casing shoe. Only when the tubing was plugged was there enough uncertainty in the flow path and pressure for a possible casing shoe leak.

The following summarizes the building of a surface-casing holes model that matched available valid data. This study presumed:

- The production casing failed prior to the injection being shut off; the parting was of such size that there was not significant pressure drop from the A-annulus into the B-annulus.
- Sufficient holes in the surface casing were formed prior to the injection being shut off. If too few holes existed at the time of injection shutoff, all gas would have exited the shoe (below the production casing leak point), and the production casing and surface casing would have measured equivalent pressures. However, the surface casing pressure was significantly lower, which indicated flow above the leak point in the surface casing—that is, surface casing hole(s) must have been open.
- The formation was highly fractured at the depth of the holes indicated by the caliper logs. The fractures could have temporarily held water from rain or fluid from well work, but at the time of injection shutoff, it was presumed that these fractures were empty and at a pressure using an air-gradient. The exact gradient was not important because the choke holes were at critical flow, and the critical pressure was significantly greater than the air-gradient. This means that the rate estimate per hole was not affected by the back pressure.
- The surface casing annulus was moderately to badly corroded with possible scale. Physical inspection of the production casing after it was pulled did reveal the presence of significantly greater roughness on the outside (B-annulus side) than on the inside (A-annulus side). The piping roughness used was a singular value of 0.016 in—an average between moderately and badly corroded and about twice the roughness used for the production casing roughness.

The following steps were involved in solving for surface casing annular flow:

1. A surface casing holes model was built based on caliper logs and borehole photographs.
2. The best estimate was used of the production casing leak-point rate, pressure, and temperature predictions (presented in section 6.2.5) as inlet conditions and flow through B-annulus using a Petroleum Experts PROSPER model with the gradient and choke calculations.

6.3.1 B-Annulus Leak-Points Model

Figure 32 and Figure 33 show the holes with area measurements at two depths [13] [14]. The hole area at 145 ft is equivalent to a circular area of 1.88 in. in diameter, and the hole area at 180 ft is equivalent to a circular area of 3.23 in. in diameter.

Figure 32: SS-25 Surface Casing Hole at 145 ft MD

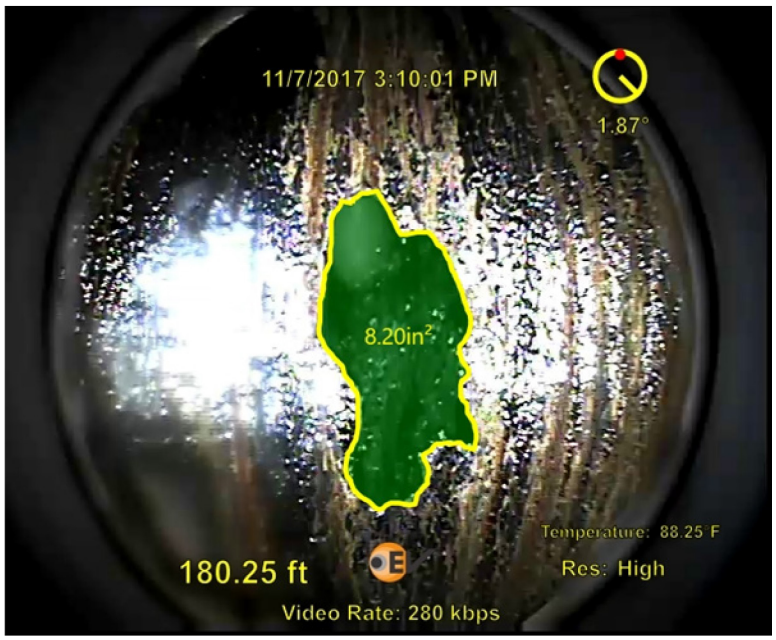

Figure 33: SS-25 Surface Casing Hole at 180 ft MD

Table 15 summarizes the resulting surface casing leak-hole model from the initial and final hole-size estimates. The holes from 230–300 were not photographed and measured because of fluid clarity, and the area of the holes at these depths was approximated based on the caliper response compared to measured holes.

Table 15: SS-25 B-Annulus Holes Summary

Depth Range (ft)		Area (in^2)
0	133	0
133	134	0.33
145	147	5.74
158	158	0.65
163	164	15.06
166	169	5.99
178	181	15.77
190	190	2.33
230	300	*2.00**
300	895	0

*Approximated based on caliper

A requirement of the leak model was that at all points in time; the size of the holes was such that all gas could leak out the holes. However, not all holes had to be available at injection shut-in. It is also possible that there were more holes and more area than shown in Table 15 available for leakage, but the above represents the minimum area that had to be open for gas to fully leak at all points in time. The model assumed there was no leak in the shoe and verified that there were sufficient holes to explain the leak.

The location of the surface casing holes was such that they opened into the fractured ground, and the flow would have been in the fractures and not in the formation itself—the path of least resistance. As the gas continued to leak into the fractures, it is possible that ice or hydrates could have formed from the water used in the kill attempts. This ice or hydrates would then have blocked flow down some fractures and thereby forced gas into other fractures. At those times when the gas leak appeared to diminish at the surface, it is likely that the gas was leaking away into a different set of fractures. It is acceptable for holes to be blocked by ice or hydrates as not all holes are required to be open at all times to leak all of the gas flow.

The shoe, at 990 ft, would have opened up into the unconsolidated Topanga sands, which are rich with clay and below the Basalt (a geologic barrier). Gas leaking into this zone would require a higher back pressure than it would require into a fractured zone (that is, the path of least resistance is out the holes in the surface casing). If the surface casing cement were damaged, it would have provided a path of less resistance for any gas to leak out the shoe and up along the surface casing. The path followed depended on the pressure of the leaked gas, and this model estimated those pressures to compare against the measured pressures. Multiple flow paths were considered and only flow paths kept were those that matched the measured data.

When comparing the pressures of the production casing, A-annulus, surface casing, and B-Annulus, an insight was given into the leak path through the casing holes versus the casing shoe. Figure 34 shows the casing head pressures for SS-25.

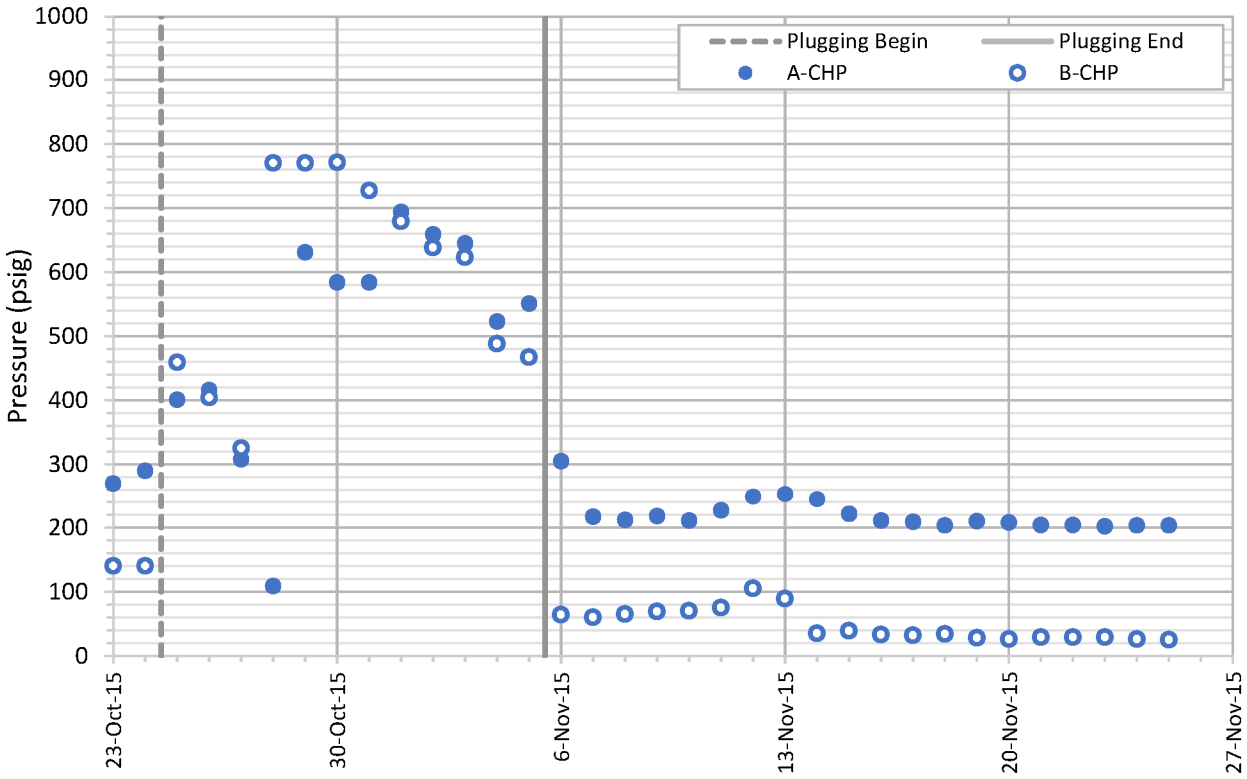

Figure 34: SS-25 A- and B-Annulus Casing Head Pressures

The following are inferences from the casing head pressure comparison:

- The casing holes existed at the beginning of the withdrawal leak. If all flow left out a casing shoe leak, the A- and B-annulus pressures would have been equivalent. The well nodal-analysis model showed that all flow left through casing holes in order to match the B-annulus casing head pressure. That is, the pressure could not have been matched with any degree of a casing shoe leak. Therefore, the estimate of rates held the assumption of no casing shoe leak at the beginning.
- From beginning to end of the plugging, the certainty of the flow path was obscured based on the relationship between the A- and B-annulus pressures. From a hydraulics standpoint, the A-annulus pressure should have always been greater than or equal to the B-annulus pressure. Also, because of the uncertainty in the pressures, the model could neither confirm nor deny a casing shoe leak. The adjustments to pressures during the plugged period for rate estimates were for:
  - Pressures not used on October 28, 2015—no rate estimate made
  - B-annulus rather than A-annulus pressures used on October 29–31, 2015, for rate estimate
- After the plugging was cleared, the hydraulic model returned to conditions akin to before plugging; a casing shoe leak was not supported.
- Since before and after the plugging indicated no casing shoe leak, the surface casing modeling assumed no casing shoe leak during the plugging; this did not affect the leak rate estimate.

6.3.2 B-Annulus Leak-Points Estimates

The procedure to estimate the leak in the surface casing for each day:

1. Used the A-annulus leak-point estimates for rate, pressure, and temperature in section 6.2.5 (results were at inlet conditions to the production casing leak).
2. Estimated pressure and temperature changes flowing from the inlet of the production casing leak in the A-annulus to the outlet of the production casing leak in the B-annulus. The hole was modeled as a choke, and the choke size was determined to fit the assumption of all gas leaking out the surface casing holes while best matching A-annulus and B-annulus pressure measurements. The leak was modeled as a 7 1/2 in. choke at all times. This determination supported the assumption that the production casing failed prior to injection shutoff. If casing had failed later, the pressure history would not have matched.
3. Solved for flow up the B-annulus from the A-annulus leak-point outlet to the first leak hole using the gradient calculation.
4. Solved for amount of gas flowing out the first leak hole using the choke calculation. The back pressure in the fractured ground was presumed to be a gas gradient. There could have been some water gradient, but the rate estimate would still not have changed because the critical pressure was always significantly larger.
5. Reduced gas flowing in annulus by the amount leaked, did gradient calculation to next leak-hole again, and did choke calculation again to determine the amount of gas leaked; this was repeated until no gas to flow was present.
6. Estimated surface pressure measurement of B-annulus assuming static gradient from last leak-hole having gas flow.

At times during the leak, it was evident that the freezing in the B-annulus and in the fractures in the ground occurred; therefore, identifying the holes that were open to flow could have been an issue. The holes began at 300 ft MD and extended upwards to 134 ft MD. The main flow-path-pressure drops were from the leak point at 892 ft MD to the first leak hole at 300 ft MD and across the leak holes into the formation. The pressure drop caused by flow from the first to last leak hole was comparatively less significant. That is, the exact depth of the holes open to flow was not that significant; rather, the significance was the total leak-hole area open to flow. As the flow rate paths froze from the initial plugging, the greater back pressure caused a lower flow rate, and the lowering of the area needed to leak off all the gas.

It was challenging to determine the pressures of the gas entering the atmosphere from the ground. The leak holes were at critical flow, and the pressure in the fractured ground was less than the pressure exiting the leak holes. This excess pressure would have flowed the gas through the ground and into the atmosphere. As back pressure built up in the ground from fluid leaked from the kill attempts, the excess pressure at the ground level would have disappeared. The leak rate did not diminish significantly as on-site reports indicated and as shown earlier in this report; rather, the mechanism of leaving the ground changed.

A well-fit model must match the surface casing head measured pressures with the estimated pressures. The complete process in determining the gas conditions leaving the well:

1. Started with the measured production casing pressure (A-annulus).

2. Used a PROSPER model to estimate the static gradient at the leak-point inlet in the production casing for conditions at the leak point. It was an iterative process with the next steps because temperatures were not measured and must be balanced.
3. Used a PROSPER model to estimate flowing gradient and inflow performance relationship to estimate bottomhole conditions and gas flow rate. The PROPER inflow and gradient calculations were used rather than the system calculation combinations of inflow and gradient. The system calculation was designed for normal flow conditions and did not calculate isenthalpic expansion temperatures at the perforations necessary for uncontrolled withdrawal conditions.
4. Used a choke model to flow gas from production casing across the failure of the production casing and into the surface casing. Multiple hole sizes were modeled until a hole size could be held constant during the entire leak.
5. Used a PROSPER model and the hole model with multiple flowing gradient and choke calculations for the leak holes to estimate the leak out the holes. This calculation was performed in steps as there was no built-in PROSPER calculation.
6. Used a PROSPER model to estimate static gradient from last hole leaked to top of surface casing for casing head conditions (B-annulus). The model estimated casing pressures and temperatures, but only pressure measurements were available to be matched against.

Figure 35 shows an excellent agreement between the measured and estimated B-annulus pressure and thereby supports the proposed wellbore model. The model matched measured data assuming the surface casing holes as measured with no casing shoe leak. Note that the estimated pressures were average daily conditions, and measured pressures at the wellhead were reported daily; with daily work occurring at the wellhead, the measured value was not always a stable value, and some discrepancy between the values is acceptable.

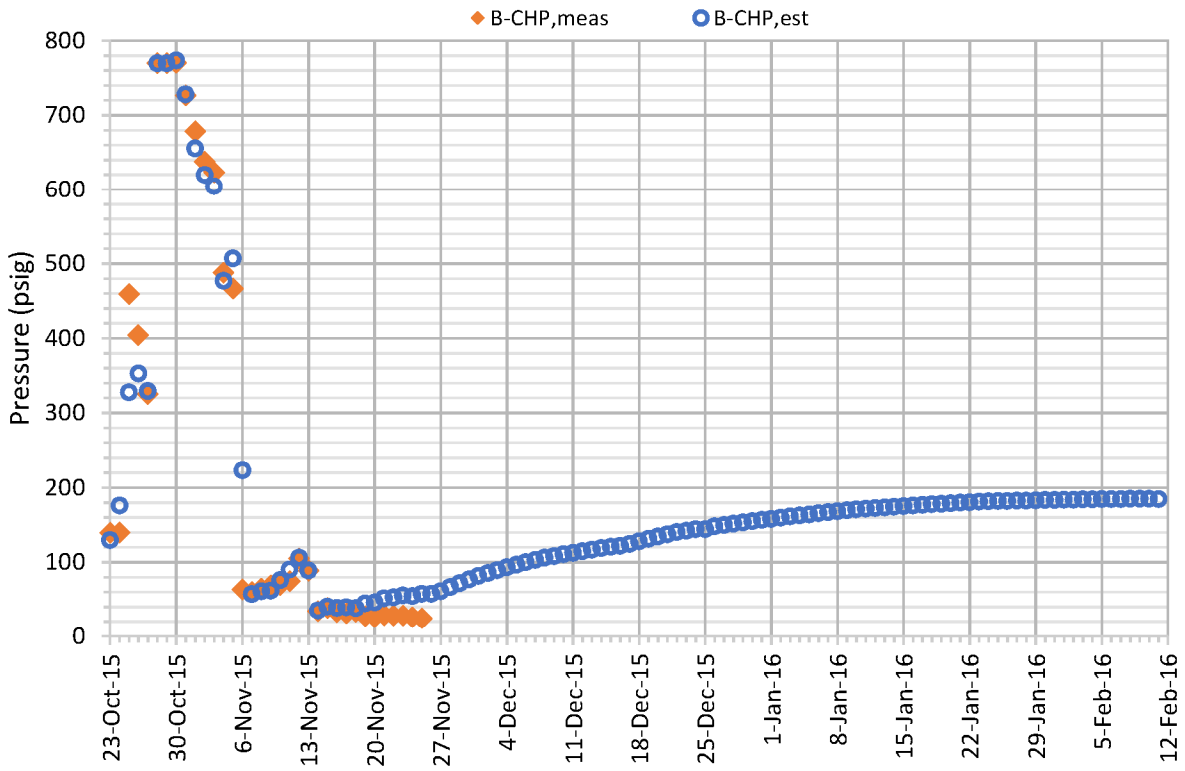

Figure 35: SS-25 B-Annulus Estimated Pressures compared to Measured Pressures

The balance in measured and estimated B-annulus pressure had some uncertainty owing to the uncertainty in the pipe roughness. The measured pressures of the withdrawal leak required flow up the B-annulus and out the holes in the surface casing, but depending on pipe roughness, it is possible that there was flow down in the direction of the shoe. Figure 36 shows that on October 23, 2015, as the pipe roughness increased up the annulus, flow could have been diverted down the annulus towards the shoe and beyond.

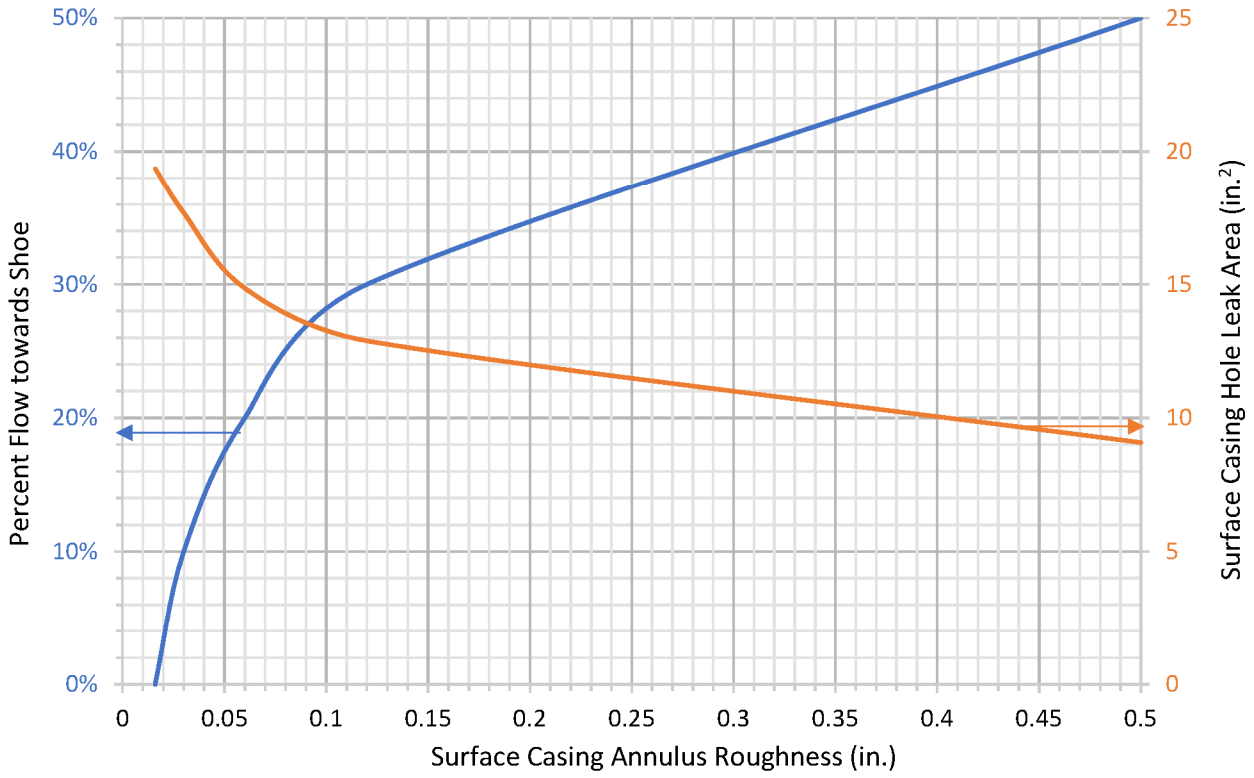

Figure 36: SS-25 Possible Flow towards Shoe on October 23, 2015

For a badly corroded pipe with a roughness of 0.03 in. and 0.06 in., approximately 10% and 20% of the flow, respectively, could have been diverted towards the shoe. The roughness required beyond this flow amount exceeded the roughness found during Blade's investigations.

Whether flow proceeded towards the shoe depended on the injectability of the formation below the shoe. A flow of 10%/9.3 MMscf/D at a formation pressure of 100 psi would have required either a matrix permeability thickness of approximately 20,000 md-ft or natural fractures that were open to flow. On October 28–30, 2015, when the pipe was plugged by ice/hydrates, a flow rate of 34 MMscf/D could have been injected for that level of permeability thickness. The low pressures require either a permeability thickness far in excess of the gas storage formation, which is approximately 3,600 md-ft, or natural fractures open to flow. There was enough uncertainty in the well modeling that a limited amount could have flowed down past the shoe, but whether this could have actually occurred would require geologic study.

Figure 37 shows the estimated B-annulus leak-point inlet temperature (B-LPIT) and outlet temperature (B-LPOT), assuming a 10 psig back pressure in the fractures, compared to the previously estimated A-annulus leak-point inlet temperatures (A-LPIT); it also shows the hydrate formation temperature at the plug-point (Hydrate-PPT).

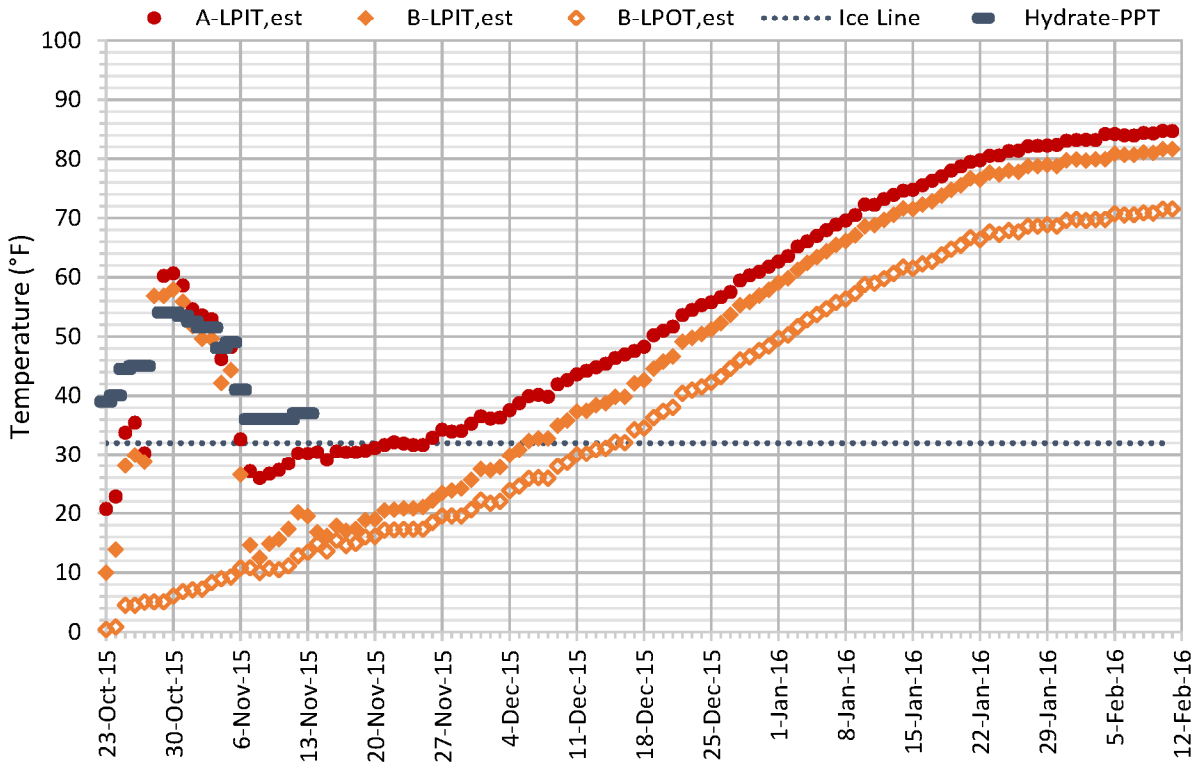

Figure 37: SS-25 Estimated Leak History—Temperatures

An average outlet temperature was reported—the outlet temperature into the ground from the bottom to the top B-annulus leak hole varied only by 0.5°F. This variance is within the accuracy of the methodology; it means that when holes are plugged by ice or hydrate, it is not necessary to know exactly which holes are plugged. The increased temperature of the gas in the A-annulus between October 23, 2015, and November 06, 2015, was caused by the increase in back pressure that resulted from freezing of the kill fluids in the piping and ground. Hydrate kinetics are such that the initial plugging would be ice and not hydrates. For several days after the plugging, hydrate formations existed, and a secondary hydrate formation could have occurred. Until the plugging was removed, the temperatures were well above the freezing point of ice but at the equilibrium point for hydrates. This suggests that the plug could have lasted if hydrates had formed after the initial ice plug. Finally, the temperature of the gas exiting the B-annulus into the ground was not as affected and would have remained below freezing until mid-December 2015.

Figure 38 shows an estimate of the total area of the holes that must be open for the gas to fully leak through the surface casing. Depending on the well flow, the flow out the surface casing leak holes and into the ground required differing amounts of holes to be open.

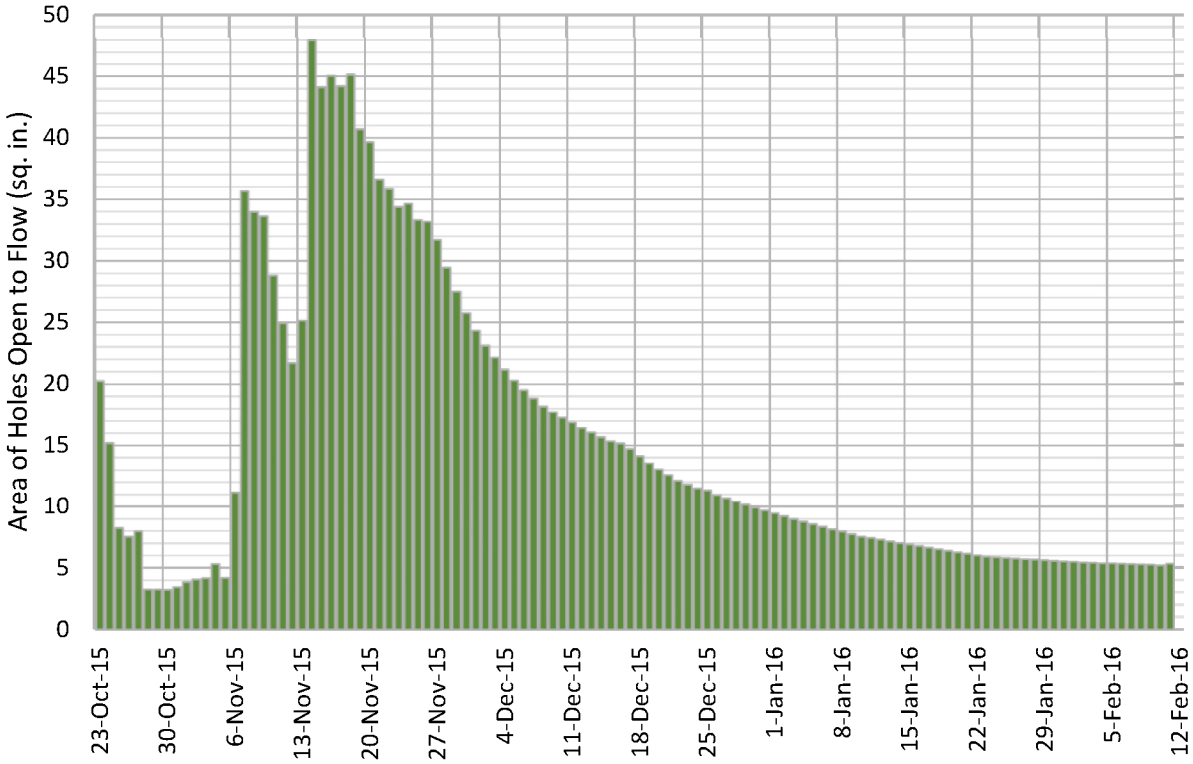

Figure 38: SS-25 Estimated Leak History—Open B-Annulus Holes

The change in area necessary to be open for flow can be explained by the well work:

- October 24, 2015—Kill #1: This kill attempt caused icing issues in the well and obstructed the flow. A smaller area of holes was made necessary as back-pressure increased and rate decreased.
- November 06, 2015—Glycol treatment for plug: The treatment removed the plug in the tubing and more area became open to flow.
- November 13, 2015—Kill attempt #2: Amount of leak-hole area open increased and *conventional* uncontrolled leak occurred.
- Remaining kill attempts #3, #4, #5, and #6: No significant effect on trend.

The surface casing model matched known occurrences and most importantly agreed with the total hole area of 46 $in.^2$ measured in the surface casing (Table 15). It is likely that the freezing blocked the majority of holes, which resulted in an increased back pressure but left enough holes open to leak all of the gas. More area than modeled would still leak all of the gas and not affect the model, while less area would imply the presence of a leak out the shoe. It is difficult to support a leaking out of the shoe given the estimated match and measured B-annulus pressures.

6.3.3 B-Annulus Leak-Points Break Points

The leak area in time shows three clear break points:

1. October 23, 2015, when the leak was first noticed. The initial area was uncertain and could be smaller but it is clear that not all holes in the surface casing were open at this time.
2. November 06, 2015, when the plug was removed from the tubing. Additional leak holes opened in the surface casing at this time.
3. November 13, 2015, when the *conventional* uncontrolled leak began. Additional leak holes opened in the surface casing at this time for the last time. The crater around the well was created at the opening of these additional holes.

The data used on October 23, 2015, were prior to any kill attempts, while the data used on October 24, 2015, were the stabilized data at the end of the day, following the first kill attempt. On October 23, 2015, a leak was noticed at the fittings at the wellhead, and this means that the previously calculated area for that day included the areas of both the surface casing holes and the fitting leak. The events on the October 23, 2015, can be used to infer the initial state of the surface casing holes because all points after that date are obscured by freezing of the kill fluid.

Figure 39 shows the area that would have been necessary in the surface casing to leak off gas that had not leaked at the wellhead, and the area of holes needed in the surface casing in the first week. All area estimates are less the first day when the fitting was leaking.

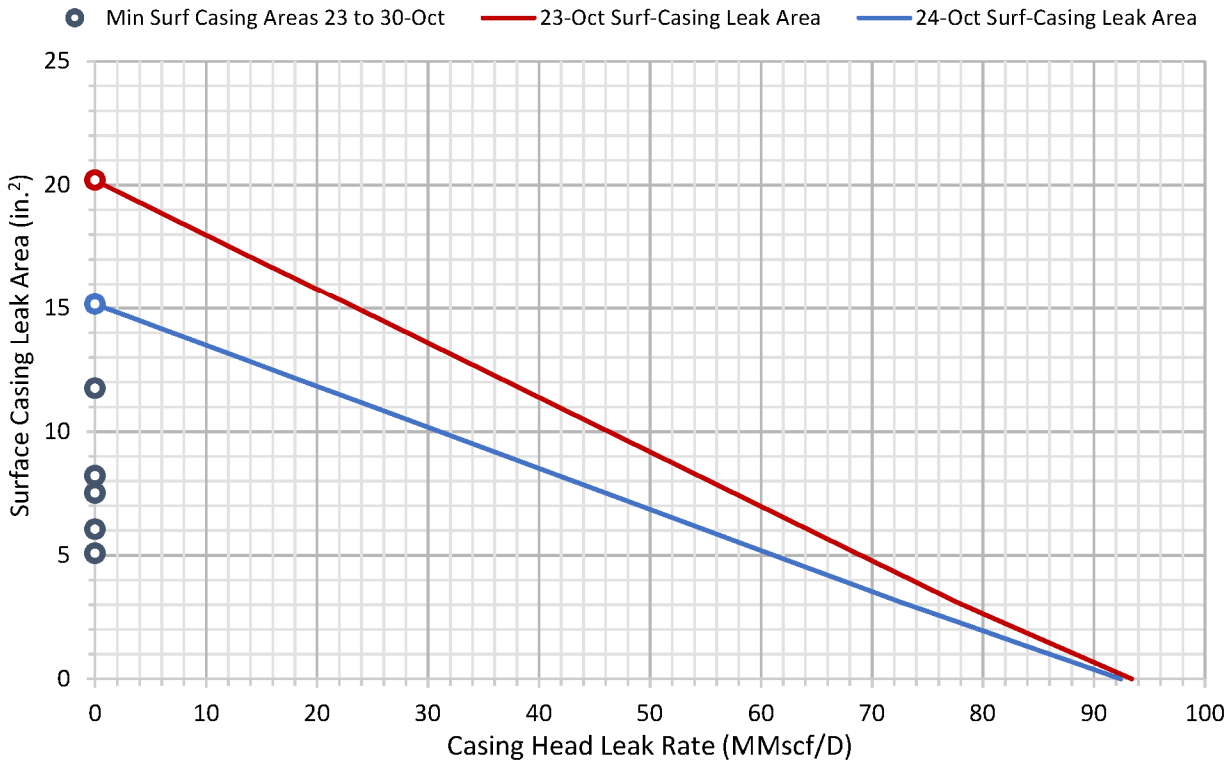

Figure 39: SS-25 Possible B-Annulus Casing Head Leak Rates

On October 23, 2015, if no leak occurred at the casing head, the leak area would have been 20 in.^{2} or greater. If a leak occurred at the casing head, then the leak area would have been smaller than 20 in.^{2} . If the hole area were too large, all the gas would have leaked off before arriving at the fitting. With the casing-head-leak stopped by the October 24, 2015, measurement, leak area would have been 15 in.^{2} or greater. The records indicate a leak on October 23, 2015, that would have been between 15 and 20 in.^{2}, significantly less than the holes measured on the surface casing; this implies that all of the holes in the surface casing were not open to flow when the leak began. Based on Figure 39, the leak at the wellhead was less than 24 MMscf/D, and the actual rate at the wellhead depended on the measured casing head pressure. Figure 40 details the casing head pressure and leak rate for various sizes of leaks at the casing head. The data on October 23, 2015, were from when a leak was evidenced, and the data on October 24, 2015, assumed what would have happened if the attempt to close the leak that day had not been successful.

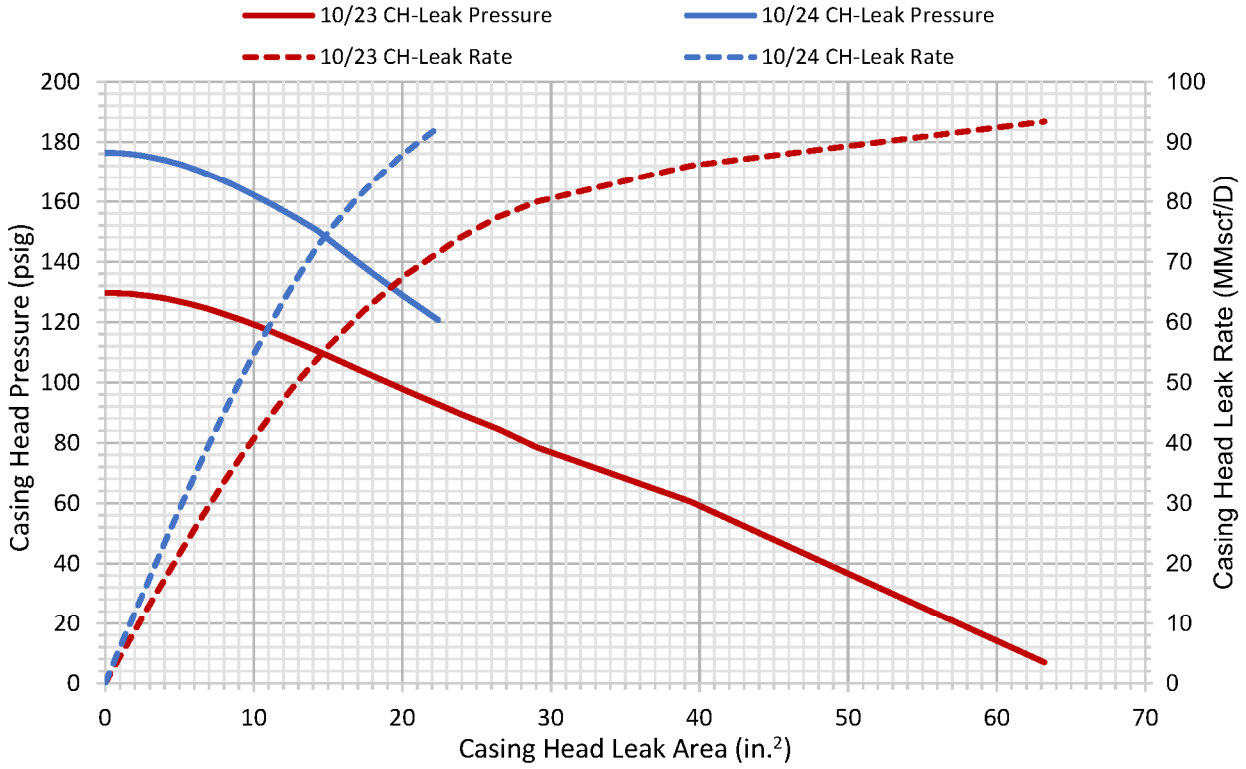

Figure 40: SS-25 Possible B-Annulus Casing Head Leak Conditions

Per Figure 40, a maximum leak rate of 24 MMscf/D on October 23, 2015 corresponded to a maximum leak opening of 5 1/2 in.^{2} and a casing head pressure drop of only 4 psi from the no-leak estimate presented earlier; that level of pressure difference was within the accuracy of the solution methodology; therefore, the extent of the leak could not be refined further.

The important conclusion is that, given a known leak rate on October 23, 2015, the best-estimated measurement for the leak holes in the surface casing at the time the leak began was 15 to 20 in.^{2} . The holes measured in the surface casing totaled 46 in.^{2} with perhaps 3 to 6 in.^{2} unmeasured. This implies that not all the holes were open to flow in the surface casing on October 23, 2015. More holes would have opened by or on November 06, 2015 when a glycol treatment freed the ice/hydrate plug from the tubing, and the final opening would have occurred on November 13, 2015.

7 Leak-Rate Comparison to Scientific Aviation

Scientific Aviation estimated the airborne emissions of the leak by analyzing data gathered by flying a specially-equipped aircraft over the leak-site [15]. Stephen Conley, the author, is president of Boulder-based Scientific Aviation and an atmospheric scientist at University of California, Davis. Figure 41 shows the estimated airborne rates (converted from metric tons of methane to standard gas rates using the EoS model presented herein).

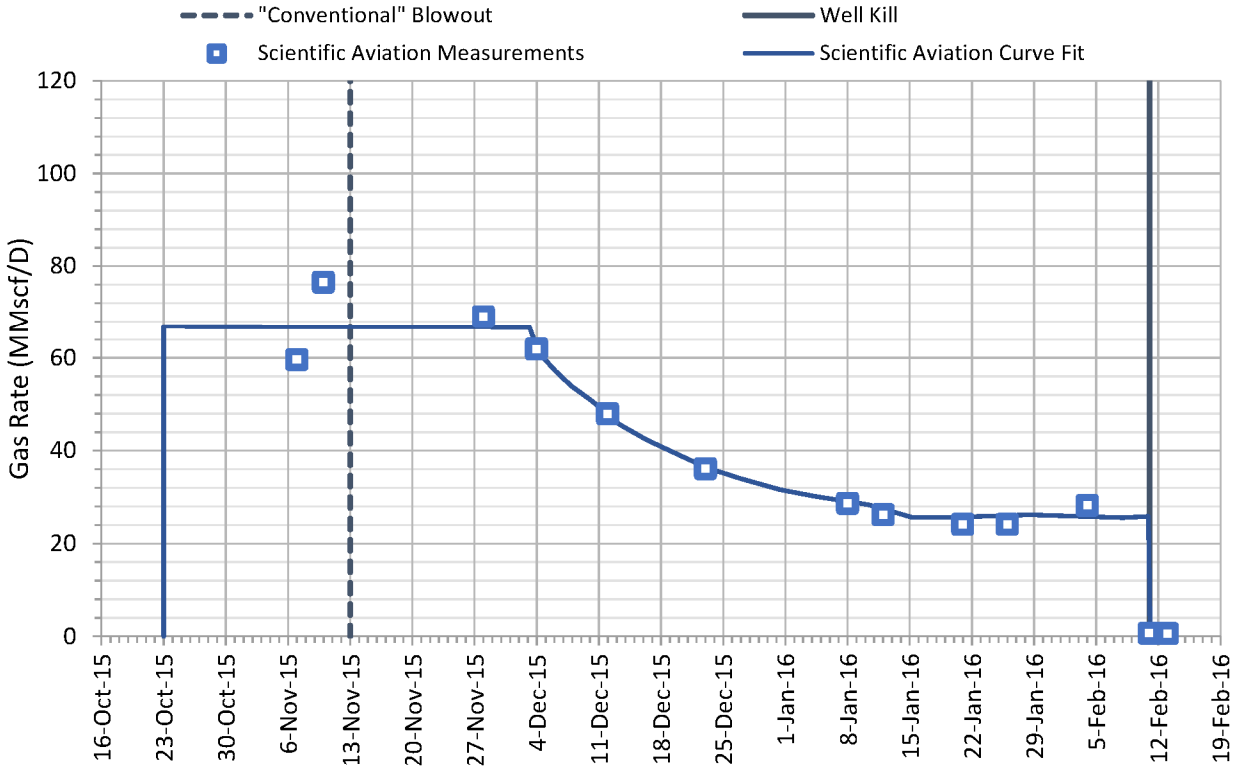

Figure 41: SS-25 Measured Leak-Rate History—Scientific Aviation

Although Scientific Aviation's plane was nearby for other measurements when the SS-25 leak occurred and could mobilize quickly to measure the leak, the initial leak rates were not measured. Also, only the airborne hydrocarbons were measured, and they did not necessarily represent the total leak. Hydrocarbons dispersed through the fracture matrix would have taken an unknown path that delayed emissions to the air. This path could have dispersed the gas to a wider area than the one that was measured. A plateau in the leak rate indicated the possibility that the initial kill attempts partially plugged the well. The *conventional* uncontrolled leak occurred on November 13, 2015, and after this point, it is likely that the rate would have experienced a continual decline. Reservoir pressure would have been continually declining from the leak withdrawal, and significant net field withdrawal from other wells would have occurred on all days from November 13, 2015, until January 24, 2016.

Figure 42 compares the rates of Scientific Aviation with those of this report.

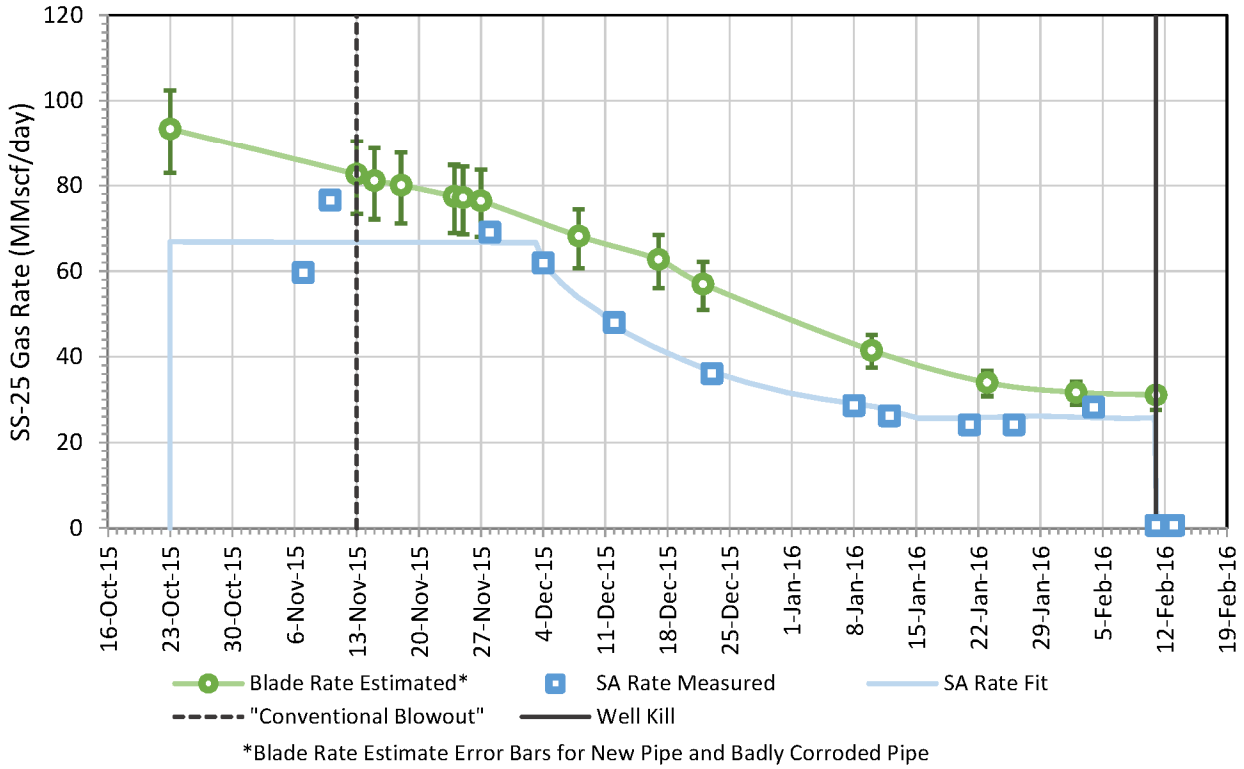

Figure 42: SS-25 Leak-Rate History Comparison—Blade and Scientific Aviation

The lower estimated rates assumed badly corroded tubing-casing and were likely lower bounds. The higher estimated rates that assumed new tubing were high and likely the upper limit, as pulled production casing showed evidence of corrosion and scaling. The best rates were from the assumed pipe roughness based on corrosion and scaling and were always just at or above the Scientific Aviation rates. Note that the plateau rate assumed by Scientific Aviation for the six weeks was a result of limited measurements—the rates were higher at the beginning and lower to a plateau around 80 MMscf/D as a result of the kill procedures.

SoCalGas provided an IPR model to DOGGR that may have been considered for kill planning. The PROSPER inflow model was built to match the kill-planning IPR with the PROSPER outflow model and remained the same as presented herein. A forecast with this kill-planning-fit IPR was then made by changing the reservoir pressure in time per the SS-5 monitoring well (same as the Blade model). Figure 43 compares the Blade, Scientific Aviation, and adjusted kill-planning IPR derived forecasts.

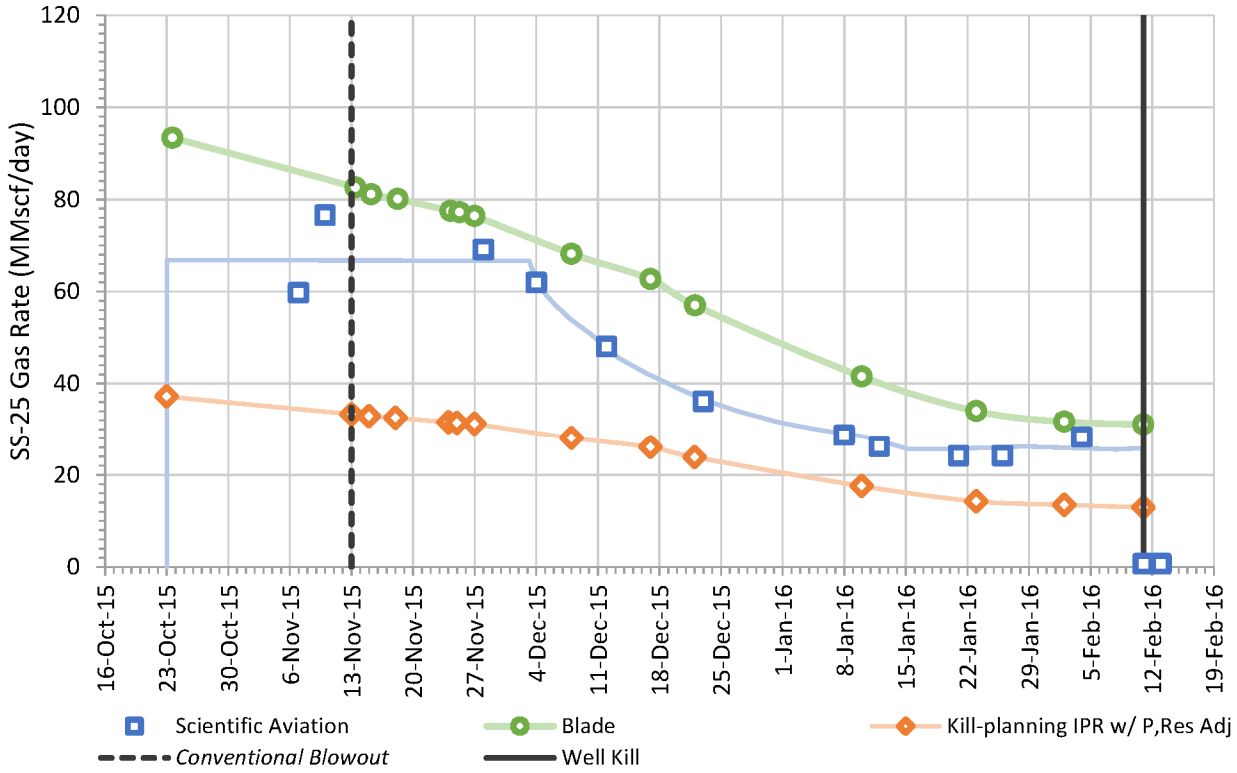

Figure 43: SS-25 Leak-Rate History Comparison—Blade and Scientific Aviation with the Kill-planning IPR

The kill planning IPR that was adjusted for reservoir pressure was consistently below the rates measured by Scientific Aviation and predicted in this study. This IPR model was previously shown to not be representative of the production well tests. The kill planning IPR model was inaccurate.

8 Conclusions

This report presented a study based on the thermo-hydraulic well model built in PROSPER of the SS-25 well for the Aliso Canyon gas leak. The model was built with matching data provided by SoCalGas and included general data about the wellbore, formation and measured injection, and withdrawal and well test data over the life of the well. By matching measured data, a model was developed to match the known conditions of the leak, and the conclusions are the following:

- A leak through the axial rupture region developed during injection where the Joule-Thompson effects cooled the tubulars to very low temperatures. This then resulted in the circumferential parting.
- After SoCalGas discovered the leak, injection was shut in. As leak gas was withdrawn from the formation, modeling of the wellhead casing measurements required the production casing to have failed before the injection shutoff.
- The leak during withdrawal would still have been cold but not as cold during injection. The tubulars during the withdrawal leak would have become warmer and warmer. The temperature of the gas leaving the surface casing would likely have been below freezing for the first two months of the leak.
- The actual leak rate and pressures exceeded those determined by the IPR provided by SoCalGas; therefore, using this IPR would have been problematic.
- The total best-estimate leak rate was greater than the one measured by Scientific Aviation and finalized by the California Air Resources Board. Those measurements were for airborne gas, and it is likely that gas was both airborne and diverted through the ground. Significant fractures in the ground were at ice and hydrate formation conditions, and it is theorized that the lingering cold temperatures in the ground could have been evidence of lingering ice and hydrates as gas diversion. The gas would have eventually leaked to the atmosphere and possibly after Scientific Aviation had stopped their measurements. Table 16 lists the total estimates.

Table 16: Aliso Canyon Hydrocarbon Leak Estimates

Source	Methane (10^6 kg)~	Other Hydrocarbon (10^6 kg)~	Carbon Dioxide (10^6 kg)~
Scientific Aviation Estimate [15]	97		
California Air Resources Board Estimate [16]	109		
Blade Best Estimate	120	11.0	2.9
Blade Estimate if Badly Corroded Pipe*	107	9.8	2.6
Blade Estimate if New Pipe*	131	12.0	3.2

~ (10^6 kg) equals (1,000 metric tons)
*The new and badly corroded pipe estimates give upper and lower bounds respectively, but Blade's well work showed that the piping was not at these limits.

9 References

[1] Blade Energy Partners, "SS-25 Transient Well Kill Analysis," 2019.

[2] Blade Energy Partners, "Analysis of the Post-Failure Gas Pathways and Temperature Anomalies at the SS-25 Site," Blade Energy Partners, Frisco, Texas, 2019.

[3] Blade Energy Partners, "Aliso Canyon Injection Network Deliverability Analysis Prior to Uncontrolled Leak," Blade Energy Partners, Frisco, TX, 2019.

[4] SS-25 Well Documentation (from SoCalGas)_N.pdf.

[5] GasComposition.pdf.

[6] SS-25 Directional Survey_ 1-16-2016 [20032].xlsx.

[7] GNPT_VSL_WL_STANDARD SESON#25_03700776_DMPT_04.12.2016.las.

[8] AC_BLD_0000001 - AC_BLD_0001955 {Temperature Surveys}.pdf, SoCalGas.

[9] "GNPT_VSL_WL_STANDARD SESON25_03700776_MID ANALYSIS_04.18.2016_WITHOUT CALIPER.pdf".

[10] SoCalGas, "Email, 28 Dec 2015, SoCalGas to DOGGR, Subject: Supplemental SoCalGas Response to Information Request - 12-23, (Information Request - 12-23 Calculations Email.docx, DOGGR -1_Supp Response Q2_ 122815.docx, Input Data for Flow Analysis.docx)".

[11] SoCalGas, "SS-25 Well Survey File.pdf," SoCalGas, 2015.

[12] AC_BLD_0088969, "AC_BLD_0088969.xlsx," SoCalGas, 2015.

[13] Video Camera Run 2017-11-07, *1st hole area.jpg.*

[14] Video Camera Run 2017-11-07, *2nd hole area.jpg.*

[15] S. Conley, G. Franco, I. Faloona, J. Peischl and D. R. Blake, "Methane emissions from the 2015 Aliso Canyon blowout in Los Angeles, CA," *Science,* 25 Feb 2016.

[16] California Air Resources Board, "Determination of Total Methane Emissions from the Aliso Canyon Natural Gas Leak Incident," 21 10 2016. [Online]. Available: https://www.arb.ca.gov/research/aliso_canyon/aliso_canyon_methane_emissions-arb_final.pdf.

SS-25 RCA Supplementary Report

Aliso Canyon Injection Network Deliverability Analysis Prior to Uncontrolled Leak

Purpose:

Model the Aliso Canyon Gas Storage Field's gas injection network and simulate the gas leak in well SS-25 to assess the impact of the leak on pressure drops at various nodes of the network and quantify additional gas volumes that could have been injected into SS-25.

Date:
May 31, 2019

2600 Network Boulevard, Suite 550
Frisco, Texas 75034

+1 972-712-8407 (phone)
+1 972-712-8408 (fax)

16285 Park Ten Place, Suite 600
Houston, Texas 77084

1-800-319-2940 (toll free)
+1 281-206-2000 (phone)
+1 281-206-2005 (fax)

www.blade-energy.com

Abstract

The gas storage well Standard Sesnon 25 (SS-25) in the Aliso Canyon Gas Storage Field located in Los Angeles County, California started leaking gas in October 2015. A relief well was drilled, and SS-25 was brought under control. The leak stopped in February 2016.

In January 2016, as part of their investigation of the leak, the California Public Utilities Commission (CPUC) and the Division of Oil, Gas, and Geothermal Resources (DOGGR) selected and gave provisional authority to Blade Energy Partners (Blade) to perform an independent Root Cause Analysis (RCA). The Blade Team and parties under Blade's direction were responsible for directing the work of subcontractors who performed the extraction of the SS-25's wellhead and tubing and casing and the preservation and protection of associated evidence. Blade RCA Reports, including this report, document and describe the key activities undertaken in support of the RCA effort.

This report describes the modeling of the Aliso Canyon gas injection surface network and analysis of the performance of the network when simulating various leak scenarios in SS-25. The key objective of this study was to simulate a gas leak in SS-25 and assess the impact of the leak on the pressure drops at various nodes of the injection network. In addition, the study quantified the additional gas volumes that could have been injected into SS-25 from other legs of the network. Blade simulated several leak scenarios in SS-25 to understand the impact of a leak on the redistribution of injection gas volumes in the West, Central, and East legs of the network.

After simulating several leak scenarios in SS-25, this study estimated:

- Pressure changes at the injection manifold, choke manifold, wellhead of SS-25, and at injection headers near the compressor station, because of a leak in SS-25.
- The excess volume of gas over the nominal allocated daily gas rate that could have been injected into SS-25 because of a leak.
- Gas volumes that could be redirected from the East and Central legs of the network and from well SS-25B because of a leak in SS-25.

The study reviewed and used several documents provided by Southern California Gas Company (SoCalGas) to build the model for the injection network in the Petroleum Experts General Allocation Package (GAP) software. GAP is a multiphase oil and gas flow simulator that models and optimizes the surface gathering network of field production or injection systems.

Blade modeled the Aliso Canyon gas injection network using the network data provided by SoCalGas. The model incorporated the length, diameter and the elevation profiles of the pipeline. The model also included the choke and check valve settings for all the wells in the network model.

The study included an analysis of the typical network injection rates and pressures for the seven days prior to the leak date of October 23, 2015. This analysis required knowledge of the allocated daily gas injection rates for the wells. The study used the reported monthly injection volume data and the daily online injection duration to estimate the monthly volume equivalent daily injected gas rate for the wells.

Using the measured discharge pressure at the Western injection header near the compressor station and the monthly volume equivalent daily injected gas rates for the wells, the study calibrated the gas injection network model to capture the performance of the network in the absence of a leak (base case). In the absence of a leak, the equivalent daily gas injection rate for SS-25 was estimated to be 3 to 5 MMscf/D. The corresponding measured discharge pressures at the Western injection header ranged from 2,800 to 2,860 psi. The model-calculated wellhead pressure (WHP) at SS-25 ranged from 2,725 to 2,775 psi for the seven days analyzed.

The calibrated network model was then used to simulate various leak scenarios in SS-25 by varying the WHP and re-calculating the network gas injection rates. The study simulated the leak by reducing the SS-25 WHP from its base case value (no leak scenario) without changing the choke setting. With every change in the WHP setting for SS-25, the gas being injected and pressure drops at various nodes were estimated.

The modeling results showed that with the change in SS-25 WHP, gas could be injected into the well at a significantly higher rate than the base case injection rate. The analysis determined that a gas rate of up to 70 MMscf/D could have been injected into SS-25 when its WHP was lowered by about 2,000 psi from the base case value to simulate a leak. This showed that in the event of a leak in SS-25, about 65 MMscf of gas volume could be redirected from the East and Central legs of the network and from well SS-25B and be additionally injected into SS-25 each day.

The pressure drop at the choke manifold was high and equivalent to the WHP reduction of 2,000 psi. However, the corresponding pressure reduction was only 15 psi at the injection manifold. Further, the equivalent change in pressure at the Western injection header for this significantly increased injection rate into SS-25 was negligible (1 psi). That is, the gas injection network could have injected up to 14 times the nominal injection rate into SS-25 in the event of a leak without any significant change in pressure at the Western injection header.

The study found that, in the event of a leak in SS-25, the pressure variations at the injection headers would have been minimal and not significant enough to be detected. If the pressure was being monitored only at the Western injection header near the compressor station, then in the event of a leak, the increased gas volume injected into SS-25 could have remained undetected.

It is best practice to monitor pressure at each node of the network such as wellheads, injection manifolds and injection headers. A real-time field-wide pressure surveillance system with intelligent evaluation capability can continuously analyze pressure measurements at various nodes of the network. It can quickly detect and activate an alarm if gas is being distributed at a significantly different rate than expected, which could indicate a surface or wellbore leak.

Table of Contents

List of Figures

List of Tables

1 Introduction

This study describes the modeling of the Aliso Canyon gas injection surface network and analysis of the performance of the network when simulating various leak scenarios in SS-25. The key objective of this study was to simulate a gas leak in SS-25 and assess the impact of the leak on the pressure drops at various nodes of the injection network. The modeling estimated pressure changes at the injection manifold, choke manifold, wellhead of SS-25, and at injection headers near the compressor station. In addition, the study quantified excess volume of gas over the nominal allocated daily gas rate that could have been injected into SS-25 from other legs of the network. Blade simulated several leak scenarios in SS-25 to understand the impact of a leak on the redistribution of injection gas volumes in the West, Central, and East legs of the network.

The study grouped wells in the East and Central legs of the network according to their physical location in the network. The study estimated each group's injection manifold pressure (before the choke) calculated by the model for pressure variations when a volume less than the nominal allocated daily gas rate was injected into those groups of wells.

Blade developed the model for the Aliso Canyon gas injection network with the actual field data using Petroleum Experts GAP software. GAP is a multiphase oil and gas flow simulator that models and optimizes the surface gathering network of field production or injection systems.

The study analyzed the typical network injection rates and pressures each day for the seven days prior to the leak date of October 23, 2015. The modeling was performed only on the surface injection with deliverability to the wellheads. The study did not conduct wellbore modeling.

1.1 Abbreviations and Acronyms

Term	Definition
CPUC	California Public Utilities Commission
DOGGR	Division of Oil, Gas, and Geothermal Resources
GAP	General Allocation Package
RCA	Root Cause Analysis
SoCalGas	Southern California Gas Company
SS-25	Standard Sesnon 25
UGS	Underground Gas Storage
WHP	Wellhead Pressure

1.2 Methodology

The study required knowledge of the allocated daily gas injection rates and daily measured wellhead pressures (WHPs) of the wells in order to conduct an analysis of the typical network injection rates and pressures for each day. However, there were limitations in the available data. The details of the data used and inherent assumptions are described in Section 2.

The study used the reported monthly injection volume data and the daily online injection duration (in hours) to estimate the monthly volume equivalent daily injected rate for each well. The calculated monthly volume equivalent daily injected gas rate for the wells is referred to as the "adjusted-allocated" daily gas injection rate in this report. This approach maximized the usage of the available data and ensured that the calculated rates employed in the model were the averages for the time period that a well was reported online, and not the total injection for the day.

The measured discharge pressure at the Western injection header node named 'PIT-WFI_DY1' near the compressor station was also used as an input to the model. The study implemented the choke and valve settings for all wells in the network model.

Blade followed a methodology as shown in Figure 1 to check the stability of the model. The results of the steps are described in Section 3.4 and Section 3.5. After ensuring the stability and accuracy of the model, this study simulated various leak scenarios for SS-25 by reducing the WHP.

The steps followed in Figure 1 are described below:

- Step 1—Implemented the measured discharge pressure at the Western injection header near the compressor station and the adjusted-allocated daily gas injection rate at each well. The main results obtained were for:
  - The total injected gas volume at the compressor station.
  - The WHP at each well.
  - The total injected gas volume in the West, Central, and East legs, respectively.
- Step 2—Calibrated the model by using the results from Step 1 as input. The main results obtained were for:
  - The pressure at the Western injection header of compressor station.
  - The gas injection rate at each well.
  - The total injected gas volume in the West, Central, and East legs, respectively.
- Step 3—Checked the results obtained from Step 2 for consistency with the input of Step 1 to assess the stability of the model. Once the model was calibrated, the study specified the WHP at each well to simulate various leak scenarios for SS-25.

This methodology was conducted for each day of the seven days preceding the leak date.

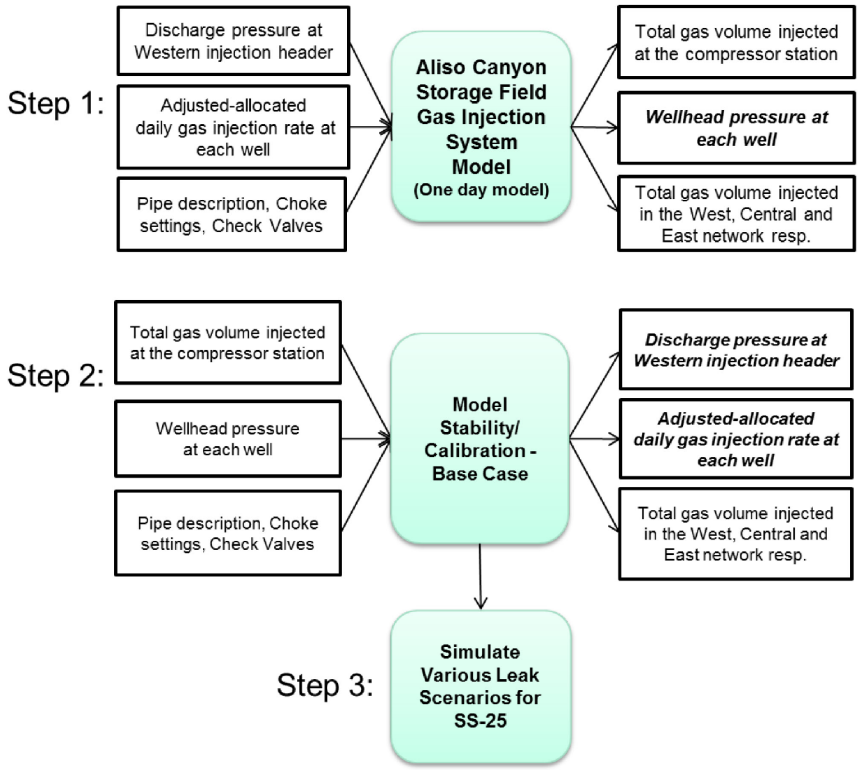

Figure 1: Methodology Used in the Stability Check for the Aliso Canyon Gas Injection Network Model

1.3 Base Case Definition

Using the measured discharge pressure at the Western injection header near the compressor station and the adjusted-allocated daily gas injection rates for wells, the study calibrated the gas injection network model to capture the performance of the network in the absence of a leak. Without a leak, the adjusted-allocated daily gas injection rate for SS-25 was estimated to be 3 to 5 MMscf/D. The corresponding measured discharge pressures at the Western injection header ranged from about 2,800 to 2,860 psi. The model-calculated WHP at SS-25 ranged from 2,725 to 2,775 psi for the seven days analyzed.

This report refers to the adjusted-allocated rates determined in the absence of a leak in SS-25 as base case settings. Without a leak, there was no pressure drop at the SS-25 wellhead.

1.4 Case Description

The model was then transposed by setting the calculated SS-25 WHP from the base case as input and then, instead, calculating the injection rates for SS-25. This study is based on the premise that at the time of the leak, the WHP at SS-25 could have been lower than the base case WHP setting. Hence, the calibrated network model was then used to simulate various leak scenarios in SS-25 by varying its WHP from the base case value and then re-calculating the network gas injection rates. The study simulated the leak by reducing the SS-25 WHP gradually by 10 psi to about 2,000 psi from its base case value (no leak scenario), without changing the choke setting. With every change in the WHP setting for SS-25, the gas being injected and pressure drops at various nodes were estimated.

2 Data and Assumptions

The study reviewed and used several documents provided by Southern California Gas Company (SoCalGas) to build the model for the injection network. This section describes the data used to build the Aliso Canyon gas injection surface network model and assumptions made to conduct this study. Section 6 provides a detailed list of the documents reviewed to obtain various inputs for the model.

2.1 Basis of Design and Data Source

The following data were used as the basis for this study:

- Measured pressure at the Western injection header named 'PIT-WFI_DY1' near the compressor station [1], [2], [3], [4], [5]
- Discharge temperature at the compressor station: 80°F [6]
- Adjusted-Allocated daily gas injection rate at each well [7], [8], [9]
- Weekly measured WHP of SS-25 [10], [11], [12], [13]
- Pipe description and choke and check valves settings as follows:
  - Google Earth Pro (Figure 5) and AC_BLD_0003725 [14], [15] were used to determine the gas injection network pipe length, diameter and elevations profile.
  - Bates range AC_BLD_0044795 to AC_BLD_0044798 [16]:
    - Pipe diameter going to the well head: 4 in.
    - Network pipeline diameter: 8 in.
    - Pipelines near the compressor station: 12 in.
  - Surface roughness: Default
  - Overall heat transfer coefficient: Default
  - Multiphase correlation: PE5
  - Choke settings (Figure 2) [17]: 1 in. choke size was modeled for SS-25 along with injection through casing string.
  - Choke model: Elf
  - Check valves settings [16]
- Gas gravity: 0.588

ALISO CANYON FIELD INJECTION SCHEDULE

DATE:
PREPARED BY:
Last updated:

WORKING GAS (BCF): 50.80
WELLS AVAILABLE: 63
WELLS NOT AVAILABLE: 50

EAST FIELD PRESSURE : 2,118 psig
WEST FIELD PRESSURE : 1,966 psig

	WELL	STR	LEG	CHOKE SIZE (T/C)	AVAIL. PRIOR.	
1	F2	T	W	1	N	No Injection
2	F4	CK	W	0.60 / 1.00	N	No Injection
3	F5	T	W	1.50 (adj)	N	No Injection
4	F6	T	W	OPEN(adj)	N	No Injection
5	F7	TK	W	OPEN / 1.50	N	No Injection
6	F8	T	W	OPEN(adj)	N	No Injection
7	FF32	C	E	1.0 / 1.60	Y 2	Choke Bypass
8	FF32A	C	E	0.70 / 1.00	Y 1	
9	FF32B	C	E	0.90 / 1.20	Y 1	
10	FF32C	C	E	1.05 / 1.00	Y 1	
11	FF32D	T	E	0.9	N 1	Choke Bypass can't be used
12	FF32F	C	E	1.00 / 1.0	Y 1	Choke Bypass
13	FF32G	C	E		N 1	Choke Bypass
14	FF33	T	E	1.5	N	No Injection
15	FF34A	TK	E	1.00 / 1.00	N	No Injection
16	FF34BR	TK	E	0.7 / 1.00	N	No Injection
17	FF35A	C	E	0.9 / 0.90	Y 1	
18	FF35B	C	E	0.9 / 0.9	Y 2	
19	FF35C	C	E	1.0 /0.90	Y 2	
20	FF35D	C	E	0.70 / 0.75	Y 2	
21	FF35E	C	E	0.80 / 1.00	Y 2	
22	FF38A	C	E	0.8 / 1.10	Y 1	Choke Bypass
23	FF38B	C	E	0.90 / 0.90	Y 1	Choke Bypass
24	FF38C	C	E	1.10/ 1.00	Y 1	Choke Bypass
25	MA1A	CK	E	0.90/ 0.90	N	No Injection
26	MA1B	CK	E	0.90/ 0.90	N	No Injection
27	MA3	--	E	OPEN	N	No Injection
28	P12	TK	E	1	N	No Injection
29	P24A	C	C	1.00 / 1.00	Y 1	Choke Bypass
30	P24B	C	C	1.00 / 1.00	Y 1	Choke Bypass
31	P25R	C	W	1.11 / 1.00	Y 4	
32	P26	C	C	0.925 / 0.8	Y 1	
33	P26A	C	C	0.90 / 1.00	Y 2	
34	P26B	C	C	1.00 / 1.00	Y 1	
35	P26C	C	C	0.80 / 1.1	Y 1	
36	P26D	C	C	1.00 / 0.90	Y 1	WKM/Instrumentation
37	P26E	C	C	0.675 / 1.00	N 1	
38	P30	C	E	0.9 / 1.2	Y 3	
39	P32	C	E	1.00 / 1.30	Y 3	
40	P32A	C	E	0.50 / 42% CCI	N 1	OOS for Wellhead work
41	P32B	C	E	1.5 / 0.9	Y 1	Choke Bypass
42	P32C	C	E	1.10 / 0.90	Y 1	Back in Service today
43	P32D	C	E	1.10 / 0.8	Y 2	
44	P32E	C	E	0.90 / 1.0	Y 2	Choke Bypass
45	P32F	C	E	1.00 / 0.8	Y 1	
46	P34	C	C	1.5 / 0.785	N	No Injection
47	P35	T	C	1.55	N	No Injection
48	P36	C	E	1.20 / 1.35	N 4	No Injection
49	P37	C	E	1.00/ 1.00	Y 3	Choke Bypass
50	P37A	C	E	1.05/ 1.20	Y 3	
51	P38	T	W	1.6	N	No Injection
52	P39	T	W	1	N	No Injection
53	P40	T	W	1.5	N	No Injection
54	P42A	C	C	0.50 / 0.5	Y 2	Choke Bypass
55	P42B	C	C	0.5 / 0.8	N 3	Choke Bypass

	WELL	STR	LEG	CHOKE SIZE (T/C)	AVAIL.	REMARKS
56	P42C	C	C	0.75 / 0.80	Y 1	Choke Bypass
57	P44	CK	C	1.00 / 1.00	N	No Injection
58	P45	CK	E	0.90 / 1.2	N	No Injection
59	P46	CK	C	1.00 / 1.00	N	No Injection
60	P47	TK	W	0.90 / 1.00	N	No Injection
61	P50A	C	E	0.5 / Open	Y 1	Choke Bypass
62	P50B	C	E	0.80/ 40% CCI	N 1	Choke Bypass
63	P50C	C	E		N 1	Choke Bypass
64	P68A	C	E	1	Y 1	
65	P68B	T	E	Open	Y 1	
66	P69A	C	C	1.10 / 1.0	Y 1	Choke Bypass
67	P69B	C	C	1.00 / 1.0	Y 1	
68	P69C	C	C	1.10 / 1.00	Y 1	
69	P69D	C	C	0.95 / 0.9	N 1	
70	P69E	C	C	1.5 / 1.00	Y 1	
71	P69F	C	C	1.10 / 1.0	Y 1	Choke Bypass
72	P69G	C	C	0.815 / 1.00	Y 1	Choke Bypass
73	P69H	C	C	1.1 / 1.0	Y 1	Choke Bypass
74	P69J	C	C	0.80 / 0.90	Y 1	
75	P69K	C	C	0.8 / 1.0	Y 1	Choke Bypass
76	P72A	C	E	0.90 / 1.0	Y 1	
77	P72B	C	E	0.90 /0.90	Y 1	
78	SF1	T	W	OPEN(adj)	N	No Injection
79	SF3	T	W	OPEN(adj)	N	No Injection
80	SF8	T	W	OPEN(adj)	N	No Injection
81	PS42	T	W	0.5	N 5	No Injection
82	SS02	C	W	0.80 / Open	Y 6	
83	SS03H	TK	W	1	N	No Injection
84	SS04	C	W	OPEN	Y 1	
85	SS04A	C	W	0.875 / 1.50	Y 1	
86	SS04-0	C	W	0.85 / 0.75	Y 4	
87	SS05	C	W	Open	N 6	W. Field Pressure Well
88	SS06	C	W	1.3 / OPEN	Y 6	
89	SS09	T	W	1.1	N 6	OOS-Rig
90	SS10	TK	W	1.5	N	No Injection
91	SS11	CK	W	1.5 / 0.5	N	No Injection
92	SS13	T	W	OPEN(ad)	N	No Injection
93	SS14	T	W	OPEN(ad)	N	No Injection
94	SS16	T	W	OPEN(ad)	N	No Injection
95	SS17	CK	W	1.5	N	No Injection
96	SS24	T	W	1.1	N	No Injection
97	SS25	C	W	0.975 / 1.00	Y 3	
98	SS25A	T	W	0.9	N 1	No check valve
99	SS25B	C	W	1.00 / 1.00	Y 4	
100	SS29	T	W	1	Y 6	
101	SS30	T	W	OPEN(ad)	N	No Injection
102	SS31	TK	W	1	N	No Injection
103	SS44A	C	W	1.00 / 0.90	N 5	Choke Bypass
104	SS44B	C	W	0.80 / 1.00	Y 3	Choke Bypass
105	W3A	T	E	0.5	N 1	E. Field Pressure Well
106						
107						
108						
109						

Figure 2: Aliso Canyon Injection Schedule Used in Modeling the Choke Settings [17]

2.2 Uncertain Parameters and Assumptions

This section describes the uncertain parameters and assumptions made to model the Aliso Canyon gas injection network. Some of the data required to build the gas injection surface model for the Aliso Canyon Gas Storage Field were not readily available, and some of the available data had discrepancies (Figure 4, Figure 19, and Figure 20). The following responses from SoCalGas describe the unavailability of the daily measured injection gas rate for each well:

> "SoCalGas does not measure gas injection or withdrawal volumes at each UGS well. SoCalGas can only measure totals for the whole field and the number of hours each day wells are either on injection or withdrawal. Monthly production and allocation data includes estimates by well" [18].
>
> "Total Injection gas volume is measured in the compressor station, and not at individual wells" [19].
>
> "An analogous Injection Worksheet is not available because Aliso Canyon does not have the ability to measure gas injection rates into individual wells. Individual Injection rates therefore are not provided to the Operations group. Instead, Aliso Canyon Operations uses parameters such as well availability, well priority, station compressor discharge pressure and flow rate to determine which injection wells are placed in service" [19].
>
> "SoCalGas does not have a written procedure for the allocation of injection gas to individual wells. Instead, injection wells are prioritized for injection. The number of wells open to injection is determined by Operations based on parameters such as Injection Call rate, number of Compressors running, field back pressure, etc. Typically, during the injection season when all compressors are running, all available injection wells are opened to injection to minimize back pressure and maximize injection rate" [19].
>
> "The Master Injection Schedule is the primary document used by Aliso Canyon Operations to prioritize wells placed on, or removed from injection. Gas Control determines the injection call rate at any given time. Operations Staff respond by placing wells on injection in the order of priority specified on the Master Injection schedule wells are prioritized 1 through 6. Priority 1 wells are placed on Injection first and removed from Injection last" [20].
>
> "The Master Injection Schedule provides the following additional, necessary information on each well to properly manage the injection process [18], [20]:
>
> - The production string to operate on each well—the tubing or casing strings.
> - The proper surface choke size(s) on the production string(s) specified.
> - The current operational status of the well (available or not-available for injection).
> - Additional notes, such as choke bypasses or status updates."

Based on the above responses from SoCalGas with regards to the unavailability of measured or allocated daily gas injection rates for each well, this study calculated the monthly volume equivalent daily injected rate for wells using the reported monthly injection volume data and the daily online injection duration (in hours) [7], [8], [9]. The other available injection volume data sheets were not used because of discrepancies in the injected volumes. Figure 19 and Figure 20 illustrate the data from those sources. Wells with a gas injection rate of less than 1 MMscf/D impacted the model's run time and efficiency. Consequently, wells that had a gas injection rate of less than 1 MMscf/D were shut in the model, and equivalently, about 5 MMscf of gas injection volume was deducted from the total volume at the compressor station.

Wells shut in for each leg of the network were:

- West leg—four wells
- Central leg—two wells

- East leg—two wells

Three separate pressure measurement documents were available for the compressor station pressure during injection operations, and each one corresponded to a pressure measurement location in the vicinity of the compressor station [1], [2], [3]. The study reviewed these documents but used the pressure measurement at the Western injection header node named 'PIT-WFI_DY1' (West Field Injection Line Y-Trench Press) because it was the closest to SS-25 [2], [21].

The model required an average discharge pressure for each day as an input. However, in the field, the discharge pressure data was measured three to five times every minute. Thus the study averaged the high frequency pressure data of each day and implemented the averaged discharge pressure in the model. Figure 3 shows the measured pressure data at the Western injection header node and also the daily corresponding averaged pressure data for the week prior to the leak.

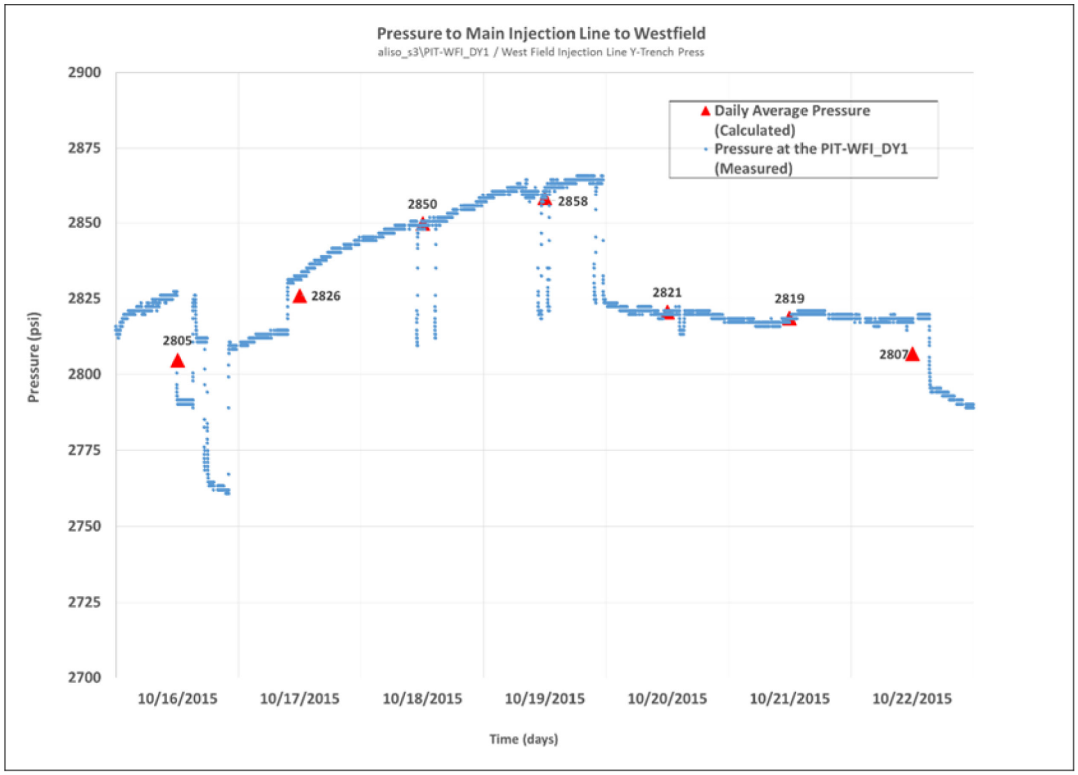

Figure 3: Measured Pressure Data at the Western Injection Header vs. Corresponding Averaged Pressure

Table 1 shows the daily average for the measured pressure data at the Western injection header, the corresponding variance over the day, and the standard deviation during each day.

Table 1: Pressure Data at the Western Injection Header 'PIT-WFI_DY1' (West Field Injection Line Y-Trench Press)

Date	Daily Average Pressure (psi) (Calculated)	Daily Pressure Variance (psi)	Daily Standard Deviation (psi)
October 16, 2015	2,805	459	21
October 17, 2015	2,826	164	13
October 18, 2015	2,850	35	6
October 19, 2015	2,858	134	12
October 20, 2015	2,821	2	2
October 21, 2015	2,819	2	2
October 22, 2015	2,807	170	13
October 23, 2015	2,811	106	10

The study also reviewed the documents provided by SoCalGas for the weekly reported WHP for SS-25 [10], [11], [12], [13]. There was a discrepancy in the reported WHP data among the referenced documents. The casing and tubing pressure data appears to be shifted by 14 days (Figure 4). This discrepancy does not change the results of the deliverability analysis.

SS-25 Temperature Suvey & Wellhead Pressure.pdf [10], [13]

	SS25 Wellhead Pressure, psi		
	Surface Casing	Casing	Tubing
08/12/15	0	2445	2445
08/20/15	0	2558	2537
08/27/15	0	0	0
09/05/15	1	2540	2540
09/11/15	0	2680	2680
09/18/15	0	2610	2600
09/25/15	0	2595	2595
10/01/15	0	0	0
10/15/15	0	0	0

AC_BLD_0075828 weekly pressure SS-25.xlsx [11], [12]

	SS25		
	A1 - Surface Casing Annulus (PSIG)	C - Production Casing Annulus (PSIG)	Tubing (PSIG)
08/12/15	0	2490	2490
08/20/15	0	2380	2380
08/27/15	0	2445	2445
09/05/15	1	2558	2537
09/11/15	0	0	0
09/18/15	0	2540	2540
09/25/15	0	2680	2680
10/01/15	0	2610	2600
10/15/15	0	2595	2595

Figure 4: Discrepancy in the Weekly Reported WHP for SS-25

3 General Allocation Package (GAP) Modeling

This section describes the various input parameters used in this study to construct the Aliso Canyon gas injection network model in GAP as outlined in Section 2.1.

3.1 Model Construction

3.1.1 Aliso Canyon Gas Injection Surface Network

Blade modeled the Aliso Canyon gas injection surface network using data provided by SoCalGas [14], [15]. The injection pipeline length, diameter and elevation change details were included in the model. Figure 5 shows the general pipeline path from the compressor station to SS-25. The study also implemented the choke settings and check valves for all wells in the network and used the 1 in. choke size and injection path through the casing string for SS-25 (Figure 2) [17].

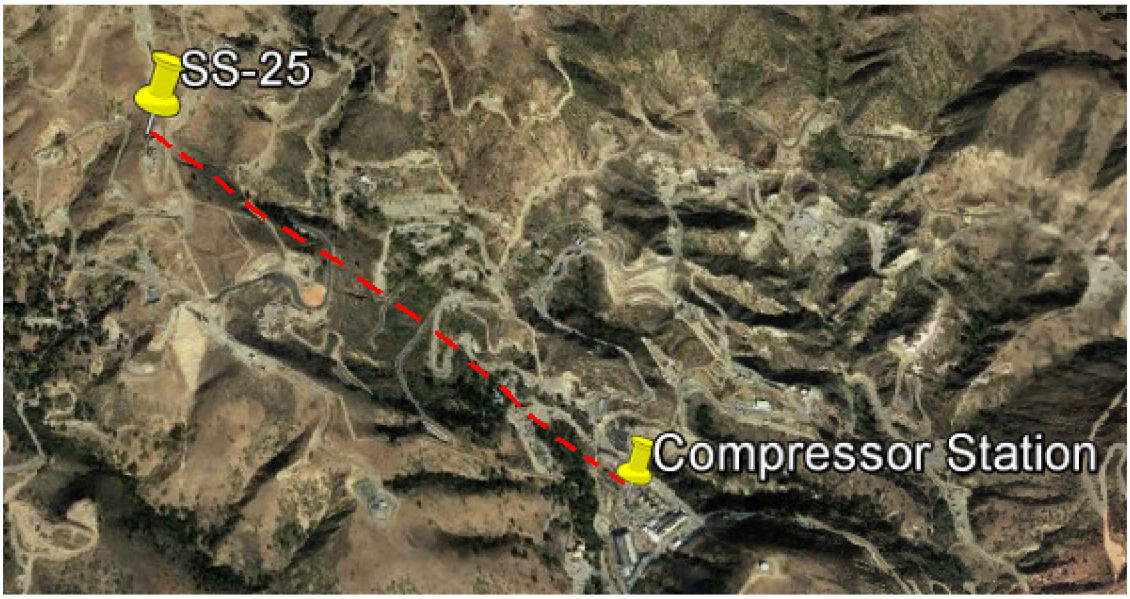

Figure 5: SS-25 Gas Injection Line Path from the Compressor Station

3.1.2 Aliso Canyon Gas Injection Network in GAP

Figure 6 illustrates an example of how this study incorporated the pipe length, diameter and elevation changes in GAP while building the injection network in order to incorporate the pressure differences due to terrain changes. The study also considered the frictional losses in the pipeline, but they did not significantly impact the modeling results.

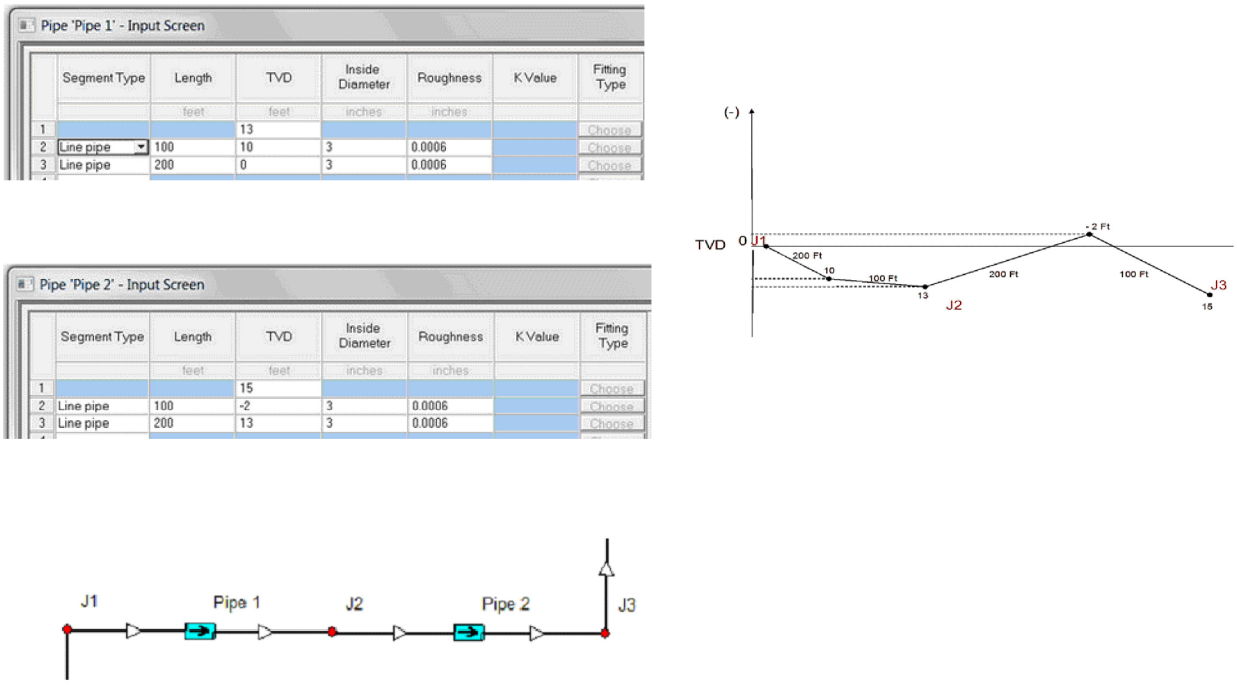

Figure 6: An Example Showing Incorporation of Pipe Length, Diameter and Elevation Changes in the GAP Model

Figure 7 shows conceptually the Aliso Canyon gas injection network modeled in GAP. In the network, numerous wells are tied to each of the three main legs of the network. The GAP modeling includes the details of each well and how a well is connected to its respective leg injection header.

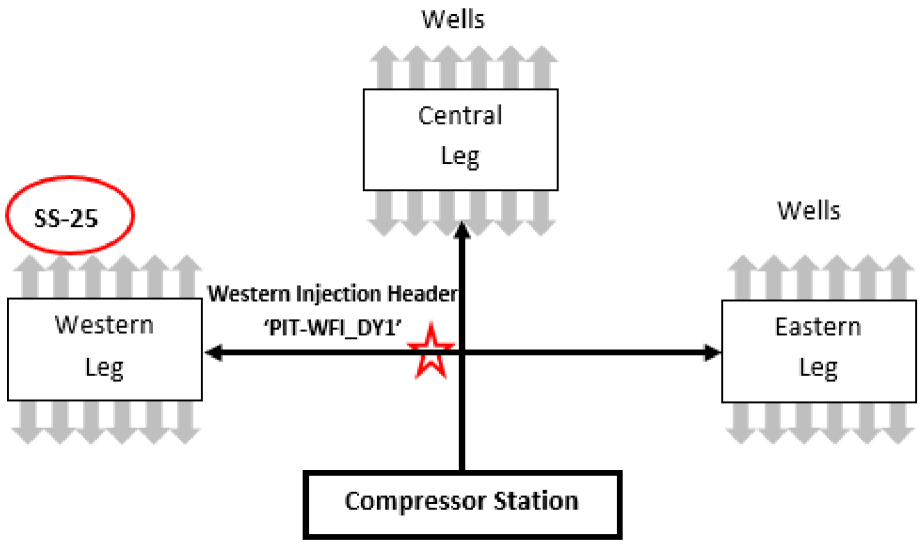

Figure 7: Aliso Canyon Gas Injection Network Block Diagram as Modeled in GAP

3.2 Various Nodes of the Network

3.2.1 Injection Manifolds of SS-25

Figure 8 shows a typical schematic of various nodes leading to SS-25 and SS-25B. The three nodes considered for the pressure observations are located at:

- The injection manifold (before SS-25 and SS-25B).
- SS-25's choke manifold.
- SS-25's wellhead.

Note that SS-25A was shut in during October 2015 [7], [22].

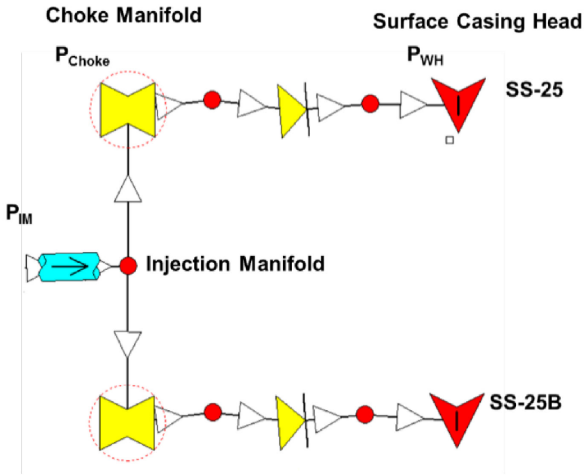

Figure 8: Nodes Diagram for Site SS-25

3.2.2 Injection Header by Network Legs

For every leak scenario simulated for SS-25, this study estimated the change in pressure at the injection headers of each leg of the network. Figure 9 schematically shows the various injection headers (represented by stars) considered for pressure variance, as set up in the model. While modeling the network, wells were grouped according to their physical location conceptually indicated by ovals in Figure 9. The pressure variance for these groups of wells was also evaluated.

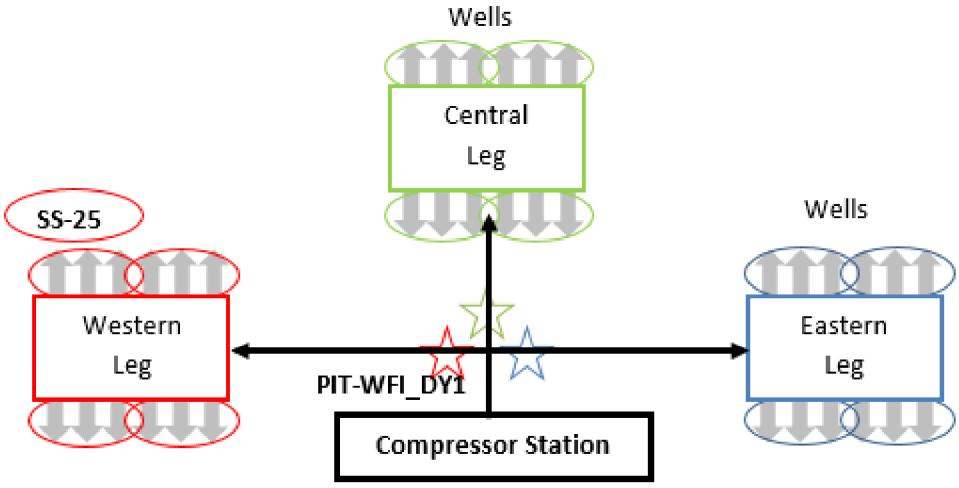

Figure 9: Block Diagram for Pressure Variance Estimation Nodes of the Aliso Canyon Gas Storage Field Network

3.3 Injection Volume

3.3.1 Allocated Daily Gas Injection Rate and Pressure at the Compressor Station

The study conducted an analysis of the typical network injection rates and pressures for each day for the seven days prior to the leak date of October 23, 2015. The calculated adjusted-allocated daily gas injection rate for each well and the total gas being injected into the network by date is shown in Table 2. Table 2 also shows the average of the discharge pressure measured at the Western injection header on each of the seven days prior to the leak.

Table 2: Adjusted-Allocated Daily Gas Injection Rate for Each Well for the Seven Days Prior to the Leak

Dates	10/16	10/17	10/18	10/19	10/20	10/21	10/22	10/23
Calculated Total Daily Injected Gas Volume (MMscf)	252.8	306.9	306.9	306.9	305.8	306.9	197.1	263.2
Pressure Transmitter to Main Injection Line to West Field.txt (psi) [2]	2,805	2,826	2,850	2,858	2,821	2,819	2,807	2,811
Injection Wells	Adjusted-Allocated Gas Injection Rate (MMscf/D)							
	10/16	10/17	10/18	10/19	10/20	10/21	10/22	10/23
FF-32	5.8	7.1	7.1	7.1	7.1	7.1	4.6	6.1
FF-32A	10.2	12.4	12.4	12.4	12.4	12.4	8.0	10.7
FF-32B	4.4	5.3	5.3	5.3	5.3	5.3	3.4	4.6
FF-32C	8.8	10.6	10.6	10.6	10.6	10.6	6.8	9.1
FF-32F	5.8	7.1	7.1	7.1	7.1	7.1	4.6	6.1
FF-35A	8.8	10.6	10.6	10.6	10.6	10.6	6.8	9.1
FF-35B	8.8	10.6	10.6	10.6	10.6	10.6	6.8	9.1
FF-35C	6.6	8.0	8.0	8.0	8.0	8.0	5.1	6.8
FF-35E	8.8	10.6	10.6	10.6	10.6	10.6	6.8	9.1
FF-38A	1.6	2.0	2.0	2.0	1.9	2.0	1.3	1.7
FF-38B	3.7	4.4	4.4	4.4	4.4	4.4	2.8	3.8
FF-38C	1.3	1.6	1.6	1.6	1.6	1.6	1.0	1.4
P-24A	5.8	7.1	7.1	7.1	7.1	7.1	4.6	6.1
P-25R	0.7	0.9	0.9	0.9	0.9	0.9	0.6	0.8
P-26	6.6	8.0	8.0	8.0	7.9	8.0	5.1	6.8
P-26A	6.6	8.0	8.0	8.0	7.9	8.0	5.1	6.8
P-26B	7.3	8.9	8.9	8.9	8.8	8.9	5.7	7.6

Injection Wells	Adjusted-Allocated Gas Injection Rate (MMscf/D)							
	10/16	10/17	10/18	10/19	10/20	10/21	10/22	10/23
P-26C	5.8	7.1	7.1	7.1	7.1	7.1	4.6	6.1
P-26D	7.3	8.9	8.9	8.9	8.8	8.9	5.7	7.6
P-30	2.9	3.5	3.5	3.5	3.5	3.5	2.3	3.0
P-32	3.7	4.4	4.4	4.4	4.4	4.4	2.8	3.8
P-32A	6.6	8.0	8.0	8.0	8.0	8.0	5.1	6.8
P-32B	0.7	0.9	0.9	0.9	0.9	0.9	0.6	0.8
P-32C	1.5	1.8	1.8	1.8	1.8	1.8	1.1	1.5
P-32D	7.3	8.9	8.9	8.9	8.8	8.9	5.7	7.6
P-32E	5.1	6.2	6.2	6.2	6.2	6.2	4.0	5.3
P-32F	8.0	9.8	9.8	9.8	9.7	9.8	6.3	8.4
P-37	0.7	0.9	0.9	0.9	0.9	0.9	0.6	0.8
P-37A	2.2	2.7	2.7	2.7	2.7	2.7	1.7	2.3
P-42B	7.3	8.9	8.9	8.9	8.8	8.9	5.7	7.6
P-42C	9.5	11.5	11.5	11.5	11.5	11.5	7.4	9.9
P-68A	8.0	9.8	9.8	9.8	9.7	9.8	6.3	8.4
P-68B	1.5	1.8	1.8	1.8	1.8	1.8	1.1	1.5
P-69A	7.3	8.9	8.9	8.9	8.8	8.9	5.7	7.6
P-69B	5.8	7.1	7.1	7.1	7.1	7.1	4.6	6.1
P-69C	6.6	8.0	8.0	8.0	7.9	8.0	5.1	6.8
P-69D	4.4	5.3	5.3	5.3	5.3	5.3	3.4	4.6
P-69E	8.8	10.6	10.6	10.6	10.6	10.6	6.8	9.1
P-69F	4.4	5.3	5.3	5.3	5.3	5.3	3.4	4.6
P-69H	4.4	5.3	5.3	5.3	5.3	5.3	3.4	4.6
P-69J	0.0	0.0	0.0	0.0	0.0	0.0	0.0	0.0
P-69K	0.0	0.0	0.0	0.0	0.0	0.0	0.0	0.0
P-72A	10.2	12.4	12.4	12.4	12.4	12.4	8.0	10.7
P-72B	8.0	9.8	9.8	9.8	9.7	9.8	6.3	8.4
SS-02	0.7	0.9	0.9	0.9	0.9	0.9	0.6	0.8
SS-06	0.7	0.9	0.9	0.9	0.9	0.9	0.6	0.8
SS-25	4.4	5.3	5.3	5.3	5.3	5.3	3.4	4.6
SS-25B	6.6	8.0	8.0	8.0	8.0	8.0	5.1	6.8
SS-44B	0.7	0.9	0.9	0.9	0.9	0.9	0.6	0.8

3.3.2 Allocated Injected Gas Volume for the Month of October 2015

Table 2 shows the calculated adjusted-allocated daily gas injection rate for each well for the seven days of October, 2015 prior to the leak. Similarly the rates were calculated for each well and day of October, 2015. Summation of calculated rates on each day of October, 2015 (Table 3) was consistent with the reported monthly volume data provided by SoCalGas for October, 2015. The reported monthly volume for October, 2015 was 5,533 MMscf (Figure 21) [7], [9].

Table 3: Adjusted-Allocated Daily Injected Gas Volumes in the West, Central, and East Legs of the Network for October 2015

October 2015	West	Central	East	Daily Total Injected Gas Volume in Network (MMscf)
October 01, 2015	15.5	102.7	116.5	234.7
October 02, 2015	16.8	111.3	126.3	254.3
October 03, 2015	16.9	111.8	126.8	255.5
October 04, 2015	16.9	111.8	126.8	255.5
October 05, 2015	16.9	111.8	134.8	263.4
October 06, 2015	16.8	111.6	134.6	263.0
October 07, 2015	13.7	90.9	115.3	219.9
October 08, 2015	10.6	70.0	98.5	179.1
October 09, 2015	5.2	34.4	50.7	90.3
October 10, 2015	14.3	100.9	145.3	260.5
October 11, 2015	16.9	118.9	171.2	306.9
October 12, 2015	12.4	87.5	126.1	226
October 13, 2015	8.7	61.1	88.0	157.7
October 14, 2015	1.6	11.7	16.7	30.0
October 15, 2015	2.4	17.1	24.7	44.2
October 16, 2015	13.9	97.9	141.0	252.8
October 17, 2015	16.9	118.9	171.2	306.9
October 18, 2015	16.9	118.9	171.2	306.9
October 19, 2015	16.9	118.9	171.2	306.9
October 20, 2015	16.8	118.4	170.7	305.8
October 21, 2015	16.9	118.9	171.2	306.9
October 22, 2015	10.8	76.3	110.0	197.1
October 23, 2015	14.5	102	146.8	263.2
October 24, 2015	1.9	62.9	90.7	155.5
October 25, 2015	0	30.2	60.0	90.2
Total Injected Volume into the Network in October 2015 (MMscf)	**311**	**2,217**	**3,006**	**5,533**

3.4 Model Calibration and Stability Check

This section shows the comparison between the measured or reported input parameters and the model back-calculated results by following the methodology shown in Figure 1. The study compared the following parameters:

- The adjusted-allocated to the model injection rates for all the active wells in the network for October 22, 2015, are shown in Table 4. The difference between them is negligible.
- The total injected gas volume in the West, Central, and East legs, to the model and found that they were in very good agreement with a difference of less than 1% (Table 4).
- The discharge pressure at the Western injection header to the model and found them to be in excellent agreement (Table 5).

This exercise established that the model could accurately capture the performance of the gas injection network and accurately determined adjusted-allocated injection volumes and discharge pressure. The simulations confirmed that the model was suitable to perform sensitivities on WHP settings to assess leak scenarios for SS-25.

Note that this exercise was done for the entire week before October 23, 2015. In addition, the study also tested the model for October 01, 2015, because SoCalGas had the reported WHP for this date.

The study checked the model's robustness by comparing the model-calculated WHP with the weekly reported WHP of SS-25. For October 01, 2015, the reported WHP was 2,610 psi [11] and the model-calculated WHP was 2,645 psi. The difference was only 1%, which could be attributed to daily temperature fluctuation effects on the pressure. In addition, the study used an average of the high frequency pressure data measured at the Western injection header, which could have contributed to the difference between the reported and model-calculated WHP.

The reported WHP was also available for October 15, 2015. The adjusted-allocated gas injection volume for the network for October 15, 2015, was only 44 MMscf. The injection volume of 44 MMscf for the network was much lower than the average daily gas injection volume of the network during the week before October 23, 2015 (Figure 12). Therefore, this study did not consider October 15, 2015, for model testing and WHP comparison.

Table 4: Comparison between the Adjusted-Allocated Injection Rates and Model-Calculated Rates for October 22, 2015

Wells	STEP 1: Adjusted-Allocated (MMscf/D)	STEP 2: Model Back-Calculated (MMscf/D)	Difference (MMscf/D)
West			
SS-25	3.4	3.2	0.2
SS-25B	5.1	5.3	-0.2
West Total:	8.5	8.5	0.0
Central			
P-24A	4.6	4.8	-0.2
P-26	5.1	4.9	0.2
P-26A	5.1	4.9	0.2
P-26B	5.7	5.8	-0.1
P-26C	4.6	4.6	0.0
P-26D	5.7	5.8	-0.1
P-42B	5.7	5.6	0.1
P-42C	7.4	7.4	0.0
P-69A	5.7	6.0	-0.3
P-69B	4.6	4.3	0.3
P-69C	5.1	5.2	-0.1
P-69D	3.4	3.5	-0.1
P-69E	6.8	6.7	0.1
P-69F	3.4	3.2	0.2
P-69H	3.4	3.2	0.2
Central Total:	76.3	75.9	0.4
East			
FF-32	4.6	4.2	0.4
FF-32A	8.0	7.7	0.3
FF-32B	3.4	2.9	0.5
FF-32C	6.8	7.1	-0.3
FF-32F	4.6	4.6	0.0
FF-35A	6.8	6.8	0.0
FF-35B	6.8	6.8	0.0
FF-35C	5.1	4.9	0.2
FF-35E	6.8	6.7	0.1
FF-38A	1.3	1.8	-0.5
FF-38B	2.8	2.8	0.0
FF-38C	1.0	1.7	-0.7

Wells	STEP 1: Adjusted-Allocated (MMscf/D)	STEP 2: Model Back-Calculated (MMscf/D)	Difference (MMscf/D)
P-30	2.3	0.9	1.4
P-32	2.8	2.9	-0.1
P-32A	5.1	4.9	0.2
P-32C	1.1	0.9	0.2
P-32D	5.7	5.6	0.1
P-32E	4.0	4.1	-0.1
P-32F	6.3	6.2	0.1
P-37A	1.7	2.1	-0.4
P-68A	6.3	5.8	0.5
P-68B	1.1	3.8	-2.7
P-72A	8.0	7.7	0.3
P-72B	6.3	6.2	0.1
East Total:	108.8	109.1	-0.3
West+Central+East Total:	193.6	193.5	0.1

3.5 Model Robustness Observations

The measured discharge pressure at the Western injection header during the seven days prior to the leak ranged between 2,800 to 2,860 psi.

For each day tested, the discharge pressure calculated by the model was consistent with the measured discharge pressure (Table 5). It should be noted that in the field, the discharge pressure data was measured 3–5 times every minute. This study averaged the high frequency pressure data of each day and implemented the averaged discharge pressure in the model.

Table 5: Western Injection Header Pressure during the Seven Days Prior to the Leak

Date	Measured Discharged Pressure at Western Injection Header (psi)	Model-Calculated Discharge Pressure at Western Injection Header (psi)
October 16, 2015	2,805	2,805
October 17, 2015	2,826	2,826
October 18, 2015	2,850	2,850
October 19, 2015	2,858	2,858
October 20, 2015	2,821	2,821
October 21, 2015	2,819	2,819
October 22, 2015	2,807	2,807
October 23, 2015	2,811	2,811

The total adjusted-allocated daily gas injection volume at the compressor station during the seven days prior to the leak ranged between 194 and 302 MMscf. For each day tested, the daily total injected gas volume at the compressor station calculated by the model was consistent with the total adjusted-allocated daily injected gas volume (Table 6).

Table 6: Total Daily Gas Injection Volume at the Compressor Station during the Seven Days Prior to the Leak

Date	Adjusted-Allocated Total Daily Injected Gas Volume at the Compressor Station (MMscf)	Model-Calculated Total Daily Injected Gas Volume at the Compressor Station (MMscf)
October 16, 2015	248.5	248.5
October 17, 2015	301.6	301.6
October 18, 2015	301.6	301.6
October 19, 2015	301.6	301.6
October 20, 2015	300.5	300.5
October 21, 2015	301.6	301.6
October 22, 2015	193.4	193.1
October 23, 2015	258.6	258.6

The daily adjusted-allocated gas injection rate into SS-25 during the seven days prior to the leak ranged between 3–5 MMscf/D. For each day tested, the daily gas injection rate into SS-25 calculated by the model was in agreement with the adjusted-allocated daily gas injection rate (Table 7), with a difference of 10% or less.

Table 7: Daily Gas Injection Rate into SS-25 during the Seven Days Prior to Leak

Date	Adjusted-Allocated Gas Injection Rate into SS-25 (MMscf/D)	Model-Calculated Gas Injection Rate into SS-25 (MMscf/D)
October 16, 2015	4.4	4.8
October 17, 2015	5.3	5.4
October 18, 2015	5.3	5.3
October 19, 2015	5.3	5.5
October 20, 2015	5.3	5.3
October 21, 2015	5.3	5.4
October 22, 2015	3.4	3.8
October 23, 2015	4.6	4.9

4 Results and Discussions

The results and observations of the study are documented in this section.

4.1 Pressure and Rate Analysis: For the Week Prior to Leak

The study simulated leak scenarios by reducing the SS-25 WHP gradually by a magnitude of up to 2,000 psi from its base case value of 2,740 psi (no leak scenario), without changing the choke settings. This exercise was repeated for each day of the week prior to the leak.

The study estimated that even when the WHP at SS-25 was reduced by 2,000 psi from the base case value, the corresponding pressure drop at the injection manifold located just before SS-25 and SS-25B was only 15 psi. This trend was observed on all the days analyzed in the one-week period prior to the leak date (Figure 10).

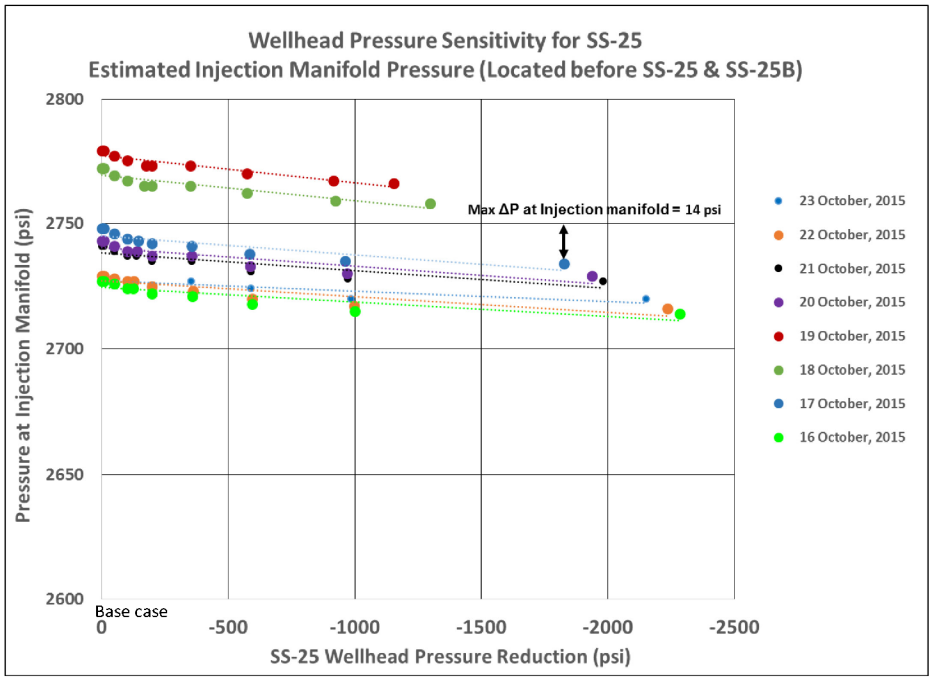

Figure 10: Estimated Injection Manifold Pressure (Located Before SS-25 and SS-25B)

In the leak scenarios simulated by lowering the SS-25 WHP setting, gas with rates from 10 to 70 MMscf/D could have been injected into SS-25 on any day during the week analyzed (Figure 11). Table 7 shows that in the absence of a leak, the adjusted-allocated daily gas injection rate in well SS-25 was estimated to be 3 to 5 MMscf/D. This volume depended on the discharge pressure at the compressor station, as well as the number of online injection hours on a particular day.

For injection rates up to 40 MMscf/D, the corresponding pressure drop at the injection manifold was in the range of 0–6 psi. However, for injection rates higher than 40 MMscf/D, the variance in pressure was 7–14 psi, which should be noticeable at the injection manifold. Therefore, if the injection manifold pressure was not being monitored closely for pressure variance, then the increased injection volume being injected into SS-25 might have gone unnoticed.

Figure 11 shows the estimated gas injection rate into SS-25 for various leak scenarios simulated by reduction in the WHP. For all the days analyzed, the model consistently estimated the gas injection rates into SS-25 with reductions in WHP, despite having different discharge pressure setting at the compressor station.

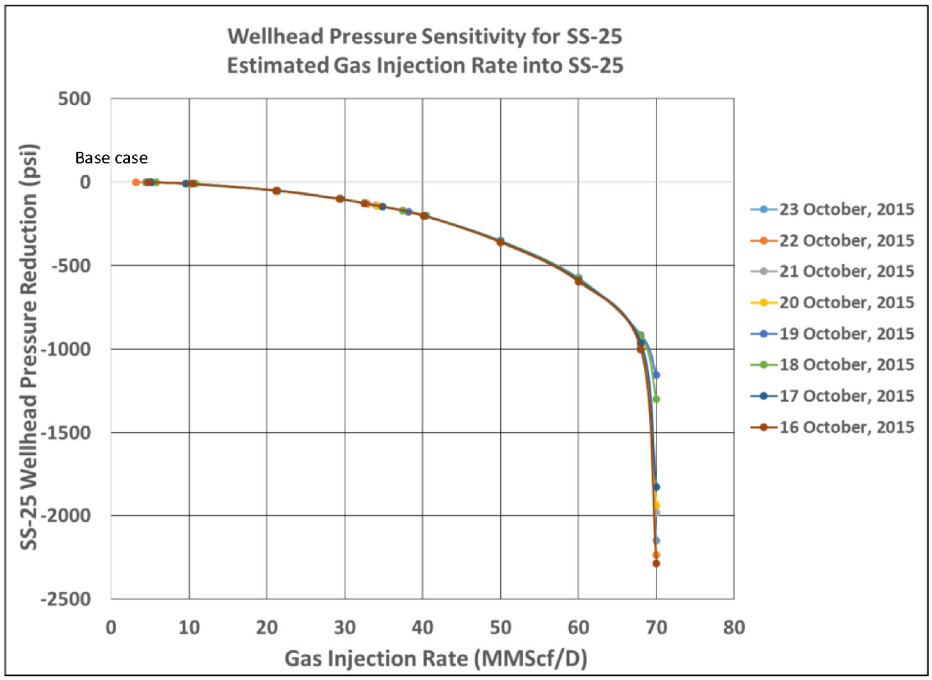

Figure 11: Estimated Gas Injection Rate into SS-25

4.2 Pressure and Rate Analysis: Selecting a Date

Figure 12 shows the adjusted-allocated daily total gas injection volumes at the Western injection header of compressor station during the seven-day period prior to the leak date. The daily gas injection volume ranged from 194 to 302 MMscf.

For all the days analyzed prior to the leak date, the model consistently estimated the gas injection rate into SS-25 with reductions in WHP, despite having different discharge pressure settings at the compressor station. Hence, this study selected one of the seven days as the representative day to analyze the gas network performance in more detail.

October 21, 2015, was selected as the representative date for further pressure and rate analysis for the following reasons:

- The adjusted-allocated injection volume for the network on October 21, 2015, was about 302 MMscf. This can be seen to be the most repeated injection volume during the week prior to the leak (Figure 12).
- The measured discharge pressure reading was also available for October 21, 2015.

Although the measured discharge pressures were also available for October 22, 2015, and October 23, 2015, this study did not select them as the representative date because during those days the injection volume for the entire network was much lower than the average daily gas injection volume of the network during that week.

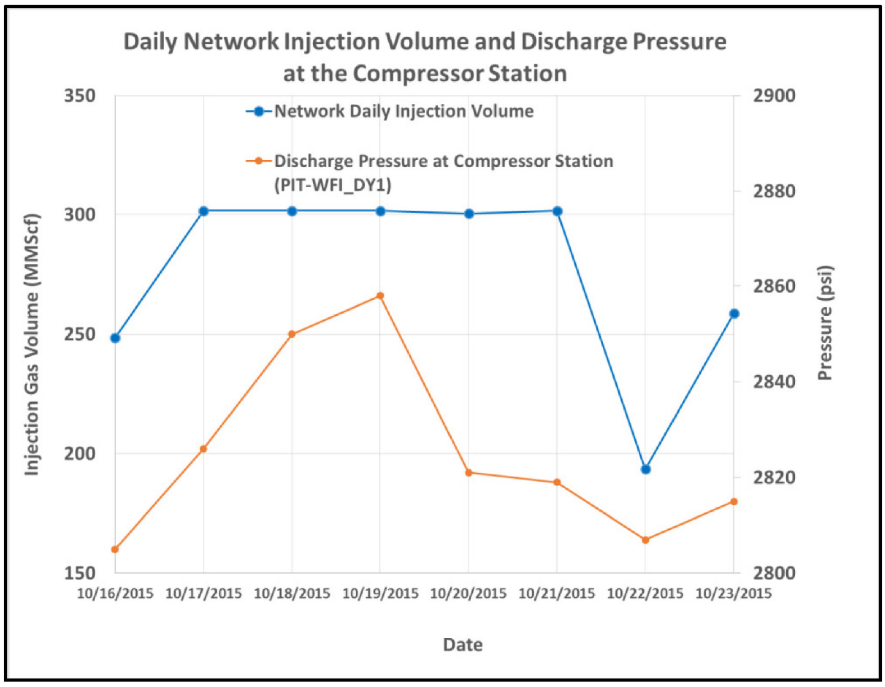

Figure 12: Adjusted-Allocated Daily Network Gas Injection Volume and Measured Discharge Pressure at the Western Injection Header near Compressor Station

4.2.1 Detailed Pressure and Rate Analysis for the Selected Day

As discussed in Section 4.2, this study selected one day out of the seven days considered as representative to conduct detailed pressure and rate analysis while simulating leak scenarios. The study compared the pressure drops and injectability between the base case and the cases when the WHP at SS-25 was lowered. The study compared:

- The pressure drops at various nodes of SS-25, i.e., the injection manifold, the choke manifold, and the wellhead.
- The pressure drops at various injection headers of the network.
- The injectability of the East, Central, and West legs of the network.
- The contribution to additional injection volume into SS-25 by each leg of the network and SS-25B.
- The wells in the East and Central networks, grouped by location in the network; this study compared the injection manifold pressure (before choke) of these groups of wells.

4.3 Pressure at Various Manifolds of SS-25

The study estimated the pressure drop at various nodes of the network (Figure 8 and Figure 9) when the WHP of SS-25 was reduced gradually by a magnitude of up to 2,000 psi from its base case value of 2,740 psi (no leak scenario). The date selected to simulate leak scenarios was October 21, 2015.

With a pressure reduction of about 2,000 psi at the wellhead of SS-25, the corresponding pressure drop at the injection manifold (located just before SS-25 and SS-25B) was less than 15 psi (Figure 13). However, with a 15 psi pressure drop at the injection manifold, SS-25 could have injected gas up to a rate of 70 MMscf/D.

The corresponding change in pressure required at the Western injection header (PIT_WFI_DY1) to increase the injection rate from 5 MMscf/D to 70 MMscf/D was negligible (1 psi) (Figure 13).

The pressure drop at the choke manifold was high and equivalent to the WHP reduction (Figure 13). It allowed the increase in injection volume to flow through the choke and into SS-25, based on the assumption that the choke settings for SS-25 were not changed during that week.

At an injection rate of 70 MMscf/D and an inlet temperature of 80°F, the pressure at the injection manifold was 2,725 psi, whereas the pressure was 755 psi after the choke. This showed that the critical flow rate could be obtained with zero or minimal change in measured pressure depending on the location of the pressure measurement node. Therefore, if the pressure was being monitored only at the Western injection header near the compressor station, then the increased gas volume being injected into SS-25 in the event of a leak could have remained undetected.

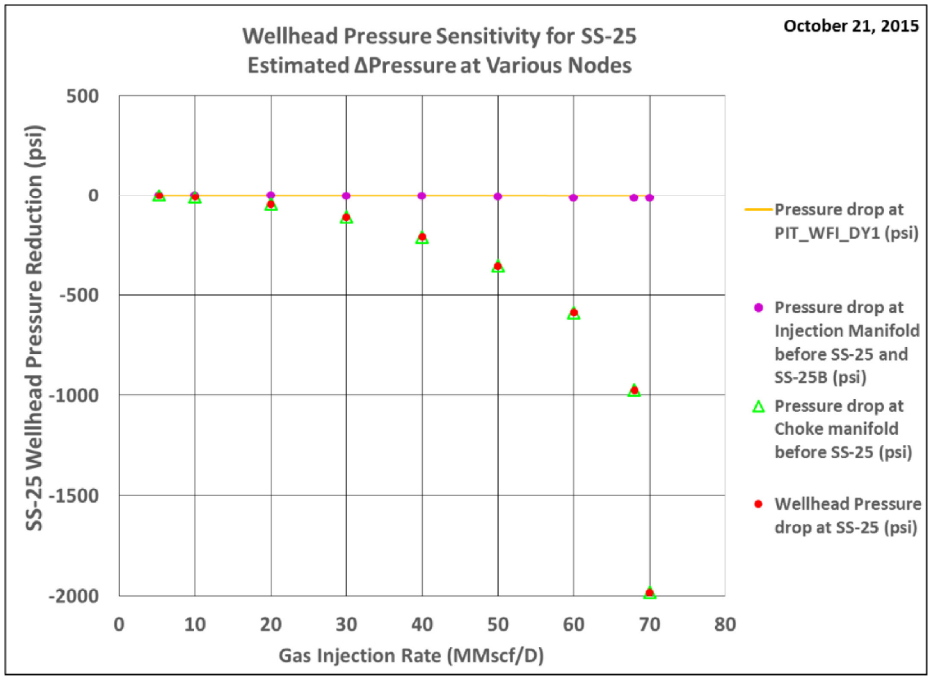

Figure 13: Estimated ΔPressure at Various Nodes of SS-25 and the Injection Network

Figure 13 shows the model-estimated pressure at various nodes of the network and their corresponding pressure drops when the injection rate into SS-25 increased from 5 MMscf/D to a critical flow rate of 70 MMScf/D.

During normal injection of 5.3 MMscf/D into SS-25 in the base case, there was approximately 80 psi of head between the injection manifold and the Western injection header near the compressor station (PIT_WFI_DY1). These two nodes are about 6,200 ft apart, which, along with elevation changes of about 1,100 ft, could have contributed to pressure changes between these two nodes. It was assumed that the pipeline had surface roughness of a new pipe and frictional losses within the pipe were negligible.

Table 8 shows estimated pressure drop at various nodes of SS-25 and the injection network.

Table 8: Estimated ΔPressure at Various Nodes of SS-25 and the Injection Network

	Base Case	Various Leak Scenarios Simulation Results						
Injection Rate at SS-25 (MMscf/D)	5.3	10	20	30	40	50	60	70
Pressure at Various Nodes of the Network (psi)								
Pressure at PIT_WFI_DY1	2,819	2,819	2,819	2,819	2,819	2,819	2,818	2,818
Pressure Drop at PIT_WFI_DY1	0	0	0	0	0	0	–1	–1
Pressure at Injection Manifold Before SS-25 and SS-25B	2,741	2,741	2,740	2,738	2,737	2,735	2,731	2,727
Pressure Drop at Injection Manifold Before SS-25 and SS-25B	0	0	–1	–3	–4	–6	–10	–14
Pressure at Choke Manifold Before SS-25	2,738	2,729	2,692	2,627	2,528	2,382	2,150	756
Pressure Drop at Choke Manifold Before SS-25	0	–9	–46	–111	–210	–356	–588	–1,982
Wellhead Pressure at SS-25	2,738	2,729	2,692	2,627	2,528	2,382	2,150	756
Wellhead Pressure Reduction at SS-25	0	–9	–46	–111	–210	–356	–588	–1,982

4.4 Injectability and Pressure Drop Analysis by Network Legs

For a measured discharge pressure of 2,820 psi at the Western injection header and a total adjusted-allocated injected gas volume of about 302 MMscf on October 21, 2015, the study concluded the following (Figure 14):

- There was redistribution of injection volumes from all legs of the network into SS-25.
- The East leg contributed most to the additional injection gas volume into SS-25, followed by the Central and West legs of the network.
- For a reduction in WHP of up to 350 psi at SS-25, the network continued to inject into both SS-25 and SS-25B. However, for WHP reduction higher than 350 psi, the entire injection gas volume of SS-25B could have been injected into SS-25.

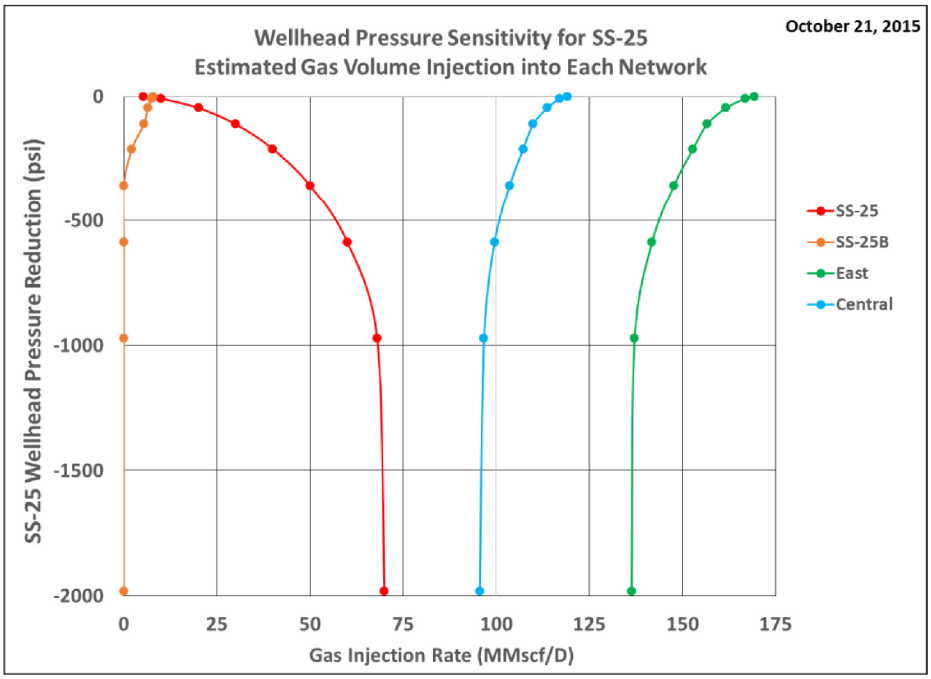

Figure 14: Estimated Gas Injection Volume into Each Leg of the Network

With each case of WHP reduction at SS-25 simulating a leak, the study estimated and plotted injection header pressure of each leg and injection manifold pressure of certain groups of wells (before choke). Figure 15 shows the results for the Central leg, and Figure 16 shows the results for the East leg of the network.

The study estimated that when the WHP at SS-25 was lowered by a magnitude of about 2,000 psi, the corresponding pressure drop at the header or injection manifolds of wells groups fluctuated from 0–8 psi at the Central leg (Figure 15) and 0–10 psi at the Eastern leg (Figure 16). These oscillations are minimal and could have been deemed as routine pressure drops within the realm of temperature fluctuations' impact on pressure measurements over the course of a day. However, in the same WHP reduction scenarios at SS-25, gas with a rate up to 70 MMscf/D could have been injected into SS-25. This corresponds to 65 MMscf of total daily gas volume that could have been redirected from the East and Central legs of the network and SS-25B and injected into SS-25, in addition to its adjusted-allocated injection rate of 5 MMscf/D.

Therefore, if the pressure was being monitored only at the injection headers of East and Central legs of the network, then the decrease in the injection volume of these legs to be injected into SS-25 in the event of a leak could have remained undetected.

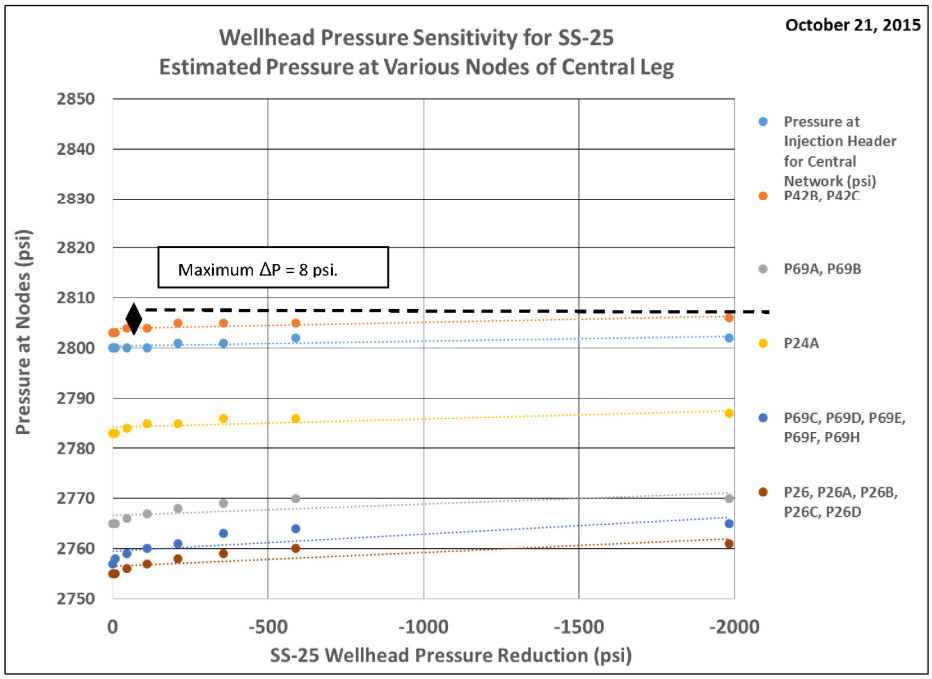

Figure 15: Estimated Injection Manifold Pressure for Central Leg of the Network

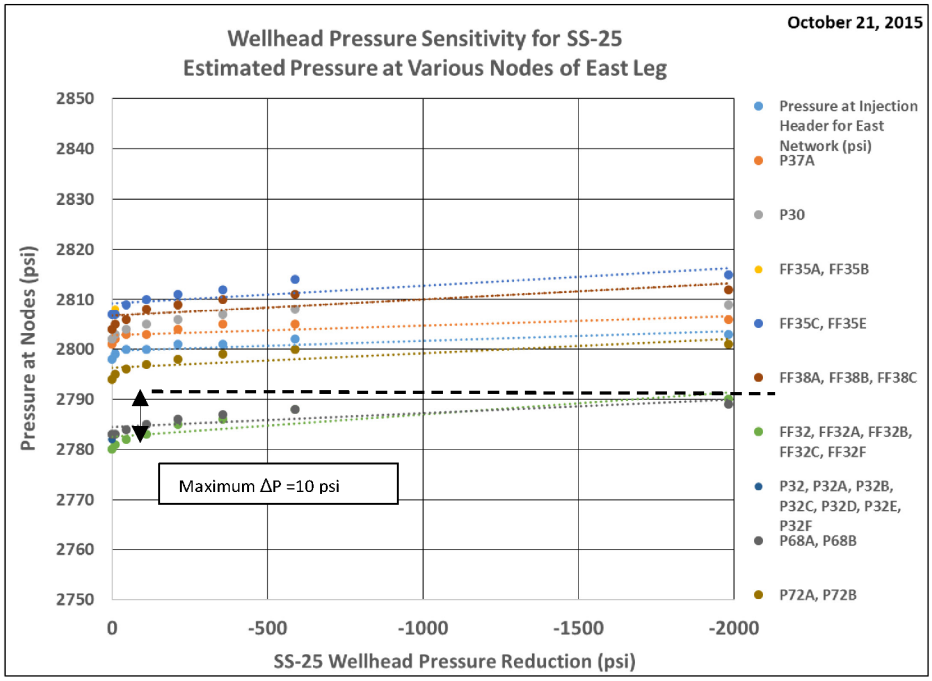

Figure 16: Estimated Injection Manifold Pressure for East Leg of the Network

Figure 17 shows the estimated gas injection contribution from each network leg into SS-25 when simulating various leak scenarios. A portion of the injection volumes from other network legs can be injected into SS-25, even with a WHP reduction of only 10 psi at SS-25 psi from its base case value of 2,740

psi. The East leg contributes the most to the additional injection gas volume into SS-25, followed by the Central and West legs of the network.

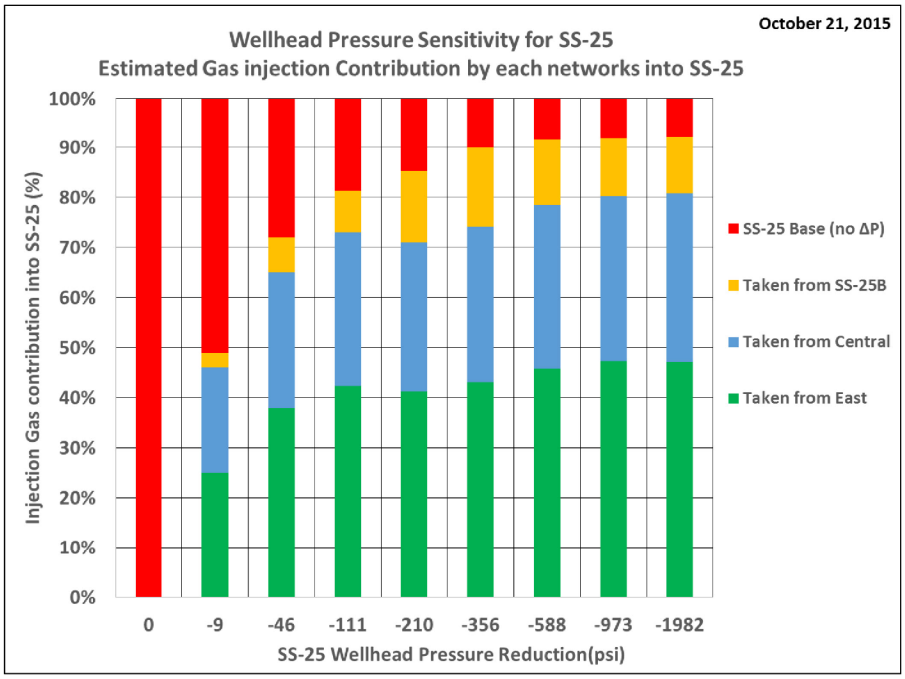

Figure 17: Estimated Gas Injection Contribution by Each Network into SS-25

Table 9 shows the contribution by each leg of the network into SS-25 in the event of leak.

Table 9: Estimated Contribution by Each Leg of the Network into SS-25

	Base Case	Various Leak Scenarios Simulation Results						
Injection Rate at SS-25 (MMscf/D)	5.3	10	20	30	40	50	60	70
Wellhead Pressure at SS-25 (psi)	2,738	2,729	2,692	2,627	2,528	2,382	2,150	756
Wellhead Pressure Reduction at SS-25 (psi)	0	–9	–46	–111	–210	–356	–588	–1,982
Model-Estimated Contribution into SS-25 (MMscf/D)								
Taken from SS-25B	0.0	0.3	1.4	2.5	5.7	7.9	7.9	7.9
Taken from Central	0.0	2.1	5.4	9.2	11.9	15.5	19.6	23.6
Taken from East	0.0	2.5	7.6	12.7	16.5	21.6	27.5	33.0
Total Δ SS-25	0.0	4.9	14.4	24.4	34.1	45.0	55.0	64.5

4.5 Results Summary

4.5.1 Pressure Monitoring at Injection Manifold

The study showed that when the WHP at SS-25 was reduced by about 2,000 psi to simulate a leak, gas at a rate of up to 70 MMscf/D could be injected into SS-25, compared to the nominal injection rate of up to 5 MMscf/D. However, the reduction of 2,000 psi at SS-25 WHP only translated into a pressure drop of less than 15 psi at the injection manifold. For injection rates higher than 60 MMscf/D, the variance in pressure was more than 10 psi, which should have been noticeable at the injection manifold.

4.5.2 Pressure Monitoring at Choke Manifold

The study indicated that when the WHP at SS-25 was lowered by about 2,000 psi and the corresponding pressure drop at the injection manifold was less than 15 psi, the pressure drop at the choke manifold was high and equivalent to the WHP reduction of about 2,000 psi. This high drop allowed the increase in injection volume to flow through the choke and into SS-25.

4.5.3 Pressure Monitoring at Injection Headers of Compression Station

Estimated Pressure at the Western Injection Header

The study concluded that the change in pressure required to increase the injection rate into SS-25 from 5 MMscf/D to 70 MMscf/D was negligible (1 psi) at the Western injection header near the compressor station closest to SS-25. The critical flow rate could be obtained with zero or minimal change in measured pressure depending on the location of the pressure measurement node. Therefore, if the pressure was being monitored only at the Western injection header near the compressor station, then the increased gas volume being injected into SS-25 in the event of a leak could have gone unidentified.

Estimated Pressure at Central and Eastern Injection Header

The study estimated that when the WHP at SS-25 was reduced by about 2,000 psi to simulate a leak, the corresponding pressure drop fluctuated up to 8 psi at Central injection header and up to 10 psi at the Eastern injection header. These oscillations are minimal and acceptable as the pressure drop within the realm of temperature fluctuations over the course of a day. However, an additional daily gas volume of about 65 MMscf could have been redirected from the East and Central legs of the network and SS-25B and been injected into SS-25. Therefore, if the pressure was being monitored only at the injection headers of East and Central legs of the network, then the decrease in the injection volume of these legs to be injected into SS-25 in the event of a leak could have remained undetected.

4.5.4 Volumetric Analysis

There was redistribution of injection volumes from all legs of the network into SS-25, even with a WHP reduction of 10 psi at SS-25 simulating a leak scenario. The East leg contributed most to the additional injection gas volume into SS-25, followed by the Central and West legs of the network.

For a reduction in WHP of up to 350 psi at SS-25, the network continued to inject into both SS-25 and SS-25B. However, for WHP reduction higher than 350 psi, the entire injection gas volume of SS-25B could have been injected into SS-25.

In the absence of a leak, the nominal injection rate for SS-25 determined in the study was 3 to 5 MMscf/D. However, the study results showed that in the event of a leak, when SS-25 WHP is reduced by about 2,000 psi, the gas injection network can inject up to 14 times the nominal injection rate into SS-25 without any significant change in pressure at the Western injection header.

5 Conclusions and Recommendations

The study found that, in the event of a leak in SS-25, the pressure variations at the injection headers would have been minimal and not significant enough to be detected. If the pressure was being monitored only at the Western injection header near the compressor station, then in the event of a leak, the increased gas volume injected into SS-25 could have remained undetected.

It is best practice to monitor pressure at each node of the network such as wellheads, injection manifolds and injection headers. A real-time field-wide pressure surveillance system with intelligent evaluation capability can continuously analyze pressure measurements at various nodes of the network. It can quickly detect and notify if gas is being distributed at a significantly different rate than expected, which could indicate a surface or wellbore leak.

6 References

[1] SoCalGas, "B16-Q1- Discharge Pr Leaving the Station.txt".

[2] SoCalGas, "B16-Q1-Pr Transmitter to Main Injection Line to West Field.txt".

[3] SoCalGas, "B16-Q1-Pressure transmitter of the turbine compressors.txt".

[4] SoCalGas, "AC_BLD_0075830.xlsx".

[5] SoCalGas, "Blade-16.pdf".

[6] SoCalGas, "B16-Q1- Temperature Turbine Compressors.txt".

[7] SoCalGas, "AC Monthly Inj & Prod July – Dec 2015 report".

[8] SoCalGas, "UGS Inj & WD Well Report".

[9] SoCalGas, "Well gas allocations 10-2015 AC_BLD_0075724.xlsx".

[10] SoCalGas, "SS-25 Wellhead Pressure_01-06-12 to 10-15-15.pdf".

[11] SoCalGas, "AC_BLD_0075828 weekly pressure SS-25.xlsx".

[12] SoCalGas, "SS-25 Wellbore Operations Jul 23-Oct 23 2015.pdf".

[13] SoCalGas, "SS-25 Temperature Suvey & Wellhead Pressure.pdf".

[14] SoCalGas, "AC_BLD_0003725".

[15] SoCalGas, "SS-25 Maps.pdf".

[16] SoCalGas, "Bates range AC_BLD_0044795 to AC_BLD_0044798".

[17] SoCalGas, "AC_BLD_0003625 (Injection + Withdrawal procedure and processes.pdf)".

[18] SoCalGas, "C025 Responses to Blade RCA Data Request February 11, 2016.pdf".

[19] SoCalGas, "C066 Blade-5.pdf".

[20] SoCalGas, "Blade-21 (Q3-6).pdf".

[21] SoCalGas, "Blade-Follow Up Request_82918_1.pdf".

[22] SoCalGas, "SS-25A - API_04_03721322_Injection_29-May-2016.xlsx".

[23] SocalGas, "B16-Q1-Pressure transmitter of the turbine compressors.pdf".

[24] SoCalGas, "B16-Q1- Discharge Pr Leaving the Station.pdf".

[25] SoCalGas, "B16-Q1-Pr Transmiter to Main Injection Line to West Field.pdf".

[26] SoCalGas, "AC Daily Injection and Withdrawal 01-2014_01-2016 [17811].xlsx".

[27] SoCalGas, "AC Inventory & Pressure-10yearsData (2)AC_BLD_0019460.xlsx".

[28] SoCalGas, "AC Injection_Withdrawal quantities (01-2014_12-2015) AC_BLD_0017451.xlsx".

[29] SoCalGas, "SS-25 - API_04_03700776_Injection_29-May-2016.xlsx".

[30] SocalGas, "SS-25B API_04_03721323_Injection_29-May-2016.xlsx".

Appendix A Compressor Pressure During injection Operations

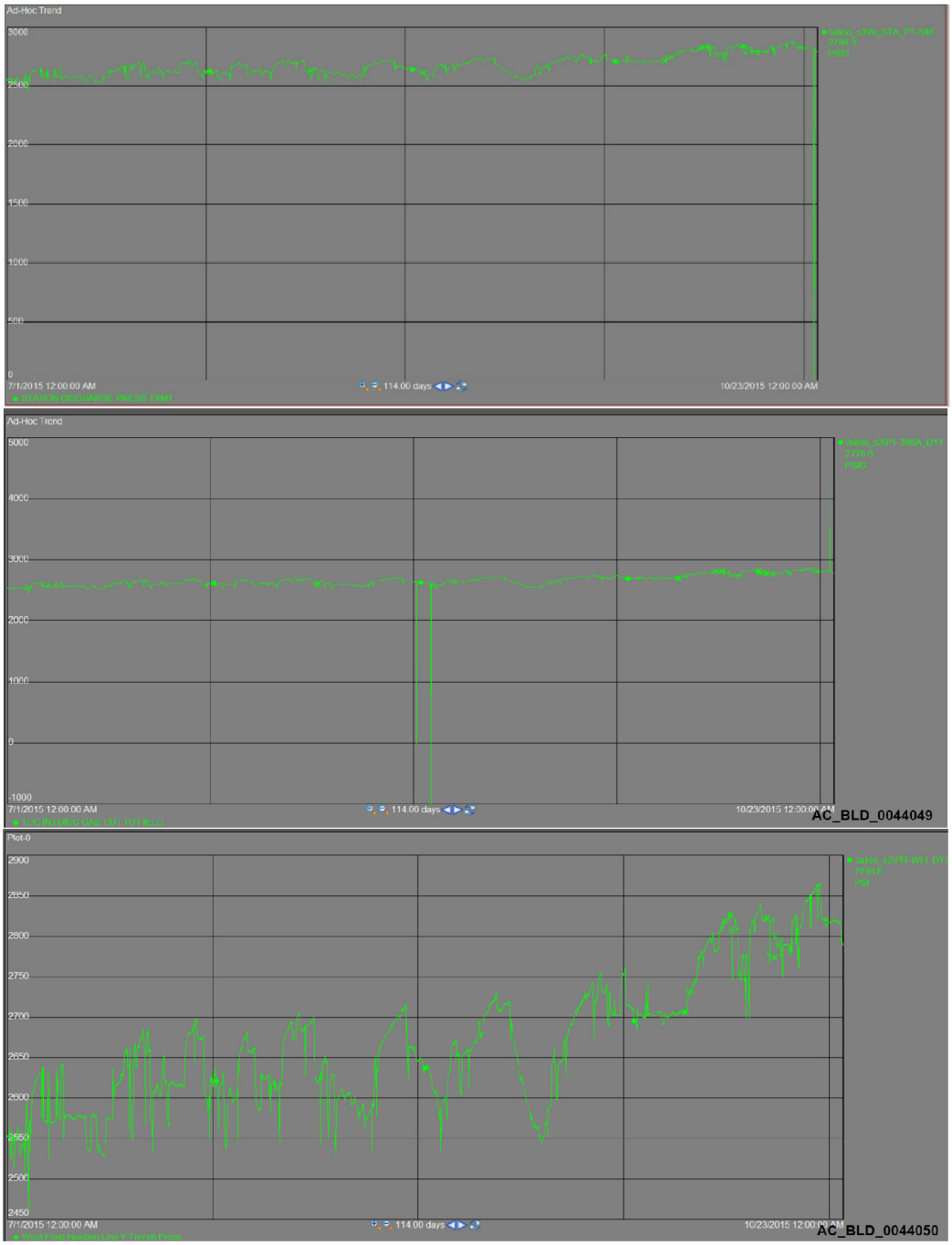

Figure 18: Discharge Pressure Leaving the Compressor Station to West Field-PIT-WFI_DY1 (West Field Injection Line Y-Trench Press) [23], [24], [25]

Appendix B Injection Data from Various Data Sources

Est. Total Gas WD (MMSCF)	40.3	49.7	49.5	49.0	47.6	42.4	41.7	41.6	92.5	39.8	41.7	42.0	171.4	39.7	53.5	41.3	41.1	35.0	7.3	2.4	4.8	7.2	20.5	20.4	19.7	11.4	0.0	0.0	0.0	0.0	0.0	
Hrs of Engine Operation	13.8	24.0	19.2	10.4	17.7	0.0	21.0	24.0	24.0	23.8	19.1	0.0	0.0	0.0	0.0	0.0	0.0	0.0	6.4	23.5	24.0	24.0	24.0	11.9	0.0	0.0	0.0	0.0	14.8	23.6	16.7	
Well Count	44	44	44	44	45	45	48	49	50	51	51	51	51	51	51	51	51	51	51	51	51	51	51	51	39	0	0	0	0	0	0	
Injection / Withdrawal	I	I	I	I	I	I	I	W	I	I	I	W	W	I	I	I	I	I	I	I	I	I	I	I	W	W	W	W	W	W	W	
Inj / WD Quantity (MMcf)	281	338	362	289	349	257	73	-64	327	297	178	-105	-32	102	197	348	381	282	136	98	38	82	8	3	-8	-1	-1	-1	-1	-1	-1	4426
% of Working Capacity	84.8%	85.1%	85.5%	85.9%	86.3%	86.7%	87.0%	87.1%	87.0%	87.4%	87.7%	87.9%	87.8%	87.7%	87.9%	88.1%	88.5%	88.9%	89.3%	89.4%	89.5%	89.6%	89.7%	89.7%	89.7%	89.7%	89.7%	89.7%	89.7%	89.7%	89.7%	
I/W	I	I	I	I	I	I	I	I	I	W	I	I	I	W	W	W	I	I	I	I	I	I	I	I	I	I	W	I	W	W	W	
Inplace (BCF)	72.713	72.858	73.067	73.386	73.724	73.987	74.324	74.563	74.687	74.593	74.798	75.105	75.244	75.193	75.139	75.103	75.301	75.604	75.950	76.332	76.683	76.812	76.891	77.006	77.078	77.102	77.098	77.098	77.098	77.098	77.098	
*Rate (MMscf/day)	113.95	144.9	209.2	319.1	337.4	263.8	336.9	239.6	124.5	-94.4	204.8	307.1	139.0	-50.6	-54.5	-35.9	197.8	303.1	345.8	382.8	350.3	129.1	79.1	115.5	71.4	24.2	-3.5	0.1	0.0	0.0	0.0	4738
Pressure SS-5	2553	2565	2570	2580	2586	2594	2601	2605	2607	2598	2604	2611	2616	2595	2586	2586	2596	2610	2620	2632	2641	2649	2655	2588	2521	2484	2447	2436	2424	2416	2407	
Pressure W-3A	2682	2686	2691	2704	2712	2723	2737	2747	2752	2753	2754	2759	2765	2765	2767	2764	2766	2771	2779	2792	2795	2795	2795	2794	2744	2788	2787	2783	2780	2777	2772	
**Pr Transmiter to Main Injection Line to West Field.txt	2723	2740	2774	2791	2788	2813	2811	2789	2762	2794	2830	2809	2803	2785	2790	2805	2826	2850	2858	2821	2819	2807										Gas injection (mmcf) (Per well in october)
Wells Injection Hours																																
FF32	0.	0.	0.	0.	0.	0.	0.	2.5	7.4	20.4	24.	17.7	12.3	2.5	3.5	19.8	24.	24.	24.	23.9	24.	15.4	20.6	12.7	8.6	0.	0.	0.	0.	0.	0.	84.905	18	18
FF32A	22.	23.9	24.	24.	24.	24.	19.5	15.	7.4	20.4	24.	17.7	12.3	2.5	3.5	19.8	24.	24.	24.	23.9	24.	15.4	20.6	12.7	8.6	0.	0.	0.	0.	0.	0.	238.614	25	25
FF32B	22.	23.9	24.	24.	24.	24.	19.5	15.	7.4	20.4	24.	17.7	12.3	2.5	3.5	19.8	24.	24.	24.	23.9	24.	15.4	20.6	12.7	8.6	0.	0.	0.	0.	0.	0.	102.263	25	25
FF32C	22.	23.9	24.	24.	24.	24.	19.5	15.	7.4	20.4	24.	17.7	12.3	2.5	3.5	19.8	24.	24.	24.	23.9	24.	15.4	20.6	12.7	8.6	0.	0.	0.	0.	0.	0.	204.526	25	25
FF32F	22.	23.9	24.	24.	24.	24.	19.5	15.	7.4	20.4	24.	17.7	12.3	2.5	3.5	19.8	24.	24.	24.	23.9	24.	15.4	20.6	12.7	8.6	0.	0.	0.	0.	0.	0.	196.351	25	25
FF35A	22.	23.9	24.	24.	24.	24.	19.5	15.	7.4	20.4	24.	17.7	12.3	2.1	3.5	19.8	24.	24.	24.	23.9	24.	15.4	20.6	12.7	8.6	0.	0.	0.	0.	0.	0.	204.349	25	25
FF35B	0.	0.	0.	0.	0.	0.	6.5	15.	7.4	20.4	24.	17.7	12.3	2.1	3.5	19.8	24.	24.	24.	23.9	24.	15.4	20.6	12.7	8.6	0.	0.	0.	0.	0.	0.	135.652	19	19
FF35C	0.	0.	0.	0.	24.	24.	19.5	15.	7.4	20.4	24.	17.7	12.3	2.	3.5	19.8	24.	24.	24.	23.9	24.	15.4	20.6	12.7	8.6	0.	0.	0.	0.	0.	0.	121.999	21	21
FF35E	0.	0.	0.	0.	0.	0.	6.3	15.	7.4	20.4	24.	17.7	12.3	2.	3.5	19.8	24.	24.	24.	23.9	24.	15.4	20.6	12.7	8.6	0.	0.	0.	0.	0.	0.	135.523	19	19
FF38A	22.	23.9	24.	24.	24.	24.	19.5	15.	7.4	20.4	24.	17.7	12.3	2.2	3.5	19.8	24.	24.	24.	23.9	24.	15.4	20.6	12.7	8.6	0.	0.	0.	0.	0.	0.	37.472	25	25
FF38B	22.	23.9	24.	24.	24.	24.	19.5	15.	7.4	20.4	24.	17.7	12.3	2.2	3.5	19.8	24.	24.	24.	23.9	24.	15.4	20.6	12.7	8.6	0.	0.	0.	0.	0.	0.	85.158	25	25
FF38C	22.	23.9	24.	24.	24.	24.	19.5	15.	7.4	20.4	24.	17.7	12.3	2.1	3.5	19.8	24.	24.	24.	23.9	24.	15.4	20.6	12.7	8.6	0.	0.	0.	0.	0.	0.	30.654	25	25
P24A	0.	0.	0.	0.	0.	0.	0.	0.	0.	20.4	24.	17.7	12.3	2.5	3.5	19.8	24.	24.	24.	23.9	24.	15.4	20.6	12.7	8.6	0.	0.	0.	0.	0.	0.	81.996	16	16
P25R	22.	23.9	24.	24.	24.	24.	19.5	15.	7.4	20.4	24.	17.7	12.3	2.5	3.5	19.8	24.	24.	24.	23.9	24.	15.4	20.6	12.7	0.	0.	0.	0.	0.	0.	0.	16.726	24	24
P26	22.	23.9	24.	24.	24.	24.	19.5	15.	7.4	20.4	24.	17.7	12.3	2.5	3.5	19.8	24.	24.	24.	23.9	24.	15.4	20.6	12.7	8.6	0.	0.	0.	0.	0.	0.	153.395	25	25
P26A	22.	23.9	24.	24.	24.	24.	19.5	15.	7.4	20.4	24.	17.7	12.3	2.5	3.5	19.8	24.	24.	24.	23.9	24.	15.4	20.6	12.7	8.6	0.	0.	0.	0.	0.	0.	153.395	25	25
P26B	22.	23.9	24.	24.	24.	24.	19.5	15.	7.4	20.4	24.	17.7	12.3	2.5	3.5	19.8	24.	24.	24.	23.9	24.	15.4	20.6	12.7	0.	0.	0.	0.	0.	0.	0.	167.264	24	24
P26C	22.	23.9	24.	24.	24.	24.	19.5	15.	7.4	20.4	24.	17.7	12.3	2.5	3.5	19.8	24.	24.	24.	23.9	24.	15.4	20.6	12.7	0.	0.	0.	0.	0.	0.	0.	133.811	24	24
P26D	22.	23.9	24.	24.	24.	24.	19.5	15.	7.4	20.4	24.	17.7	12.3	2.5	3.5	19.8	24.	24.	24.	23.9	24.	15.4	20.6	12.7	8.6	0.	0.	0.	0.	0.	0.	170.438	25	25
P30	22.	23.9	24.	24.	24.	24.	19.5	15.	7.4	20.4	24.	17.7	12.3	2.5	3.5	19.8	24.	24.	24.	23.9	24.	15.4	20.6	12.7	8.6	0.	0.	0.	0.	0.	0.	68.175	25	25
P32	22.	23.9	24.	24.	24.	24.	19.5	15.	7.4	20.4	24.	17.7	12.3	2.5	3.5	19.8	24.	24.	24.	23.9	24.	15.4	20.6	12.7	8.6	0.	0.	0.	0.	0.	0.	85.219	25	25
P32A	0.	0.	0.	0.	0.	0.	0.	0.	1.5	20.4	24.	17.7	12.3	2.5	3.5	19.8	24.	24.	24.	23.9	24.	15.4	20.6	12.7	8.6	0.	0.	0.	0.	0.	0.	92.758	17	17
P32B	22.	23.9	24.	24.	24.	24.	19.5	15.	7.4	20.4	24.	17.7	12.3	2.5	3.5	19.8	24.	24.	24.	23.9	24.	15.4	20.6	12.7	0.	0.	0.	0.	0.	0.	0.	16.726	24	24
P32C	22.	23.9	24.	24.	24.	24.	19.5	15.	7.4	20.4	24.	17.7	12.3	2.5	3.5	19.8	24.	24.	24.	23.9	24.	15.4	20.6	12.7	8.6	0.	0.	0.	0.	0.	0.	34.086	25	25
P32D	22.	23.9	24.	24.	24.	24.	19.5	15.	7.4	20.4	24.	17.7	12.3	2.5	3.5	19.8	24.	24.	24.	23.9	24.	15.4	20.6	12.7	8.6	0.	0.	0.	0.	0.	0.	170.424	25	25
P32E	22.	23.9	24.	24.	24.	24.	19.5	15.	7.4	20.4	24.	17.7	12.3	2.4	3.5	19.8	24.	24.	24.	23.9	24.	15.4	20.6	12.7	8.6	0.	0.	0.	0.	0.	0.	119.294	25	25
P32F	22.	23.9	24.	24.	24.	24.	19.5	15.	7.4	20.4	24.	17.7	12.3	2.4	3.5	19.8	24.	24.	24.	23.9	24.	15.4	20.6	12.7	8.6	0.	0.	0.	0.	0.	0.	187.45	25	25
P37	22.	23.9	24.	24.	24.	24.	19.5	15.	7.4	20.4	24.	17.7	12.3	2.5	3.5	19.8	24.	24.	24.	23.9	24.	15.4	20.6	12.7	8.6	0.	0.	0.	0.	0.	0.	17.044	25	25
P37A	22.	23.9	24.	24.	24.	24.	19.5	15.	7.4	20.4	24.	17.7	12.3	2.5	3.5	19.8	24.	24.	24.	23.9	24.	15.4	20.6	12.7	0.	0.	0.	0.	0.	0.	0.	50.179	24	24
P42B	22.	23.9	24.	24.	24.	24.	19.5	15.	7.4	20.4	24.	17.7	12.3	2.	3.5	19.8	24.	24.	24.	23.9	24.	15.4	20.6	12.7	8.6	0.	0.	0.	0.	0.	0.	170.243	25	25
P42C	22.	23.9	24.	24.	24.	24.	19.5	15.	7.4	20.4	24.	17.7	12.3	1.9	3.5	19.8	24.	24.	24.	23.9	24.	15.4	20.6	12.7	8.6	0.	0.	0.	0.	0.	0.	221.296	25	25
P50B	22.	23.9	24.	24.	24.	24.	19.5	15.	7.4	20.4	24.	17.7	12.3	2.5	3.5	19.8	24.	24.	24.	23.9	24.	15.4	20.6	12.7	8.6	0.	0.	0.	0.	0.	0.		25	25
P50C	0.	0.	0.	0.	0.	0.	9.2	15.	7.4	20.4	24.	17.7	12.3	2.5	3.5	19.8	24.	24.	24.	23.9	24.	15.4	20.6	12.7	8.6	0.	0.	0.	0.	0.	0.		19	0
P68A	22.	23.9	24.	24.	24.	24.	19.5	15.	7.4	20.4	24.	17.7	12.3	2.5	3.5	19.8	24.	24.	24.	23.9	24.	15.4	20.6	12.7	8.6	0.	0.	0.	0.	0.	0.	197.482	25	25
P68B	22.	23.9	24.	24.	24.	24.	19.5	15.	7.4	20.4	24.	17.7	12.3	2.5	3.5	19.8	24.	24.	24.	23.9	24.	15.4	20.6	12.7	8.6	0.	0.	0.	0.	0.	0.	34.088	25	25
P69A	22.	23.9	24.	24.	24.	24.	19.5	15.	7.4	20.4	24.	17.7	12.3	2.5	3.5	19.8	24.	24.	24.	23.9	24.	15.4	20.6	12.7	8.6	0.	0.	0.	0.	0.	0.	170.431	25	25
P69B	22.	23.9	24.	24.	24.	24.	19.5	15.	7.4	20.4	24.	17.7	12.3	2.5	3.5	19.8	24.	24.	24.	23.9	24.	15.4	20.6	12.7	8.6	0.	0.	0.	0.	0.	0.	135.338	25	25
P69C	22.	23.9	24.	24.	24.	24.	19.5	15.	7.4	20.4	24.	17.7	12.3	2.4	3.5	19.8	24.	24.	24.	23.9	24.	15.4	20.6	12.7	0.	0.	0.	0.	0.	0.	0.	150.521	24	24
P69D	22.	23.9	24.	24.	24.	24.	19.5	15.	7.4	20.4	24.	17.7	12.3	2.4	3.5	19.8	24.	24.	24.	23.9	24.	15.4	20.6	12.7	8.6	0.	0.	0.	0.	0.	0.	102.248	25	25
P69E	22.	23.9	24.	24.	24.	24.	19.5	15.	7.4	20.4	24.	17.7	12.3	2.4	3.5	19.8	24.	24.	24.	23.9	24.	15.4	20.6	12.7	0.	0.	0.	0.	0.	0.	0.	200.681	24	24
P69F	22.	23.9	24.	24.	24.	24.	19.5	15.	7.4	20.4	24.	17.7	12.3	2.4	3.5	19.8	24.	24.	24.	23.9	24.	15.4	20.6	12.7	8.6	0.	0.	0.	0.	0.	0.	102.241	25	25
P69H	22.	23.9	24.	24.	24.	24.	19.5	15.	7.4	20.4	24.	17.7	12.3	2.4	3.5	19.8	24.	24.	24.	23.9	24.	15.4	20.6	12.7	8.6	0.	0.	0.	0.	0.	0.	102.236	25	25
P69J	22.	23.9	24.	24.	24.	24.	19.5	15.	7.4	20.4	24.	17.7	12.3	2.4	3.5	19.8	24.	24.	24.	23.9	24.	15.4	20.6	12.7	8.6	0.	0.	0.	0.	0.	0.	0.095	25	25
P69K	22.	23.9	24.	24.	24.	24.	19.5	15.	7.4	20.4	24.	17.7	12.3	2.3	3.5	19.8	24.	24.	24.	23.9	24.	15.4	20.6	12.7	8.6	0.	0.	0.	0.	0.	0.	0.102	25	25
P72A	22.	23.9	24.	24.	24.	24.	19.5	15.	7.4	20.4	24.	17.7	12.3	2.3	3.5	19.8	24.	24.	24.	23.9	24.	15.4	20.6	12.7	8.6	0.	0.	0.	0.	0.	0.	238.526	25	25
P72B	22.	23.9	24.	24.	24.	24.	19.5	15.	7.4	20.4	24.	17.7	12.3	2.3	3.5	19.8	24.	24.	24.	23.9	24.	15.4	20.6	12.7	8.6	0.	0.	0.	0.	0.	0.	187.409	25	25
SS02	22.	23.9	24.	24.	24.	24.	19.5	15.	7.4	20.4	24.	17.7	12.3	2.3	3.5	19.8	24.	24.	24.	23.9	24.	15.4	20.6	12.7	0.	0.	0.	0.	0.	0.	0.	16.719	24	24
SS06	22.	23.9	24.	24.	24.	24.	19.5	15.	7.4	20.4	24.	17.7	12.3	2.3	3.5	19.8	24.	24.	24.	23.9	24.	15.4	20.6	12.7	0.	0.	0.	0.	0.	0.	0.	18.719	24	24
SS25	22.	23.9	24.	24.	24.	24.	19.5	15.	7.4	20.4	24.	17.7	12.3	2.3	3.5	19.8	24.	24.	24.	23.9	24.	15.4	20.6	0.	0.	0.	0.	0.	0.	0.	0.	97.491	24	24
SS25B	22.	23.9	24.	24.	24.	24.	19.5	15.	7.4	20.4	24.	17.7	12.3	2.2	3.5	19.8	24.	24.	24.	23.9	24.	15.4	20.6	0.	0.	0.	0.	0.	0.	0.	0.	148.23	24	24
SS44B	22.	23.9	24.	24.	24.	24.	19.5	15.	7.4	20.4	24.	17.7	12.3	2.2	3.5	19.8	24.	24.	24.	23.9	24.	15.4	20.6	12.7	0.	0.	0.	0.	0.	0.	0.	16.717	24	24

Figure 19: Injection and Pressure Data for the Month of October 2015, Gathered from Various Data Sources

UGS Inj and WD Well reports.xlsx
AC Monthly Inj and Prod Jul-Dec 2015.xls
SS-25 - API_04_03700776_Injection_29-May-2016.xlsx
SS-25B API_04_03721323_Injection_29-May-2016.xlsx
AC Daily Injection and Withdrawal 01-2014_01-2016 [17811].xlsx
AC Inventory & Pressure-10yearsData (2)AC_BLD_0019460.xlsx
Pr Transmiter to Main Injection Line to West Field.txt

Figure 20: Color Codes of Corresponding Source Data Sheet for Figure 19 [2], [7], [8], [26], [27], [28], [29], [30]

Appendix C Well Gas Allocations 10-2015

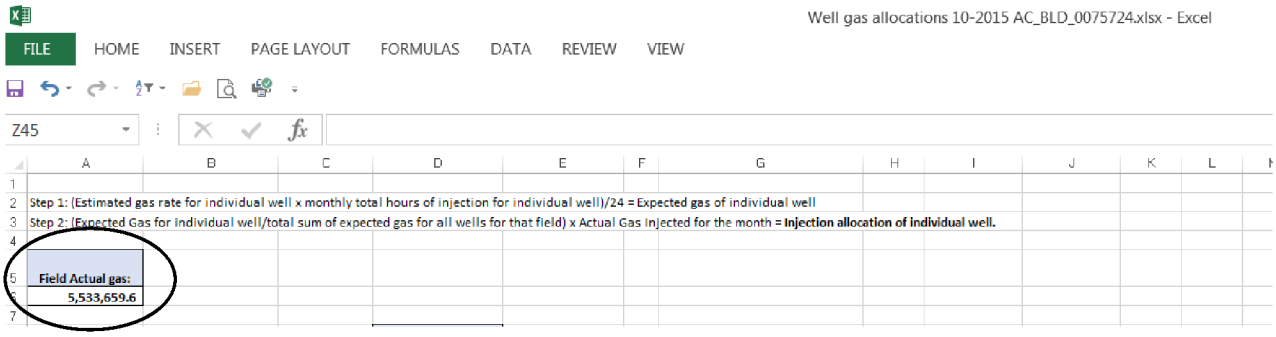

Figure 21: Gas Injected for the Month [9]

SS-25 RCA Supplementary Report

Analysis of the Post-Failure Gas Pathways and Temperature Anomalies at the SS-25 Site

Purpose:
Develop a model to define the post-leak gas pathway using a thermal reservoir simulation model consistent with the anomalous temperature measurements at the SS-25 site

Date:
May 31, 2019

2600 Network Boulevard, Suite 550
Frisco, Texas 75034

+1 972-712-8407 (phone)
+1 972-712-8408 (fax)

16285 Park Ten Place, Suite 600
Houston, Texas 77084

1-800-319-2940 (toll free)
+1 281-206-2000 (phone)
+1 281-206-2005 (fax)

www.blade-energy.com

Abstract

The gas storage well Standard Sesnon 25 (SS-25) in the Aliso Canyon Gas Storage Field located in Los Angeles County, California started leaking gas in October 2015. A relief well was drilled, and SS-25 was brought under control. The leak stopped in February 2016.

In January 2016, as part of their investigation of the leak, the California Public Utilities Commission (CPUC) and the Division of Oil, Gas, and Geothermal Resources (DOGGR) selected and gave provisional authority to Blade Energy Partners (Blade) to perform an independent Root Cause Analysis (RCA). The Blade Team and parties under Blade's direction were responsible for directing the work of subcontractors who performed the extraction of the SS-25's wellhead and tubing and casing and the preservation and protection of associated evidence. Blade RCA Reports, including this report, document and describe the key activities undertaken in support of the RCA effort.

The objectives of the analysis described in this report were the following:

- Determine the earliest time that the 7 in. casing failure could have occurred.
- Determine the evolution of the leak path of the gas from the initial 7 in. casing failure to after the coiled tubing deicing operation was carried out on November 6, 2015.
- Explain the unusual temperature observations in the ground at the SS-25 site.

The SS-25 gas leak began sometime after 03:00 on October 23, 2015, no more than about 12 hours prior to the shut-in of SS-25. The metallurgical analyses showed that the 7 in. casing initially underwent a ductile (warm temperature) failure, followed by a brittle (cold) temperature parting. The 7 in. casing temperature needed to be between –76°F (–60°C) to –38°F (–39°C) to cause the brittle parting. Analysis showed that injection gas prior to the shut-in of SS-25 could reach these low temperatures. After shut-in, the reservoir gas at the leak point (892 ft), although still cold (10°F (–12°C) to 20°F (–6°C)), would not be cold enough to cause this type of brittle failure. Therefore, both 7 in. casing failure events occurred prior to the shut-in of SS-25.

The gas at first flowed out the holes in the surface casing between 134 and 300 ft. However, in the first kill attempt, fluid pumped down the tubing, and the 7 in. x 2 7/8 in. annulus froze and blocked this pathway. The pressure rose, and the high gas pressure likely caused the rock around the surface casing shoe to fracture. Consequently, gas started flowing out of the well around the shoe. The coiled tubing deicing operation removed the blockages and allowed the gas to flow out the holes at the top again. Pressure in the 11 3/4 in. x 7 in. annulus fell, and the fractures around the shoe closed. As the reservoir pressure declined, the leaked gas temperature rose, and the gas warmed the shallow formation around SS-25. A crater then formed; the warm gas vented into the atmosphere and preserved the cold temperatures in the formation farther away from SS-25. When SS-25 was finally killed, the cold gas away from SS-25 flowed back toward the crater and cooled down SS-25 and the area near it. To model how the leak evolved, we built a thermal reservoir simulation model using the information from the shallow geology work. The simulated temperatures compared well with the observed data, which lends credence to our model.

Table of Contents

List of Figures

List of Tables

1 Introduction

The objectives of the analysis described in this report were the following:

- Determine the earliest time that the 7 in. casing failure could have occurred.
- Determine the evolution of the leak path of the gas from the initial 7 in. casing failure to after the coiled tubing deicing operation was carried out on November 6, 2015.
- Explain the unusual temperature observations in the ground at the SS-25 site.

The many pressure, temperature, and fluid level measurements taken in SS-25, SS-25A, and SS-25B were analyzed to model the evolution of the leak.

Blade used CMG's thermal reservoir simulator, STARS, to model the leak and predict the evolution of the temperatures in the formation from the shut-in of SS-25 on October 23, 2015 until the end of August 2017. The model investigated the temperature in an area that also included SS-25A and SS-25B. The area of investigation was about 40 ft away from SS-25. Comparing the simulated temperatures with the observed temperatures provided a test of the model of the leak.

In Section 2, we review the shallow geology to identify flow channels and estimate porosity, permeability, and water saturations. These data were needed to build the static reservoir simulation model. In Section 3, we trace the early development of the leak, and in Section 4, we discuss our scenario of how the leak evolved. The leak in the simulation model is treated as a gas injector. We used our scenario to guide how we operated this gas injector in the simulation model. In Section 5, we review and gather all the observed temperature data. These will be compared with the simulated temperatures and will provide a test of our leak scenario. In Section 6, we provide details of the simulation model and the results of the comparison of the simulated and observed temperatures.

The purpose of this simulation study is to test our understanding of the leak and not to tune the parameters (porosity, permeability, rock thermal properties, and so forth) to get a match. We used reasonable estimates of these parameters, along with rates and fluid temperatures obtained from other Blade reports, and tested how well the simulation model of the leak reproduced the observed temperatures. We performed some sensitivity studies to check how robust our model was to changes to these sensitivity study parameters.

The metallurgical analyses showed that the 7 in. casing failed in two separate events [1]. The initial failure was a ductile (warm temperature) failure. The second failure was a brittle (cold temperature) failure. The metallurgical analyses showed that the metal temperature at the time of the brittle failure was between –76°F (–60°C) to –38°F (–39°C). PROSPER, a commercial wellbore hydraulics simulator from Petroleum Experts, showed that after SS-25 was shut in, the temperature of the leaking gas was no colder than 10°F (–12°C) to 20°F (–6°C) [2]. This parting failure, therefore, could not have happened after SS-25 was shut in. Section 3 will show that prior to the shut-in, the injection gas could have reached the low temperatures that the metallurgical analyses indicated.

In this report we frequently refer to the 7 in. x 2 7/8 in. annulus and 11 3/4 in. x 7 in. annulus. The 7 in. x 2 7/8 in. annulus is the space between the 7 in. casing and the 2 7/8 in. tubing and is the upstream side of the leak; it is also referred to as "A". The 11 3/4 in. x 7 in. annulus is the space between the surface casing (11 3/4 in. casing) and the 7 in. casing and is the downstream side of the leak; it is also referred to as "B".

Previous work concluded only that the leak could not have occurred earlier than October 15, 2015; this was based on the last 0 psi reading inside the 11 3/4 in. x 7 in. annulus pressure [3]. Section 3 further

refines this estimate and shows that the SS-25 gas leak began sometime after 03:00 on October 23, 2015, no more than 12 hours prior to the shut-in of SS-25.

Section 3 and Section 4 together describe the entire life of the leak. Section 3 focuses on the period from ductile failure to shut-in of SS-25. Section 4, supported by the analyses in Appendix B through Appendix E, extends the analysis of how the gas leak path evolved out to the end of August 2017. Results from both sections were fed to the thermal reservoir simulation model, as discussed in Section 6.

The cold temperatures seen in and around SS-25 were due to the Joule-Thomson (J-T) cooling effect. During a flow test of SS-25, the produced gas was passed through a choke, and the temperature and pressure data upstream and downstream of the choke were collected. In Appendix A, we estimate the J-T coefficient from these data. The J-T coefficient can provide an estimate of the temperature drop due to pressure drop.

Between October 28 and November 6, 2015, measured pressures in the 7 in. x 2 7/8 in. annulus and the 11 3/4 in. x 7 in. annulus were 400 to 800 psi. PROSPER calculated the leaking gas temperatures at 892 ft to be 40 to 60°F [2]. This period is referred to as the warm leaked gas period. The rising pressure suggested that blockages were developing in the well or along the flow path of the escaping gas. Appendix B analyzes the SS-25 pressure data and observations noted in the daily reports to understand how the gas flowed out the well and how the blockages inside the well were developing during this period. The results of these analyses were used to fill in details of the leak model during the warm leaked gas period.

There were temperature measurements and other observations in the SS-25 tubing string on October 28 and 29, 2015. However, these measurements and observations were inconsistent. Appendix C reviews these data and explains why we concluded that the temperature was 19°F and the solid plugs that were blocking the gas flow were ice and not hydrate on these days. Our simulation results will be compared to the 19°F temperature.

Appendix D shows that if the gas had continued to flow out of the holes between 134 and 300 ft in the surface casing during the warm leaked gas period, heat transfer inside the well would have been fast enough to thaw out the upper section of the well. We did not see evidence of this, and concluded that the gas escaped the well through a path that preserved the cold temperatures in the tubing.

There had been speculation that the plugs blocking the flow were initially ice and that the ice transformed into hydrate by the time of the warm leaked gas period [2]. Because hydrate is stable at the high temperatures and pressures in the 7 in. x 2 7/8 in. annulus and the 11 3/4 in. x 7 in. annulus, warm gas could have continued to flow up the 11 3/4 in. x 7 in. annulus without thawing out the well. Appendix E explains why this transformation was unlikely to have occurred.

One hypothesis to explain how 85 MMscf/D of 40 to 60°F reservoir gas during the warm leaked gas period was unable to melt the ice in the tubing string in 9 days is that the rocks around the surface casing shoe were fractured by the high gas pressure, which then provided an alternative path for the gas to escape; this path avoids the upper section of the surface casing. Appendix F estimates the fracturing pressure at the surface casing shoe.

1.1 Abbreviations and Acronyms

Term	Definition
BHP	Bottom Hole Pressure
Blade	Blade Energy Partners

Term	Definition
CBL	Cement Bond Log
CHDT	Cased Hole Dynamics Tester
CMG	Computer Modeling Group
CPUC	California Public Utilities Commission
DOGGR	Division of Oil, Gas, and Geothermal Resources
DTS	Distributed Temperature Sensing
FMI	Formation MicroImager
ID	Inside Diameter
J-T	Joule-Thomson (Cooling)
LCM	Loss Circulation Material
LP	Leak Point
NIST	National Institute of Standards and Technology
NMR	Nuclear Magnetic Resonance (Log)
OD	Outside Diameter
SSV	Surface Safety Valve

2 Shallow Geology

In this section, we develop a qualitative picture of the shallow geology that guided the development of the static reservoir simulation model. We were interested in identifying pathways and barriers for the leaking gas to flow away from SS-25. We were also interested in the lithology, porosity, permeability, and water saturations. These properties were needed to build the static simulation model.

The shallow geology in the Aliso Canyon area is complex, and it can change quickly from site to site. For this reason, there can be and are inconsistencies in the large amount of geological data at the SS-25 site and the nearby SS-9 and P-39 sites. In the modeling, we gave the greatest weight to data from the SS-25 site and to data that were consistent across the three sites. In this discussion, we point out where there are multiple interpretations and state which interpretation we have chosen. This section discusses only the data that were needed to build the static simulation model. A detailed review of the shallow geology is provided in reference [4].

Lost circulation means that drilling mud is leaking into the formation and not coming back to the surface. It is used to identify channels through which the leaking gas could flow away from SS-25. Figure 1 summarizes the depth at which the wells SS-25, SS-25A, and SS-25B experienced loss of circulation. We list here our observations concerning lost circulation of these wells:

- The drilling record of SS-25 [5] (pages 129-135) showed 5 hours of lost circulation at 169 ft and 3.75 more hours of lost circulation at 741 ft. Loss circulation material (LCM) was added to control the losses. The long time it took to stop the loss indicated that the formation at 169 ft had high permeability and pore volume and was a possible channel for the gas to leak away from SS-25. The lost circulation at 741 ft did not necessarily mean that there was another channel there. It was possible that the loss zone at 169 ft reopened.
- The drilling record of SS-25A [6] (page 41) showed lost circulation at 67, 371, 779, and 808 ft.
- The drilling record of SS-25B [7] (page 36) showed lost circulation beginning at 330 ft. No LCM was used, and the hole was drilled with no return of drilling fluid to surface down to 900 ft. Because mud loss was not stopped at 330 ft, it was not possible to tell if there were more lost circulation zones below 330 ft.
- The lost circulation zones at shallow depths in SS-25A and SS-25B suggested that the channel identified at SS-25 (169 ft) likely extended out to SS-25A and SS-25B. Because we saw lost circulation at approximately 740 ft in both SS-25 and SS-25A and possibly also in SS-25B, it was likely that there is a second channel at that depth. We presumed that there was a second channel at approximately 740 ft.

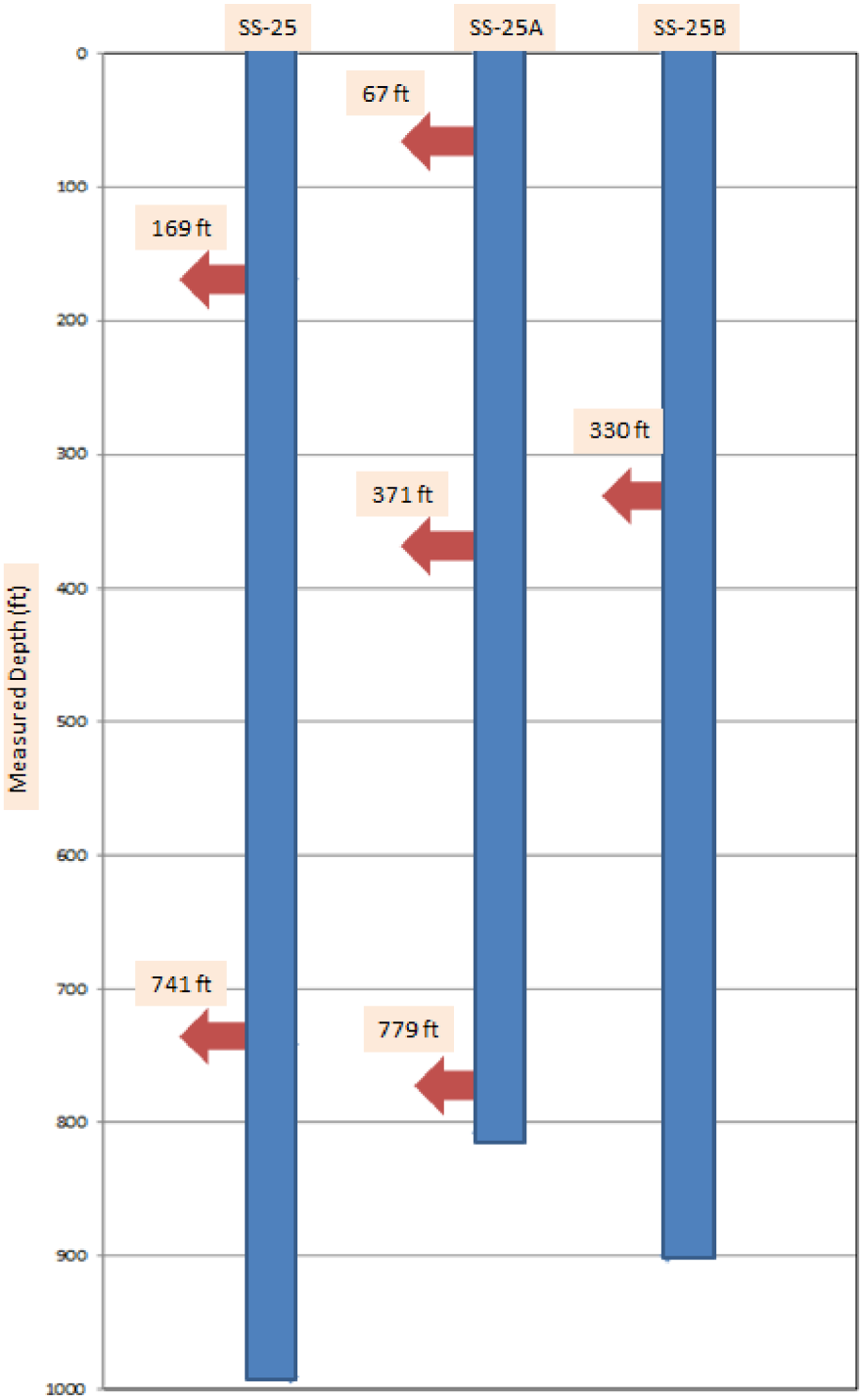

Figure 1: Depth where Loss of Circulation Occurred

Advisian, an independent consulting firm hired by Blade to study the shallow geology at site SS-25, cored and logged several shallow boreholes at the SS-25 site [8]. The deepest hole was 150 ft. Advisian noted that the rock was heavily weathered. Heavy weathering suggested high permeability and porosity in the matrix. Advisian also ran Nuclear Magnetic Resonance (NMR) logs in the four shallow boreholes. The deepest log was 123 ft in BH-3. The water content typically ranged from 10 to 20%.

Water content is the ratio of the water volume to the total volume (including the rock volume) and should not be confused with water saturation, which is the ratio of the water volume to the total pore volume (excluding the rock volume). Water content is divided into clay-bound water, capillary water, and mobile water, based on the degree to which the water is bound to the rock. Bound water typically does not freeze and was neglected in the reservoir simulation. Capillary water typically does not flow and is what is called the critical water saturation in petroleum engineering. Mobile water is water in the fractures and larger matrix pores and vugs.

The borehole NMR logs indicated that the bulk of the water in the boreholes was capillary water. The high capillary water content of 10 to 20% implied that the rock matrix porosity was at least of the same range. It was not certain how much of this capillary water came from the drilling operation. It was also not certain how deep the weathered layer was.

Borehole TH-1 was drilled and logged down to 1,100 ft at the SS-9 site located about 600 ft south and 100 ft below the SS-25 site. Geosyntec Consultants concluded from the lost circulation that the entire 1,100 ft was "substantially fractured" [9] (page 19). The TH-1's mud log [9] (page 835) described the cuttings carried back up to the surface by the drilling fluid during the drilling operation. It provided a map of lithology versus depth. Because total lost circulation started at 550 ft, the mud log ended at this depth.

The TH-1 mud log showed layers of soft, moist material interbedded with layers of hard siltstone. The soft layers were usually silt with varying amount of clay and sand. Clay is made up of fine particles, and it swells and clumps when wetted. Clay can plug pores and seal fractures and faults. Such soft, moist layers with large amounts of clay are likely barriers to flow. Siltstone has low permeability and porosity and could act as a barrier. However, some of the siltstone layers encountered in the TH-1 are heavily weathered. In addition, siltstone is brittle and likely to be fractured. If fractured and weathered siltstone layers do not contain clay, they have high permeability and porosity and are potential channels for gas to flow through.

The surface location of the relief well, P-39A, is 300 ft below and about 1,475 ft southeast of the SS-25 site. On the mud log [10], the geologist noted that total lost circulation occurred at 362 ft [10]. This mud log was more detailed than that of TH-1 and went deeper than 1,000 ft. The soft material in the upper 500 ft (Modelo formation [4]) was mainly clay. Below 500 ft, there were layers of sand and clay, and many of the sand layers also contained clay. The soft layers were expected to be barriers. The hard materials seen in this hole were porcelanite, siltstone, and claystone. The geologist noted that fracture faces in the hard layers near the surface were coated with tar. The coating of tar implied that the fractures were preexisting and not caused by the drilling process. The number of fractures coated with tar decreased with depth, and the tar-coated fractures disappeared by 250 ft. This does not mean that the deeper fractures were drilling induced; there could have been no tar there.

In these mud logs, the geologists saw the major lithological formations Modelo and Topanga. (See reference [4] for information on these formations.) These flow units are sufficiently thick to extend across all three sites. The P-39A mud log, along with some old SS-25 electric and gamma ray logs, were used to delineate coarse layers at SS-25 in Blade's preliminary assessment of the shallow geology [11]. The thinner flow units seen in the mud logs are difficult to correlate between the wells and may not extend across all three sites. These layers were not included in this model. Our static simulation model used the layering in the initial Blade assessment [11]. These thick flow units were assumed to be flat layers extending with unvarying thicknesses across the entire simulation model.

The mud logs provided a picture of layers of barriers interbedded with channels that can flow gas. A sufficient number of thick barriers should exist to restrict gas flow in the vertical direction, unless faults or fractures cut across them. Preliminary analysis of formation microimager logs (FMI) for borehole TH-1

showed faults that may be conductive locally [12]. Due to abundant clay layers, clay smear can seal these faults when adjacent surfaces of these faults slide past each other. These faults may appear conductive locally but may not be conductive over a longer distance. In this work we presume that these faults are sealing, and the vertical flow of gas is restricted.

The FMI log also showed that the Topanga basalt has fractures, but not conductive ones. The P-39A mud log showed clay mixed in with the basalt, which may explain why there was no conductive fracture in this layer. The basalt was treated as a barrier.

The locations of the channels at 169 ft and 741 ft in SS-25 were determined based on where mud loss occurred.

The Cement Bond Log (CBL) for the SS-25 surface casing [13] showed poor cement bonding behind casing above 400 ft. The report of the cement job of the surface casing indicated little if any cement made it up this high [5] (pages 129-135). Gas leaking from the holes in the surface casing between 134 and 300 ft could have readily flowed through the gaps in the cement and away from SS-25 via the channel identified at 169 ft.

The surface casing shoe was at 990 ft. The CBL showed better cementing at this depth than above 400 ft, but there was micro annulus. The CBL showed that between 700 ft and 900 ft, the cement quality was also poor. When the 11 3/4 in. x 7 in. annulus pressure built to as high as 800 psi, the gas might have fractured the rock around the surface casing shoe and further damaged the cement behind the surface casing. (See Appendix F.) The gas leaking from the shoe could have then flowed up behind the casing and away from SS-25 through the channel at 741 ft.

In summary, the lost circulation records of the wells in the SS-25 site showed two channels for gas to flow away from SS-25. The mud and FMI logs showed that there are flow barriers that restrict gas from flowing vertically inside the formation. The CBL showed cement behind the surface casing was poor and thus provided a path for leaking gas to flow up behind the surface casing to the two identified channels.

3 Early Period of the Leak

Metallurgical analyses showed that the 7 in. casing failed in two separate events. The first failure event was a warm temperature ductile failure that created an axial crack approximately 2 ft long. This entire 2 ft ductile failure occurred very fast. The second failure event was a cold temperature brittle parting of the 7 in. casing [1]. The metallurgical analysis of the parting surface showed that the metal temperature was –76°F (–60°C) to –38°F (–39°C), whereas the lowest temperature of the leaking gas after the shut-in of SS-25 was 10°F (–12°C) to 20°F (–6°C) [2]. Our analysis of pressure and temperature, described in this section, showed that prior to the shut-in of SS-25, the injection gas temperature could have reached –30°F, close to the range of temperatures indicated by the metallurgical analyses. We therefore concluded that both the ductile and the brittle failures occurred prior to the shut-in.

Previous work used the last 0 psi pressure reading inside the 11 3/4 in. x 7 in. annulus to conclude that the leak could not have occurred earlier than October 15, 2015 [3]. This section refines the estimate and determines that the leak could not have occurred earlier than about 12 hours prior to the shut-in of SS-25 on October 23, 2015. The length of this period and temperature of the gas during this period are used to build the reservoir simulation model in Section 6.

To determine the earliest time the ductile failure could have occurred and how cold the injection gas could have been at 892 ft, we made two assumptions:

- The holes in the surface casing before the shut-in of SS-25 were the same size as the holes after the shut-in.
- The leak out of the holes in the surface casing was choked after the shut-in of SS-25.

The second assumption allowed us to estimate the equivalent hole size in the surface casing after the shut-in of SS-25 without having to know precisely what the pressure was in the formation between 134 and 300 ft. (The equivalent hole size is the circular hole with an area equal to the total area of the openings in the casing. We can then use the choke model to estimate the gas flow rate, pressure drop and temperature.) The second assumption is correct if the formation pressure was less than about 75 psi. Cased Hole Dynamic Tester (CHDT) measurements taken in 2018 found pressure between 16 and 34 psi at depths between 372 and 490 ft [14]. (Note that after leaking for a period, the formation pressure will rise and this assumption may no longer be valid. We are essentially approximating the flow resistance of the surface casing holes and the formation with a choke.)

Together, these two assumptions allowed us to estimate the pressure in the 11 3/4 in. x 7 in. annulus prior to the shut-in of SS-25 from 134 to 300 ft. We then used this information to estimate pressure, rate, and temperature at various points in the flow path. Figure 2 shows the problem configuration which we seek to solve.

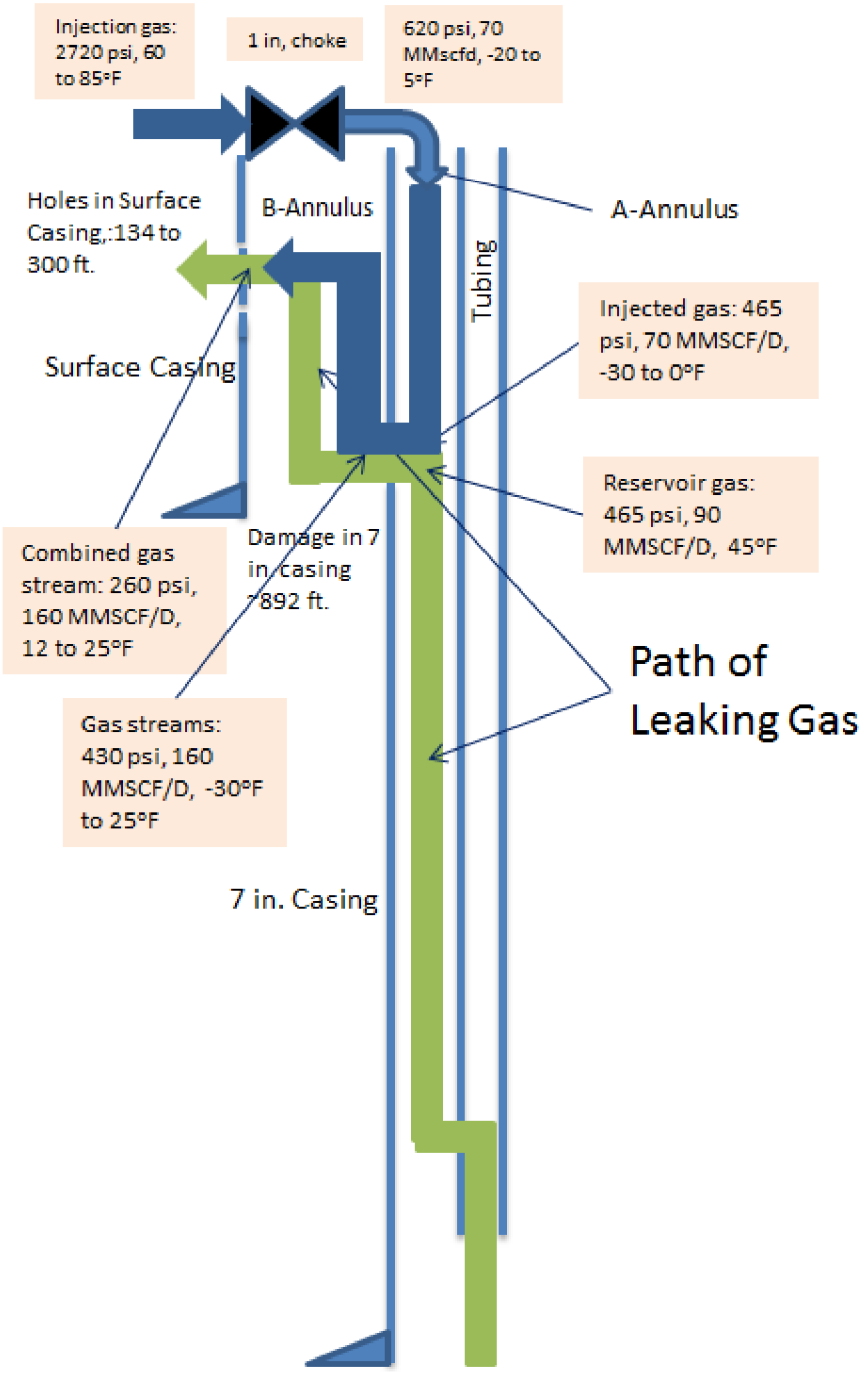

Figure 2: Summary of the PROSPER Calculations Prior to the Shut-In of SS-25

The procedure to solve this problem is to make an initial estimate of the gas rate from the injection line and from the reservoir. PROSPER then uses these estimates to calculate the rates and pressures along the flow path. If the results do not match these initial estimates, these estimates are updated, and this process is repeated until convergence is achieved. It is an iterative process. Figure 3 shows the flowchart of the solution procedure.

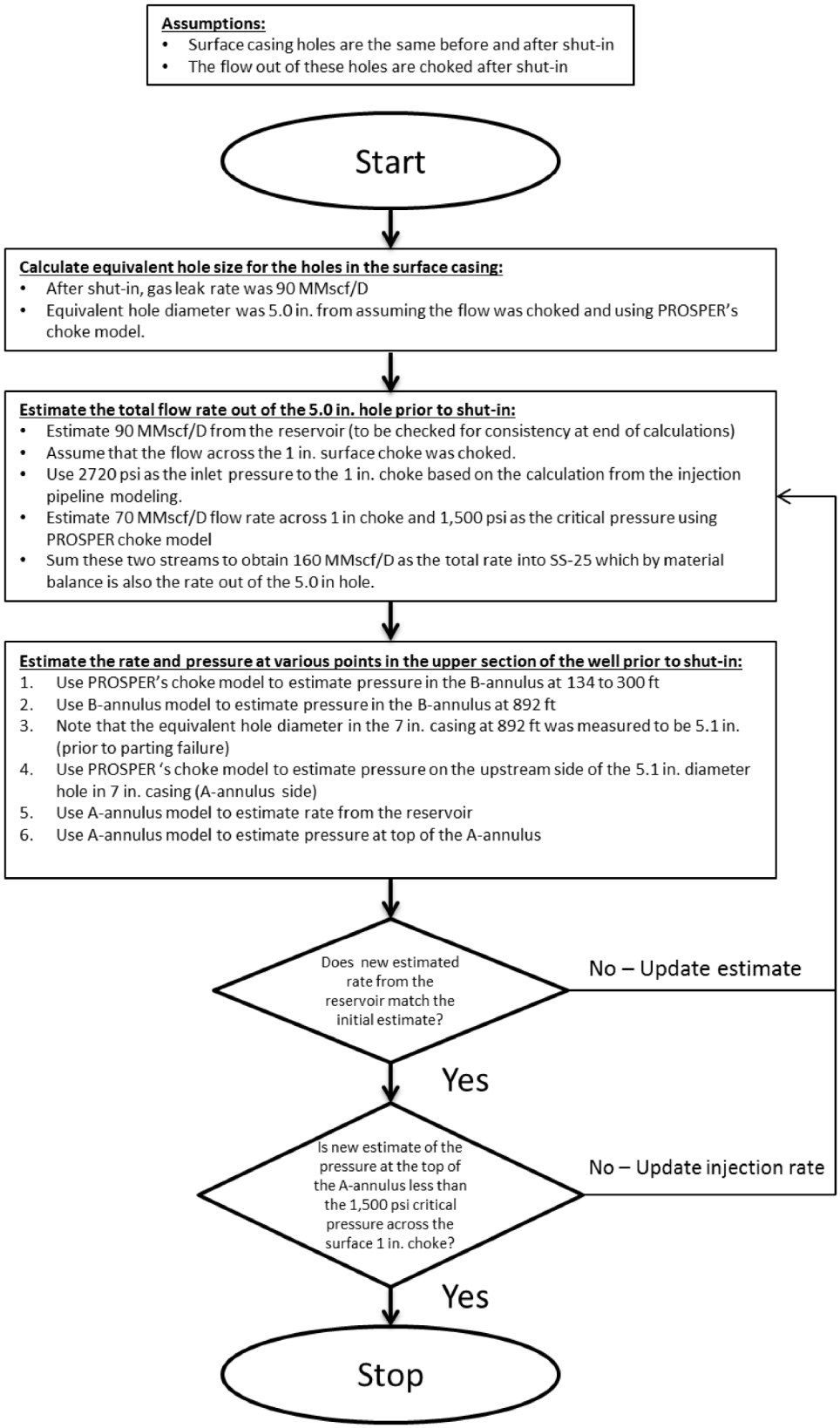

Figure 3: Flowchart of the Pressure and Rate Calculations in SS-25 Prior to Shut-In

Let's begin the calculations by estimating the equivalent hole size of the holes in the surface casing between 134 and 300 ft. After the shut-in of SS-25, the measured 11 3/4 in. x 7 in. annulus pressure was 140 psi. The estimated leak rate was about 90 MMscf/D [2]. Because we assumed that the flow was choked, PROSPER's choke model estimated that the equivalent hole diameter for the holes in the surface casing was 5.0 in.

Next, we estimate the gas injection rate into SS-25 prior to the shut-in. Figure 4 shows the pressure and temperature of the gas at the injection header from October 22 to October 23, 2015. This injection header is near the compressor station where the flow from the compressor is split among the trunk lines to the western, eastern, and central area. The pressure gauge labeled PIT-WFI_DY1 is on the trunk line leading to the western part of the field, including SS-25. AI_STA_TE-506 is the temperature gauge on the line coming from the compressor station into the injection header [15].

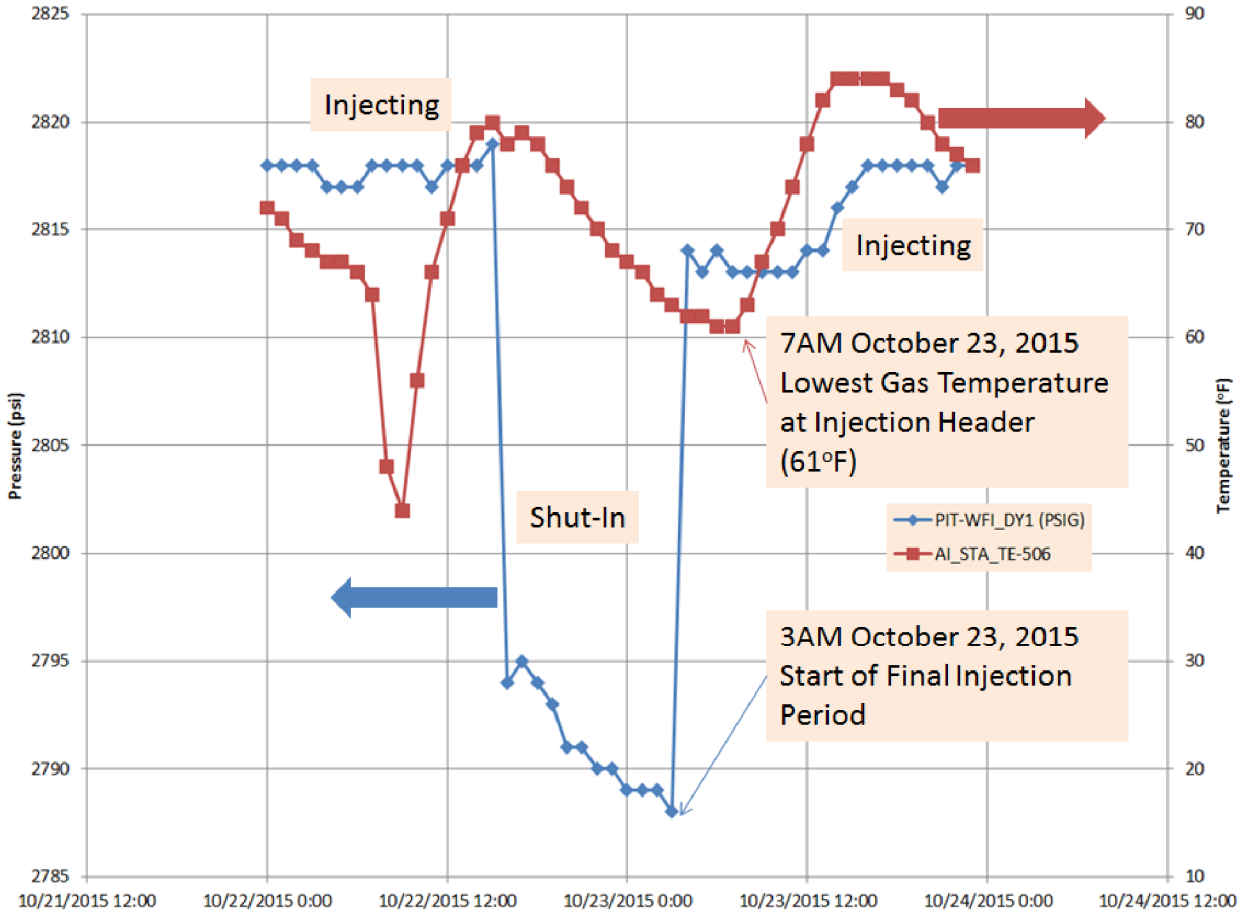

Figure 4: Hourly Pressures and Temperatures at the Injection Header by the Compression Station [15]

The PIT-WFI_DY1 pressures varied between about 2,815 and 2,790 psi. When the pressure gauge read about 2,815 psi, the wells were injecting. When the gauge read 2,790 psi, the wells were shut-in. We used this to determine when gas was injecting into SS-25 [16]. Figure 4 shows that the final time SS-25 was brought back on line as an injector was between 03:00 and 04:00 on October 23, 2015. (SoCalGas reported 20.6 hours of injection on October 23, 2015 [17]. This would place the injection start time at 03:24. In this report, we will use 03:00 as the start of SS-25's final injection period for convenience.) Using the pressure corresponding with this time and the pipeline configuration, reference [16] estimated the pressure at SS-25 to be about 2,720 psi.

Assuming the flow across the 1 in. choke was choked and using the estimated 2,720 psi at the inlet of the 1 in. choke, PROSPER calculated that the critical flow rate was 70 MMscf/D. This will be the injection gas flow rate down the SS-25 7 in. x 2 7/8 in. annulus if the flow was choked. We will show shortly that the assumption that the flow was choked was correct.

In addition to the injected gas stream, there was a second stream flowing up from the reservoir. We will assume 90 MMscf/D and will show that this assumption was correct shortly. Material balance then required the leak rate out of the holes in the surface casing (out of well SS-25) to be 160 MMscf/D, the sum of the two streams coming into SS-25.

PROSPER estimated that a pressure of 260 psi in the 11 3/4 in. x 7 in. annulus was needed to push 160 MMscf/D out of the 5 in. equivalent diameter hole in the surface casing between 134 and 300 ft. To drive 160 MMscf/D of gas up the 11 3/4 in. x 7 in. annulus and for the gas to arrive at the holes in the surface casing with a pressure of 260 psi, required a pressure of 430 psi at 892 ft on the 11 3/4 in. x 7 in. annulus side of the 7 in. casing. The initial ductile failure of the 7 in. casing had an equivalent hole size of 5.1 in. [1]. A pressure of 465 psi on the 7 in. x 2 7/8 in. annulus side at 892 ft was needed to drive 160 MMscf/D across the failure in the 7 in. casing.

PROSPER estimated that with a pressure of 465 psi at 892 ft in the 7 in. x 2 7/8 in. annulus, the flow rate from the reservoir was about 90 MMscf/D. (See Table 5.) Therefore, the earlier assumption of 90 MMscf/D from the reservoir was correct.

To drive 70 MMscf/D from the surface down to 892 ft in the 7 in. x 2 7/8 in. annulus and for the gas to arrive with a pressure of 465 psi required a pressure of 620 psi at the top of the 7 in. x 2 7/8 in. annulus.

The inlet pressure to the SS-25 1 in. choke was 2,720 psi [16]. The critical pressure from PROSPER's choke model was 1,500 psi. The pressure, 620 psi, was well below 1,500 psi, so the gas flowing through the 1 in. choke was choked. The critical flow rate was 70 MMscf/D. Our assumptions that the flow was choked and the injection rate was 70 MMscf/D were correct.

The estimate of 70 MMscf/D from the injection line assumed that the SSV was open. The pressure in the 7 in. x 2 7/8 in. annulus at 892 ft was 465 psi and at the well head was 620 psi. The well head pressure was above the set point of the SS-25 surface safety valve (SSV) (270 to 300 psi [5] (page 78)). In fact, even if the pressure was 260 psi at 892 ft on the 7 in. x 2 7/8 in. annulus side, the pressure at the well head would still have been 500 psi based on PROSPER calculation. The pressure at 892 ft could not be as low as 260 psi because this was the pressure in the 11 3/4 in. x 7 in. annulus at the holes in the surface casing. The SS-25 SSV therefore would not have tripped during injection even if the ductile failure in the 7 in. casing had already occurred. The assumption that the SSV remained open was correct.

The only time the pressure at SS-25 was low enough to cause the SSV to close was when the well was shut-in and when the 7 in. casing had failed. This is why when SS-25's injection valve was shut in at 15:30 on October 23, 2015, the SSV closed immediately [5] (page 78). (For the pressures and flow rates after SS-25 was shut-in, see [2].)

We make use of this fact, Figure 4, and references [3] and [17] to refine the estimate of when the initial failure occurred. From reference [3], the last 0 psi pressure reading in SS-25's 11 3/4 in. x 7 in. annulus was on October 15, 2015. The failure had not occurred by this date. Reference [17] showed that between October 15 and October 23, 2015, all the active injection wells were on injection the same number of hours each day. Furthermore, the same set of wells was injecting throughout this period. This suggested that the injection to the field during this period was controlled with a single valve by the compression station rather than with multiple valves at the well sites and inlet to the trunk lines supplying gas to the eastern, central, and the western part of the field. In other words, during the shut-in periods between

October 15 and October 23, there was no closed valve between PIT-WFI_DY1 and SS-25. If this was true, the pressure gauge, PIT-WFI_DY1 should have been reading the pressure in the trunk line to the western area, including SS-25 during the shut-in periods.

Figure 4 showed that during the shut-in period prior to the final injection period, the pressure was about 2,790 psi. If the ductile failure occurred during this shut-in period, the holes in the 7 in. casing would have evacuated the gas in the trunk line leading to SS-25, and the pressure would be closer to 300 psi. (For an 8 in. line, at 2,800 psi, there is about 350,000 scf/mi of pipeline. At 2,700 psi line pressure, SS-25 would have leaked 50,000 scf/min. Also note that the wells have check valves, which prevent the other open injection wells from replenishing the pipeline and maintaining pressure.) Because the pressure was 2,790 psi, the 7 in. casing did not fail during the shut-in period prior to the final injection period. The 7 in. casing therefore failed during the final injection period or after 03:00 on October 23, 2015 at the earliest.

If the assumption that there was no closed valve between PIT-WFI_DY1 and SS-25 during the shut-in periods was wrong, when this closed valve was reopened for the injection periods, PIT-WFI_DY1 should register a sudden drop in pressure and the pressure should remain low until the line was re-pressurized. The operator would have noticed this. We have not found any record of this in the data provided by SoCalGas.

Let's estimate the gas temperatures after the initial ductile failure but before the shut-in of SS-25 to see if the gas could have been cold enough to cause the brittle parting failure observed. Figure 5 shows the record of an SS-25 flow test conducted in 1978 [5] (page 710). During this flow test, the reservoir gas was passed through a choke to reduce the gas pressure. Both the pressure and the temperature upstream and downstream of the choke were measured. The inlet pressure to the choke for this test was about 2,700 psi. The outlet pressure was 485 psi. The inlet temperature was about 85°F, and the outlet temperature was about 0°F. These inlet conditions are close to the inlet conditions of SS-25's 1 in. choke. (See Figure 2.) The J-T coefficient estimated from this flow test was 0.56°F/14.7 psi, and this should be a good estimate for the J-T coefficient across SS-25's 1 in. choke after the initial ductile failure.

WELL NO: SS-25 DATE: 7-18-78 OPERATOR: _____ TEST NO: [illegible]

B. H. CHOKE: NONE " SURF CHOKE: .400 " (LATERAL) VESSEL TEST

FLOWING STRING: (CSG) / TBG SAFETY VALVE IS IN (OUT) OF WELL . BOMBS RUN: (YES) NO

PROBE ID NO'S--RISER: _____ US#1 _____ US#2 _____ DS#1 _____ DS#2 _____

PROBE AND BULL PLUG REMARKS: NO PROBES

WATER CUT (% BS & W): _____ OIL GRAVITY: _____ @ _____ °F

ELAPSED TIME	TIME OF DAY	AIR TEMPERATURE	CSG PRESSURE	TBG PRESSURE	UPSTREAM SURFACE CHOKE		DOWNSTREAM SURFACE CHOKE		GAS FLOW RATE				LIQUIDS
					PRESSURE	TEMPERATURE	PRESSURE	TEMPERATURE	STATIC	DIFFERENTIAL	TEMPERATURE	RATE	
SI IN	9 05 A		2760	2780									39794.95
0:00	9 10 A		START	FLOW	TEST								
0:05													
0:10													
0:15													
0:25													
0:35													
0:45													
1:00	10 A			2745	2705	82	490	-0	7.12	3.54	31°	11,378	
1:15													
1:30													
1:45													
2:00	11 10 A			2750	2710	83	490	-0	7.12	3.5	8°	11,250	
2:30													
3:00	12 10 N			2750	2715	85	485	-0	7.12	3.48	5	11,186	
3:30													
4:00	1 10 N			2760	2720	85	485	+1	7.12	3.48	5	11,186	
4:30													
5:00	2 10 P			2760	2720	85	490	+2	7.12	3.48	5	11,186	
5:30													
6:00	3 10 P			2750	2720	86	490	+2	7.11	3.48	5	11,170	
6:30													
7:00	4 10 P			2760	2720	86	490	+1	7.11	3.5	5	11,234	
7:30													
8:00	5 10 P			2754	2720	86	480	-0	7.11	3.43	5	11,009	
JWT/wlc (rev. 7/19/78) Field Test Data Sheet WCC									7.11	3.44		11,642	45174

Figure 5: Reproduction of the SS-25 Well Test Record Conducted on September 18, 1978

Figure 4 shows that the temperature at the injection header was between 60 and 85°F. SS-25 is about 1,000 ft higher in elevation than the injection header. Therefore, the inlet gas temperatures to the SS-25 1 in. choke were likely several degrees lower.

The pressure drop across the 1 in. choke was estimated to be 2,100 psi. Using the 0.56°F/14.7 psi J-T coefficient, this translated to a drop in temperature of about 80°F. The outlet temperature of this 1 in. choke therefore ranged from –20 to 5°F. PROSPER estimated that the flow down the 7 in. x 2 7/8 in. annulus led to an additional 8°F temperature drop (assuming minimal heat gain or loss through the 7 in. casing). The estimated temperature of the 70 MMscf/D gas at 892 ft was between –30 and 0°F.

The initial ductile failure was about 2 ft long [1]. The stream from the injection line and the gas from the reservoir would have collided somewhere below 892 ft in the 7 in. x 2 7/8 in. annulus where the 2 ft long crack was. PROSPER estimated that the gas from the reservoir was 45°F when it arrived at 892 ft. Volume averaging the temperature of the 70 MMscf/D stream from the injection line and the 90 MMscf/D stream from the reservoir yielded an average temperature between 12 and 25°F. These estimates represented the upper bound on the temperature of the combined streams and the 7 in. casing. This would not have been cold enough to cause the brittle parting failure.

Figure 6 shows a possible scenario that could have yielded lower temperatures. The cold injection gas as it exited the 7 in. casing at the upper section of the axial crack could have blown the warm reservoir gas away from the 7 in. casing surface, thus keeping the 7 in. casing cold. Depending on how effective this transpiration cooling effect was, the 7 in. casing could have reached the injection gas temperature of –30 to 0°F. References [18] and [19] studied the transpiration cooling effect experimentally and numerically. The magnitude of this effect depends on the ratio of the blowing stream rate (injection gas in our case) and the bulk stream rate (reservoir gas in our case). In these references, this ratio was less than 1%. In the SS-25 case, this ratio was 70 to 80%. Therefore, the magnitude of the transpiration cooling effect would have been significantly larger than what was shown in these two references.

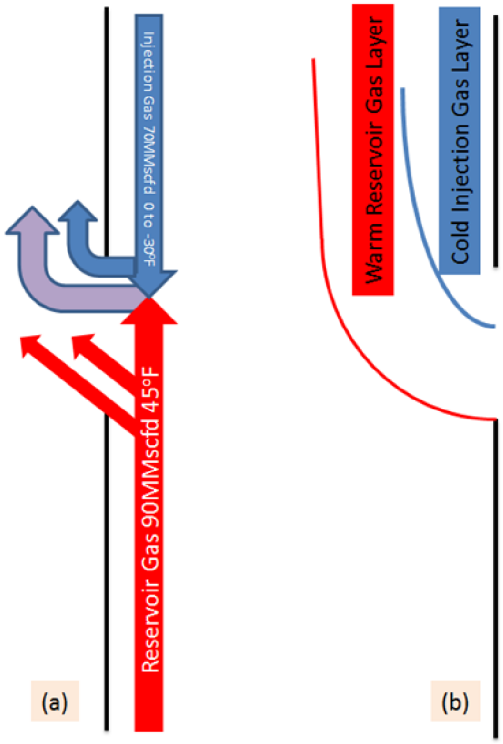

(a) shows the flow paths of the cold injection gas flowing down from above (blue arrow) and the warm reservoir gas flowing up from below (red arrow). The axial crack (initial ductile failure) is about 2 ft long at depth of 892 ft. Part of the reservoir gas exits at the lower section of the axial crack. The rest continues upward to collide with the injection gas. Similarly, part of the injection gas flowing downward exits at the upper section of the crack before colliding with the remnants of the reservoir gas. Remnants of both streams mix and exit the 7 in. casing near the point of collision (purple arrow). All the leaked gas then flows upward and out the holes in the surface casing between 130 and 300 ft.

(b) shows that the cold injection gas pushes the warm reservoir gas layer away from the surface of the 7 in. casing, shielding the 7 in. casing from the warm reservoir gas. Depending on how effective this transpiration cooling effect is, it is possible the 7 in. casing temperature can drop to -30°F.

Figure 6: Schematic of Flow Paths of the Injection Gas Stream and Reservoir Gas Stream

If transpiration cooling was effective, there would be a jacket of –30°F gas protecting the 7 in. casing. As this jacket of gas flows upward, its pressure falls by 170 psi, which will cause further cooling. This gas jacket could precool the injection gas, resulting in gas temperatures even colder than –30°F down by 892 ft. This counter current heat exchanger problem is beyond the scope of this work. We will consider –30°F reasonably close to the temperature range indicated by the metallurgical study.

The conclusion from these analyses was that the gas temperature at the leak point was between –30 and 25°F. (25°F is when there is no transpiration effect, and the gas leaving the injection header was 85°F.) Figure 7 summarizes the gas flow paths from initial failure to just prior to kill attempt #1 on October 24, 2015. The initial ductile failure occurred after 03:00 on October 23, 2015. If a –30°F temperature was needed to cause the parting failure, it would likely have occurred when the injection gas at the injection header was the coolest. Figure 4 shows that this would have been between 07:00 and 08:00 on October 23, 2015. This would have been the latest that the initial ductile failure could have occurred.

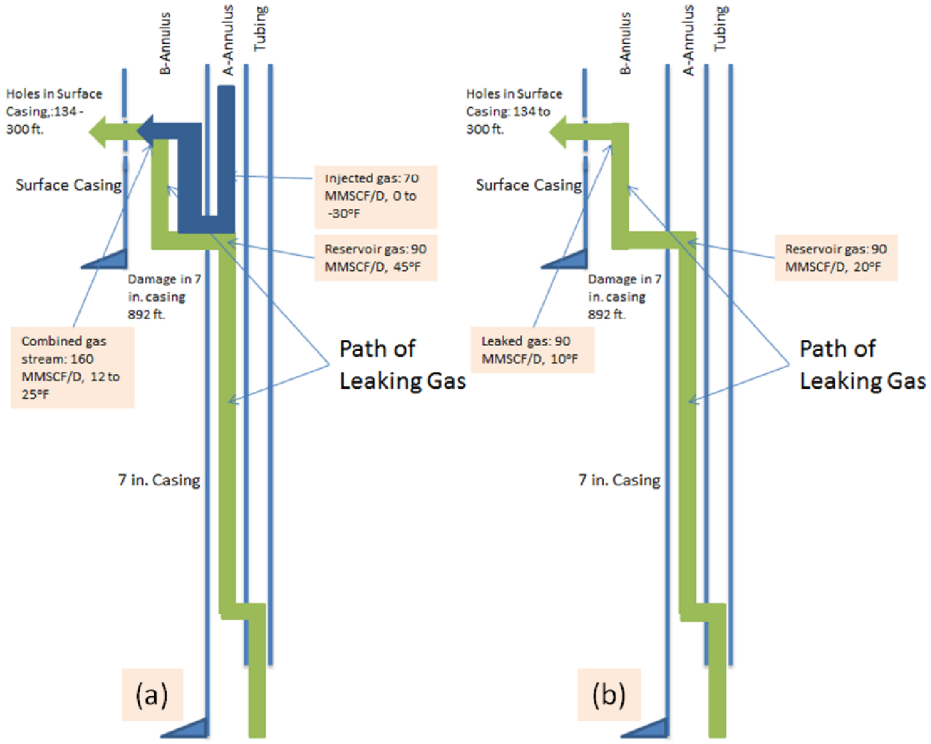

(a) Gas flow path after 7 in. casing failure but before shut-in of SS-25 (10/23/15 04:00 to 16:00). The cold injection gas exits the 7 in. casing near the top of the 20 in. axial crack. We believe this lead to transpiration cooling which shielded the 7 in. casing from the warm reservoir gas. This cold temperature caused the 7 in. casing near 892 ft to become brittle and the casing to part.
(b) Gas flow path after SS-25 was shut in. Gas is provided solely by the reservoir. The pressure at the 7 in. casing leak point falls to 280 psi and temperature of the reservoir gas arriving at 892 ft falls to between 10 and 20°F.

Figure 7: The Gas Flow Paths Prior to Kill Attempt #1 October 24, 2015

Let's estimate the time required to cool 892 ft of 7 in. casing. Since there were only about 12 hours between the initial ductile failure and the shut-in, the time to cool the 7 in. casing should be less than this amount of time. There are two steps to cooling down the 7 in. casing. The first is to flow enough injection gas to absorb the required amount of heat. The second is for forced convection to transfer the heat from the metal to the injected gas. These two steps occur in parallel, so the required time is the longer of the two.

The following analysis assumes that the transpiration cooling is effective, the injection gas temperature is –30°F, and the 7 in. casing will be cooled from 80°F to nearly the gas temperature.

The volume of gas needed (first step) is the largest when the final 7 in. temperature is the lowest. Table 1 shows that for a final 7 in. casing temperature of –25°F, it will take 1.2 hours to flow enough gas to absorb the required amount of heat. Table 2 shows that for a final temperature of –29°F, it will take 6.1 hours. Please see Appendix D for details on this type of calculations.

Table 1: Estimated Time Required to Bring 892 ft of 7 in. Casing from 80 to –25°F

Initial Temperature	°F	80
Tubing Weight	lbm/ft	6.5
7 in. Casing	lbm/ft	23
Total Weight of Metal /ft	lbm/ft	29.5
Heat Capacity	Cp Btu/lb-°F	0.12
Metal Temperature	°F	–25
Change in Temperature	°F	–105
From Sensible Heat	Btu/ft	–371.7
Total Length	ft	892
Total Btus Required	Btu	–331,556

Gas (Methane)

Rate	MMSCF/D	70
Heat Capacity	Btu/lbm-F	0.461
Density @ 68°F /1 atm	lbm/ft^3	0.0417
Gas Temperature	°F	–30
Change in Temperature	°F	–5
Available Btus	Btu/10 mins	–46,724
Total Time Required	Hr	1.2

Table 2: Estimated Time Required to Bring 892 ft of 7 in. Casing from 80 to –29°F

Initial Temperature	°F	80
Tubing Weight	lbm/ft	6.5
7 in. Casing	lbm/ft	23
Total Weight of Metal /ft	lbm/ft	29.5
Heat Capacity	Cp Btu/lb-°F	0.12
Metal Temperature	°F	–29
Change in Temperature	°F	–109
From Sensible Heat	Btu/ft	–385.86
Total Length	Ft	892
Total Btus Required	Btu	–344,187

Gas (Methane)		
Rate	MMSCF/D	70
Heat Capacity	Btu/lbm-°F	0.461
Density @ 68°F /1 atm	lbm/ft^3	0.0417
Gas Temperature	°F	–30
Change in Temperature	°F	–1
Available Btus	Btu/10 min	–9,345
Total Time Required	Hr	6.1

The overall heat transfer coefficient for forced convection inside the 7 in. x 2 7/8 in. annulus is given by the same correlation shown in Appendix D. Table 3 shows that for a final 7 in. casing temperature of –25° F, the required time to transfer the needed amount of heat is 0.04 hours. Table 4 shows that for a –29°F final 7 in. casing temperature, the required time is 0.21 hours by forced convection. In either case, the rate-limiting step is the time needed to flow enough gas to absorb the heat from the 7 in. casing. This time ranges from 1 hour to 6 hours depending on the final metal temperature. This range is within the 12 hours between the ductile failure and the shut-in of SS-25.

Table 3: Time Required for Forced Convection Inside the 7 in. x 2 7/8 in. Annulus to Transfer the Required Amount of Heat when 7 in. Casing Temperature is –25°F

Temperature (°F)	–30.00
Z Factor	0.87
Pressure (psi)	480.00
Inner Diameter D1 (ft)	0.24
Outer Diameter D2 (ft)	0.53
Density rho (lbm/ft^3)	1.91
Volumetric Flow Rate (MMSCF/D)	70.00
Gas Viscosity mu (lbm/(hr-ft)	0.01
Gas Specific Heat c (Btu/lbm-°F)	0.62
Gas Conductivity k (Btu/hr-ft^2-(°F/ft)	0.02
Flow Area (ft^2)	0.18
Effective Diameter De (ft)	0.29
Velocity u (ft/hr)	366,263
Reynold's Number Nre	20,287,328
Prandtl's Number Npr	0.31
Npr's Exponent	0.33
Nusselt Number Nnu	14388.50
Heat Transfer Coefficient h (Btu/hr-ft^2-°F)	1003.36
Difference in Temperature (°F)	5
7 in. Casing External Surface Area (ft^2/ft)	1.83
Total Length (ft)	892

Temperature (°F)	–30.00
Heat Transferred Rate (Btu/hr)	8,200,797
Time Required (hr)	0.04

Table 4: Time Required for Forced Convection Inside the 7 in. x 2 7/8 in. Annulus to Transfer the Required Amount of Heat when 7 in. Casing Temperature is –29°F

Temperature (°F)	–30.00
Z Factor	0.87
Pressure (psi)	480.00
Inner Diameter D1 (ft)	0.24
Outer Diameter D2 (ft)	0.53
Density rho (lbm/ft^3)	1.91
Volumetric Flow Rate (MMSCF/D)	70.00
Gas Viscosity mu (lbm/(hr-ft)	0.01
Gas Specific Heat c (Btu/lbm-°F)	0.62
Gas Conductivity k (Btu/hr-ft^2-(°F/ft)	0.02
Flow Area (ft^2)	0.18
Effective Diameter De (ft)	0.29
Velocity u (ft/hr)	366,263
Reynold's Number Nre	20,287,328
Prandtl's Number Npr	0.31
Npr's Exponent	0.33
Nusselt Number Nnu	14388.50
Heat Transfer Coefficient h (Btu/hr-ft^2-°F)	1003.36
Difference in Temperature (°F)	1
7 in. Casing External Surface Area(ft^2/ft)	1.83
Total Length (ft)	892
Heat Transferred Rate (Btu/hr)	1,640,159
Time Required (hr)	0.21

4 Model of the Leak

The analyses in Section 3 showed that the leak started after 03:00 on October 23, 2015 and provided estimates of rates, pressure, and temperatures in the well during the period between the start of the leak and the shut-in of SS-25. This section covers the period after the shut-in of SS-25.

On October 23, 2015, the SS-25 injection valve was shut in, and the SSV automatically closed. The tubing pressure was 1,700 psi, 7 in. x 2 7/8 in. annulus pressure was 270 psi, and 11 3/4 in. x 7 in. annulus pressure was 140 psi [5] (page 78). From these readings, PROSPER estimated a leak rate of 90 MMscf/D and a temperature of the gas at the leak point (892 ft) inside the 7 in. x 2 7/8 in. annulus of 10 to 20°F [2].

Initial temperature surveys showed anomalously low temperatures in the shallow portion of the well, which suggested a breach in the 7 in. casing at a shallow depth. When there is a gas leak like the one at SS-25, failure of the surface casing shoe and poor cementing of the surface casing are the usual suspected places where the gas leaks out of the well. Our initial theory was that gas escaped through the opening in the 7 in. casing into the 11 3/4 in. x 7 in. annulus and then flowed around the surface casing shoe and up the poorly cemented backside of the surface casing and out into the formation. However, when the 7 in. casing was pulled, holes were found in the surface casing between 134 and 300 ft [20]. This raised the question as to whether the gas flowed out the holes, or around the casing shoe, or both.

The ratio of the pressure in the 7 in. x 2 7/8 in. annulus to the pressure inside the 11 3/4 in. x 7 in. annulus was about 2, which initially suggested that the leak was choked by the opening in the 7 in. casing. The estimated equivalent hole size to choke 90 MMscf/D was approximately 4 in. However, when the 7 in. casing was pulled, it was found that the 7 in. casing not only had a large hole and long axial crack (with a measured area of 20 $in.^2$ – 5.1 in. equivalent hole diameter), but it was also parted at 892 ft. Section 3 showed that these damages were there by the time of shut-in. Such large openings would not choke the 90 MMscf/D gas flow. The pressure on the 11 3/4 in. x 7 in. annulus side would have been close to the pressure on the 7 in. x 2 7/8 in. annulus side of the leak (about 270 psi). The pressure at the top of the 11 3/4 in. x 7 in. annulus was 140 psi, and the PROSPER modeling indicated that there would be substantial pressure drop if the bulk of the 90 MMscf/D flowed up the 11 3/4 in. x 7 in. annulus and out the holes between 134 and 300 ft [2]. If a substantial portion of the gas flowed out the casing shoe and not out the holes, the 11 3/4 in. x 7 in. annulus pressure reading would be close to 270 psi and not 140 psi. From these pressure measurements, we deduced that the bulk, if not all, of the 90 MMscf/D flowed up the 11 3/4 in. x 7 in. annulus and out the holes there. This also implied that the temperature inside the upper section of the well was close to the gas temperature, which was 10 to 20°F less the extra cooling due to the additional pressure drop as the gas flowed up the 11 3/4 in. x 7 in. annulus (about 5°F).

On October 28, 2015, fluid level was at 43 ft in the 11 3/4 in. x 7 in. annulus and 164 ft in the 7 in. x 2 7/8 in. annulus [21]. These fluid levels were actually the top of ice plugs that had formed in the well. The source of this water was the 89 bbl of the 8.6 ppg KCl pumped down the 7 in. x 2 7/8 in. annulus on October 24, 2015, as part of kill attempt #1. Part of this water was entrained by the gas flowing up the 11 3/4 in. x 7 in. annulus; it coated the walls of the surface casing and froze. This coating of ice was thick enough to appear as a fluid level. The pressure in the 11 3/4 in. x 7 in. annulus also rose to 450 psi from 140 psi by October 25, 2015, and 800 psi by October 30, 2015 (Table 9). The holes in the 11 3/4 in. x 7 in. annulus were likely obstructed by ice.

The estimated fracturing pressure at the shoe was 400 to 815 psi (Appendix F). During the period from October 25, 2015, to when the well was finally deiced on November 6, 2015, the pressure in the 11 3/4 in. x 7 in. annulus ranged from 400 to 800 psi. We presumed that the rocks around the surface casing shoe

were fractured during this period. This provided the path for the gas out of the well during the warm leaked gas period.

It is not certain whether the path around the casing shoe was also obstructed by ice. In principle, the 7 in. x 2 7/8 in. annulus pressure can be used to estimate the relative amount of flow up the 11 3/4 in. x 7 in. annulus and around the casing shoe. In Appendix B, we present evidence that there was a blockage between the pressure gauge at the top of the 7 in. casing and the leak point at 892 ft after pumping the kill fluid down the 7 in. x 2 7/8 in. annulus in kill attempt #1. Due to this obstruction, the 7 in. x 2 7/8 in. annulus pressure gauge reading lags the pressure at the leak point. In fact, there are times when the 7 in. x 2 7/8 in. annulus pressure reading appears to be lower than the 11 3/4 in. x 7 in. annulus pressure reading, which is impossible. The 7 in. x 2 7/8 in. annulus' pressure reading therefore cannot be used to determine whether the casing shoe was also obstructed. We assumed that the leak path around the casing shoe was not blocked, and the leak during the warm leaked gas period was mainly around the casing shoe.

The available data did not indicate when the flow was redirected from the holes in the surface casing to the casing shoe. We assumed the ice formed in the 11 3/4 in. x 7 in. annulus in a day, and selected October 25, 2015, as the day when the gas was redirected. This redirection was important because pressure was as high as 800 psi between this date and November 6, 2015. Table 5 shows PROSPER's estimate of the gas rates and temperatures for various pressures at 892 ft after the shut-in. Table 5 shows that at pressure above 400 psi, the estimated temperature of the reservoir gas at the leak point is above freezing. If a portion of this warm gas flowed up the 11 3/4 in. x 7 in. annulus, the upper section inside the well would have warmed up. However, this is not what occurred. (See Appendix D.)

Under this scenario, gas flow at the surface should have diminished because the gas leaked deeper underground. A DOGGR onsite representative indeed reported that the gas leak rate at the surface was diminishing. On November 2, 2015, he reported that "most of the cracks and the hillside were no longer leaking gas to surface. Gas leakage was primarily confined to the well cellar and was reduced from before. There was some leakage still on the hillside, but this was barely noticeable." [22]

There were temperature readings ranging from 19 to 59°F on October 28 and 29, 2015, inside the SS-25 tubing. Appendix C discusses these data in detail and explains why we concluded that the temperature was 19°F. Because we believed that the temperature was below freezing, we concluded that most if not all the gas flowed out of the well around the casing shoe and avoided thawing out the upper section of the well.

The daily reports mentioned that hydrates formed in the tubing during kill attempt #1. The implication was that, with hydrates, a temperature well above 32°F was required to thaw out the hydrate plug.

However, the hydrate formation kinetic is slow [2]. It would not have been possible to form enough hydrates in the several minutes that it took to plug up the tubing. In addition, the salt that was in the kill fluid would have inhibited the formation of hydrates.

Table 5: Results of PROSPER Modeling with Various Conditions at Leak Point

LP PRS (psi)	LP Q (MMscf/D)	LP TEMP (°F)	Depth >32°F (ft)
280	93	22	1,200
300	92	26	1,100
350	92	29	1,000
400	91	33	-
500	91	39	-
800	87	56	-
1000	84	67	-
1200	80	76	-
1400	76	84	-
1600	70	91	-
1800	63	97	-
2000	55	103	-
2200	45	107	-
2300	39	109	-
2350	36	110	-
2400	32	111	-
2500	24	111	-
2600	14	108	-
2680	0	80	-

- Leak point (LP) is at 892 ft.
- LP PRS is the pressure on the upstream side of the leak at the leak point.
- LP Q is the volumetric rate up the casing associated with "LP PRS".
- LP TEMP is the estimated temperature of the gas upstream of the leak at the LP.
- DEPTH >32°F is the depth below which the gas temperature is above freezing (32°F).

On November 6, 2015, 10.8 ppg $CaCl_2$ and glycol were pumped into SS-25 through coiled tubing to unplug the tubing (deicing operation). The operation was successful. The pressure in the 11 3/4 in. x 7 in. annulus fell from 500 psi to 60 psi after deicing. The 60 psi was even lower than the 140 psi measured immediately after shutting in SS-25. This lower 60 psi pressure could have been the result of new fissures forming between the shut-in and the deicing operations. Ice that formed from kill fluids might have plugged these new fissures soon after their formation, and the deicing operation unplugged them. In any case, in the simulation model, gas was allowed to flow up the 11 3/4 in. x 7 in. annulus again on November 6, 2015. Because the pressure in the 11 3/4 in. x 7 in. annulus fell, the fracture around the casing shoe would likely close and once again cause all the gas to leak out the holes in the upper portion of the surface casing. The DOGGR onsite representative reported that after the deicing operation, "Gas was once again leaking at the well head and on the surrounding hillsides after a period of quiescence." [22]

On November 13, 2015, a crater started forming around SS-25. The pressure in the 11 3/4 in. x 7 in. annulus fell to 30 psi. Most of the leaked gas was vented out the crater and did not affect the formation temperatures away from SS-25.

Several other unsuccessful kill attempts were made with the final kill attempt on December 22, 2015. The crater continued to enlarge with each subsequent kill attempts.

On February 11, 2016, SS-25 was killed from relief well P-39A. Gas trapped in the formation flowed out the crater, and the formation around SS-25 depressurized.

The gas leak rates and temperatures from the shut-in to when SS-25 was killed came from the PROSPER modeling using the reported 7 in. x 2 7/8 in. annulus pressure and the shut-in well head pressure of the observation well SS-5 [2].

Figure 8 summarizes the evolution of the leak inside the well from the initial ductile failure to after the deicing operation. The observations on the changes in the leak rate noted by the DOGGR representative at the SS-25 site are consistent with our scenario [22].

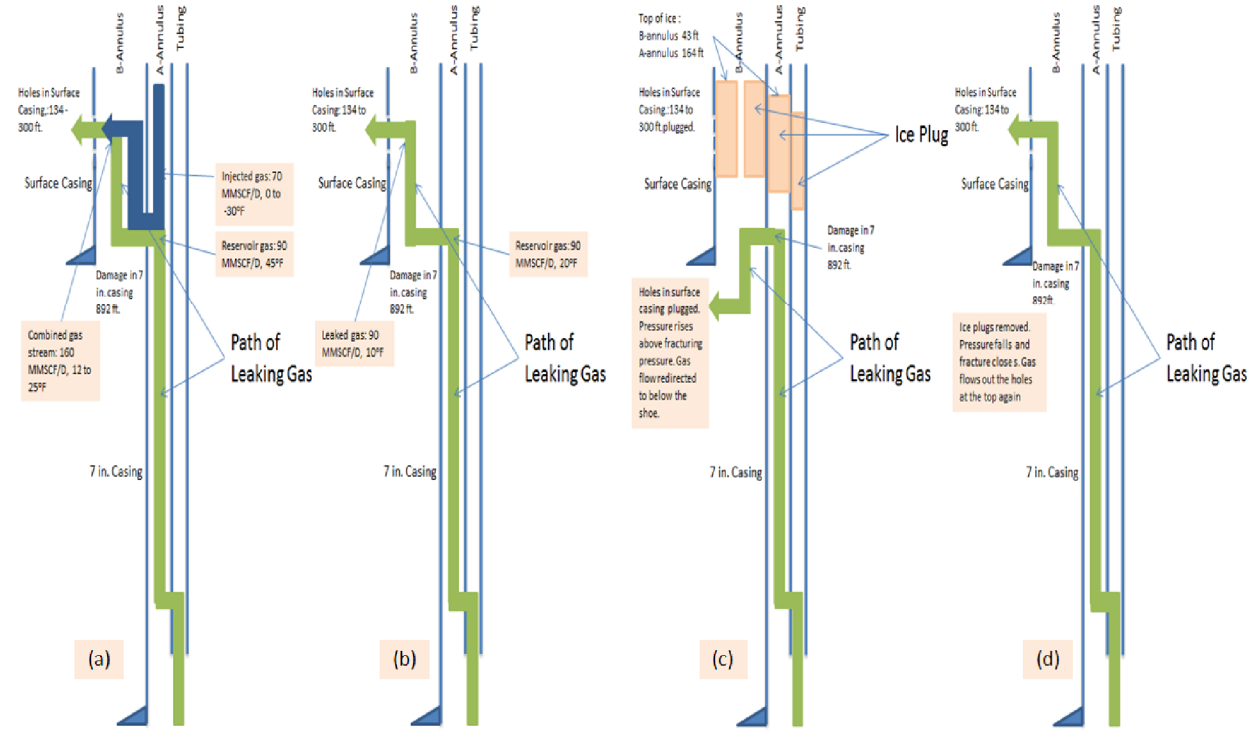

(a) Gas flow path after 7 in. casing failure but before shut-in of SS-25 (10/23/15 03:00 to 16:00). The cold injection gas exits the 7 in. casing near the top of the 20 in. axial crack. This cold temperature cased the 7 in. casing near 892 ft to become brittle and the casing to part.
(b) Gas flow path after SS-25 was shut in. Gas is provided solely by the reservoir. The pressure at the 7 in. casing leak point falls to 280 psi and temperature of the reservoir gas arriving at 892 ft falls to between 10 and 20°F.
(c) After the kill attempt #1, ice plugged the upper section of the well. (Ice or hydrate might have also plugged the pathways out in the formation.) The ice restricted the flow out the holes in the upper section. Pressure rose fracturing the shoe. Gas flow is redirected below the shoe leaving the upper section cold.
(d) After the coil tubing deicing operation (6-Nov-15), the ice plugs were removed. This allowed gas to once again flow out the top. Pressure falls and the fracture closes.

Figure 8: Gas Leak Path out of the Well from the Initial Failure to Coiled Tubing Deicing Operation

5 Temperature Observations

In this section, we gather all the recorded temperature measurements and temperatures deduced from reported field observations. These temperatures will be compared to the simulation model results.

On October 23, 2015, SS-25 was shut in. The tubing pressure was 1,700 psi, 7 in. x 2 7/8 in. annulus pressure was 270 psi, and 11 3/4 in. x 7 in. annulus was 140 psi [5] (page 78). Using PROSPER, the flow rate was estimated to be 90 MMscf/D with a temperature of 20°F, or possibly 10°F, depending on the heat transfer coefficient value and roughness factor used in PROSPER [2].

On October 24, 2015, the 10.0 ppg $CaCl_2$ / XC polymer pill was pumped down the 2 7/8 in. tubing [23]. Tubing pressure rose to 3,500 psi and pumping had to be stopped. The fluid had frozen in the tubing after several minutes of pumping. The freezing point of a 10.0 ppg $CaCl_2$ solution is –8°F. However, a review of the pumping record of kill attempt #1 down the tubing indicated that there was some 8.6 ppg KCl still left in the line ahead of the 10.0 ppg $CaCl_2$ (Figure 22). There was about 1 bbl of KCl and $CaCl_2$ mixture (slop) (Figure 22). The 8.6 ppg KCl has a freezing point of 26°F. The freezing point of this slop, therefore, was between –8 and 26°F. Because the slop froze in the tubing, the temperature of the tubing was in or below this range.

On October 28, 2015, 8.7 ppg Flowzan (8.6 ppg KCl and xanthan polymer from GEO Drilling Fluids, Inc.) was pumped down the tubing. However, because of the ice plug already in the tubing (the bailer tagged ice at 467 ft prior to pumping the solution), pressure rose, and this pumping operation was stopped. An hour later, the bailer was sent back down and again tagged ice at 467 ft, which indicated that the Flowzan® had not frozen yet. However, the presence of the ice plug at 467 ft suggested that the temperature in the tubing was still below freezing.

The following morning, the bailer was sent down and found that this fluid had frozen overnight, and the bailer temperature was 19°F. (The data on October 28 and 29, 2015, were inconsistent. See Appendix C for discussion of this data and why we concluded the temperature was 19°F.) Because it took the Flowzan hours to freeze while the slop pumped on October 24, 2015, took only a few minutes, the temperature on October 24, 2015, was likely lower than 19°F.

On November 8, 2015, Core Lab ran a temperature survey [24] down the SS-25 tubing and obtained a temperature reading of 17°F at an approximate depth of 300 ft.

The February 16, 2016, temperature survey [25] run in the SS-25 tubing showed temperatures of about 65°F in the upper section. This is unexpected considering that the temperatures seen at SS-25, SS-25A, and SS-25B at a later date were near freezing.

The April 12, 2016, temperature survey run in the SS-25 tubing showed a temperature of about 46°F [26].

Temperature surveys [27] run in SS-25B between August 2 and 16, 2016, showed temperatures of 38°F at an approximate depth of 100 ft.

The temperature survey [28] run in SS-25A between August 13 and 30, 2016 showed temperatures of around 30°F at an approximate depth of 100 ft.

Other temperature surveys and Distributed Temperature Sensing (DTS) measurements [29], [30], [31], [32], and [33] were taken between August 2016 and July 2017. Table 6 shows the date and temperature for the STARS thermal model to match to.

Between September and October 2016, the temperature at SS-25A rose from freezing to 40°F and then fell back down to freezing again. Analysis of the DTS data and the review of well work performed on

SS-25A during this period suggested that this was caused by fluid movement in the well. The anomalous temperature behavior did not reflect the temperature of the formation around SS-25A at this time [26]. These higher temperatures were ignored.

Persistent temperatures of 30 to 40°F extending 20 to 40 ft from SS-25 14 months after the incident were unexpected. We used these anomalous temperature observations to test our scenario of the leak.

Table 6: Temperatures to Match

Date	Temperature
10/24/2015	SS25 <19°F
10/28/2015	SS25 < 32°F (below freezing)
10/29/2015	SS25 <19°F
11/8/2015	SS25 <17°F
2/16/2016	~65°F around SS25
4/12/2016	46°F around SS25
8/16/2016	~30°F at SS25A and 38°F at SS25B
9/30/2016	~40°F at SS25A and 40°F at SS25B
10/8/2016	38°F at SS25B
10/29/2016	~32°F at SS25, ~37°F at SS25A
11/29/2016	~32°F at SS25, ~32°F at SS25A
12/10/2016	~32°F at SS25, ~33°F at SS25A
7/31/2017	32°F at SS25, 48°F at SS25A

6 Simulation Model

In this section we show how the shallow geology was used to construct the static thermal reservoir simulation model and how our picture of the leak was used to construct the model's well operating schedule. After the simulation model was constructed, we examined how well the simulated temperatures matched the observed values.

Figure 9 shows an aerial view of the SS-25 pad and the relative location of SS-25, SS-25A, and SS-25B. These wells are vertical over the first 1,000 ft, so SS-25A is approximately 20 ft and SS-25B is approximately 38 ft from SS-25 over the entire vertical interval of interest. The blue box is the area to be simulated. By assuming symmetry, only one quadrant needed to be modeled.

Figure 9: Plan View of What was Modeled by the STARS's Simulation Model

Figure 10 shows the vertical cross section of the simulation grid aligned with the SS-25 stratigraphic log [11]. The simulation grid was 10 X-slices (i) by 10 Y-slices (j) by 9 Z-layers (k). Layer 1 mimicked the atmosphere. The 10th i and j vertical slices provided a constant temperature bath surrounding the area of interest. The air temperature (layer one) was set to 60°F. Temperature surveys and DTS measurements showed that the temperature ranged from 60 to 80°F (excluding the cold zones) over the top 1,000 ft of the ground. In the simulation model, the remaining layers (ground) were set initially to 80°F.

SS-25 did not have any of the modern logs needed for determining the lithology. The lithology log was constructed from the mud log of the relief well P-39A, which is 1,475 ft southeast of SS-25. Figure 10 shows only the major lithological units (flow units), and because these flow units are thick, they are likely to extend across the SS-25 site. Within these major flow units there are thinner flow units, but they were not modeled because we lacked the data to trace them for SS-25, SS-25A, and SS-25B.

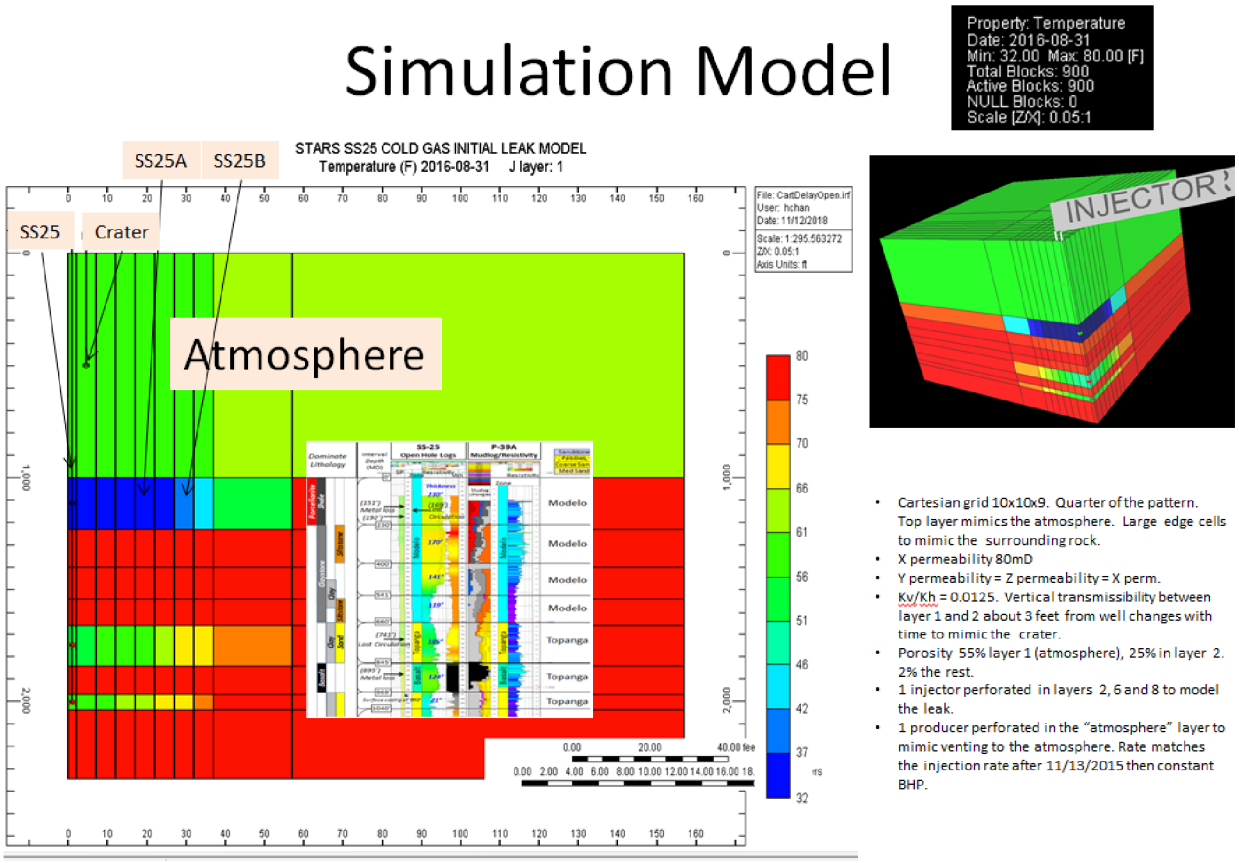

Figure 10: Simulation Grid

Advisian's [8] shallow geology work indicated that at least down to the depth of 150 ft, the ground is heavily weathered. This weathered zone may extend deeper. To mimic this, the top ground layer (simulation layer 2), which extends down to 230 ft, was given a porosity of 25%. Layers 3 to 9 were given 2% porosity.

The permeability values of all layers were assigned 80 md in the horizontal directions (X and Y). (Permeability of 80 md was what was used in the well bore hydraulic modeling of the Sesnon reservoir zone [2].) Although the permeability in the channels would be much higher, these channels do not occupy the entire 230 ft of layer 2. There are barriers between the channels. Furthermore, 80 md or higher does not make much difference as far as temperature goes. We ran a sensitivity case with permeability of 1,000 md to demonstrate this.

Flow in the vertical direction was expected to be restricted, as explained in Section 2, Shallow Geology. Except for layer 2, which is heavily weathered and was given a vertical permeability of 80 md, all the other layers (3 to 9) were given 1 md. The vertical to horizontal permeability is, therefore, 0.0125. Starting on November 13, 2015, a large crater started to form around SS-25. This crater formation was mimicked by increasing the vertical transmissibility between layers 1 and 2 (atmosphere and top ground layer) by 10,000-fold only in the area within 3 ft of the well starting on that day.

Advisian's NMR work [8] showed 10 to 20% water content in the top 123 ft of the ground. The water saturation in layer 2 was assigned a value of 60% (15% water content). It was not certain how much of the water seen by the NMR was from the borehole drilling operation. It should be noted that California was experiencing the third year of a severe drought in 2015 when the incident occurred [34]. Southern

California did not see relief until end of 2016 and beginning of 2017. This suggested that there was little rainwater in the ground at the time of the incident. However, about 4,000 bbl of water was pumped into SS-25 between October 24 and December 22, 2015, and that might have been the source of the water. The 4,000 bbl of water would have extended out 22 ft from SS-25 if the channel were shaped like a 100 ft thick disc with porosity of 25% and water saturation of 60%. We ran a sensitivity case with 1% water saturation. Recall that the bulk of the water seen in the NMR log was capillary water, the type of water that does not flow. The critical water saturation was set to 75% to prevent water from flowing.

We assigned 35 Btu/ft^3/°F [35] to the rock heat capacity (assuming a rock density of 2.6 gm/cm^3), 24 Btu/(ft-day-°F) [35] to the rock thermal conductivity, 8.6 Btu/(ft-day-°F) [36] to the thermal conductivity of water, and 0.48 Btu/(ft-day-°F) [37] to the thermal conductivity of methane. Because STARS assumed the rock and fluid were at temperature equilibrium in each grid cell, the heat transfer coefficient between the gas phase and the rock was infinite.

CMG's STARS suggested a rock thermal conductivity value, in the absence of data, of 44 Btu/(ft-day-°F) [36]. We ran a sensitivity case with 50 Btu/(ft-day-°F), twice the base case value.

We modeled the leak as an injector. We initially perforated layer 2 to mimic the leak. The column of grid cells the well was in (cells i=1, j=1, and k=2 to 8) represented the backside of the surface casing. We assumed that even though the cement behind the surface casing was poor, it still provided some resistance to flow in the vertical direction. This column of grid cells was given a permeability of 80 md.

The leak started prior to the shut-in of SS-25. This period of leak was brief, about half a day. We set the leak rate to 160 MMscf/D, with 90 MMscf/D from the reservoir and 70 MMscf/D from the injection line. We assumed that the leak temperature was 0°F and the leak duration was half of a day. (See Section 3.) We simulated this case and the case in which this brief leak did not occur. There were differences in the temperatures at early time, but after shut-in, the flow of the warmer reservoir gas quickly erased the signs of the earlier colder leak. By the time the temperature data were available from SS-25A and SS-25B (August 2016), both cases were the same. Because it was not possible to discriminate between the two cases, we show only the results without the earlier leak.

We perforated layers 6 and 8 and shut layer 2 when the holes in the 11 3/4 in. x 7 in. annulus were plugged. The gas flowed out above and below the basalt. In the earlier discussion on the shallow geology, only two channels were identified based on lost circulation. The first was at 169 ft and the second at 741 ft. The channel at 741 ft was above the basalt, and that corresponded to layer 6. We perforated layer 8 because it was where the surface casing shoe landed (below the basalt), and the P-39A mud log did show sand layers below the basalt.

We added a producer well to layer one (atmosphere) to mimic the crater that formed near SS-25. We activated it on November 13, 2015 when the large crater started to form. We set the production rate to equal the leak rate. We switched the producer to a constant bottomhole pressure producer (140 psi) on February 11, 2016 to depressurize the formation after the well was killed by the relief well. Table 7 shows the changes in the well rate and temperature with time. Table 6 shows the temperatures to match.

As shown in Table 7, on October 29, 2015, the pressure in the 11 3/4 in. x 7 in. annulus was 600 to 800 psi; for this date, we set the gas temperature to 40°F even though PROSPER estimated the gas temperature to be 50 to 60°F. We presumed that the gas depressurized as it flowed up the back side of the surface casing or out in the formation, and the additional expansion may have reduced the temperature to 40°F. The simulation results showed that because of this choice, the temperatures in layer 6 and 8 were about 20°F lower than observed. Because our focus is on the temperatures around SS-25, SS-25A, and SS-25B in layer 2, we did not adjust the leaked gas temperature to improve the match.

The ground around SS-25A and SS-25B was still cold at the end of August 2016; one plausible explanation for this is that this was due to ice or hydrates undergoing phase change. STARS does not have the ability to model hydrates, but it has the ability to model ice formation and melting. We used the ice option.

It is difficult to determine whether it was ice or hydrate formation that maintained the freezing temperatures in SS-25, SS-25A, and SS-25B long after SS-25 was killed. The anomalous temperature was about 32°F. Ice phase changes at 32°F; hence, ice can explain this anomaly. It would be difficult to distinguish between ice or hydrate formation based on the observed temperatures alone. The heat of fusion of ice and the heat of dissociation of hydrates are also about the same. One difference between the two is the thermal conductivity (0.61 W/m-K for hydrates [38] and 2.22 W/m-K for ice [39]), but this difference is masked by the uncertainty of the rock thermal conductivity and the amount of water in the formation.

Table 7: Changes in the Leak Rates and Temperatures with Time Used in the Thermal Simulation Model

Date	Temperature	Comment
10/23/2015	Set injection rate to 90 MMSCF/D 10°F. Open well to layer two.	Leak rate and temperature from PROSPER. Leak flowing out of holes between 134 and 300 ft.
10/26/2015	Shut layer two and open layers six and eight. Raise injection temperature to 40 °F.	Ice forms in B annulus. B annulus pressure 600 to 800 psi and may frac the casing shoe. PROSPER estimates gas temperature of 50 to 60 °F. Diverting flow around surface casing shoe.
11/6/2015	Close well to layers six and eight. Open well to layers two. Set injection temperature to 10 °F.	Deicing operations unplugs well and formation around the well. "A" and "B" pressures fall. Leak point temperature falls back down to 20 °F.
11/13/2015	Set injection rate to 80 MMSCF/D 20°F.	Leak rate and temperature from PROSPER.
11/13/2015	Open communication between layer one (atmosphere) to layer two.	Blowout vent opened shooting debris into the air.
12/8/2015	Set injection rate to 70 MMSCF/D 40°F.	Leak rate and temperature from PROSPER.
12/17/2015	Set injection rate to 60 MMSCF/D 50°F.	Leak rate and temperature from PROSPER.
12/24/2015	Set injection rate to 50 MMSCF/D 60°F.	Leak rate and temperature from PROSPER.
1/10/2016	Set injection rate to 40 MMSCF/D 70°F.	Leak rate and temperature from PROSPER.
2/11/2016	Switch to BHP. Set BHP to 140 psi.	Well killed. Depressurize the formation.
12/11/2016	No change.	-
8/31/2017	End of simulation.	Last temperature log

The temperatures of the leaked gas between 10/23/2015 and 11/13/2015 included additional 10°F drop for possible J-T cooling.

The rest of this section compares the simulated temperatures with the observed temperatures. The area of interest is in layer 2 around the three wells, SS-25, SS-25A and SS-25B. The approximate locations of these wells are colored in the temperature maps. Yellow is SS-25, pink is SS-25A, and blue is SS-25B.

Figure 11 and Figure 12 show the simulated temperatures of the base case. The simulated temperatures from shut-in to November 8, 2015 satisfy the observed temperature requirements. The simulated temperature for February 16, 2016 is 49°F, which is lower than the observed 65 to 70°F. Figure 13 shows the temperatures on February 11, 2016, four days earlier. The temperature at SS-25 is 70°F and matches the observed temperature.

On February 11, 2016, SS-25 was killed and the reservoir depressurized through the crater, which drew cold gas toward the well and cooled down SS-25. This is why the temperature in SS-25 declined after the

well was killed, consistent with the field observations. The faster cool down of SS-25 indicates that the simulation model might be depressurizing the formation too fast.

On April 12, 2016, the measured temperature was 46°F. The simulated temperature (not shown) is 34°F. The difference again may be due to depressurizing the formation too fast. Also, it should be noted that the February 11 and April 12, 2016, measurements were wireline surveys. They tend to measure higher temperatures than the DTS does. For example, on December 30, 2016, a wireline survey measured a low temperature of 37°F [26], whereas the DTS gave a low reading of 32°F [29].

The temperature matches later around SS-25 are good. The temperature is still 32°F out to end of August 2017 as observed in the field.

The SS-25B temperature matches between August 2016 and end of October 2016 are also good (the only temperature data available for SS-25B).

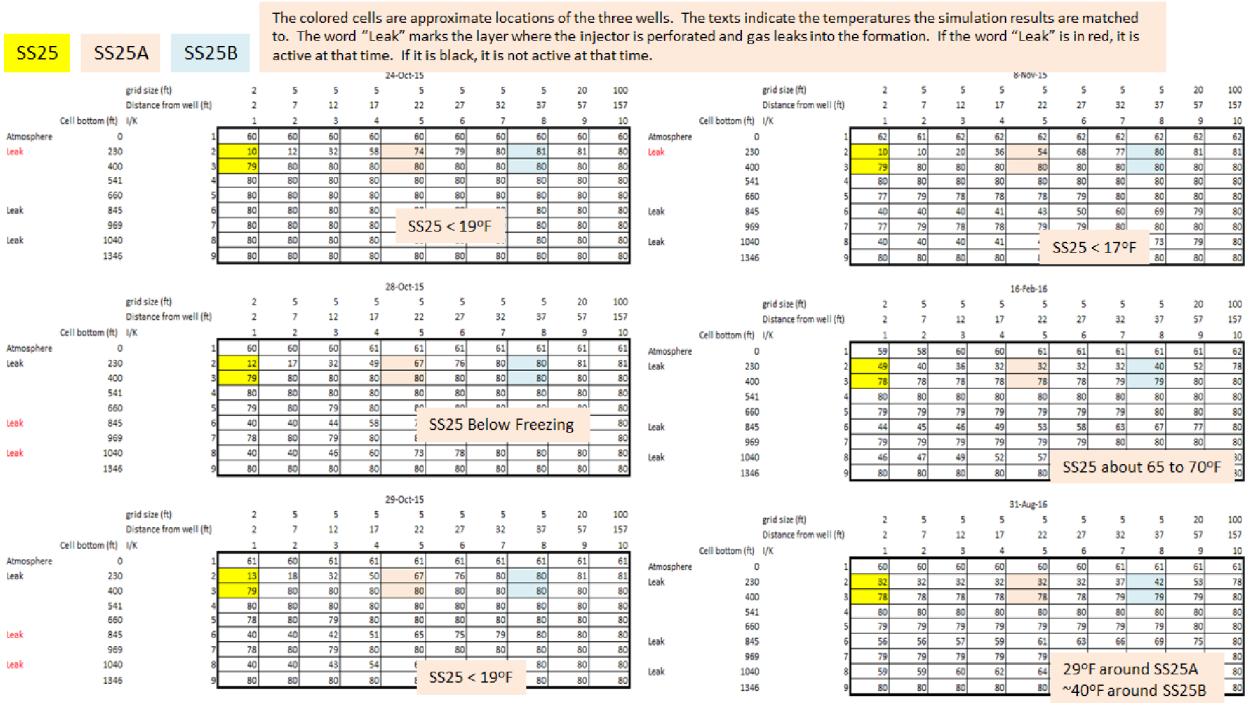

Figure 11: Simulated Temperatures October 24, 2015, to August 31, 2016

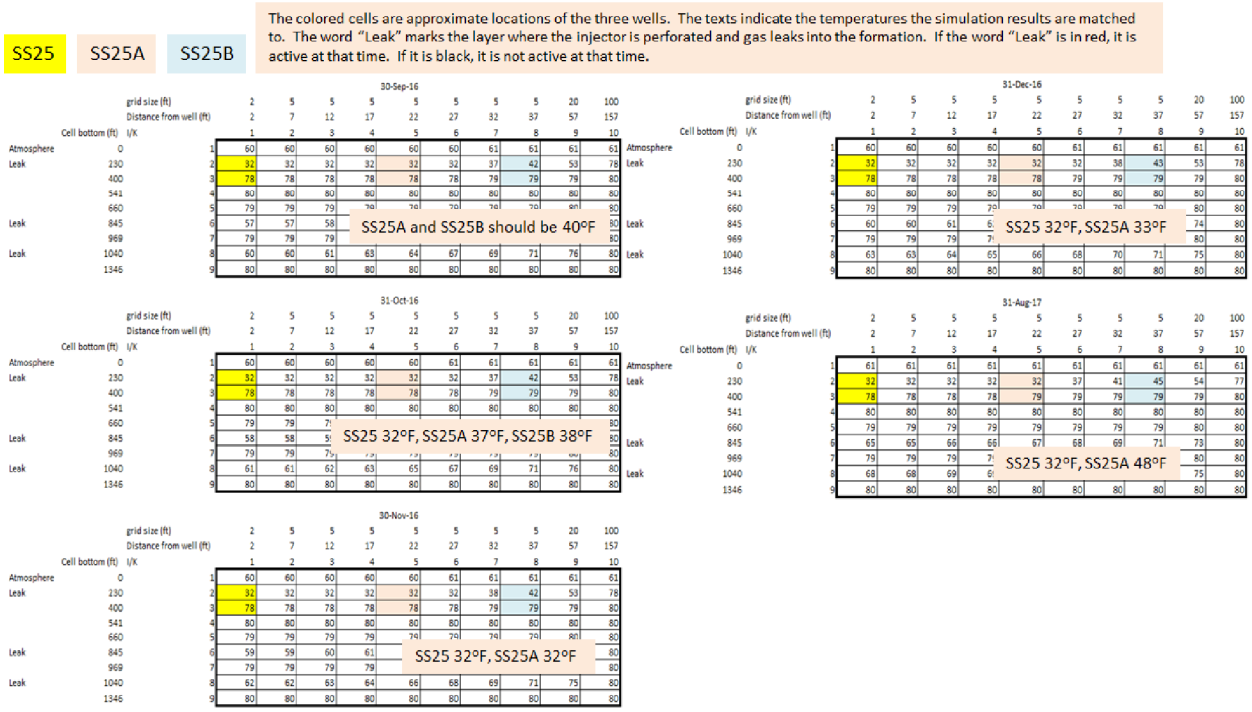

Figure 12: Simulated Temperatures between September 30, 2016, and August 31, 2017

SS25 SS25A SS25B

11-Feb-16

	grid size (ft)		2	5	5	5	5	5	5	5	20	100
	Distance from well (ft)		2	7	12	17	22	27	32	37	57	157
Cell bottom (ft)	I/K		1	2	3	4	5	6	7	8	9	10
Atmosphere	0	1	70	67	63	62	62	62	63	63	63	64
Leak	230	2	70	69	54	32	31	31	32	37	51	78
	400	3	78	78	78	78	78	78	79	79	80	80
	541	4	80	80	80	80	80	80	80	80	80	80
	660	5	79	79	79	79	79	79	79	80	80	80
Leak	845	6	44	44	46	49	53	58	63	67	77	80
	969	7	79	79	79	79	79	79	80	80	80	80
Leak	1040	8	46	46	48	52	56	61	66	70	78	80
	1346	9	80	80	80	80	80	80	80	80	80	80

Figure 13: Simulated Temperatures for February 11, 2016

As discussed in reference [26], the rise and fall of temperature at SS-25A between September and October 2016 are not representative of the formation temperature. Excluding these measurements, simulated temperatures of SS-25A compare well with the observed values, except at late time. Simulated temperature is still freezing at the end of August 2017, whereas the observed temperature is 48°F.

One explanation may be the amount of water assumed in the model was too high. Figure 14 shows the temperature map at the end of August 2016 for the case with 1% water saturation. The case with 60% water saturation does show warmer temperatures beyond SS-25B. This is because freezing water adds heat to the gas stream leaving it with less capacity to cool the cells further away from SS-25.

Figure 15 shows the same information at end of August 2017. The 1% water saturation case shows warmer temperatures than the 60% water saturation case. With 1% water, the temperature match at

SS-25A improves but is still 10 degrees cooler than observed. The simulated temperature at SS-25 is 37°F, whereas the observed temperature is 32°F. Water is important for keeping the temperatures low.

The match at SS-25A can be improved by restricting the kill water pumped down SS-25 to the vicinity of SS-25 and refining the simulation grid to force the escape gas to follow a more tortuous path through the wet zone. However, this requires more detailed knowledge of the shallow geology than we have. This additional level of model tuning is not warranted for the purpose of this study.

SS25 SS25A SS25B

			31-Aug-16					60% water saturation (15% water content)				
	grid size (ft)		2	5	5	5	5	5	5	5	20	100
	Distance from well (ft)		2	7	12	17	22	27	32	37	57	157
Cell bottom (ft)	I/K		1	2	3	4	5	6	7	8	9	10
Atmosphere	0	1	60	60	60	60	60	60	61	61	61	61
Leak	230	2	32	32	32	32	32	32	37	42	53	78
	400	3	78	78	78	78	78	78	79	79	79	80
	541	4	80	80	80	80	80	80	80	80	80	80
	660	5	79	79	79	79	79	79	79	79	80	80
Leak	845	6	56	56	57	59	61	63	66	69	75	80
	969	7	79	79	79	79	79	79	79	79	80	80
Leak	1040	8	59	59	60	62	64	66	68	71	76	80
	1346	9	80	80	80	80	80	80	80	80	80	80

			31-Aug-16					1% water saturation (0% water content)				
	grid size (ft)		2	5	5	5	5	5	5	5	20	100
	Distance from well (ft)		2	7	12	17	22	27	32	37	57	157
Cell bottom (ft)	I/K		1	2	3	4	5	6	7	8	9	10
Atmosphere	0	1	59	59	60	60	60	60	60	60	60	61
Leak	230	2	33	33	33	33	33	34	35	37	43	75
	400	3	78	78	78	78	78	78	78	78	79	80
	541	4	80	80	80	80	80	80	80	80	80	80
	660	5	79	79	79	79	79	79	79	79	80	80
Leak	845	6	56	56	57	59	61	63	66	69	75	80
	969	7	79	79	79	79	79	79	79	79	80	80
Leak	1040	8	59	59	60	62	64	66	68	71	76	80
	1346	9	80	80	80	80	80	80	80	80	80	80

Figure 14: Effect of Water Saturation on Temperatures on August 31, 2016

SS25 SS25A SS25B

31-Aug-17 60% water saturation (15% water content)

	Cell bottom (ft)	I/K	1	2	3	4	5	6	7	8	9	10
		grid size (ft)	2	5	5	5	5	5	5	5	20	100
		Distance from well (ft)	2	7	12	17	22	27	32	37	57	157
Atmosphere	0	1	61	61	61	61	61	61	61	61	61	61
Leak	230	2	32	32	32	32	32	37	41	45	54	77
	400	3	78	78	78	78	79	79	79	79	79	80
	541	4	80	80	80	80	80	80	80	80	80	80
	660	5	79	79	79	79	79	79	79	79	80	80
Leak	845	6	65	65	66	66	67	68	69	71	73	80
	969	7	79	79	79	79	79	79	79	79	80	80
Leak	1040	8	68	68	69	69	70	71	72	73	75	80
	1346	9	80	80	80	80	80	80	80	80	80	80

31-Aug-17 1% water saturation (0% water content)

	Cell bottom (ft)	I/K	1	2	3	4	5	6	7	8	9	10
		grid size (ft)	2	5	5	5	5	5	5	5	20	100
		Distance from well (ft)	2	7	12	17	22	27	32	37	57	157
Atmosphere	0	1	60	60	60	60	60	60	60	60	60	61
Leak	230	2	37	37	38	39	39	41	42	44	48	75
	400	3	78	78	78	78	78	78	78	78	79	80
	541	4	80	80	80	80	80	80	80	80	80	80
	660	5	79	79	79	79	79	79	79	79	80	80
Leak	845	6	65	65	66	66	67	68	69	71	73	80
	969	7	79	79	79	79	79	79	79	79	80	80
Leak	1040	8	68	68	69	69	70	71	72	73	75	80
	1346	9	80	80	80	80	80	80	80	80	80	80

Figure 15: Effect of Water Saturation on Temperatures on August 31, 2017

Figure 16 shows the temperature maps for the 80 md and 1,000 md cases at end of August 2016. The two maps are the same. Permeability has little impact on the temperatures.

SS25 SS25A SS25B

31-Aug-16 80 mD

	Cell bottom (ft)	I/K	1	2	3	4	5	6	7	8	9	10
		grid size (ft)	2	5	5	5	5	5	5	5	20	100
		Distance from well (ft)	2	7	12	17	22	27	32	37	57	157
Atmosphere	0	1	60	60	60	60	60	60	61	61	61	61
Leak	230	2	32	32	32	32	32	32	37	42	53	78
	400	3	78	78	78	78	78	78	79	79	79	80
	541	4	80	80	80	80	80	80	80	80	80	80
	660	5	79	79	79	79	79	79	79	79	80	80
Leak	845	6	56	56	57	59	61	63	66	69	75	80
	969	7	79	79	79	79	79	79	79	79	80	80
Leak	1040	8	59	59	60	62	64	66	68	71	76	80
	1346	9	80	80	80	80	80	80	80	80	80	80

31-Aug-16 1000 mD

	Cell bottom (ft)	I/K	1	2	3	4	5	6	7	8	9	10
		grid size (ft)	2	5	5	5	5	5	5	5	20	100
		Distance from well (ft)	2	7	12	17	22	27	32	37	57	157
Atmosphere	0	1	60	60	60	60	60	60	61	61	61	61
Leak	230	2	33	33	32	32	32	32	37	42	52	78
	400	3	78	78	78	78	78	78	79	79	79	80
	541	4	80	80	80	80	80	80	80	80	80	80
	660	5	79	79	79	79	79	79	79	80	80	80
Leak	845	6	56	56	57	59	61	63	66	69	75	80
	969	7	79	79	79	79	79	79	79	79	80	80
Leak	1040	8	59	59	60	62	64	66	69	71	76	80
	1346	9	80	80	80	80	80	80	80	80	80	80

Figure 16: Temperature Maps for 80 md and 1,000 md Cases on August 31, 2016

The formation of the crater is important in keeping the formation below freezing. Figure 17 compares the temperature map at the end of August 2016 for the case with and without the crater. Without the crater, the temperatures are above 65°F at SS-25.

The crater vented the warm reservoir gas, thus keeping temperatures low away from SS-25. After the well was killed, the cold gas in the formation away from SS-25 flowed back toward the crater and cooled SS-25 back down. This rise and then fall in temperatures at SS-25 was observed in the field.

SS25 SS25A SS25B

31-Dec-16 With Venting

	grid size (ft)		2	5	5	5	5	5	5	5	20	100
	Distance from well (ft)		2	7	12	17	22	27	32	37	57	157
Cell bottom (ft)	I/K		1	2	3	4	5	6	7	8	9	10
Atmosphere	0	1	60	60	60	60	60	61	61	61	61	61
Leak	230	2	32	32	32	32	32	32	38	43	53	78
	400	3	78	78	78	78	78	79	79	79	79	80
	541	4	80	80	80	80	80	80	80	80	80	80
	660	5	79	79	79	79	79	79	79	79	80	80
Leak	845	6	60	60	61	62	64	65	67	69	74	80
	969	7	79	79	79	79	79	79	79	79	80	80
Leak	1040	8	63	63	64	65	66	68	70	71	75	80
	1346	9	80	80	80	80	80	80	80	80	80	80

31-Aug-16 Without Venting

	grid size (ft)		2	5	5	5	5	5	5	5	20	100
	Distance from well (ft)		2	7	12	17	22	27	32	37	57	157
Cell bottom (ft)	I/K		1	2	3	4	5	6	7	8	9	10
Atmosphere	0	1	67	67	67	67	67	67	68	68	69	70
Leak	230	2	65	65	64	62	59	56	54	51	47	75
	400	3	77	77	77	77	77	77	77	78	78	80
	541	4	80	80	80	80	80	80	80	80	80	80
	660	5	79	79	79	79	79	79	80	80	80	80
Leak	845	6	56	56	57	59	61	64	66	69	75	80
	969	7	79	79	79	79	79	79	79	80	80	80
Leak	1040	8	59	59	60	62	64	66	69	71	76	80
	1346	9	80	80	80	80	80	80	80	80	80	80

Figure 17: Temperature Maps with and without Crater Formation on August 31, 2016

The rock thermal conductivity also has an effect on temperatures. In the CMG user manual [36], the suggested typical rock conductivity (when no data are available) is 44 Btu/ft-day-°F. Figure 18 compares the temperature maps at the end of August 2016 for rock thermal conductivity of 24 and 50 Btu/ft-day-°F. Temperatures in general are higher for the higher rock thermal conductivity case. However, between SS-25 and SS-25A in layer 2, the results are the same. Figure 19 shows the same comparison at the end of August 2017. The temperatures of the higher rock conductivity case are noticeably higher.

The thermal conductivity of 44 Btu/ft-day-°F is high for the type of rock seen in the Modelo and Topanga [11] in the upper 1,000 ft of SS-25. The value used in the base case is 24 Btu/ft-day-°F. The value for basalt is 24 to 30, siltstone is 22, clay is 11 to 21, sand is 16 to 30, and limestone is 33 to 49 Btu/ft-day-°F [35]. The top Modelo layer does have some limestone in it, but it is intermixed with layers of clay, chert, and shale. The thermal conductivity and especially the vertical thermal conductivity (harmonic average of the layers' thermal conductivities) are not expected to be nearly as high as those of pure limestone.

SS25 SS25A SS25B

31-Aug-16 24 Btu/ft-day-°F

	Cell bottom (ft)	I/K										
		grid size (ft)		2	5	5	5	5	5	5	5	20	100
		Distance from well (ft)		2	7	12	17	22	27	32	37	57	157
				1	2	3	4	5	6	7	8	9	10
Atmosphere	0		1	60	60	60	60	60	60	61	61	61	61
Leak	230		2	32	32	32	32	32	32	37	42	53	78
	400		3	78	78	78	78	78	78	79	79	79	80
	541		4	80	80	80	80	80	80	80	80	80	80
	660		5	79	79	79	79	79	79	79	79	80	80
Leak	845		6	56	56	57	59	61	63	66	69	75	80
	969		7	79	79	79	79	79	79	79	79	80	80
Leak	1040		8	59	59	60	62	64	66	68	71	76	80
	1346		9	80	80	80	80	80	80	80	80	80	80

31-Aug-16 50 Btu/ft-day-°F

	Cell bottom (ft)	I/K										
		grid size (ft)		2	5	5	5	5	5	5	5	20	100
		Distance from well (ft)		2	7	12	17	22	27	32	37	57	157
				1	2	3	4	5	6	7	8	9	10
Atmosphere	0		1	60	60	60	60	60	60	61	61	61	61
Leak	230		2	32	32	32	32	32	36	41	45	53	77
	400		3	78	78	78	78	78	79	79	79	79	80
	541		4	80	80	80	80	80	80	80	80	80	80
	660		5	79	79	79	79	79	79	79	79	80	80
Leak	845		6	65	65	65	66	67	68	69	70	73	80
	969		7	79	79	79	79	79	79	79	79	80	80
Leak	1040		8	68	68	68	69	69	70	71	72	75	80
	1346		9	80	80	80	80	80	80	80	80	80	80

Figure 18: Temperature Comparison for 24 and 50 Btu/ft-day-°F on August 31, 2016

SS25 SS25A SS25B

31-Aug-17 24 Btu/ft-day-°F

	Cell bottom (ft)	I/K										
		grid size (ft)		2	5	5	5	5	5	5	5	20	100
		Distance from well (ft)		2	7	12	17	22	27	32	37	57	157
				1	2	3	4	5	6	7	8	9	10
Atmosphere	0		1	61	61	61	61	61	61	61	61	61	61
Leak	230		2	32	32	32	32	32	37	41	45	54	77
	400		3	78	78	78	78	79	79	79	79	79	80
	541		4	80	80	80	80	80	80	80	80	80	80
	660		5	79	79	79	79	79	79	79	79	80	80
Leak	845		6	65	65	66	66	67	68	69	71	73	80
	969		7	79	79	79	79	79	79	79	79	80	80
Leak	1040		8	68	68	69	69	70	71	72	73	75	80
	1346		9	80	80	80	80	80	80	80	80	80	80

31-Aug-17 50 Btu/ft-day-°F

	Cell bottom (ft)	I/K										
		grid size (ft)		2	5	5	5	5	5	5	5	20	100
		Distance from well (ft)		2	7	12	17	22	27	32	37	57	157
				1	2	3	4	5	6	7	8	9	10
Atmosphere	0		1	61	61	61	61	61	61	61	61	61	61
Leak	230		2	42	42	43	44	45	47	49	50	56	77
	400		3	79	79	79	79	79	79	79	79	79	80
	541		4	80	80	80	80	80	80	80	80	80	80
	660		5	79	79	79	79	79	79	79	79	80	80
Leak	845		6	72	72	72	72	72	72	73	73	74	79
	969		7	79	79	79	79	79	79	79	79	79	80
Leak	1040		8	74	74	74	74	74	74	75	75	76	80
	1346		9	80	80	80	80	80	80	80	80	80	80

Figure 19: Temperature Comparison for 24 and 50 Btu/ft-day-°F on August 31, 2017

The need to divert the flow of gas to the casing shoe is to match the freezing temperature on October 28, 2015, (inferred from the ice plug in the tubing), and the 19°F temperature measured on October 29, 2015. There were other higher temperature measurements at this time, but we used 19°F, as explained in Appendix C. Figure 20 shows the temperature map comparison on October 29, 2015, for the case when

the gas was rerouted to the leak at the surface casing shoe, and the case when the gas continued to leak out of the holes between 134 and 300 ft in the surface casing. Not surprisingly, the temperature is warmer in the latter case. We no longer matched the 19°F temperature as expected. However, by the time we had additional data at SS-25A and SS-25B to test the two scenarios, the temperatures were the same as shown in Figure 21. The only impact if the flow was diverted is the temperature matches on October 28 and 29, 2015.

SS25 SS25A SS25B

Leak Out of Surface Casing Shoe

29-Oct-15

		grid size (ft)		2	5	5	5	5	5	5	5	20	100
		Distance from well (ft)		2	7	12	17	22	27	32	37	57	157
	Cell bottom (ft)	I/K		1	2	3	4	5	6	7	8	9	10
Atmosphere	0		1	61	60	61	61	61	61	61	61	61	61
Leak	230		2	13	18	32	50	67	76	80	80	81	81
	400		3	79	80	80	80	80	80	80	80	80	80
	541		4	80	80	80	80	80	80	80	80	80	80
	660		5	78	80	79	80	80	80	80	80	80	80
Leak	845		6	40	40	42	51	65	75	79	80	80	80
	969		7	78	80	79	80	80	80	80	80	80	80
Leak	1040		8	40	40	43	54	68	76	79	80	80	80
	1346		9	80	80	80	80	80	80	80	80	80	80

29-Oct-15

Leak Continue to Leak Out of Holes in Surface Casing

		grid size (ft)		2	5	5	5	5	5	5	5	20	100
		Distance from well (ft)		2	7	12	17	22	27	32	37	57	157
	Cell bottom (ft)	I/K		1	2	3	4	5	6	7	8	9	10
Atmosphere	0		1	61	60	61	61	61	61	61	61	61	61
Leak	230		2	40	40	32	34	43	57	70	77	80	81
	400		3	79	80	79	80	80	80	80	80	80	80
	541		4	80	80	80	80	80	80	80	80	80	80
	660		5	80	80	80	80	80	80	80	80	80	80
	845		6	80	80	80	80	80	80	80	80	80	80
	969		7	80	80	80	80	80	80	80	80	80	80
	1040		8	80	80	80	80	80	80	80	80	80	80
	1346		9	80	80	80	80	80	80	80	80	80	80

Figure 20: Temperature Comparison When Gas Is Diverted to the Surface Casing Shoe and When the Leak Continues to Flow out of the Holes at the Upper Section of the Surface Casing on October 29, 2015

SS25 SS25A SS25B

31-Aug-16 Leak Out of Surface Casing Shoe

		grid size (ft)	2	5	5	5	5	5	5	5	20	100
		Distance from well (ft)	2	7	12	17	22	27	32	37	57	157
	Cell bottom (ft)	I/K	1	2	3	4	5	6	7	8	9	10
Atmosphere	0	1	60	60	60	60	60	60	61	61	61	61
Leak	230	2	32	32	32	32	32	32	37	42	53	78
	400	3	78	78	78	78	78	78	79	79	79	80
	541	4	80	80	80	80	80	80	80	80	80	80
	660	5	79	79	79	79	79	79	79	79	80	80
Leak	845	6	56	56	57	59	61	63	66			80
	969	7	79	79	79	79	79	79	79			80
Leak	1040	8	59	59	60	62	64	66	68			80
	1346	9	80	80	80	80	80	80	80	80	80	80

29°F around SS25A
~40°F around SS25B

31-Aug-16 Leak Continue to Leak Out of Holes in Surface Casing

		grid size (ft)	2	5	5	5	5	5	5	5	20	100
		Distance from well (ft)	2	7	12	17	22	27	32	37	57	157
	Cell bottom (ft)	I/K	1	2	3	4	5	6	7	8	9	10
Atmosphere	0	1	60	60	60	60	60	60	60	60	61	61
Leak	230	2	32	32	32	32	32	32	36	39	48	76
	400	3	77	77	78	78	78	78	78	78	79	80
	541	4	80	80	80	80	80	80	80	80	80	80
	660	5	80	80	80	80	80	80	80	80	80	80
	845	6	80	80	80	80	80	80	80	80	80	80
	969	7	80	80	80	80	80	80	80			80
	1040	8	80	80	80	80	80	80	80			80
	1346	9	80	80	80	80	80	80	80	80	80	80

29°F around SS25A
~40°F around SS25B

Figure 21: Temperature Comparison When Gas Is Diverted to the Surface Casing Shoe and When the Leak Continues to Flow out of the Holes at the Upper Section of the Surface Casing August 31, 2016

The simulation of our leak scenario using reasonable reservoir and leak gas parameters reproduced the anomalously cold temperature observations reasonably well. The presence of water and the formation of the crater near SS-25 were important in explaining the cold temperatures. The choice of the rock thermal conductivity did impact the temperature match. The 24 Btu/ft-day-°F value was more representative than 44 Btu/ft-day-°F for the type of rocks seen in the mud logs. The lower value yielded a good temperature match. The good temperature match suggested that our leak scenario is plausible.

7 Conclusions

We integrated information from drilling records, daily reports, pressure and temperature readings, logs, shallow geology studies, and metallurgical studies to develop a model of how the SS-25 leak evolved.

The SS-25 gas leak developed sometime after 03:00 on October 23, 2015, no more than 12 or 13 hours before SS-25 was shut in. The 7 in. casing failed in the following manner:

1. The initial rupture was a warm temperature ductile failure, which caused the pressure at the leak point to drop. Because SS-25 was injecting at this time and the injection pressure was around 2,720 psi, J-T cooling could produce injection gas temperature as low as –30°F subsequent to this initial ductile failure.
2. The cold gas made the 7 in. casing brittle, which contributed to the parting failure. Metallurgical analysis indicated that the metal temperature was –76°F (–60°C) to –38°F (–39°C) when this parting occurred.

This extreme cooling and casing parting failure all occurred prior to the shut-in of SS-25. This is because after SS-25 was shut in, the leaked gas supplied by the reservoir was 10°F (–12°C) to 20°F (–6°C). This would not be cold enough to cause the brittle parting.

Initially, the gas flowed out the holes in the surface casing between 134 and 300 ft. Part of the kill fluid pumped down the tubing during kill attempt #1 froze. Part of the fluid pumped down the 7 in. x 2 7/8 in. annulus crossed over to the 11 3/4 in. x 7 in. annulus and also froze, which hindered the gas from leaking out the surface casing holes between 134 and 300 ft. These blockages caused the pressure in the 11 3/4 in. x 7 in. annulus to rise, and we believed that the high pressure caused the rocks around the surface casing shoe to fracture. The gas that was blocked from the holes at the top of the surface casings flowed around the shoe and into the formation near the lower section of the surface casing. The deicing operation unblocked the pathways and therefore allowed the gas to flow out the holes at the top again. As the reservoir pressure declined, the gas temperature rose, which warmed up the formation around SS-25. The crater formed, and the warm gas vented into the atmosphere, thus preserving the cold temperatures in the formation farther away from SS-25. When SS-25 was finally killed, the cold gas away from SS-25 flowed back toward the crater and cooled back down the area around SS-25.

This scenario of how the leak evolved would lead to unusual temperature readings at SS-25 and the surrounding area. Unusual low temperature readings were recorded at SS-25, SS-25A, and SS-25B. These temperature measurements provided a test of our scenario.

To test our scenario, we built a thermal reservoir simulation model using CMG's thermal reservoir simulator, STARS. We kept the model simple and the grid coarse to avoid going beyond the limited available data. Where data were missing, we assumed reasonable values. We did not tune these parameters to achieve a better match, but we did perform sensitivity studies to test how robust our results were to the choices we made.

The simulated temperatures compared reasonably well with the observed data, which lent credence to our scenario.

The sensitivity studies showed that the choice of rock thermal conductivity could affect the results (warmer than observed) at the end of August 2017. However, the values we used were more representative of the rocks in the formation.

Water (ice formation) also affected the results. With water, the temperature was still freezing at SS-25A whereas the observed temperature was 48°F at end of August 2017. Without water, the simulated temperature at SS-25A was 38°F – an improvement, but still low. However, the simulated temperature at SS-25 was 37°F, which was above the observed value of 32°F. The mismatch could be due to using a simple coarse grid and not keeping the water around SS-25 only. We accepted the limitations of our model and did not attempt to tune the geology and water saturation to improve the match.

There had been speculation that hydrates formed in the tubing during the first kill attempt. Because the formation of hydrates is a slow process, whereas the blockage developed in minutes, it is unlikely that the blockage was caused by hydrate formation.

As to whether it was ice or hydrates that kept the ground cold, we could not make that determination because the relevant properties of ice and hydrates are similar. Whether we modeled it as ice or hydrate should not affect the results.

The need to divert the gas from flowing up the 11 3/4 in. x 7 in. annulus during the warm leaked gas period hinged on what the temperature readings were on October 28 and 29, 2015. However, the temperature data on these days was inconsistent. We believed the lower measured temperature, 19°F, was the correct reading and presumed the solid plugs in the well were ice and not hydrates. For freezing temperatures to have persisted for this long, gas during the warm leaked gas period must have been prevented from flowing up the 11 3/4 in. x 7 in. annulus and thawing out the upper section of the well.

If the higher temperature readings of 45 to 59°F were correct, then there was no need to divert the gas to the surface casing shoe. However, the choice of whether to divert the gas or not would only affect the temperature match for these two days, October 28 and 29, 2015. These two scenarios match the observed temperatures equally well for all the later times.

8 References

[1] Blade Energy Reports, "SS-25 Casing Failure Analysis," Blade Energy Reports, Houston, 2019.

[2] Blade Energy Partners, "SS-25 Well Nodal-Analysis with Uncontrolled Leak Estimation," Blade Energy Partners, Houston, 2019.

[3] SoCalGas, "SS-25 Wellbore Operations Jul 23-Oct 23 2015.pdf," SoCalGas, Los Angeles, 2016.

[4] Blade Energy Partners, "SS-25 Geology Summary," Blade Energy Partners, Houston, 2019.

[5] SoCalGas, "SS-25 Well Documentation (from SoCalGas)_N.pdf," SoCalGas, Los Angeles, 2016.

[6] SoCalGas, "03721322_DATA_1-1-2008.pdf," SoCalGas, 2010.

[7] SoCalGas, "03721323_DATA_1-1-2008.pdf," SoCalGas, 2008.

[8] Advisian, "2016 Geophysical Investigation Aliso Canyon SS-25," Advisian, Calgary, 2017.

[9] Geosyntec, "Subsurface Assessment Report Investigative Order R4-2016-0035," Geosyntec, Los Angeles, 2018.

[10] Petrolog, "AC_BLD_0042434.pdf," Petrolog, Ventura, 2016.

[11] Blade Energy Partners, "6_SS-25_P-39A mudlog description by major lith zone_PLOT COPY.pptx," Blade Energy Partners, Houston, 2016.

[12] Schlumberger, "SoCalGas_TH-1_FMI_110-1102ft_Summary.pptx (preliminary)," Schlumberger, Los Angeles, 2018.

[13] Schlumberger, "03700776_Standard_Sesnon_25_IBC_UCI_CPET_SoCalGas_Report_with_logs_revised.pdf," Schlumberger, Los Angeles, 2018.

[14] Blade Energy Partners, "SS-25 Well Info Master Rev 11.xlsx," Blade Energy partners, Houston, 2018.

[15] SoCalGas, "AC_BLD_0075830.xlsx," SoCalGas, 2018.

[16] Blade Energy Partners, "Aliso Canyon Injection Network Deliverability Analysis Prior to Uncontrolled Leak," Blade Energy Partners, Houston, 2019.

[17] SoCalGas, "01957 - Inj&Wthdrwl Hours (July-Dec 2015).xlsx," SoCalGas, 2016.

[18] S. Schweikert, J. Wolfersdorf, M. Selzer and H. Hald, "Experimental Investigation on Velocity and Temperature Distributions of Turbulent Cross Flows over Transpiration Cooled C/C Wall Segments," in *5th European Conference for Aeronautics and Space Sciences (EUCASS)*, Munich, 2013.

[19] W. Dahmen, T. Gotzen, S. Muller and M. Rom, "Numerical Simulation of Transpiration Cooling through Porous Material," *International Journal for Numerical Methods in Fluids,* vol. 76, no. 6, pp. 331-365, 2014.

[20] Blade Energy Partners, "SS-25 Inspection Logs Analysis," Blade Energy Partners, Houston, 2019.

[21] Add Energy, "Dynamic Simulations Aliso Canyon SS-25," Add Energy, Houston, 2016.

[22] Department of Conservation, "SS-25 Chronology Summary.docx," Department of Conservation, 2015.

[23] SoCalGas, "02-00 DOGGR Data (Operator_SoDaily Report 10-23-2015 thru 11-15-2015.pdf," SoCalGas, 2016.

[24] Core Lab, "Completion Profiler Report," Core Lab, Los Angeles, 2015.

[25] Western Wireline, "SS-25 Noise Temperature 16Feb2016 AC_BLD_0035425 - AC-BLD_0035427.las,"

Western Wireline, Bakersfield, 2016.

[26] Blade Energy Partners, "SS-25 Temperature, Pressure, and Noise Logs Analysis," Blade Energy Partners, Houston, 2019.

[27] Blade Energy Partners, "SS-25-B_Survey 8-16-2016.xlsx," Blade Energy Partners, Houston, 2016.

[28] Schlumberger, "SS-25-A_Survey 8-30-2016.xlsx," Schlumberger, Houston, 2016.

[29] Blade Energy Partners, "SS-25 DTS Data.xlsm," Blade Energy Partners, Houston, 2016.

[30] Schlumberger, "SS-25A DTS Data.xlsm," Schlumberger, Houston, 2016.

[31] Blade Energy Partners, "SS-25B DTS Data.xlsm," Blade Energy Partners, Houston, 2016.

[32] Schlumberger, "SS-25-A_Survey_8-13-2018.xlsx," Schlumberger, Los Angeles, 2018.

[33] Schlumberger, "SS-25_Survey_07-31-2017.xlsx," Schlumberger, Los Angeles, 2018.

[34] Wikipedia, "2011-2017 California drought," Wikipedia, 16 11 2018. [Online]. Available: https://en.wikipedia.org/wiki/2011%E2%80%932017_California_drought. [Accessed 26 11 2018].

[35] L. Eppelbaum, I. Kutasov and A. Pilchin, Applied Geothermics, Lecture Notes in Earth System Sciences, New York: Springer, 2014.

[36] CMG, "STARS User Manual," CMG, Calgary, 2015.

[37] Engineering Tool Box, "Methane - Thermophysical Properties," Engineering Tool Box, 2008. [Online]. Available: http://www.engineeringtoolbox.com/methane-d_1420.html. [Accessed 23 11 2018].

[38] USGS, "Thermal Properties of Methane Gas Hydrates," USGS, 7 2007. [Online]. Available: https://pubs.usgs.gov/fs/2007/3041/pdf/FS-2007-3041.pdf. [Accessed 23 11 2018].

[39] Engineering ToolBox, "Ice - Thermal Properties," Engineering ToolBox, 2004. [Online]. Available: https://www.engineeringtoolbox.com/ice-thermal-properties-d_576.html. [Accessed 23 11 2018].

[40] E. McAllister, Pipeline Rules of Thumb Handbook 5th Edition, New York: Gulf Professional Publishing, 2002, p. 483.

[41] NIST, "Thermophysical Properties of Fluid Systems," NIST, 2018. [Online]. Available: https://webbook.nist.gov/chemistry/fluid/. [Accessed 23 11 2018].

[42] Haliburton, "C086 Halliburton - Cement Job Summary 24OCT2015 [AC_BLD_0041890].pdf"," Haliburton, 2016.

[43] SoCalGas, "SS-25 Casing Pr. 10-30 to 12-25-15 (3).xlsx," SoCalGas, 2018.

[44] Engineering Toolbox, "Laten Heat of Melting for some common Materials," Engineering Toolbox, 2003. [Online]. Available: https://www.engineeringtoolbox.com/latent-heat-melting-solids-d_96.html. [Accessed 21 January 2019].

[45] Engineers Edge, "Specific Heat Capacity of Metals Table Chart," Engineers Edge, 2018. [Online]. Available: https://www.engineersedge.com/materials/specific_heat_capacity_of_metals_13259.htm. [Accessed 21 January 2019].

[46] B. Wischnewski, "Some scientific and engineering data online," Peace Software, [Online]. Available: http://www.peacesoftware.de/einigewerte/methan_e.html. [Accessed 22 January 2019].

[47] R. H. Perry and C. H. Chilton, "Heat Transmission," in *Chemical Engineer's Handbook 5th edition*, New York, McGraw Hill, 1973, p. Section 10.

[48] Engineering Tool Box, "Emissivities of some common materials," Engineering Tool box, 2003. [Online]. Available: https://www.engineeringtoolbox.com/radiation-heat-emissivity-d_432.html. [Accessed 22 January 2019].

[49] Engineering ToolBox, "Solubility of Gases in Water," Engineering ToolBox, 2008. [Online]. Available:

https://www.engineeringtoolbox.com/gases-solubility-water-d_1148.html. [Accessed 18 January 2019].

[50] K. Wegner, "Mass Transfer Estimation of Diffusivities Lecture 8," Swiss Federal Institute of Technology, Zurich, 2017.

[51] T. Komai, S. P. Kang, J. H. Yoon, Y. Yamamoto, T. Kawamura and M. Ohtake, "In Situ Raman Spectroscopy Investigation of the Dissociation of Methane Hydrate at Temperatures Just below the Ice Point," *Journal of Physical Chemistry B,* pp. 8062-8068, 18 May 2004.

[52] ORNL, "One dimensional diffusion," [Online]. Available: https://web.ornl.gov/sci/diffusion/Theory/One-dimensional%20diffusion.pdf. [Accessed 18 January 2019].

[53] Engineering Tool Box, "Diffusion Coefficients of Gases in Water," Engineering Tool Box, 2008. [Online]. Available: https://www.engineeringtoolbox.com/diffusion-coefficients-d_1404.html. [Accessed 23 January 2019].

[54] B. Tohidi, A. Danesh and A. C. Todd, "On the Mechanism of Gas Hydrate Formation in Subsea Sediments," in *American Chemical Society: 213th ACS National Meeting*, San Francisco, 1997.

Appendix A Joule-Thomson Coefficient

In August 1978, a flow test was conducted by SoCalGas on SS-25 [5] (pages 693-713). In this flow test, the produced gas stream was sent through a choke. The temperature and pressure upstream and downstream of the choke were measured. These data enabled us to estimate the J-T coefficient, which ranged from 0.58 to 0.78 with an average of 0.64°F/14.7 psi. Table 8 lists all the estimates of the J-T coefficients. The rule of thumb for natural gas is 1.0°F/14.7psi [40]. This is also the value for methane from NIST [41] at 10°F. The variation in the estimates is likely due to the differences in the composition, temperature, and pressure. These J-T coefficients can be used to give a quick estimate of temperature drop due to pressure drop.

Table 8: J-T Coefficients Calculated from the Flow Test Data

Upstream Pressure (psi)	Upstream Temperature (°F)	Downstream Pressure (psi)	Downstream Temperature (°F)	Pressure Drop (psi)	Temperature Change (°F)	J-T (°F /14.7 psi)
1,850	84	565	16	1,285	68	0.78
1,880	82	565	16	1,315	66	0.74
1,892	80	565	18	1,327	62	0.69
1,890	77	565	18	1,325	59	0.65
1,890	76	565	18	1,325	58	0.64
1,890	74	565	18	1,325	56	0.62
1,890	74	565	18	1,325	56	0.62
1,890	73	565	18	1,325	55	0.61
2,090	80	600	12	1,490	68	0.67
2,095	80	605	10	1,490	70	0.69
2,100	80	600	12	1,500	68	0.67
2,100	80	555	13	1,545	67	0.64
2,105	82	505	12	1,600	70	0.64
2,105	82	510	14	1,595	68	0.63
2,105	82	560	11	1,545	71	0.68
2,095	82	560	10	1,535	72	0.69
2,290	96	540	13	1,750	83	0.70
2,290	93	530	15	1,760	78	0.65
2,300	91	540	17	1,760	74	0.62
2,300	90	540	19	1,760	71	0.59
2,295	89	540	18	1,755	71	0.59
2,295	88	535	16	1,760	72	0.60
2,300	88	535	13	1,765	75	0.62
2,450	91	520	4	1,930	87	0.66
2,445	92	520	6	1,925	86	0.66

Upstream Pressure (psi)	Upstream Temperature (°F)	Downstream Pressure (psi)	Downstream Temperature (°F)	Pressure Drop (psi)	Temperature Change (°F)	J-T (°F /14.7 psi)
2,450	92	538	8	1,912	84	0.65
2,450	89	525	8	1,925	81	0.62
2,445	86	525	10	1,920	76	0.58
2,445	88	525	8	1,920	80	0.61
2,440	88	525	8	1,915	80	0.61
2,440	88	525	8	1,915	80	0.61
2,510	98	505	4	2,005	94	0.69
2,515	100	505	6	2,010	94	0.69
2,520	98	505	7	2,015	91	0.66
2,525	96	505	7	2,020	89	0.65
2,520	95	510	10	2,010	85	0.62
2,520	94	505	11	2,015	83	0.61
2,520	94	505	10	2,015	84	0.61
2,510	94	505	8	2,005	86	0.63
2,580	93	500	10	2,080	83	0.59
2,590	97	500	12	2,090	85	0.60
2,600	97	500	9	2,100	88	0.62
2,600	96	500	9	2,100	87	0.61
2,600	96	500	9	2,100	87	0.61
2,595	95	500	10	2,095	85	0.60
2,580	95	500	8	2,080	87	0.61
2,575	95	500	8	2,075	87	0.62
2,615	92	530	7	2,085	85	0.60
2,610	95	525	8	2,085	87	0.61
2,610	94	525	8	2,085	86	0.61
2,610	95	515	4	2,095	91	0.64
2,610	95	530	6	2,080	89	0.63
2,605	94	525	8	2,080	86	0.61
2,605	94	530	8	2,075	86	0.61
2,600	94	530	8	2,070	86	0.61

Appendix B SS-25 Tubing and Annuli Pressure Readings Review

There are actually four temperatures associated with SS-25 in the upper section of the well, which are:

- The temperature in the tubing (Table 6).
- The temperature of the gas in the 7 in. x 2 7/8 in. annulus at the leak point.
- The temperature of the gas when it expands and cools further in the formation and is used as the injected gas temperature in the simulator (Table 7).
- The simulated reservoir temperature of the well cell (the colored cells in the temperature maps).

It is assumed that the overall heat transfer coefficient is such that the reservoir rock temperature next to the well is close to the temperature in the tubing. How well they match the measurements is what we use to judge the plausibility of our leak model.

When there is no blockage, and the 7 in. x 2 7/8 in. annulus pressure is low, the first three temperatures should be close to each other. Table 9 and Table 10 show the pressures recorded in the SS-25 tubing string, the 7 in. x 2 7/8 in. annulus, and the 11 3/4 in. x 7 in. annulus. The pressures are compiled from reference [23], [21], and [5](page 78). Pressures in the 7 in. x 2 7/8 in. annulus and the 11 3/4 in. x 7 in. annulus starting on October 29, 2015, were over 500 psi. Although this caused only a small decline in the rate, the leak temperature increased to between 40 and 60°F, based on PROSPER's calculations [2]. The measured temperature in the tubing string was 19°F. In this appendix, we analyze the SS-25 pressure data to get a better understanding of the flow paths and blockages in the upper 1,000 ft of the well during the period between shut-in and the deicing operations (October 23 and November 6, 2015). We seek an explanation that can accommodate both sets of temperatures. This explanation then guides how we model the leak in the simulation model. We also describe in this appendix how this is mimicked in the CMG STARS simulation.

Table 9: SS-25 Pressure Record and Associated Activities October 23 to October 31, 2015

Date	Time	Tubing (psi)	"A" (psi)	"B" (psi)	Comment
23-Oct-15	16:00	1,700	270	140	Right after shut-in
24-Oct-15	12:27	3,500	290	140	Tubing froze
24-Oct-15	13:20	2,700			
24-Oct-15	13:30	50			Bleed tubing back to frac tank
24-Oct-15	14:07	50	290	140	Before pumping down A annulus
24-Oct-15	14:30		400		End of pumping down A annulus
24-Oct-15	17:00	177	306		
24-Oct-15	17:23	200	307		
24-Oct-15	17:30	210	309		
24-Oct-15	17:40	218	310		
24-Oct-15	17:50	226	311		

Date	Time	Tubing (psi)	"A" (psi)	"B" (psi)	Comment
24-Oct-15	18:00	232	312		
24-Oct-15	18:10	239	314		
24-Oct-15	18:30	251	316		
24-Oct-15	19:00	262	318		
24-Oct-15	19:30	274	322		
25-Oct-15	8:45	616	377	450	
25-Oct-15	15:00	674	401	459	
26-Oct-15	10:15			428	Checked at start of day.
26-Oct-15	15:30	680	419	413	Begin flowing B annulus 16/64
26-Oct-15	16:45	446	416	404	Open choke to 23/64 8 MSCF/D
27-Oct-15	7:15	34	307	325	
27-Oct-15	13:30		15		Open Orbitz valve on withdrawal line Bring A annulus prs from 260 to 15 psi
27-Oct-15	14:45	78	16	308	Begin bleeding B annulus on 11/64 choke Prs 275 psi 3MSCF/D.
27-Oct-15	15:30	78	25	310	Open choke to 23/64 prs 300 psi. A annulus 21 psi, tubing 75 psi. Close Choke
28-Oct-15	8:00	170	128	325	Checked at start of day.
28-Oct-15	10:00		134		Bled A annulus from 134 to 124 psi
28-Oct-15	11:30	87	109		Sending down bailer. Opened up well. Fluid level 300'(tubing) Bailer tagged at 467'
28-Oct-15	14:15				Shot fluid level. B annulus 43' A annulus 164'
29-Oct-15	7:30	429	353	505	Checked at start of day.
29-Oct-15	8:30	360	420	560	
29-Oct-15	11:00	375	462	591	Bled A annulus from 452 to 440 psi
29-Oct-15	13:15	54	-	-	Sending down bailer. Tubing 54 psi. Tubing temperature 19°F
29-Oct-15	16:30	51	685	731	
29-Oct-15	17:00	55	634	697	
29-Oct-15	17:30	-	631	770	
30-Oct-15	7:30	-	614	823	Checked at start of day.
30-Oct-15	10:50			750	
30-Oct-15	15:00		585	770	
30-Oct-15	16:00		584	771	

Date	Time	Tubing (psi)	"A" (psi)	"B" (psi)	Comment
31-Oct-15	7:15		574	716	Checked at start of day.
31-Oct-15	12:30		578	749	
31-Oct-15	16:30		584	727	

Table 10: Pressure Record and Associated Activities November 1 to November 15, 2015

Date	Time	Tubing (psi)	"A" (psi)	"B" (psi)	Comment
1-Nov-15	7:30		676	690	Checked at start of day.
1-Nov-15	12:30		694	679	
2-Nov-15	7:15		686	663	Checked at start of day.
2-Nov-15	12:00		682	638	
2-Nov-15	16:10		659	284	
3-Nov-15	6:00		626	599	Checked at start of day.
3-Nov-15	12:30		645	623	
4-Nov-15	6:00		512	555	Checked at start of day.
4-Nov-15	17:30		523	488	
5-Nov-15	6:00		551	467	Checked at start of day.
5-Nov-15	15:00			515	
6-Nov-15	6:00		560	460	This day they used coil tubing to unplug the tubing.
6-Nov-15	17:30	0	305	64	
7-Nov-15	6:00	940	229	60	
7-Nov-15	7:00	1,100			
7-Nov-15	9:30	1,146	228	59	
7-Nov-15	10:00	1,170	231	60	
7-Nov-15	11:45	1,298	222	60	
7-Nov-15	13:45	1,407	227	60	
7-Nov-15	17:00	1,584	217	60	
8-Nov-15	6:00	1,660	218	65	
8-Nov-15	8:15	1,681	192	62	
8-Nov-15	13:15	1,615	212	65	
9-Nov-15	6:00	1,620	215	66	
9-Nov-15	12:15	1,585	216	69	
9-Nov-15	18:00	1,585	218	69	

Date	Time	Tubing (psi)	"A" (psi)	"B" (psi)	Comment
10-Nov-15	6:00	1,624	211	70	
11-Nov-15	6:00	1,705	227	75	
11-Nov-15	15:00	1,707	229	85	
11-Nov-15	15:30	1,703	220	84	
12-Nov-15	6:00	1,737	240	108	
12-Nov-15	15:30	1,694	245	105	
13-Nov-15	6:00	1,202	229	69	Well blew out shooting debris 75' into the air. Gas, oil, brine flow out of fissures.
13-Nov-15	7:00	1,201			
13-Nov-15	11:15	1,526	253	89	
13-Nov-15	17:00	278	293	42	
14-Nov-15	6:00	1,610	245	35	
14-Nov-15	15:15	1,690	213	32	
15-Nov-15	6:00	1,607	217	32	
15-Nov-15	11:15	0	107	22	
15-Nov-15	12:20		205	35	
15-Nov-15	13:00	220	190	38	
15-Nov-15	14:00	600	190	40	
15-Nov-15	15:00	980	220	39	
15-Nov-15	16:00	1,159	251	37	

Figure 22 shows the pumping record of the first kill attempt conducted on October 24, 2015 [42]. The portion of interest is the shutdown of the first kill attempt pumped down the 7 in. x 2 7/8 in. annulus (the vertical blue line on the far-right side). Notice that the pressure falls by 100 psi when the pump is shut down. This sharp pressure decline is because the fluid is no longer moving, and the friction loss vanishes instantaneously. This 100 psi pressure drop is very high for a friction loss in the 7 in. x 2 7/8 in. annulus.

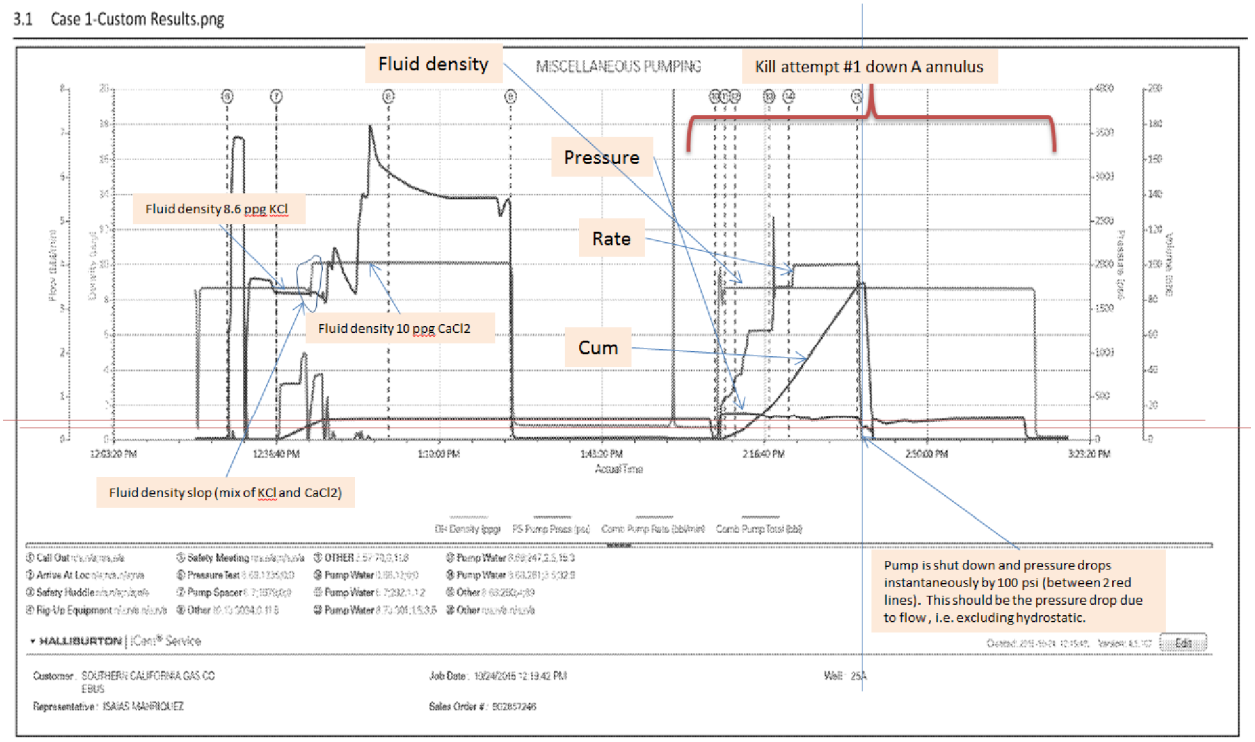

Figure 22: Pumping Record of First Kill Attempt [42]

Table 11 shows the estimated pressure drop in an annulus. Case A is the configuration for the 7 in. x 2 7/8 in. annulus with no ice buildup. The pressure drop for water flowing at 4 BPM over 1,000 ft is less than 3 psi. The pressure drop in the kill line is also expected to be low. This can be seen from the start of the pump job where rising pump rates resulted in negligible increase in pressure. The 100 psi pressure drop due to friction from the instantaneous shut-in pressure, therefore, indicates that restriction (ice) formed in the 7 in. x 2 7/8 in. annulus during the kill attempt. Table 11 show estimates of the pressure drop for various gap sizes. Note that the pressure drop calculation is for a length of 1,000 ft. If the blockage covered a shorter interval, the pressure drop would be proportionally less.

The 100 psi pressure drop we found is at the end of pumping kill fluid down the 7 in. x 2 7/8 in. annulus. After pumping stopped, any liquid above the ice plug continues to drain through the crack(s). This liquid also freezes, thus reducing the crack size further; the ice plug can become a significant restriction even for gas movement. There is still pressure communication between the upper and lower portion of the 7 in. x 2 7/8 in. annulus, but it is so tight that there is significant lag. See, for example, around November 3, 2015, in Figure 23. Notice how the blue curve (7 in. x 2 7/8 in. annulus pressure) lags the red curve (11 3/4 in. x 7 in. annulus pressure).

From the fluid level measurements made on October 28, 2015, the fluid level (top of ice) is at 43 ft in the 11 3/4 in. x 7 in. annulus and 164 ft in the 7 in. x 2 7/8 in. annulus. This indicates that there is ice in the 11 3/4 in. x 7 in. annulus also. The pumping record of kill attempt #1, however, does not yield information

on the constriction in the 11 3/4 in. x 7 in. annulus. For this, we turn to the continuous pressure data shown in Figure 23.

Table 11: Estimated Pressure Due to Flow in Annulus for Various Amounts of Ice Buildup

The gap is centered within the A annulus mimicking uniform ice growth from both walls of the annulus. This is for length of 1,000 ft, 4 BPM and roughness of 0.0012 in. Case A has no ice buildup.

Case	Annulus ID (in.)	Annulus OD (in.)	Gap (in.)	Pressure Drop (psi)
A	2.875	6.336	1.7305	2.44
B	3.875	5.336	0.7305	31.2
C	4.125	5.086	0.4805	117
D	4.175	5.036	0.4305	164
E	4.225	4.986	0.3805	237

Figure 23 shows the continuous pressure data of the tubing, the 7 in. x 2 7/8 in. annulus, and the 11 3/4 in. x 7 in. annulus between October 30 to November 15, 2015 [43]. On November 6, 2015, 10.8 ppg $CaCl_2$ solution and glycol were pumped down the tubing to remove the ice plug, and this is marked on Figure 23. The first thing to notice in this pressure plot is that the pressures of the 7 in. x 2 7/8 in. annulus and the 11 3/4 in. x 7 in. annulus fall sharply (400 psi) after the deicing operation. The second thing to notice is that before pumping the deicing solutions, the 11 3/4 in. x 7 in. annulus pressure (red curve) shows a significant amount of fluctuation, while the 7 in. x 2 7/8 in. annulus pressure (blue curve) does not. After the pumping of the deicing solution, the opposite is true.

Let us first examine the pressures prior to deicing. During this period, the 11 3/4 in. x 7 in. annulus pressure is fluctuating by more than 50 psi. We are fairly certain that the cracks in the 7 in. casing are not plugged by ice, and the size of the cracks is sufficiently large to avoid choking. There should be good pressure communication between the 7 in. x 2 7/8 in. annulus and the 11 3/4 in. x 7 in. annulus, and therefore the 7 in. x 2 7/8 in. annulus pressure should show same amount of fluctuations. The reason 7 in. x 2 7/8 in. annulus shows no fluctuation is because of the blockage between the upper section of the 7 in. x 2 7/8 in. annulus (where the pressure gauge is) and the lower section. This restriction filters out high-frequency fluctuations in the pressure. (Recall how the 7 in. x 2 7/8 in. annulus pressure lags the 11 3/4 in. x 7 in. annulus pressure.) The fact that there is fluctuation in the 11 3/4 in. x 7 in. annulus indicates that there is no comparable tight flow restriction in the 11 3/4 in. x 7 in. annulus.

Although there is good pressure communication between the upper and lower section of the 11 3/4 in. x 7 in. annulus, the top of the ice plug was measured at 43 ft. The ice coating the walls of the 11 3/4 in. x 7 in. annulus is thick enough to appear as a fluid level. This and the rising pressure indicate that the holes in the surface casing are obstructed by ice, possibly to the point of sealing these exits from the gas. If the holes were sealed then there needs to be an alternative path for the gas to escape.

The pressures during this period are within the estimated range of the fracturing pressure (400 to 815 psi) of the rocks around the surface casing shoe. (See Appendix F) If the shoe failed, it can provide the alternative path for the gas to leak out of the 11 3/4 in. x 7 in. annulus. Once out, the gas can flow away from the well through the flow channel where the shoe landed. It is also possible for the gas to flow behind the casing to the channel suspected at 741 ft. In either case, the warm gas avoids the upper

section of the well and avoids thawing it out. Appendix C discusses the evidence that the upper section of the well was below freezing.

One remaining question is what caused the fluctuations in the 11 3/4 in. x 7 in. annulus pressure. Between October 30 and November 6, 2015, there was no operation on SS-25 that would affect the well's pressures. These fluctuations in the 11 3/4 in. x 7 in. annulus pressure were due to the pressure fluctuations in the well itself, as seen in the tubing pressure fluctuations after deicing, and probably to the blockages breaking and reforming in the leak pathways.

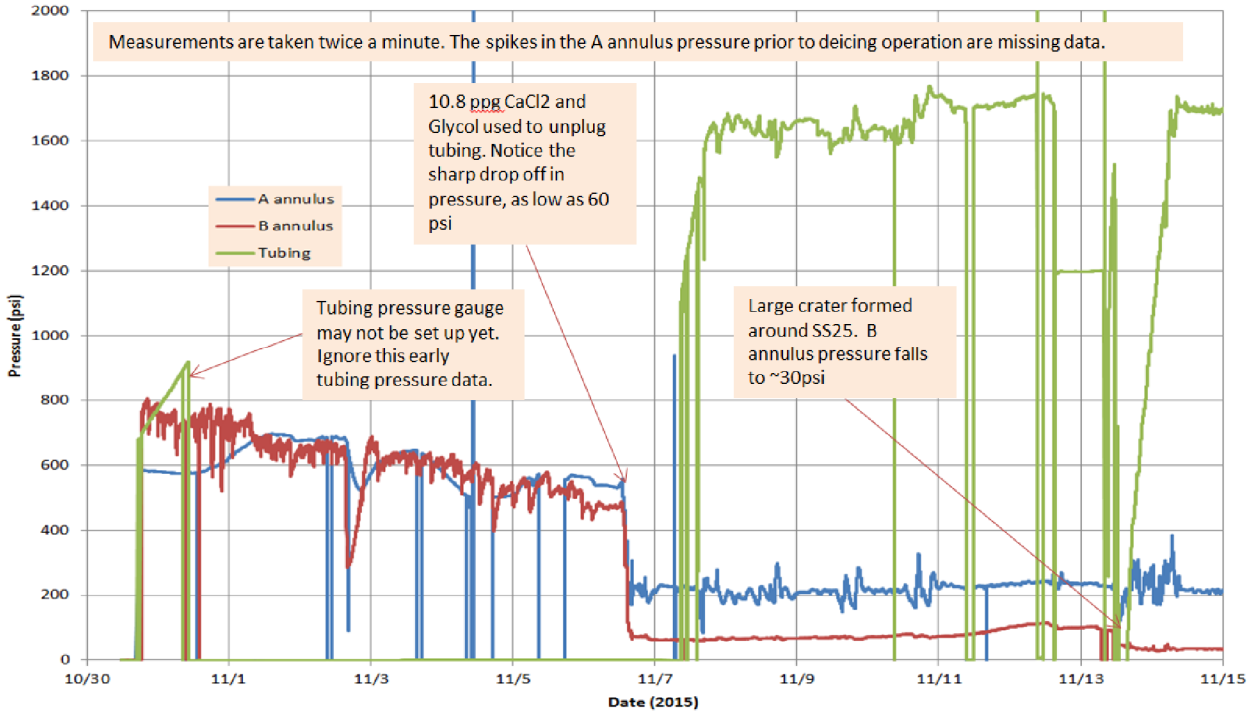

Figure 23: Continuous Pressure Measurements of SS-25 Tubing and Annuli [43]

After the deicing operation, the 7 in. x 2 7/8 in. annulus pressure fluctuations increased, which indicates that its ice plug had been removed. The ice in the 11 3/4 in. x 7 in. annulus is likely to have melted also, thus exposing the holes in the surface casing. The 11 3/4 in. x 7 in. annulus pressure was as low as 60 psi, which is less than the 140 psi measured on October 23, 2015, immediately after shut-in of SS-25. It is possible that the leaking gas and pumped fluid could have opened up additional passageways after shut-in, and they became unclogged after the deicing operations. In any case, the deicing operation had also removed the near wellbore ice or hydrate blockages.

Notice that the difference between the 7 in. x 2 7/8 in. annulus and the 11 3/4 in. x 7 in. annulus pressure is approximately 140 psi. The size of the damage to the 7 in. casing was too large to be choking back the leak. The 140-psi pressure drop was due to flow up the 11 3/4 in. x 7 in. annulus. Most, if not all, of the gas was flowing out of the holes in the 11 3/4 in. x 7 in. annulus again.

On November 13, 2015, a large crater started to form near SS-25. Figure 23 shows the 11 3/4 in. x 7 in. annulus pressure falling to 30 psi.

The pressure data and notes from the daily reports helped to fill in the details of what happened inside and outside the well between the times of shut-in and deicing operations. It is possible to accommodate

the 19°F measurement in the tubing and the 40 to 60°F temperatures estimated by PROSPER during warm leaked gas period. Figure 8c and Figure 8d summarize the flow paths discussed in this appendix.

What happened in the well between October 23 and November 6, 2015, is complex. In CMG's STARS simulator, the leak was modeled as an injector. The gaps in the cement behind the surface casing were modeled with a column of simulation cells where the well was spotted in the model. On October 23, 2015, the injector was perforated in the simulation layer 2, which corresponded to the suspected channel, at 169 ft. During the warm leaked gas period October 25 to November 6, 2015, the perforation in layer 2 is closed and layers 6 and 8 are opened. These two layers corresponded to the suspected channel at 741 ft (above the basalt) and possibly some sands below the basalt where the surface casing shoe landed. This redirected the gas to flow around the casing shoe and above and below the basalt layer. The injected gas temperature was set to 40°F. After the deicing operation on November 6, 2015, the ice blocking the holes in the 11 3/4 in. x 7 in. annulus was removed. The pressure also fell, and the fractures around the casing shoe closed. This was mimicked by reopening the perforations in layer 2 while closing perforation in layers 6 and 8.

Appendix C Observations at SS-25 on October 28 and 29, 2015

On October 28 and 29, 2015, there were temperature measurements in the tubing and there were also observations at SS-25 well from which we could infer a temperature. This data can provide a test of our leak model. Unfortunately, the data during this period are contradictory so there can be multiple interpretations. In this appendix, we will review the data, lay out the different interpretations, and explain which interpretation we consider most likely.

Figure 24 and Figure 25 show the portions of the daily report for October 28 and 29, 2015. On October 28, 2015 between 11:30 and 12:15, a bailer sent down the tubing tagged a solid plug at 467 ft. The bailer was found to be coated with polymer after it was retrieved, and the tool temperature was 47°F. They also reported the liquid level at 300 ft, indicating that there was a 167 ft column of liquid (containing polymer) above the solid plug.

The fluid found in the tubing was the 10 ppg $CaCl_2$ XC pumped down the tubing during kill attempt #1. This fluid contained polymer and has a freezing point of –8°F. Because the leaking gas temperature was estimated to be around 10 to 20°F after SS-25 was shut in, this 10 ppg $CaCl_2$ XC was not expected to freeze. This column of liquid, therefore, was not unexpected.

Ahead of the $CaCl_2$ was 8.6 ppg KCl. It contained no polymer and had a freezing point of 26°F. This was what froze and was likely the solid that the bailer tagged at 467 ft.

If the 47°F reading was correct, then the solid plug in the tubing was hydrate and not ice. During kill attempt #1, the fluid pumped down the tubing froze in a matter of minutes. Because hydrate formation kinetic is too slow, hydrate could not have formed this quickly [2]. The initial blockage was an ice plug. Therefore, if the solid plug was now hydrate, then the ice must have transformed into hydrate in the four days since kill attempt #1. Appendix E shows that because methane diffusion in solids is slow, this initial ice plug was unlikely to have transformed into hydrate plug in four days.

Another reason that the solid plug is unlikely to be hydrate is because hydrate is unstable at 47°F and 257 psi, the conditions at 467 ft. (The tubing pressure reading was 170 psi. The 167 ft column of liquid added another 87 psi of hydrostatic pressure.)

Figure 26 shows the hydrate stability curve. The conditions, 47°F and 257 psi, were well outside the methane hydrate stability region. The pressure on October 27, 2015 (a day earlier) was 165 psi (78 psi + 87 psi hydrostatic). Assuming the temperature was also 47°F, this condition was even further outside of the stability region. If the solid was hydrate, it was in the unstable region for more than a day by the time the bailer tagged it at 467 ft. Hydrate dissociation rates reported in the literature are inconsistent, so we are not certain that the hydrate plug would have dissociated in a day though.

Because the solid was not likely to be hydrate, we concluded the 47°F reading was not representative of the temperature in the tubing at 467 ft.

Well Summary		
Standard Senson 25 has broached to surface with several fissures on pad site.		
11-3/4" casing to 990 ft. 7" casing to 8,585 ft. 5-1/2" slotted liner to 8,745 ft. 2-7/8" tubing to 8,510 ft. Packer depth 8,468 ft.		
Hour	**Hour**	**Activity on Site**
6:45	7:15	Traveled from hotel to location.
7:15	7:45	Attended morning safety/operations meeting.
7:45	8:00	Performed site assessment. Gas flow from fissures on well pad appear to have decreased.
8:00	9:30	Checked pressures on 25 well. 7" x 11-3/4" - 325 psi. 2-7/8" x 7" - 128 psi. 2-7/8" - 170 psi. Bled tubing pressure to 86 psi.
9:30	11:30	Closed all casing valves. Installed A-Frame on well. Continued rigging up slick line. (10:00) Checked pressure on
		2-7/8" x 7" annulus - 134 psi. Bled to 124 psi.
11:30	12:15	Made up 1-5/8" sample bailer. Stabbed lubricator. Opened up well. 2-7/8" x 7" - 109 psi. 2-7/8" - 87 psi. RIH with sample bailer
		Sat down hard at 467 ft. Pulled out of the hole. Inspected sample bailer. Observed polymer on tool. Tool temperature 47 deg F.
		Fluid level - 300 ft.
12:15	12:45	Lunch.
12:45	14:15	Shot fluid levels on 7" x 11-3/4" and 2-7/8" x 7" annulus. 7" x 11-3/4" - 43 ft. 2-7/8" x 7" - 164 ft.
14:15	15:30	Lined up Halliburton to pump 8.7 ppg Flozane down tubing.
15:30	16:15	Filled kill line with 9.5 bbls. Pumped 3.1 bbls. Pump pressure increased to 350 psi. Monitored 5 minutes. Pressure increased
		to 377 psi. Pumped 0.2 bbls. Tubing pressure 500 psi. Monitored for 5 minutes. Tubing pressure increased to 525 psi.
		Pumped 0.5 bbls. Tubing pressure increased to 776 psi. Monitored for 5 minutes. Tubing pressure increased to 801 psi.
		Pumped 0.1 bbls. Tubing pressure 998 psi. Monitored for 5 minutes. Tubing pressure increased to 1,027 psi. Pumped 0.1 bbls.
		Tubing pressure 1,220 psi. Monitored for 5 minutes. Tubing pressure increased to 1,337 psi. Pumped 0.1 bbls. Tubing pressure
		1,480 psi. Monitored for 5 minutes. Tubing pressure 1,603 psi.
16:15	17:00	Tubing pressure 1,824 psi. Bled to 1,790 psi. Continued monitoring well. (16:50) Tubing pressure 2,400 psi. Closed tubing
		head valve. Tubing pressure remained constant. Pressure on pump truck increased to 2,595 psi. Suspect communication with
		field injection lines. Made up 1-5/8" sample bailer.
17:00	17:30	Ran in hole with sample bailer. Tagged hard at 467 ft. Pulled out of the hole. Secured well.
17:30	18:00	Attended end of the day meeting.
18:00	18:30	Travel to hotel.

Figure 24: Portion of the Daily Report for October 28, 2015 [21]

Date:	29-Oct-2015	Well Name and Number:	Standard Senson 25	Report #	5
Well Summary					
Standard Senson 25 has broached to surface with several fissures on pad site. Surface casing pressure fluctuates between 505 psi and 770 psi.					
11-3/4" casing to 990 ft. 7" casing to 8,585 ft. 5-1/2" slotted liner to 8,745 ft. 2-7/8" tubing to 8,510 ft. Packer depth 8,468 ft.					
Hour	**Hour**	**Activity on Site**			
6:30	7:00	Traveled from hotel to location.			
7:00	7:30	Attended morning safety/operations meeting.			
7:30	8:15	Performed site assessment. Observed ice on fissures around cellar. Fissures appeared to have made fluid overnight. Checked			
		pressures on SS 25. 2-7/8" - 429 psi. 2-7/8" x 7" - 353 psi. 7" x 11-3/4" - 505 psi.			
8:15	8:30	7" x 11-3/4" pressure - 515 psi. Flowed annulus for fifteen minutes. Shut in. Casing pressure 509 psi.			
8:30	9:30	Moved in and rigged up crane. Laid down lubricator. Removed A-Frame from well. 2-7/8"- 360 psi. 2-7/8" x 7" - 420 psi.			
		7" x 11-3/4" - 560 psi. Checked pressures on 25B. 2-7/8" - 2,450 psi. 2-7/8" x 7" - 2,450 psi. 7" x 11-3/4" - 44 psi.			
9:30	10:30	Western wireline added sinker bar and lubricator.			
10:30	10:45	Shot fluid levels on SS 25.			
10:45	11:00	Bled 2-7/8" x 7" annulus f/ 456 psi t/ 440 psi.			
11:00	12:00	Installed 2-9/16" 5M upper master valve. 2-7/8" - 375 psi. 2-7/8" x 7" - 462 psi. 7" x 11-3/4" - 591 psi.			
12:00	12:30	Held PJSM to discuss slick line operations.			
12:30	13:15	Made up 1.625" sample bailer. Stabbed lubricator. RIH. Sat down at 37 ft. POOH. Tool temperature 59 deg F. 2-7/8" - 54 psi.			
13:15	13:45	Stabbed lubricator. RIH with 1.625" sample bailer. Sat down at 37 ft. POOH. Tool temperature - 19 deg F. Observed ice			
		in sample bailer. Rigged down slick line.			
13:45	14:15	Met with HALCO representatives to discuss coiled tubing operations. A coiled tubing unit is being mobilized from Houma, LA.			
14:15	15:30	Blew down with draw and kill lines from 450 psi to 50 psi. Discussed removing lines to isolate SS 25 from facility lines.			
15:30	16:00	Attended end of the day meeting. Coiled tubing unit will take 2 days to arrive at location. Will remove lateral lines from SS 25.			
		Will move Halliburton pump truck closer to SS 25. SCGC will continue running diagnostics on nearby wells.			
16:00	18:00	Continued monitoring pressures. (16:30) 2-7/8" - 51 psi. 7" - 685 psi. 11-3/4" 731 psi. (17:00) 2-7/8" - 55 psi. 7" - 634 psi.			
		11-3/4" - 697 psi. (17:30) 2-7/8" - Shut in. 7" - 631 psi. 11-3/4" - 770 psi.			
18:00	18:30	Traveled to hotel.			

Figure 25: Portion of the Daily Report for October 29, 2015 [21]

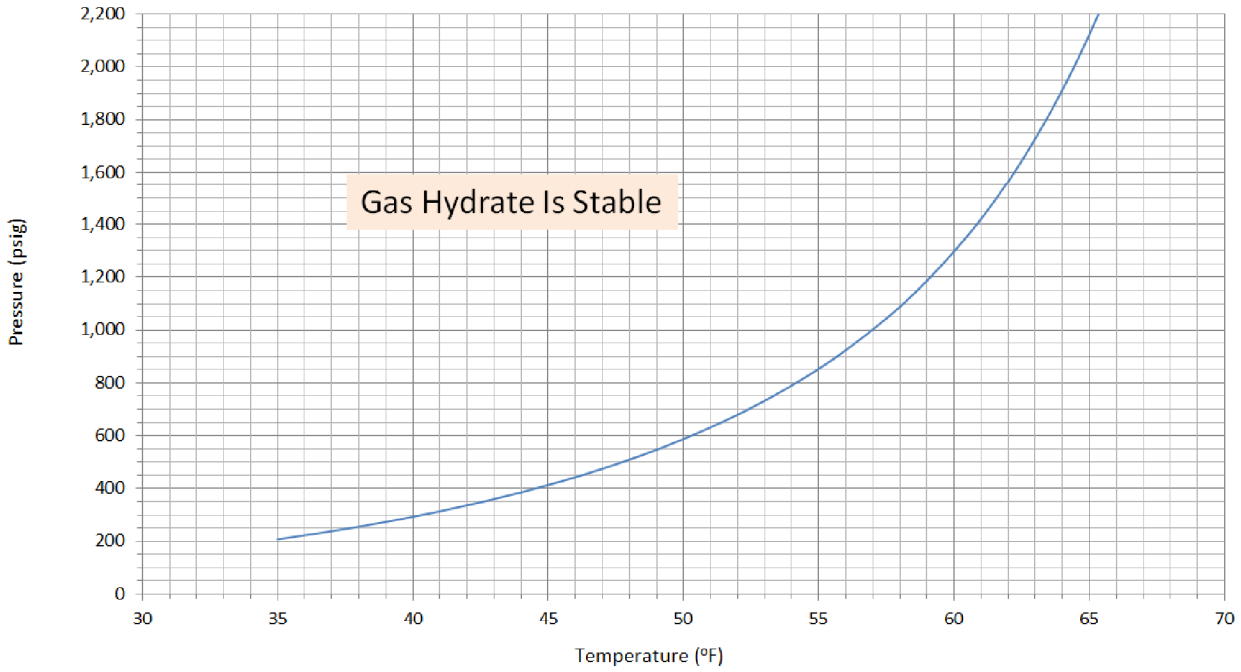

Figure 26: PROSPER Estimated Gas Hydrate Stability Curve [2]

At 15:30 to 16:15 on October 28, 2015, 8.7 ppg Flowzan with freezing point of 26°F was pumped down the tubing. The operation was terminated due to a jump in the pressure. The bailer was sent back down at 17:30 to 18:00 and tagged solid at 467 ft. The kill fluid had not frozen after about an hour. Furthermore, the methane in the tubing above 300 ft had been displaced out of the well. There was little or no methane in the tubing above the solid plug at 467 ft.

At 13:15 to 13:45 October 29, 2015, the bailer was sent down the tubing and tagged a solid plug at 37 ft. The tool temperature was 59°F. The bailer was sent down the tubing again and tagged a solid plug at 37 ft again, but this time the tool temperature was 19°F. A solid plug had formed in less than 20 hours. If the 59°F temperature reading was correct, the new solid plug had to be hydrate. The tubing pressure was 429 psi, and the temperature needed to be less than 45°F for hydrate to be stable. If the 59°F temperature reading is correct, the pressure needed to be above 1,200 psi for the hydrate to be stable. Although the tubing was at 2,400 psi on October 28, 2019, there was no methane. One possible scenario is that a large amount of methane leaked through the solid plug at 467 ft to enable hydrate to form. However, a simpler explanation is that the 19°F was the correct temperature reading, and this new solid plug was ice and not hydrate.

From these observations, we concluded that the temperature in the tubing was likely below freezing on October 28, 2015, and was 19°F on October 29, 2015. Furthermore, the solid plugs in the well were likely ice and not hydrate. The upper section of the well was cold. The ice plug in the tubing was not removed until November 6, 2015 (deicing operation), and this suggested that the temperature was still below 32°F until then. However, because of the 500 to 800 psi pressure measured in the 7 in. x 2 7/8 in. annulus and the 11 3/4 in. x 7 in. annulus between October 28, 2015, and November 6, 2015, PROSPER predicted leaking gas temperature between 40 and 60°F. Appendix D shows that if this warm gas continued to flow up the 11 3/4 in. x 7 in. annulus and out the holes in the surface casing, the upper section of the well would have thawed out. This is not what was observed. Therefore, the gas must have taken another path that avoided the upper section of the well.

Appendix F estimates the fracturing pressure of the surface casing shoe to be between 400 and 815 psi, which is in the range of the observed pressure in the 11 3/4 in. x 7 in. annulus. It is possible the rocks around the surface casing shoe fractured and the gas leaked out the well around the casing shoe. This path would avoid the upper section of the well and would avoid thawing this section out. This is what we believe happened during this warm leaked gas period.

Appendix D Energy Balance & Heat Transfer Inside SS-25

During the period of October 28 to November 6, 2015 (9 days), the 7 in. x 2 7/8 in. annulus pressures were 400 to 800 psi, and PROSPER estimated the leaking gas temperatures were 40 to 60°F. The goal of this appendix is to show that if this warm gas flowed up the 11 3/4 in. x 7 in. annulus and escaped through the holes in the surface casing between 134 and 300 ft (Figure 27), then the temperature in the upper section of SS-25 would have been above freezing, and all the ice would have melted by November 6, 2015.

To demonstrate this, it is necessary to show that the heat energy in the leaked gas was sufficient to warm up the well within these 9 days. In addition, it is necessary to show that the needed amount of heat could have been transferred to the tubing string within this same period.

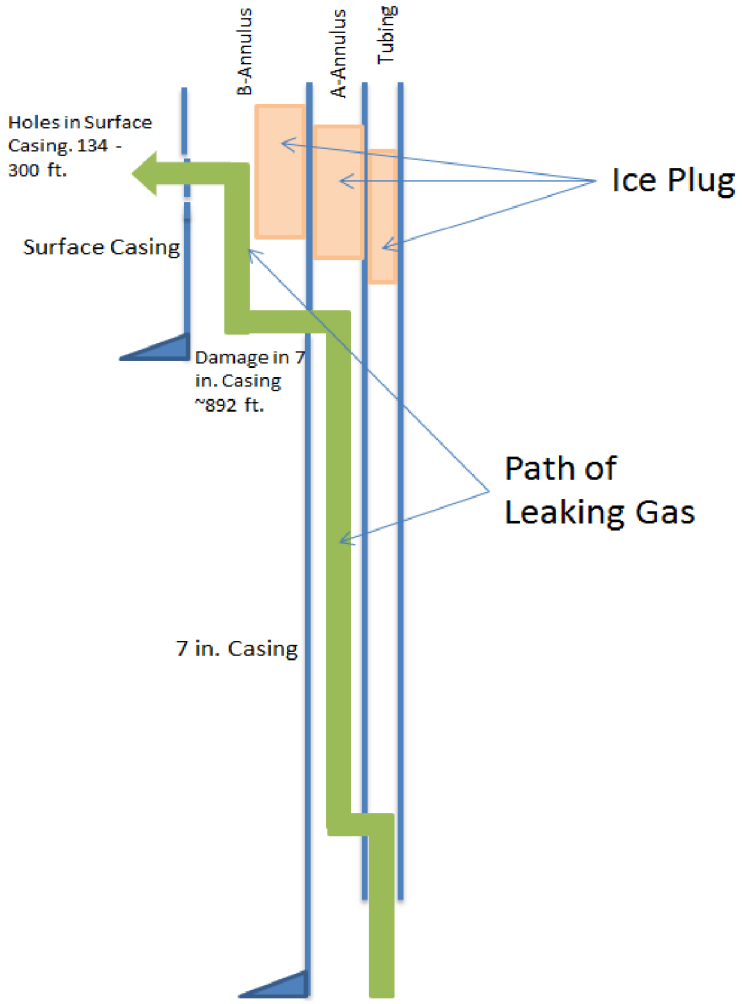

Figure 27: Leaking Gas Path If Holes in Surface Casing Not Blocked

The energy required to melt the ice in the well is equal to the energy needed to raise the temperature of the well (tubing and casing plus the ice and water) from 10°F to the melting point of ice. PROSPER simulation estimated that the temperature of the leaking gas when SS-25 was shut in was 10 to 20°F. We assume that the upper section of the well had equilibrated to the gas temperature of 10°F. Due to brine rejection, the ice should be nearly pure water with a melting point of 32°F. For this calculation, though, we will use 45°F. Therefore, the calculation will overestimate the amount of energy needed. The energy

needed consists of the sensible heat (mass times heat capacity times the change in temperature, 35°F) and heat of fusion of water (144 Btu/lbm [44]). The heat capacity of steel is 0.12 Btu/lbm-°F [45]. To simplify the calculation, we used 1 Btu/lbm-°F for the heat capacity of water and ice (ice is 0.5 Btu/lbm-°F). Although part of the 89 bbl of 8.6 ppg KCl would have been entrained in the escaping gas, the entire 89 bbl was assumed to remain in the well for this calculation. The *Kill Fluid* and *Tubular and Casing* sections of Table 12 summarize the calculation for the required amount of energy needed to melt the ice in the well.

The calculation for the amount of sensible heat energy the escaping gas can deliver is shown in the *Gas (methane)* section of Table 12. PROSPER estimates a gas flow rate of about 80 MMscf/D [2] during this period. The heat capacity of methane at 700 psi and 50°F is 0.62 Btu/lbm-°F [46]. The density of methane at standard condition is 0.0417 lbm/ft^3 [46]. Dividing the required amount of heat energy by the rate at which heat energy can be delivered by the leaking gas shows about 14 hours would have been needed. This is much less than the 9 days available, so there would have been an ample amount of heat in the leaking gas to melt the ice in the well.

Table 12: Energy Balance to Estimate How Long It Takes to Thaw SS-25's Upper Section

Kill Fluid

Vol Pumped	bbl H_2O	89
	ft^3 H_2O	500
	lbm H_2O	31,189
Heat Capacity	Cp Btu/lb-°F	1
Final Fluid Temperature	°F	45
Change in Temperature	°F	35
Heat of Fusion	Btu/lbm	144
From Sensible Heat (Heat Capacity)	Btu	1,091,616
From Heat of Fusion (Phase Change)	Btu	4,491,219
Total	Btu	5,582,834

Tubular and Casing

Tubing Weight	lb/ft	6.5
7 in. Casing	lb/ft	23
Surface Casing	lb/ft	42
Total Weight of Metal /ft	lb/ft	71.5
Heat Capacity	Cp Btu/lb-°F	0.12
Metal Temperature	°F	45
Change in Temperature	°F	35
From Sensible Heat	Btu/ft	300.3
Total Length	ft	1000
Total Btu	Btu	300,300
Total Btu Required	Btu	5,883,134

Gas (Methane)

Rate	MMSCF/D	80
Heat Capacity	Btu/lbm-F	0.62
Density @ 68°F and 1 atm	lbm/ft^3	0.0417
Gas Temperature	°F	50
Change in Temperature	°F	5
Available Btu	Btu/10 min	71,776
Total Time Required	hr	13.7

The estimation of how long it takes to transfer this amount of energy is broken down into two steps. The first step is to bring the 7 in. casing to 45°F. The second step is for the 7 in. casing to warm the inside of

the 7 in. x 2 7/8 in. annulus and melt the ice. Both steps occur in parallel, so the time needed to transfer the required Btu is the longer of the two steps.

The primary mechanism for warming the 7 in. casing is by forced convection of gas up the 11 3/4 in. x 7 in. annulus. Formulas for this calculation can be found in reference [47] and are summarized below:

$$D_e = \frac{{D_{outer}}^2 - {D_{inner}}^2}{D_{outer} + D_{inner}},$$

$$N_{re} = \frac{\rho U D_e}{\mu},$$

$$N_{pr} = \frac{\mu C_p}{k},$$

$$N_{nu} = 0.02 {N_{re}}^{0.8} {N_{pr}}^{1/3} \left(\frac{D_{outer}}{D_{inner}}\right)^{0.53},$$

$$h = \frac{N_{nu} k}{D_e}, \text{ and}$$

$$q = h \Delta T A.$$

N_{re}, N_{pr}, and N_{nu} are the dimensionless group Reynolds number, Prandtl, number and Nusselt number, respectively. D_{outer} is the inner diameter of the surface casing, D_{inner} is the outer diameter of the 7 in. casing, U is the gas velocity, ρ is the gas density, μ is the gas dynamic viscosity, k is the gas thermal conductivity, h is the heat transfer coefficient, T is the temperature, A is the surface area, and q is the heat transfer rate. The values of the gas properties can be found in reference [46].

Table 13 shows the time for forced convection to transfer the amount of heat needed (5.9 million Btu). The required time is about 2 hours assuming an average temperature difference of 5°F. This is much less than 9 days, so warming up the 7 in. casing will not be an obstacle to melting the ice in the well.

Table 13: Forced Convection Heat Transfer Coefficient in the 11 3/4 in. x 7 in. Annulus with 80 MMscf/D Flow Rate

Gas in 11 3/4 in. x 7 in. Annulus	
Temperature (°F)	50.00
Z Factor	0.90
Pressure (psi)	700.00
Inner Diameter D1 (ft)	0.58
Outer Diameter D2 (ft)	0.92
Density rho (lbm/ft^3)	2.28
Volumetric Flow Rate (MMSCF/D)	80.00
Gas Viscosity mu (lbm/(hr-ft)	0.03
Gas Specific Heat c (Btu/lbm-°F)	0.61
Gas Conductivity k (Btu/hr-ft^2-(°F/ft)	0.02
Flow Area (ft^2)	0.40
Effective Diameter De (ft)	0.34
Velocity u (ft/hr)	153,726
Reynold's Number Nre	4,342,192
Prandtl's Number Npr	0.84
Npr's Exponent	0.33
Nusselt Number Nnu	4920.41
Heat Transfer Coefficient h (Btu/hr-ft^2-°F)	292.37
Difference in Temperature (°F)	5
7 in. Casing External Surface Area(ft^2/ft)	1.83
Total Length (ft)	1000
Heat Transfer Rate (Btu/hr)	2,678,986
Time Required (hr)	2.20

The second step, transferring the heat from the 7 in. casing into the 7 in. x 2 7/8 in. annulus is more complicated. After the ice in the 7 in. x 2 7/8 in. annulus starts to melt and shrinks away from the 7 in. casing wall, the dominant heat transfer mechanism may change. The three main mechanisms are conduction, natural convection, and radiative heat transfer. There is another possible mechanism that can occur if the two halves of the 7 in. casing are not aligned at the parting. In this case, gas can shoot up the top half of the 7 in. casing on one side with return flow coming back down on the other side. Once the gap between the ice plug and the 7 in. casing's wall is wide enough, warm gas can flow up the gap and forced convective heat transfer can start. Forced convective heat transfer can quickly finish the job of warming the 7 in. x 2 7/8 in. annulus and tubing to the gas temperature.

The analysis of all these heat transfer mechanisms is beyond the scope of this work. Instead, we solve just the radiative heat transfer problem to determine how long it takes radiative heat transfer to melt the ice in the 7 in. x 2 7/8 in. annulus. We assume that after that happens convective heat transfer will melt the remaining ice in the tubing string quickly.

The Stefan-Boltzmann equation is used to estimate the radiative heat transfer rate [47].

$$q = 0.1713\text{x}10^{-8} A\epsilon\left({T_{outer}}^4 - {T_{inner}}^4\right).$$

T_{outer} is the temperature of the 7 in. casing and the T_{inner} is the temperature of the ice surface in Rankine. A is the inner surface area of 7 in. casing in ft^2, ϵ is the emissivity, and q is the heat transfer rate in Btu/hr. The emissivity of ice is 0.98 [48].

The upper part of Table 14 shows the calculation for the amount of energy needed to melt a 500 ft column of ice in the 7 in. x 2 7/8 in. annulus. The bottom part of this table calculates the radiative heat transfer rate per foot of 7 in. casing. Dividing the amount of energy required, by the radiative heat transfer rate over 500 ft of 7 in. casing shows that 5 days are required. We expect that a sufficiently wide gap between the 7 in. casing and the ice plug would have formed for convective heat transfer to become dominant sooner than that. In any case, the ice in the upper section of well SS-25 should have melted by November 6, 2015. However, this is not what was observed. The warm gas during this period of high pressure must have found another route out of the well to keep the upper section of the well cold.

Table 14: Time Required to Melt a Column of Ice in the 7 in. x 2 7/8 in. Annulus by Radiative Heat Transfer

Outer Diameter (ft)	0.53
Inner Diameter (ft)	0.24
Annulus Volume (ft^3/ft)	0.18
Total Ice Mass in Annulus (lbm/ft)	10.98
Length (ft)	500
Heat of Fusion (Btu/lbm)	144
Temperature Change (°F)	25
Heat Capacity of Ice (Btu/lbm-°F)	1
Total Btu Required (Btu/ft)	859,142
T1 (°F)	45
T2 (°F)	35
Emissivity	0.98
Area / Length of 7 in. casing (ft^2/ft)	1.67
Btu/hr-ft	13.93
Time Required (days)	5.1

Appendix E Conversion of Ice Plug to Hydrate Plug

Reference [2] speculates that although during the first kill attempt the kill fluid formed ice and not hydrate, later the ice could have converted into hydrate. During the period between October 28 and November 6, 2015 (9 days) when the temperatures and pressures were high, the conditions in the upper section of the well (the 7 in. x 2 7/8 in. annulus and the 11 3/4 in. x 7 in. annulus) were in the stable hydrate region. Gas flowing up the B annulus would not have been warm enough to cause the hydrate to dissociate. Gas, therefore, does not have to find another route out of the well. In the remainder of this appendix we will show that the ice phase changing into hydrate is unlikely.

The difficulty with this theory is that to convert ice into hydrate, methane must diffuse through the ice. (To make methane hydrate, methane is needed.) The molar concentration of methane needed to satisfy stoichiometry is one molecule of methane for about six molecules of water [49], or about 14% by mole. The diffusivity of gas in solids is low, between 10^{-8} to 10^{-10} cm^2/s [50]. Kaomi et.al. [51] reported methane diffusivity values between $1.7x10^{-9}$ and $6.7x10^{-10}$ cm^2/s. Because of the low diffusivity, methane is not expected to penetrate deep into the ice and the diffusion problem can be simplified to diffusion in the X-direction only (ignoring curvature), as shown in Figure 28. The solution to this problem can be found in reference [52]. Figure 29 shows the ratio of the methane molar concentration at 0.2 in. from the interface to the concentration at the interface (methane diffusivity used is 10^{-8} cm^2/s). It shows that after 2 weeks the concentration is still less than 1% of the interface concentration at depth of 0.2 in. Methane has not penetrated in appreciable amount to a depth of 0.2 in. by November 6, 2015. This means that there may at most be a thin crust of hydrate encasing the ice plug during the period of high pressure and temperature. The bulk of the solid blockage remains ice and will melt if the temperature rises above 32°F. (Note that due to brine rejection, the melting point will be 32°F and not 26°F.)

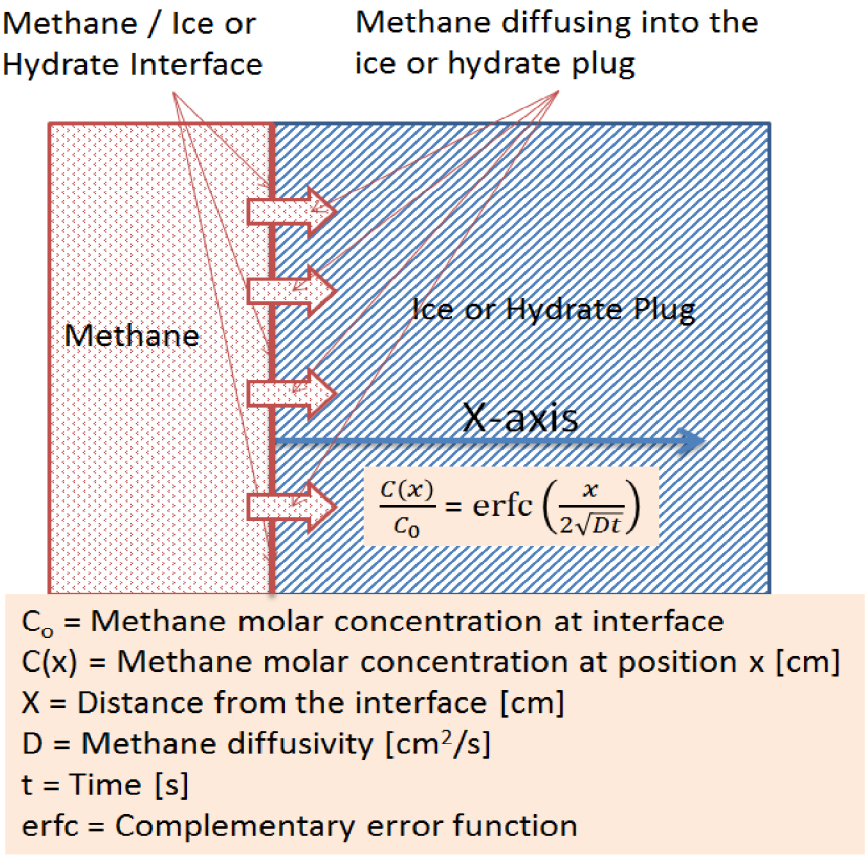

Figure 28: One Dimensional Diffusion Problem with Equation for the Methane Concentration at Position X from the Methane/Ice or Hydrate Interface

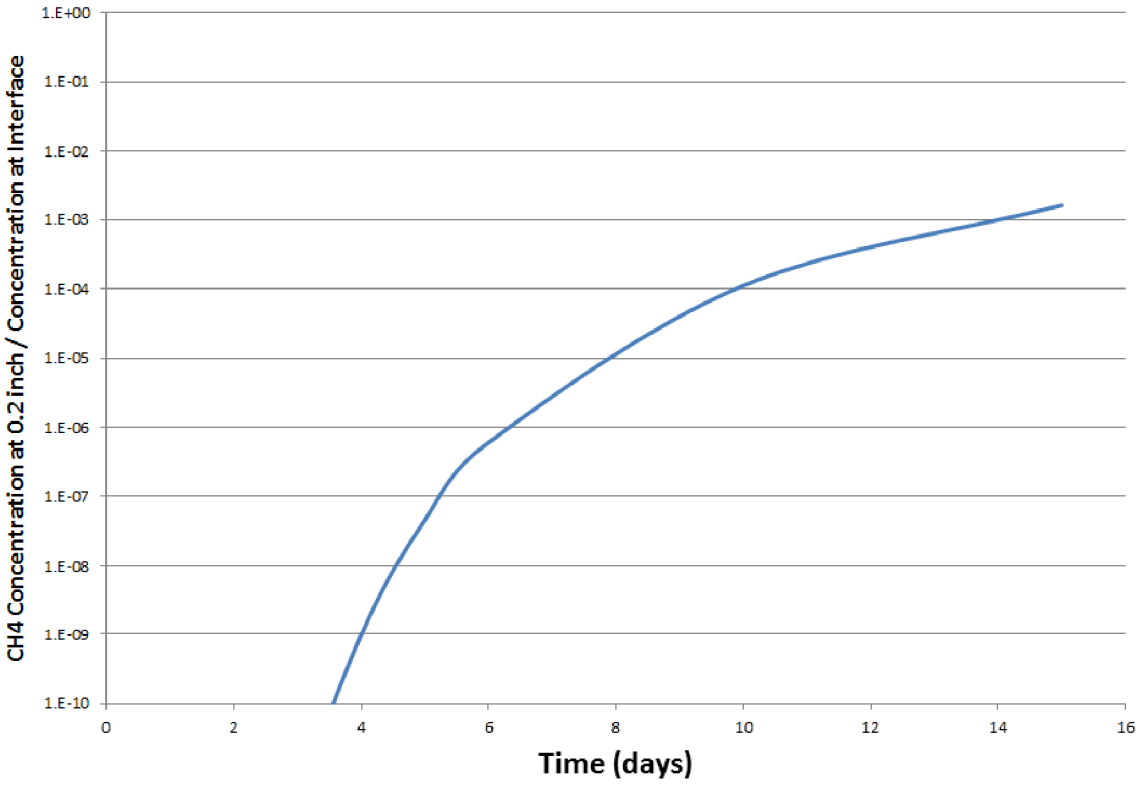

Figure 29: Methane Molar Concentration 0.2 In. from the Surface

There is another possibility, which is that during the high temperature period, the ice starts to melt at the surface and the hydrate forms then. Methane diffusion coefficient in water is $1.5x10^{-5}$ cm^2/s [53], three orders of magnitude higher than in ice. In this case, if the hydrate formation kinetic is slow compared to the water drainage rate, the liquid will simply drain away before any hydrate forms. If hydrate formation kinetics is faster, then again hydrate will encrust the ice. Methane diffusion rate will again limit how much of the ice plug will convert to hydrate. In either case, this scenario will not convert the solid ice block into solid hydrate block. The blockage will melt away once the temperature rises above 32°F.

One can argue that there is enough methane dissolved in the original kill fluid and there is no need for methane to diffuse into the ice plug. The solubility of gas increases with pressure. Let's examine the solubility of methane in the kill fluid pumped down the tubing string. The pressure is highest there compared with the 7 in. x 2 7/8 in. annulus and the 11 3/4 in. x 7 in. annulus. The solubility of methane in water is low, 0.04 gm/kg of water at 32°F and 1 atm [49]. Using Henry's law to adjust to 1,700 psi, the initial pressure at top of the tubing after shutting in SS-25, the molar concentration of dissolved methane is 0.5%, far from the 14% required by stoichiometry. Tohidi et al. [54] made a more detailed thermodynamic calculation and showed that hydrate yield is about a mole percent with just the methane initially dissolved in water. There is not enough dissolved methane in the water to convert the ice plug to hydrate plug.

Because we cannot rule out the possibility of an initial form of the ice plug (porous ice for example) that could circumvent the slow methane diffusion problem, we cannot assert that the ice plug that formed during the kill attempt #1 did not convert to hydrate. However, if the initial blockage was a solid block of ice these calculations showed that the ice plug would not have converted to hydrate. We will presume that the blockage was initially a solid ice plug and the conversion to hydrate did not occur. The presence of the ice blockage indicated that the temperature was below 32°F.

Appendix F Estimating Fracturing Pressure

A noise-temperature survey on May 20, 2018 showed that there is no leak at the surface casing shoe at 990 ft [20]. This test was performed by loading the 11 3/4 in. x 7 in. annulus with fluid and listening for sound of fluid flow. However, the leak around the surface casing is necessary to provide a path for the gas to flow out the well without going up the 11 3/4 in. x 7 in. annulus during the warm leaked gas period (October 28 and November 6, 2015).

In this appendix, the fracturing pressure is estimated. The fracturing pressure at the surface casing shoe can be estimated using the Terzaghi equation:

$$HS_{min} = \left(P_{overburden} - P_{pore}\right) * \frac{Poisson\ Ratio}{1-Poisson\ Ratio} + P_{pore} + Tectonic\ Forces,$$

where HS_{min} is the fracturing pressure, $P_{overburden}$ is the overburden pressure, and P_{pore} is the pore or formation pressure at the depth of the surface casing shoe.

The depth of the surface casing shoe is 990 ft. If we assume rock bulk density over this 990 ft interval to be 2.2 gm/cm^3, the overburden pressure is 945 psi.

CHDT measurements were taken in the well in 2017 [14]. The pore pressure estimated between 872 ft and 1,006 ft ranged between 132 and 202 psi. For the lower bound on the fracturing pressure we will use 130 psi. For the lower bound on the fracturing pressure, the tectonic force is also neglected. For Poisson ratio of 0.25 (hard rock), the fracture pressure is 402 psi. For Poisson ratio of 0.35 (soft rock), the fracture pressure is 569 psi.

At shallow depths and in presence of strong tectonic forces, it is possible for minimum stress to be in the vertical direction. The stress in the vertical direction is overburden pressure minus the formation pressure or 815 psi. This would be the upper bound on the fracturing pressure of the casing shoe.

The expected range of the fracturing pressure around the surface casing shoe is 400 to 815 psi. This is in the range of pressures observed between October 29 and November 6, 2015.

As to the noise test of the integrity of the surface casing shoe conducted on May 20, 2018, the height of the fluid column was 690 ft or a hydrostatic pressure of about 300 psi. This may not be sufficient to reopen the fractures around the surface casing shoe.

SS-25 RCA Supplementary Report

SS-25 Transient Well Kill Analysis

Purpose:

Present and discuss the results of transient kill simulations for the seven SS-25 kill attempts performed from October 24 to December 22, 2015, and the analysis of the kill attempts.

Date:
May 31, 2019

2600 Network Boulevard, Suite 550
Frisco, Texas 75034

+1 972-712-8407 (phone)
+1 972-712-8408 (fax)

16285 Park Ten Place, Suite 600
Houston, Texas 77084

1-800-319-2940 (toll free)
+1 281-206-2000 (phone)
+1 281-206-2005 (fax)

www.blade-energy.com

Abstract

The gas storage well Standard Sesnon 25 (SS-25) in the Aliso Canyon Gas Storage Field located in Los Angeles County, California started leaking gas in October 2015. A relief well was drilled, and SS-25 was brought under control. The leak stopped in February 2016.

In January 2016, as part of their investigation of the leak, the California Public Utilities Commission (CPUC) and the Division of Oil, Gas, and Geothermal Resources (DOGGR) selected and gave provisional authority to Blade Energy Partners (Blade) to perform an independent Root Cause Analysis (RCA). The Blade Team and parties under Blade's direction were responsible for directing the work of subcontractors who performed the extraction of the SS-25's wellhead and tubing and casing and the preservation and protection of associated evidence. Blade RCA Reports, including this report, document and describe the key activities undertaken in support of the RCA effort.

Southern California Gas Company (SoCalGas) and their suppliers, made seven unsuccessful attempts to kill SS-25 between October 24 and December 22, 2015. Blade set up a model to simulate the gas leak conditions in the 7 in. casing at 892 ft, with gas flowing to surface. One of the objectives of this study was to analyze efficacy of each kill attempt based on the reported operations that included the density and volume of fluid pumped and pump rate. This analysis was done by modeling each kill attempt, which simulated the kill operational parameters and estimated flow rate of the well. Another objective was to identify if there was a set of kill parameters that could have successfully killed the well.

This report describes the approach and presents the results and a discussion of the transient kill simulation study performed by Blade.

Blade reviewed the kill attempt operations to understand what was done and what could have been done differently to improve the likelihood of a successful kill. The modeling showed a low likelihood of a successful well kill when using the low-density clear fluids, volumes, and pump rates utilized in the original kill attempts. We present alternative fluid density and pump rates for successful kill operations.

Some key findings include the apparent lack of modeling in the early kill attempts and the underestimation of the gas flow rate during the kill attempts. We found some evidence of the kill modeling developed by, we presume, the well-control company for the December 22, 2015, attempt. The kill attempt was unsuccessful, likely related to operational problems. The lack of success in the early kill attempts shows why kill modeling was necessary. The numerous kill attempts caused a crater to form, which made further well intervention into SS-25 hazardous and unsafe.

Table of Contents

List of Figures

List of Tables

1 Introduction

We include in this report the results of our transient kill simulation study. We used this study to evaluate the likelihood of success of the actual kill attempts and propose alternative kill scenarios for successful kill operations. We also discuss the actual kill operations performed in the field and analyze what occurred and what could have been done differently.

1.1 Transient Kill Simulations

Blade conducted a transient kill simulation analysis of the SS-25 gas leak, which began in October 2015, and was successfully killed on February 11, 2016 from the relief well Porter 39A (P-39A).

The analysis was conducted in four phases:

1. Simulation and evaluation of the seven kill attempts ranging from Kill Attempt #1 on October 24, 2015, to Kill Attempt #7 on December 22, 2015
2. Simulation and evaluation of alternative kill responses with higher density fluids, pump rates, and fluid volumes for each of the seven kill attempts to achieve a success kill
3. Simulation and evaluation of alternative kill responses for Kill Attempt #1 and Kill Attempt #2 with hypothetical low gas flow rate conditions (representative of the lower flow rate assumptions made during the actual kill attempts)
4. Simulation and evaluation of alternative kill responses for Kill Attempt #4 with an assumed leak depth of 440 ft

The SS-25 *base case* analysis was constructed from initial pressure conditions and an estimate of the Inflow Performance Relationship (IPR). The IPR was based on historic well test data analyzed in the report SS-25 Well Nodal Analysis with Uncontrolled Leak Estimation [1] by Blade. Using these conditions, a base case gas flow rate of 93 MMscf/D was estimated as the initial condition for Kill Attempt #1 on October 24, 2015. The initial reservoir pressure at the time of this attempt was estimated to be 3,195 psia.

The model was set up to reflect initial conditions for each of the seven scenarios. The dynamic kill approach applied for these simulations involved kill fluid being pumped down the 2 7/8 in. tubing with returns flowing up the 7 in. x 2 7/8 in. annulus to achieve the kill. For the purposes of the analyses in this report, a successful kill is defined as the ability to stop the influx gas within one complete circulation of kill fluid without exceeding the surface pressure limit of 5,000 psi[i].

An alternative set of initial conditions with a hypothetical low gas flow rate was created by implementing a Forchheimer influx model with a reservoir pressure of 2,400 psia and an Absolute Open Flow (AOF) of 30 MMscf/D. This low gas rate scenario was considered in this analysis because these reservoir conditions could be representative of what was assumed at the time of the kill attempts in 2015.

A leak depth of 440 ft was hypothesized in the US Department of Energy report Ensuring Safe and Reliable Underground Natural Gas Storage [2]. We simulated the kill responses at 440 ft to see what effect a shallow leak depth would have had on the ability to kill the well assuming these conditions.

[i] The SS-25 wellhead and tree had a working pressure rating of 5,000 psi.

The analysis reported in this study was primarily performed by using the software Drillbench Blowout Control version 6.2.2. The use of this tool facilitated the required transient, multiphase analysis of the dynamic kills with geometry representative of the physical system being considered.

Kill modeling using two-phase flow simulators have been available since the early 1990s for the purpose of contingency planning as part of emergency response plans and modeling well control events [3].Well kill simulators use the dynamic two-phase pipe flow simulator OLGA [4]. These models are equipped to handle time transients of the kill operations, complicated multiphase flow regimes and flow paths, and interactions with the reservoir.

1.2 Discussion of Kill Attempt Operations

Blade reviewed and analyzed the actual kill attempt operations based on data provided by SoCalGas.

A well-control company was contracted and brought on site after Kill Attempt #1 to provide well control expertise for Kill Attempts #2–7 and for drilling the relief well P-39A. Section 6 includes general comments about each kill attempt.

Figure 1 shows a timeline of the SS-25 events from the time the leak was identified until the time the well was killed from P-39A.

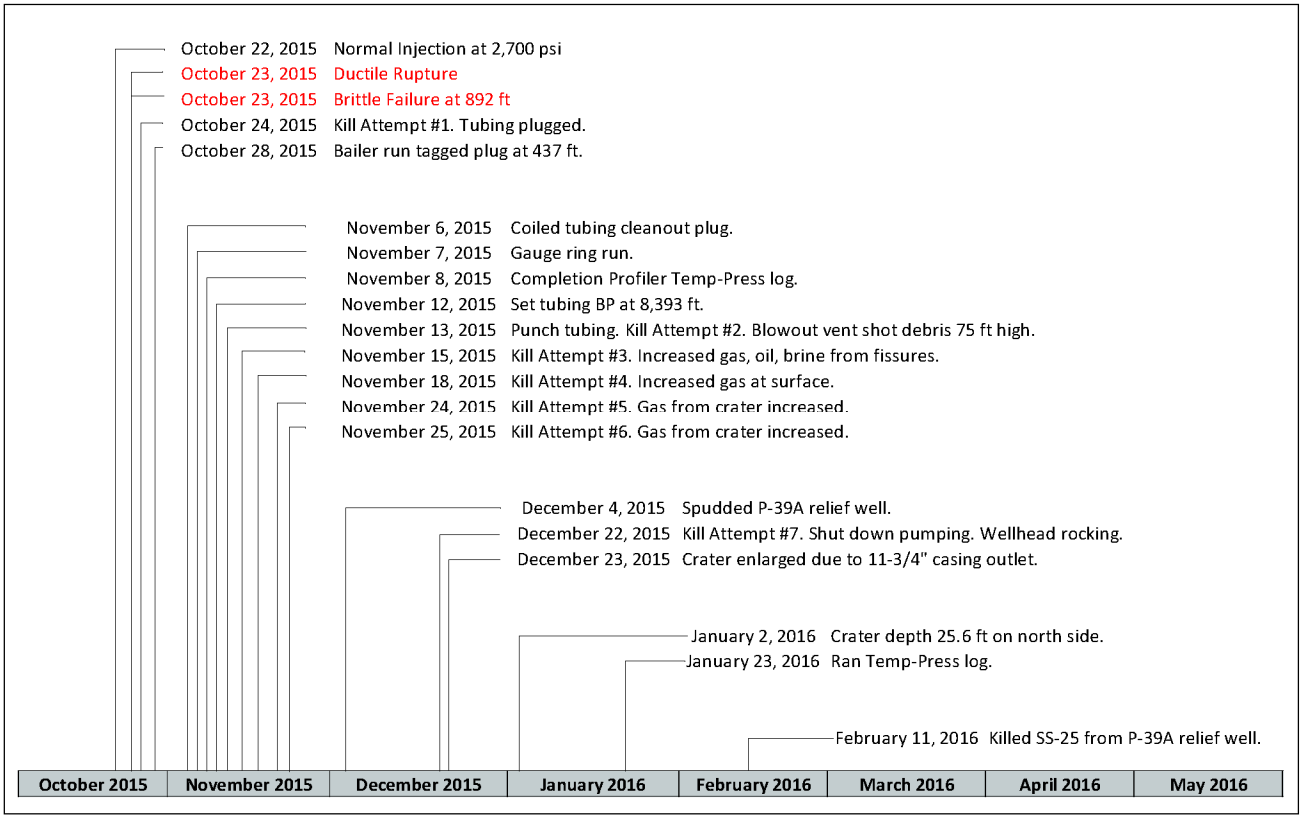

Figure 1: Timeline of the SS-25 Kill Attempts

1.3 Abbreviations and Acronyms

Term	Definition
AOF	Absolute Open Flow
BHP	Bottomhole Pressure
BP	Bridge Plug
$CaCl_2$	Calcium Chloride
CHP	Casing Head Pressure
cP	centipoise
CPUC	California Public Utilities Commission
DOGGR	Division of Oil, Gas, and Geothermal Resources
FBHP	Flowing Bottomhole Pressure
FF	Fernando Fee
GR	Gamma Ray
HHP	Hydraulic Horsepower
ID	Internal Diameter
IPR	Inflow Performance Relationship
KP	Kill Point
LBNL	Lawrence Berkley National Laboratory
LCM	Loss Circulation Material
MD	Measured Depth
MMscf/D	Million Standard Cubic Feet per Day
OD	Outside Diameter
P	Porter
PI	Productivity Index
ppg	Pounds per Gallon
psi	Gauge pressure units of Pounds Force per Square Inch
psia	Absolute pressure units of Pounds Force per Square Inch
Q	Volumetric Flow Rate
RCA	Root Cause Analysis
SoCalGas	Southern California Gas Company
SS	Standard Sesnon
STB	Stock Tank Barrel
TFA	Total Flow Area
THP	Tubing Head Pressure
WBM	Water-Based Mud
WGR	Water-to-Gas Ratio
WLM	Wireline Measurement

Term	Definition
XC	Xanthan Gum

2 Analysis Approach and Key Assumptions

This section summarizes:

- The general analysis approach.
- The method used to construct the physical system.
- The matching conditions at Key Points (KPs) in time with available data.
- The field observations and other analyses.
- The process of calibrating the software model.

Blade performed the transient kill analysis by using the software Drillbench Blowout Control, provided by Schlumberger, for the analysis of dynamic kills (where kill fluid is pumped down the tubing).

Throughout our modeling of potential kills, the intent was to determine under what conditions, if any, the well could have been killed. We achieved this by varying combinations of kill fluid density, pump rate, and duration of pumping.

2.1 Base Case

We constructed the SS-25 base case analysis based on:

- Our estimate of gas flow from the IPR and reservoir pressure at the time of the kill attempt [1].
- Our inference of the drawdown applied to the reservoir based on the observed shut-in conditions before and after the leak and well pressure data from the monitoring of SS-5.
- Our estimate of the initial gas rate on October 24, 2015, of 93 MMscf/D. This estimate was checked against the available data covering the initial period and refined as necessary. Similarly, we estimated the reservoir pressure to be 3,195 psia, which was assumed as the base case gas flow rate and reservoir pressure.
- Our assumption that a leak already existed prior to the attempted kills. Log data indicated a leak location at 895 ft WLM. The 7 in. casing was later confirmed to be parted at 892 ft MD.
- Our model's relief conduit for the flow exiting the 7 in. x 2 7/8 in. annulus at the leak. The conduit's internal diameter, D_R, was calibrated to achieve the observed 7 in. x 2 7/8 in. annulus pressure at the base case gas rate.

We then performed kill simulations for the SS-25 base case conditions (Key Point #1) and the subsequent six kill attempts. We investigated the kill through the tubing for a range of kill fluid densities and pump rates. It should be noted that we performed these simulations with the relief conduit open to flow to reflect conditions under which the kill would have succeeded. Based on this analysis, we were able to determine if the well was killable for each of the seven kill attempts.

2.2 Analysis of Kill Attempts

The analysis began with the base case conditions described in Section 2.1 as the starting point, that is, those conditions presumed to be present when the first kill was attempted.

Kill Attempt #1 on October 24, 2015, failed because the tubing plugged after just 11.8 bbl of 10 ppg polymer pill were pumped. The field operations continued with an unsuccessful pump and bleed[ii] attempt by pumping down the 7 in. x 2 7/8 in. annulus. It was not meaningful to evaluate this kill attempt because of its early termination.

The remaining six kill attempts were analyzed in detail. The Halliburton Job Report operational parameters (pump rate, kill fluid density, surface pressures, and pumping duration) [5] [6] [7] [8] [9] [10] [11] and daily reports for each kill attempt were used to set up each kill attempt in the simulator. The gas flow rate was based on estimated reservoir pressure at the time of each kill attempt by using the Productivity Index (PI) maintained at base case conditions. As such, the reservoir pressure and gas rate were adjusted for each kill attempt and reflected the conditions present on that date.

2.3 Definition of Kill

A well is said to be killed for modeling purposes, when the combination of hydrostatic pressure, surface pressure, and annular friction (in the case of dynamic kill attempts) is such that gas flow rate from the reservoir goes to zero, within the time required, for approximately one complete circulation of kill fluid at the specified pump rate and without exceeding the surface equipment pressure limit of 5,000 psi.

2.4 Physical System

This section describes some key assumptions in the set-up of the SS-25 physical system within the Drillbench Blowout Control software (Figure 2), the consistency checks used, and the details of our technical approach.

After shut-in and prior to Kill Attempt #1 on October 24, 2015, it was presumed that gas had flowed from the reservoir into the bottom of the tubing, entered the 7 in. x 2 7/8 in. annulus via ports near the packer, flowed up the 7 in. x 2 7/8 in. annulus, exited the 7 in. casing through a leak at 892 ft and finally flowed to surface through the formation. When the pumping of the kill fluid down the tubing of this physical system was initiated, the influx gas and kill fluid met in the tubing, and the combined flow entered the annulus through the ports.

Prior to Kill Attempt #2 on November 13, 2015, a plug had been set in the tubing at 8,393 ft, and the tubing had been perforated a few feet above the plug. Within the software, the plug and perforations were represented as a bit with nozzles forming the equivalent flow area of the perforations. When the pumping of kill fluid down the tubing of this physical system was initiated, the kill fluid entered the annulus via the bit nozzles (perforations) while influx gas flowed up from below.

The difference in annular flow conditions in the two physical setups in the software (before and after installation of the plug and perforations) was negligible for the purpose of this study. The primary impact of the installation of the plug and perforations was an increased restriction of kill fluid entry into the annulus. This restriction impacted the pumping pressure of the kill fluid.

For the initial conditions for both physical systems considered, we presumed that the 7 in. x 2 7/8 in. annulus was occupied by static reservoir gas from the assumed leak location to the wellhead. Similarly,

[ii] Pump and bleed refers to the process of removing gas from a well by pumping a given volume of fluid down the well to create an additional hydrostatic pressure that corresponds to the height and density of the fluid pumped and by bleeding gas pressure at surface with an amount equal to approximately the hydrostatic pressure from the fluid pumped. For example, if the hydrostatic pressure of the fluid volume pumped is 50 psi, bleed and reduce the pressure by approximately 50 psi.

we presumed that the tubing was occupied by static reservoir gas from the ports near the packer or perforations, depending on the system being considered, to the wellhead. Therefore, pressure at the leak location within the 7 in. x 2 7/8 in. annulus could be calculated by adding an estimated fluid hydrostatic pressure at the leak to the 7 in. x 2 7/8 in. annulus surface pressure. Likewise, the flowing bottomhole pressure (FBHP) could be calculated by adding an estimated fluid hydrostatic pressure at the ports near the packer to the tubing surface pressure. These serve as critical calibration checks for any simulation that reflects specific well conditions.

The flow from the assumed leak in the 7 in. casing through the formation to surface was modeled by using a fixed length *relief* conduit of constant internal diameter, D_R (as discussed previously). Based on assumed initial conditions for the Kill Attempt #2, the D_R was calibrated for a specified gas flow rate by choosing the relief well internal diameter so that pressure inside the 7 in. x 2 ⅞ in. annulus was consistent with the initial pressure conditions for that gas flow rate.

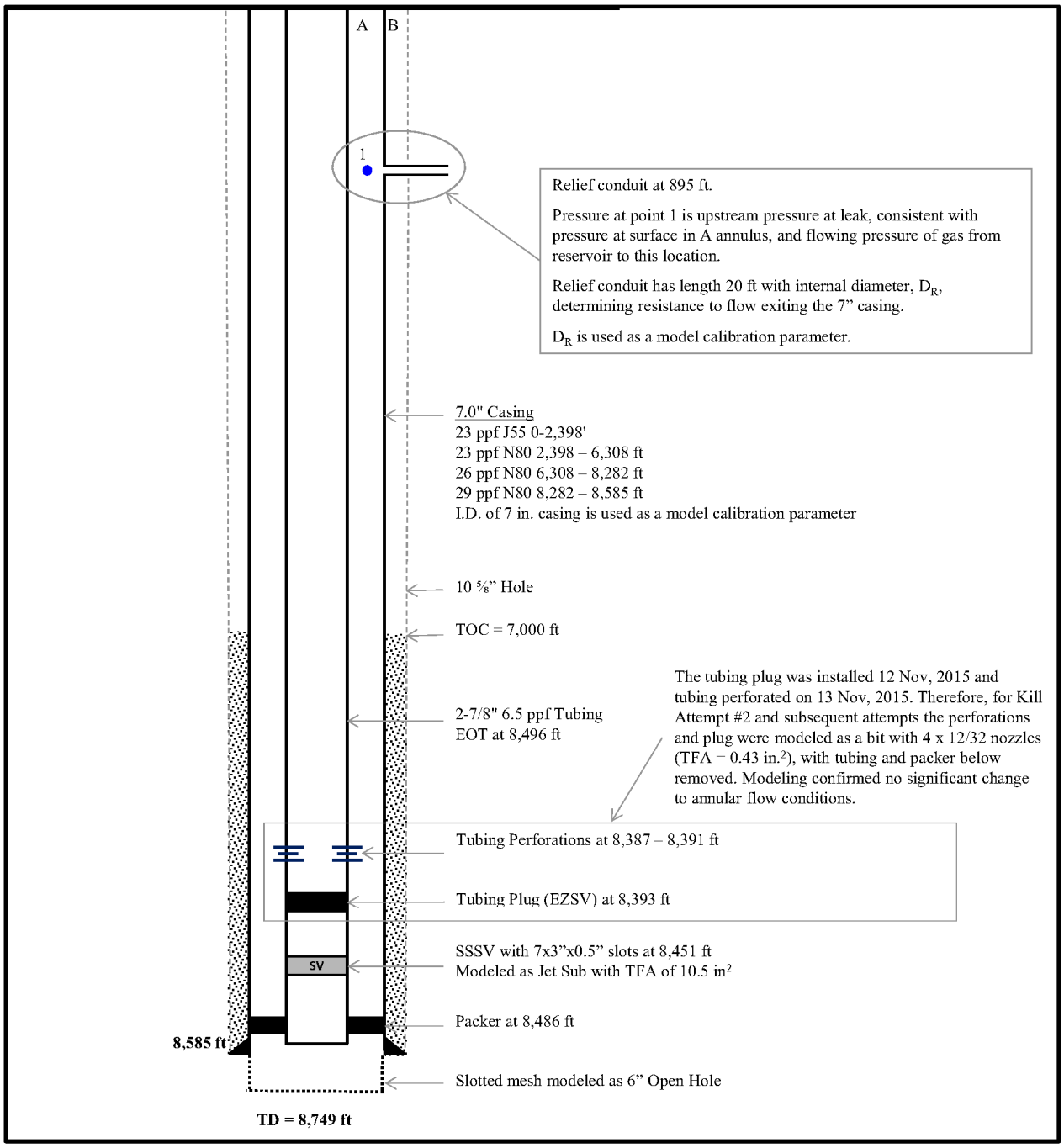

Figure 2: Physical Model as Set up in the Drillbench Blowout Control Model

2.5 Equivalent Resistance Diagram

Figure 3 shows an equivalent resistance diagram of the physical model being analyzed. This diagram allows for a simple understanding of the system and its response to changes in certain parameters.

In simulations, the different conditions of flow and pressure required to calibrate a model are achieved by essentially controlling each of the resistances. For example, we can see that the equivalent resistances R_1, R_2, and R_3 are inversely proportional to the relief conduit ID, reservoir pressure, and 7 in. casing ID, respectively. Increasing the R_1 (by reducing the relief conduit diameter D_R) results in a higher back pressure P_i at the leak location in the 7 in. x 2 7/8 in. annulus. Likewise, increasing the R_2 reduces the gas flow rate from the reservoir for a given drawdown. Finally, increasing the R_3 increases resistance to flow through the A annulus, thereby resulting in a higher FBHP for a given P_i. Thus, by balancing these resistances, it is possible to achieve the desired values for the CHP, THP, FBHP, and gas flow rate through iterative adjustments of the resistance to flow from the casing leak (R_1), the resistance to flow from the formation for a given drawdown pressure (R_2), and the annular friction pressure loss (R_3).

Conceptually, the model calibration approach described in Section 2.7 follows the above physical description. As such, since the fluid in the tubing (reservoir gas) is assumed to be static for the model calibration, an equivalent resistance is not shown within the tubing in the equivalent resistance diagram of the physical model (Figure 3).

Needless to say, numerically obtaining the correct balance to be consistent with data and observations requires multiple iterations.

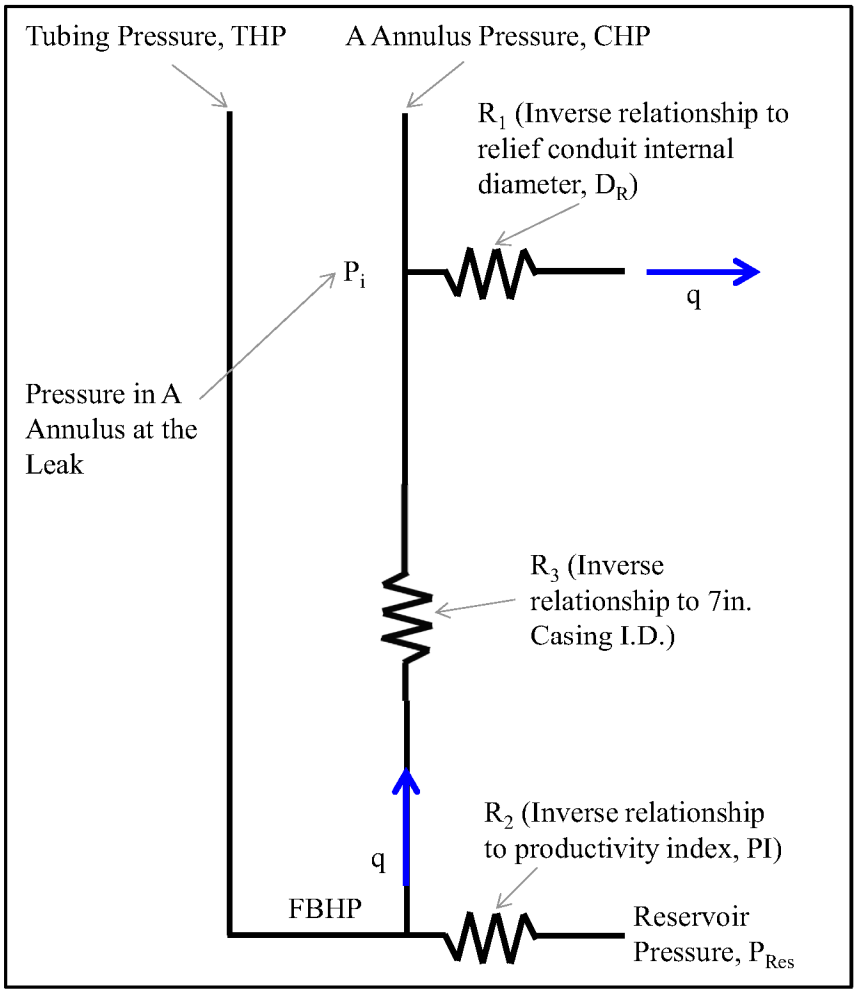

Figure 3: Equivalent Resistance Diagram of the Physical Model

2.6 Key Point Definition and Conditions

Throughout this analysis, the initial conditions from which various kill attempts were simulated are referred to as KP conditions. Based on this definition, KP #1 refers to the initial conditions existing prior to Kill Attempt #1. Similarly, KP #2 refers to the starting conditions for Kill Attempt #2, and so forth.

The summary of KP target conditions (Table 1) shows values for the CHP, THP, gas flow rate, and reservoir pressure for KP #1 through KP #7. In each case, KP conditions were assumed to represent approximate steady-state conditions from which a kill attempt may have proceeded.

The KP conditions have been carefully considered and kept consistent in the various analyses conducted by Blade. These data points include a combination of direct field data (CHP and THP), modeled and benchmarked data (gas flow rate), and field data estimated from an offset well (reservoir pressure).

Specifically, while the CHP and THP values were taken directly from daily reports, the gas flow rate and reservoir pressure were obtained from the report Blade Well Nodal Analysis [1]. Within the well nodal analysis, the tubing and IPR models were set up and benchmarked against historical production data for SS-25. In addition, reservoir pressures for SS-25 were obtained from the estimated reservoir pressure values for SS-5 [1].

Table 1: Summary of Key Point Target Conditions

Key Point Summary							
Key Point	KP #1	KP #2	KP #3	KP #4	KP #5	KP #6	KP #7
Date	Oct 24	Nov 13	Nov 15	Nov 18	Nov 24	Nov 25	Dec 22
Time	6:00	11:15	6:00	6:30	6:30	6:30	7:10
CHP (psia)	285	268	232	214	214	214	215
THP (psia)	1,715	1,541	1,622	1,612	1,653	1,666	1,230
Q (MMscf/D)	93.4	82.6	81.1	80.1	77.5	77.2	57.0
$R_{eservoir}$ (psia)	3,195	2,865	2,815	2,785	2,705	2,695	2,095

2.7 Model Calibration

The model was calibrated at the outset to achieve the targeted initial conditions corresponding to KP #2. Calibration of KP #2 was achieved by adjusting the relief conduit diameter (D_R), PI, 2 7/8 in. tubing ID, and 7 in. casing ID. Other parameters, including surface roughness of casing and tubing, reservoir fluid type, Condensate Gas Ratio, and Water-to-Gas Ratio (WGR) were also considered for the initial calibration of KP #2.

All parameters, except for reservoir pressure and conduit diameter, were maintained constant and used as assumptions for all other KPs after extensive model calibration for KP #2. This was crucial to maintain consistency of the physical system.

It should also be noted that the Well Nodal Analysis report [1] used a Forchheimer influx model to match known pressures and gas flow rates. This model was used in the kill simulations by calculating an equivalent linear PI for KP #2 conditions. The aim was to achieve a calibration with minimal adjustment of the equivalent linear PI if possible. This was an important step given that the reservoir pressure was assumed to be known and, therefore, consistent values for gas flow rate and FBHP could have only existed with similar PI values.

The final calibration parameters for KP #2 were adjusted as follows:

- The relief conduit ID, D_R was adjusted to 6.93 in.
- The Reservoir Linear PI was adjusted to 0.083 MMscf/D/psi. (The equivalent linear PI calculated from the Forchheimer model based on KP #1 conditions was 0.087 MMscf/D/psi.)
- The 2 7/8 in. tubing ID was adjusted to 2.525 in. (increased from the average measured ID of 2.473 in. to calibrate and match the observed pump pressure during Kill Attempt #2).
- The 7 in. casing ID was adjusted to 5.98 in. (reduced from the existing combination of 6.366/6.280/6.185 in.). The 7 in. casing ID required an adjustment to achieve annular friction pressure losses consistent with the tubing model values from the Well Nodal Analysis report [1] (which were benchmarked against historical production data for SS-25).

It should be noted that the magnitude of a relief conduit diameter had no direct quantitative meaning to the existing physical system. This parameter was used only to achieve the correct casing pressure and may have been considered a qualitative measurement of the resistance to fluid flow from the 7 in. casing leak and the formation. It was difficult to quantify or model the exact nature of flow in the formation once the

gas exited the casing leak. However, the impact of the gas exiting the leak, as far as the wellbore conditions were concerned, would have been merely to apply a resistance to flow and, consequently, an exit pressure at the leak. As long as the resistance was such that the resulting wellbore conditions remained consistent with the KP calibrations, the analysis accurately reflects conditions that were presented for each case.

Once the final calibration of KP #2 conditions was achieved, only the relief conduit diameter and reservoir pressure were adjusted for calibration of subsequent KPs, and all other calibration and input parameters remained constant. KP #2 was used for the calibration rather than KP #1 due to availability of data enabling calibration with respect to pump pressure during the kill attempt.

The reservoir pressure was assumed to be known at each subsequent KP, and given as an input, while the relief conduit diameter, D_R, was adjusted to achieve the specified CHP for each subsequent KP. Interestingly, within the range of D_R values required for this analysis, changes in the CHP (due to the changing D_R) produced no significant change in the FBHP and gas rate because changes in the CHP are almost directly offset by consequential changes to the annular friction within this range of D_R values and gas flow rates. Only substantial changes in D_R resulted in appreciable change in flow rates, and this effect quickly became nonlinear.

The KP model calibration summary (Table 2) summarizes the KP conditions calibrated in the Drillbench model[iii] and compares to the results from the tubing and IPR models used in the Well Nodal Analysis report [1]. These results also show the percentage error from the KP target conditions shown in the summary of KP target conditions (Table 1).

In general, a very good agreement exists between the Drillbench model and the tubing/IPR models. The software input parameters required the creation of KP conditions, i.e., P_{res} and D_R, which were the only input parameters changed within the Drillbench model (for KPs) other than KP #2. That is, the resulting CHP, THP, and gas flow rate are the parameters representing the physical system in the model. The agreement between the two models was necessary to further utilize Drillbench to assess the kill attempts.

Since the reservoir pressures were estimated from SS-5 values, the two wells are known to be in communication. Withdrawal from the field occurred during this time; therefore, more weight was put on the expected reservoir pressures than the reported THP field values [1]. Reducing the reservoir pressure necessarily reduces the FBHP and, therefore, the THP. As such, although KP #2 was calibrated accurately to the target THP value, subsequent KP THP values were allowed to reduce as a consequence of reducing the reservoir pressure.

Table 2: Key Point Model Calibration Summary

Key Point	Date	Model	Inputs		Outputs						
			D_R (in.)	$P_{reservoir}$ (psia)	CHP (psia)	Error (%)	THP (psia)	Error (%)	Rate (MMscf/D	Error (%)	FBHP (psia)
KP #1	Oct 24	Drillbench	6.93	3,195	282	–0.9%	1,718	0.2%	91.5	–2.0%	2,083
		Tubing/IPR	NA	3,195	285	0.0%	1,715	0.0%	93.4	0.0%	2,080
KP #2	Nov 13	Drillbench	6.93	2,865	267	–0.3%	1,535	–0.4%	82.8	0.2%	1,859
		Tubing/IPR	NA	2,865	268	0.0%	1,541	0.0%	82.6	0.0%	1,855
KP #3	Nov	Drillbench	7.38	2,815	231	–0.3%	1,506	–7.1%	81.3	0.2%	1,841

[iii] "Drillbench model" refers to the simulation model constructed in the *Drillbench Blowout Control* software.

Key Point	Date	Model	Inputs		Outputs						
			D_R (in.)	$P_{reservoir}$ (psia)	CHP (psia)	Error (%)	THP (psia)	Error (%)	Rate (MMscf/D	Error (%)	FBHP (psia)
	15	Tubing/IPR	NA	2,815	232	0.1%	1,530	–5.7%	81.1	0.0%	1,817
KP #4	Nov 18	Drillbench	7.64	2,785	214	0.1%	1,487	–7.7%	80.5	0.5%	1,819
		Tubing/IPR	NA	2,785	214	0.1%	1,484	–7.9%	80.1	0.0%	1,797
KP #5	Nov 24	Drillbench	7.58	2,705	214	0.1%	1,449	–12.3%	78.0	0.6%	1,769
		Tubing/IPR	NA	2,705	214	0.1%	1,438	–13.0%	77.5	0.0%	1,740
KP #6	Nov 25	Drillbench	7.58	2,695	214	0.1%	1,444	–13.3%	77.7	0.6%	1,762
		Tubing/IPR	NA	2,695	214	0.1%	1,434	–13.9%	77.2	0.0%	1,733
KP #7	Dec 22	Drillbench	7.06	2,095	215	0.1%	1,136	–7.6%	59.5	4.4%	1,382
		Tubing/IPR	NA	2,095	215	0.1%	1,092	–11.2%	57.0	0.0%	1,316

3 Simulation of SS-25 Kill Attempts

In this section, we present the results of the remaining six kill attempts, from Kill Attempt #2 on November 13, 2015, to Kill Attempt #7 on December 22, 2015.

For each kill attempt, the operational parameters representative of the kill attempt (pump rate, kill fluid density, and pumping duration) were modeled primarily to gain an understanding of the FBHP, influx rate, and likelihood of success throughout the process.

The gas flow rate and tubing pressure at each KP were based on the estimated reservoir pressure at the time of the kill attempt because all input parameters, other than the reservoir pressure and relief conduit diameter, D_R, were maintained constant at KP #2 values for all kill attempts, except for Kill Attempt #2. This is reasonable because only the reservoir pressure and the nature of flow in the formation are likely to have changed with time as the situation unfolded. As discussed in more detail in Section 2.7, within the range of D_R values required for this analysis, the varying D_R value had little impact on the gas flow rate from the reservoir. It was used predominantly to calibrate CHP for each set of KP conditions.

The summary of kill attempt operations (Table 3) shows a brief summary of each kill attempt. It summarizes whether the simulation suggested that the kill should have been successful and also shows the total pumped kill fluid volume, the maximum pump rate and pressure during the kill, and the kill fluids used throughout each attempt. The maximum pump pressure of 5,000 psi was exceeded in the simulations for Kill Attempts #5 and #6. However, the well-control company field reports show a maximum pressure of 4,167 psi [12] for Kill Attempt #5 and 4,173 psi [12] for Kill Attempt # 6. The reason for the discrepancy in pressure readings could not be fully reconciled from the available data. A possible explanation is that the addition of polymer (GeoZan) to the kill fluid acted as a friction reducer, causing the actual fluid friction pressure to be lower than calculated in the model. The Add Energy report [12] also discusses a discrepancy in the simulated pressure and the pressure observed.

Table 3 also shows that the model suggests that each of the subsequent kill attempts would not have succeeded, except for Kill Attempt #7. The simulation results for Kill Attempt #7, illustrated in Figure 9, shows that the FBHP exceeds the reservoir pressure and, therefore, the influx ceased, and the surface pressure remained within the equipment limits. Kill Attempts #5 and #6 are marked as not successful because the simulated pressure exceeded the successful kill criterion of a maximum pump pressure less than 5,000 psi. As noted later in the report, the actual results of Kill Attempts #5 and 6 resulted in the surface pressure at or near zero for a short period of time before the pressure increased.

The upcoming sections include a summary of each kill attempt, including specific job details, such as pumped volumes of each kill fluid and field observations during each attempt. In addition, graphical simulation results are illustrated in Figure 4 through Figure 9.

The simulated pump pressure and field data (where available) for tubing pressure[iv] are included in the simulation results shown in the figures. For the purposes of this analysis, the tubing head pressure during a dynamic kill attempt is considered synonymous with the pump pressure. That is, piping from the pump to the wellhead is not considered in these results because the distance from the pump to the wellhead is small compared to the length of the well downhole flow paths.

[iv] The field data for the tubing pressure are shown as series "Tubing Pressure (field)" in Figure 4 through Figure 9 and are from a SoCalGas data recording system that was set up to monitor and record well SS-25's pressures vs. time.

Table 3: Summary of Kill Attempt Operations

Kill Attempt #	Date	Simulated Kill Successful? Yes/No	Total Pumped Volume	Maximum Rate (bpm)	Reported Maximum Pump Pressure (psi)	Fluids Pumped
2	Nov 13	No	706	8	1,526	9.4 ppf $CaCl_2$,9.4 ppf Polymer Pill, Brine Water
3	Nov 15	No	239	8	1,645	9.4 ppf $CaCl_2$, 18 ppg Barite Pill
4	Nov 18	No	315	9	1,975	9.4 ppf $CaCl_2$, 18 ppg Barite Pill
5	Nov 24	No[a]	1,091	13	4,167	9.4 ppf GEO Zan Pill, Fresh Water, 18 ppg Barite Pill, 9.4 ppg $CaCl_2$
6	Nov 25	No[a]	1,116	13	4,164	9.4 ppg GEO Zan LCM Pill, Fresh Water, 9.4 ppg $CaCl_2$
7	Dec 22	Yes	332	5.8	1,157	15 ppg WBM, 15 ppg WBM with LCM

[a] The simulation estimated pressure exceeded the successful kill criteria of pump pressure of less than 5,000 psi, which is the reason for showing not successful.

3.1 Kill Attempt #2 on November 13, 2015

The following are details from Kill Attempt #2 field operations:

- 10 bbl of 9.4 ppg polymer pill
- 683 bbl of 9.4 ppg CaCl2
- 10 bbl of 9.4 ppg polymer pill
- 3 bbl of 8.6 ppg brine water
- Maximum pump rate 8 bpm
- Maximum pump pressure 1,526 psi

The following are field observations from Kill Attempt #2:

- Observed increased gas flow and liquid from fissures.
- Pony motor went down. Shut down pumping.
- Brine, oil, and gas flowing from fissures on pad.
- Well blew out in the conventional sense. Blowout vent opened 20 ft from wellbore, shooting debris 75 ft into the air.

As Figure 4 shows, the calculated pump pressure is in line with the field observations. However, the FBHP (solid red curve) never approaches the reservoir pressure; this implies that the well could not have been killed during Kill Attempt #2.

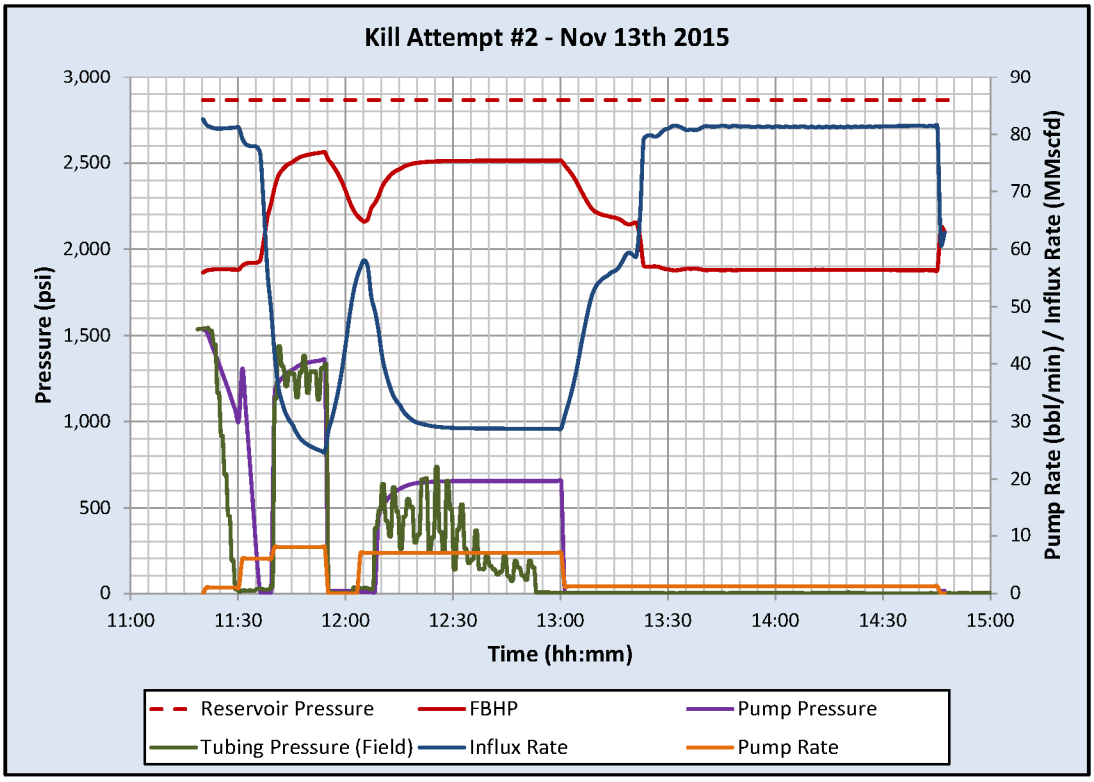

Figure 4: Simulation Results for Kill Attempt #2

3.2 Kill Attempt #3 on November 15, 2015

The following are details from Kill Attempt #3 field operations:

- 170 bbl of 9.4 ppg $CaCl_2$
- 19 bbl of 18 ppg barite pill
- 50 bbl of 9.4 ppg $CaCl_2$
- Maximum pump rate 8 bpm
- Maximum pump pressure 1,645 psi

The following are field observations from Kill Attempt #3:

- Gas rate from fissures increased, followed by oil and brine.
- Flow from fissures stopped briefly and then began to flow gas.

Figure 5 shows that the calculated pump pressure is generally in line with the field observations for tubing pressure. However, the FBHP never approaches the reservoir pressure; this implies that the well could not have been killed during Kill Attempt #3.

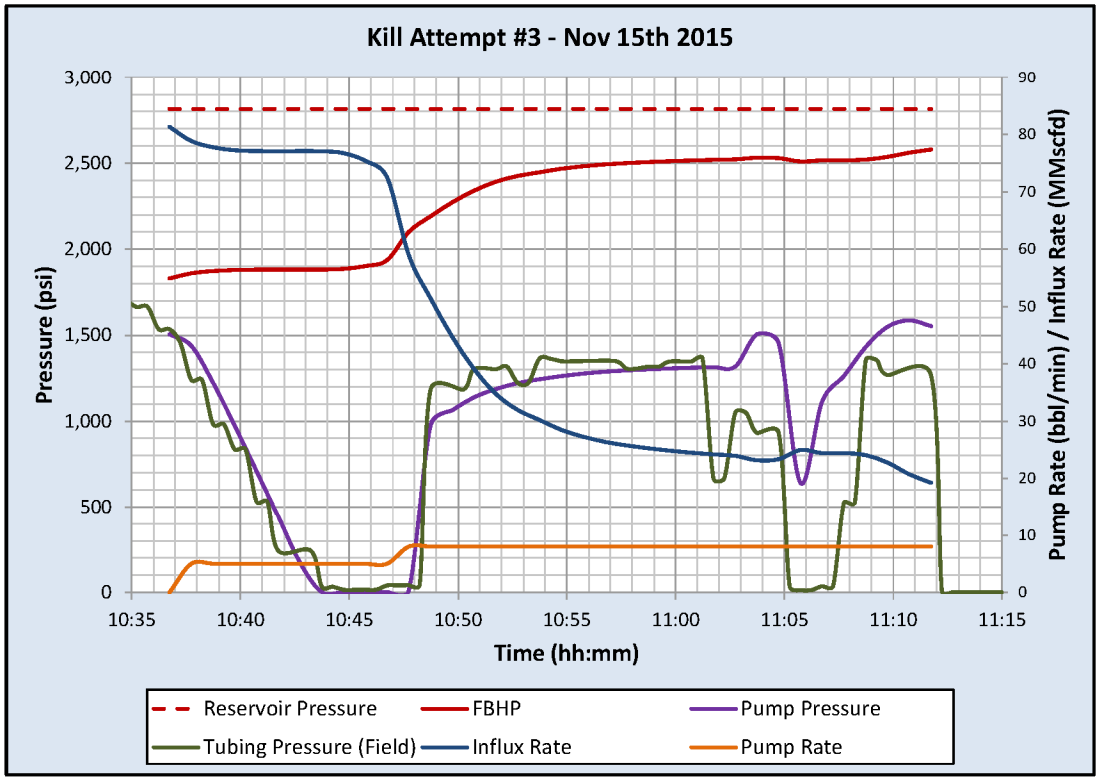

Figure 5: Simulation Results for Kill Attempt #3

3.3 Kill Attempt #4 on November 18, 2015

The following are details from Kill Attempt #4 field operations:

- 230 bbl of 9.4 ppg $CaCl_2$
- 35 bbl of 18 ppg barite pill
- 50 bbl of 9.4 ppg $CaCl_2$
- Maximum pump rate 9 bpm
- Maximum pump pressure 1,975 psi

The following are field observations from Kill Attempt #4:

- Gas rate from fissures increased. Observed oil and brine from fissure.
- Barite to surface was reported.

Figure 6 shows that the FBHP never approaches the reservoir pressure, which implies that the well could not have been killed during Kill Attempt #4.

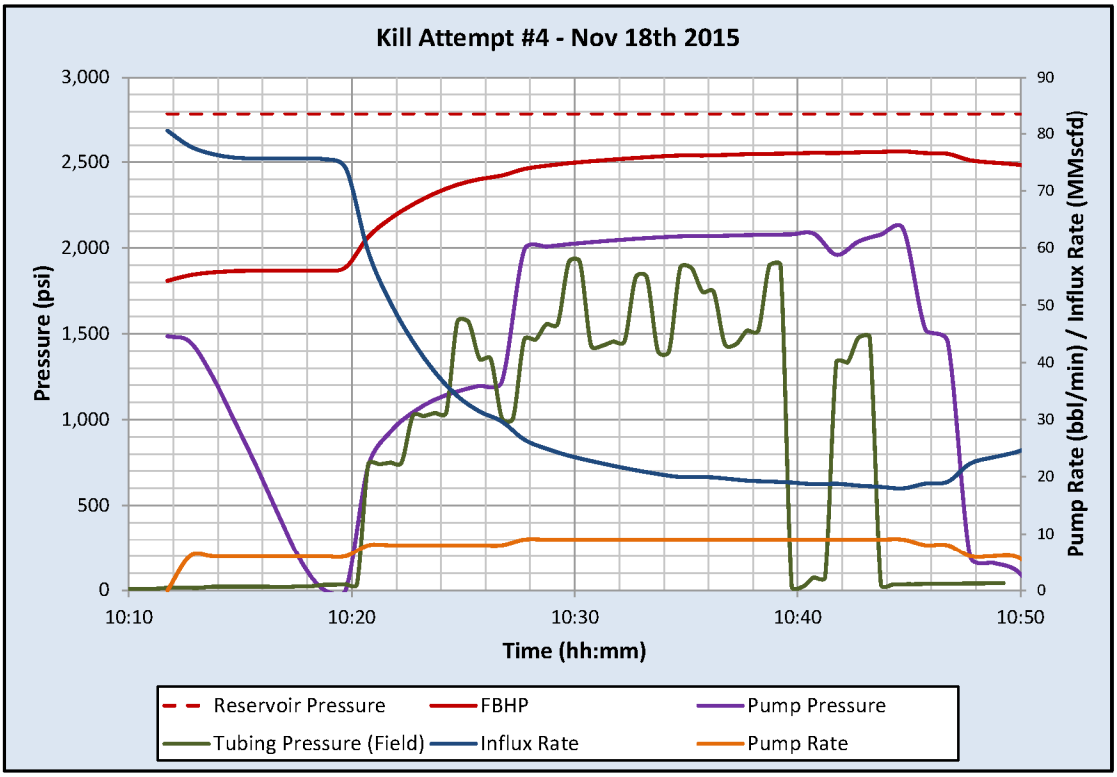

Figure 6: Simulation Results for Kill Attempt #4

3.4 Kill Attempt #5 on November 24, 2015

The following are details from Kill Attempt #5 field operations:

- 50 bbl of 9.4 ppg GEO Zan pill
- 950 bbl of fresh water
- 35 bbl of 18 ppg barite pill
- 56 bbl of 9.4 ppg $CaCl_2$
- Maximum pump rate 13 bpm
- Maximum pump pressure 4,167 psi (Reported value. Telemetry system shows maximum tubing pressure of approximately 3,600 psi)

The following are field observations from Kill Attempt #5:

- Gas rate from crater increased.
- Recovered 700 bbl of fluid from location.

Figure 7 shows that the calculated pump pressure is much greater than the pressure observed in the field for tubing pressure. It also shows that the influx flow goes to zero. However, given the high pump rates for this kill attempt and the discrepancy between calculated and reported pump pressures, this brings into question the reported rates. Section 4 shows that a slight decrease in pump rate from the reported values would have resulted in an unsuccessful kill as observed from the actual attempt.

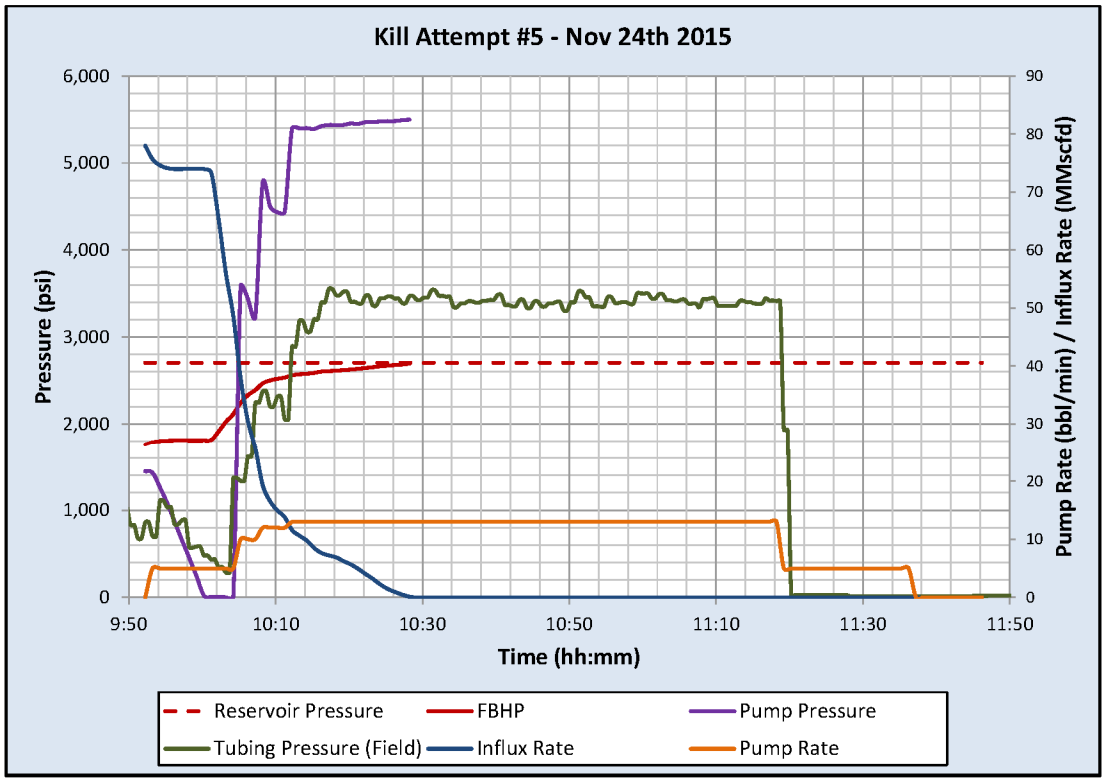

Figure 7: Simulation Results for Kill Attempt #5

3.5 Kill Attempt #6 on November 25, 2015

The following are details from Kill Attempt #6 field operations:

- 50 bbl of 9.4 ppg GEO Zan LCM pill
- 910 bbl of fresh water
- 100 bbl of 9.4 ppg GEO Zan LCM pill
- 56 bbl of 9.4 ppg $CaCl_2$
- Maximum pump rate 13 bpm
- Maximum pump pressure 4,164 psi

The following are field observations from Kill Attempt #6:

- Gas activity increased in crater.
- Water flow from crater increased.

- Flow line from 7 in. and tubing head broke. Nipple on wellhead broke. Pump line to 7 in. casing head broke.
- Cratering around the wellhead increased and damaged several casing valves.
- Tubing pressure went to zero, and then started increasing.

Figure 8 shows simulation results for Kill Attempt #6; at the time, field data for tubing pressure from the SoCalGas pressure monitoring system were not available. However, Halliburton's field data [13] were available for Kill Attempt #6 and are shown in the figure; the data suggest a pump pressure of approximately 4,200 psi during this attempt—significantly lower than calculated. However, given the high pump rates for this kill attempt and the discrepancy between the calculated and the reported pump pressures, this brings into question the reported rates. Section 4 shows that a slight decrease in pump rate from the reported values would have resulted in an unsuccessful kill. The simulation shows that the influx flow goes to zero and that a tubing pressure of zero was observed at the end of the job but increased after a period of time.

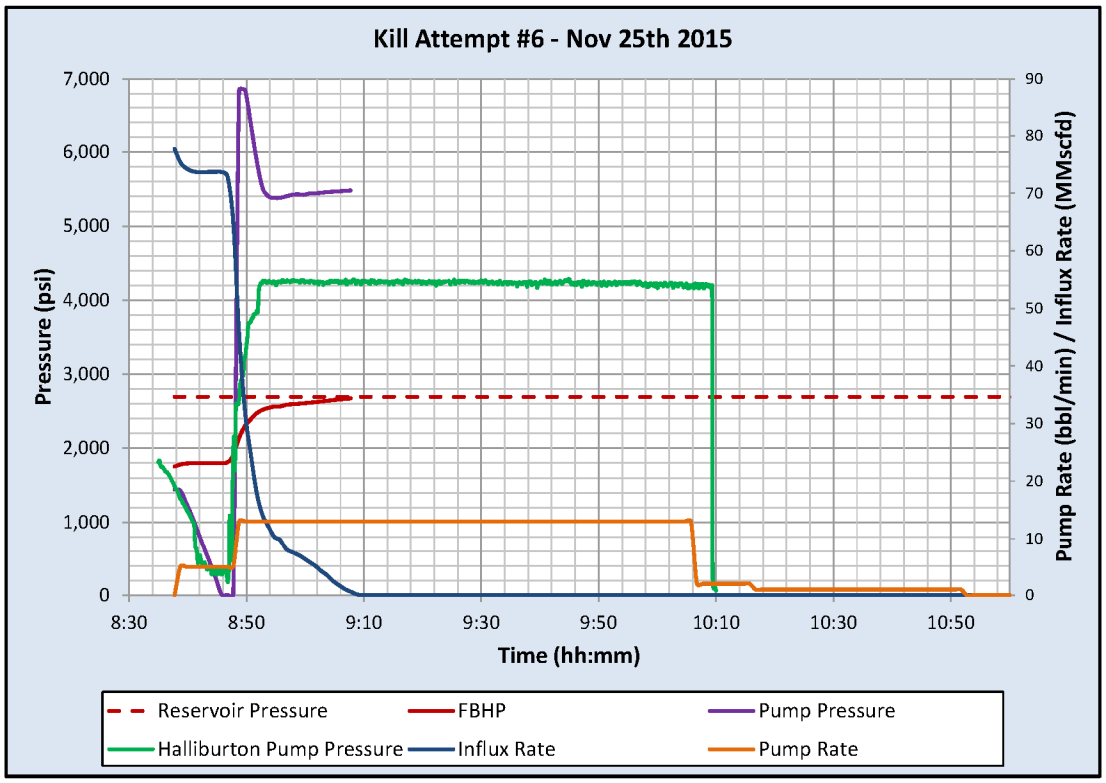

Figure 8: Simulation Results for Kill Attempt #6

3.6 Kill Attempt #7 on December 22, 2015

The following are details from Kill Attempt #7 field operations:

- 107 bbl of 15 ppg WBM
- 100 bbl of 15 ppg WBM with LCM
- 125 bbl of 15 ppg WBM
- Maximum pump rate 5.8 bpm

- Maximum pump pressure 1,157 psi (at start conditions)

The following are field observations from Kill Attempt #7:

- Mud, oil mist in crater.
- Liquid began to come out of the casing at surface.
- Shut down due to rocking of wellhead and unloading mud from crater.
- Pump line to top tee broke off due to movement of wellhead.
- Tubing pressure went to zero, and then started increasing.

The actual kill attempt was not successful, although the tubing pressure went to zero before increasing. Possible reasons why this kill attempt was not successful include shutting down pumping early due to the wellhead rocking or momentum of the kill fluid u-tubing in the tubing and annulus. The u-tubing may have caused an underbalanced condition and allowed the well to flow after the pumps had been shut down. Another possible reason why the kill attempt was not successful is not being able to keep the well filled.

The simulation results for Kill Attempt #7 (Figure 9) show a successful kill where the FHBP is equal to the reservoir pressure at the end of the simulation.

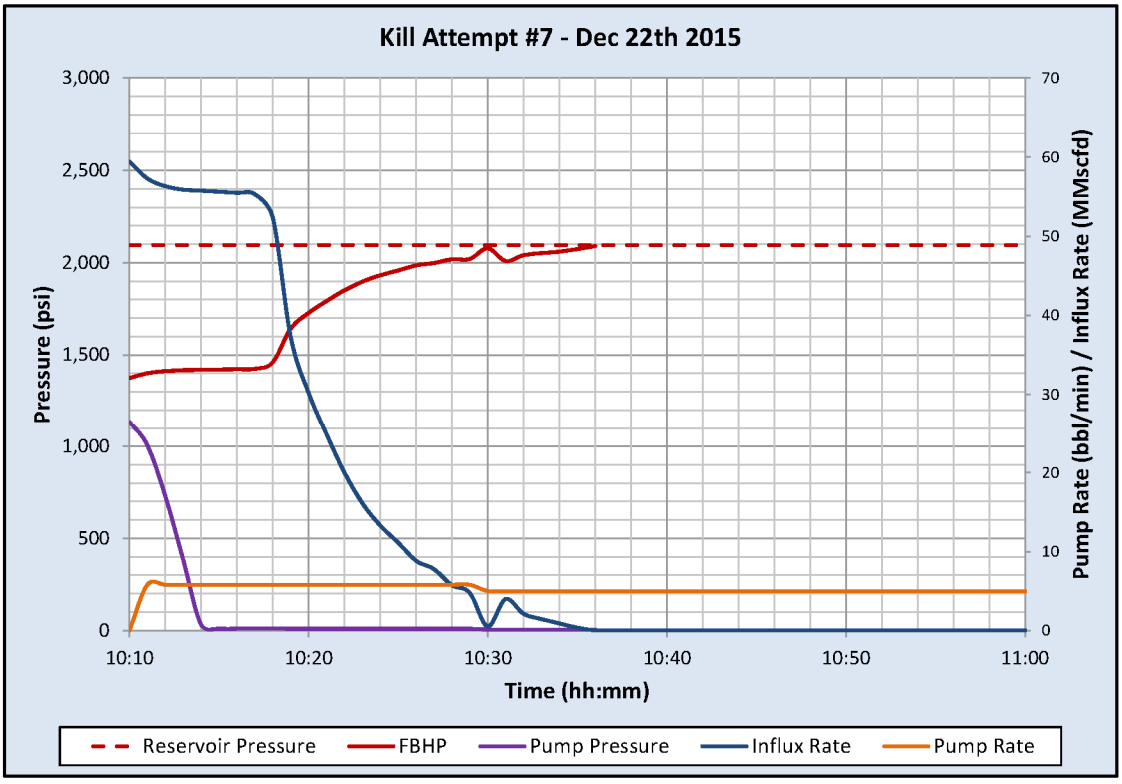

Figure 9: Simulation Results for Kill Attempt #7

4 Dynamic Kill Sensitivity Study

In this section we summarize the results from our evaluation of alternative dynamic kill scenarios. These scenarios initiated from the seven KPs that correspond to the initial conditions from which the kill attempts were executed. We performed sensitivity studies based on varying kill fluid densities and pump rates to show a range of pump rates for each fluid density.

The range of pump rates extended up to the minimum rate to achieve a successful kill, or if a successful kill could not be achieved, the rate at which the surface equipment pressure limit of 5,000 psi was exceeded.

The following three kill fluid densities were considered for each KP:

- 15 ppg fluid
- 12 ppg fluid
- Lower density fluid based on the following fluids used in the actual kill attempts:
  - 10 ppg fluid for Kill Point #1
  - 9.4 ppg $CaCl_2$ for Kill Point #2, #3 and #4
  - Fresh water for Kill Point #5, #6 and #7 (only 15 ppg fluid was used in actual Kill Attempt #7)

Table 4 through Table 10 show the results for the kill fluid density and pump rate sensitivity studies for the dynamic kill simulations initiated from KP #1 through KP #7, respectively.

For example, referring to Table 4, we can see that when considering a kill fluid of 10 ppg for a dynamic kill for Kill Point #1 (as attempted with Kill Attempt #1), it is not possible to achieve a successful kill without exceeding surface pressure limitations, whereas a successful kill can be achieved at pump rates of 10 bpm and 7 bpm with kill fluids of 12 ppg and 15 ppg, respectively. The highlighted rows indicate the successful kills in each of the tables.

Similarly, a successful dynamic kill is not possible without exceeding surface pressure limitations with a kill fluid of 9.4 ppg fluid (Table 5) as attempted with Kill Attempt #2. A successful kill can be achieved at pump rates of 9 bpm and 6 bpm with kill fluids of 12 ppg and 15 ppg kill fluids, respectively.

Looking broadly across the results from Table 4 to Table 10, we can note that achieving a successful dynamic kill for a comparable fluid density becomes easier with subsequent KPs. This is generally to be expected due to the reducing reservoir pressure that existed for successive kill attempt conditions.

Given that the lowest density fluid considered for Key Point #1 through Key Point #6 corresponds to the density fluid used in the actual kill attempts, it may be concluded that a successful kill was not possible with the attempted methods.

Another broad conclusion from observing these results is that a successful kill could be made with 12 ppg fluid across the entire range of KPs being considered. When using 15 ppg fluid, the dynamic kill method is more efficient. For each of the KP conditions, except KP #1, the pump pressure is on a vacuum when the influx ceases.

An important note when interpreting these results is that the maximum pump pressure reported in Table 4 through Table 10 is the pressure when the influx cessation first occurred or the initial tubing pressure, whichever is greater. Therefore, the pump pressures reported do not include any further increase in

pump pressure due to establishing a full annular column (from total depth to the leak zone at 892 ft) of kill fluid while balancing annular pressure with losses.

Modeling was used to determine combinations of fluid density, pump rates, and volumes of kill fluid that are likely to kill the well. In an actual well kill, the maximum FBHP obtainable after it reaches reservoir pressure would depend on other parameters, such as formation fracture and initiation pressures. This limitation on FBHP—not considered here—would be reflected in the pump pressure after the cessation of the initial influx. For this reason, the pump pressures reported in this analysis should be considered approximate. Keeping the well full of fluid after the well is killed is beyond the scope of kill modeling.

Table 4: Dynamic Kill Fluid Density and Pump Rate Sensitivity Results for KP #1

Alternative Kill Methods Results Summary										
Initial Conditions										
Key Point	Gas Rate (MMscf/D	Kill Fluid	Kill Rate (bpm)	Gas Flow Stopped? Yes/No	Time to Stop Gas Flow (min.)	Time for One Circulation (min.)	Time Less than One Circulation Yes/No	Surface Pressure when Influx Ceased (psia)	Maximum Pump Pressure (psi)	Successful Kill? Yes/No
KP #1	93	10 ppg	10	No	-	28	-	4,322	4,337	No
			11	Yes	41	25	No	5,372	5,387	No
			12	Yes	28	23	No	7,213	7,228	No
		12 ppg	7	No	-	39	-	1,109	1,733	No
			8	Yes	70	35	No	2,226	2,241	No
			9	Yes	38	31	No	3,224	3,239	No
			10	Yes	27	28	Yes	4,327	4,342	Yes
		15 ppg	5	No	-	55	-	Vacuum	1,733	No
			6	Yes	78	46	No	Vacuum	1,733	No
			7	Yes	38	39	Yes	628	1,733	Yes

Table 5: Dynamic Kill Fluid Density and Pump Rate Sensitivity Results for KP #2

Alternative Kill Methods Results Summary										
Initial Conditions										
Key Point	Gas Rate (MMscf/D	Kill Fluid	Kill Rate (bpm)	Gas Flow Stopped? Yes/No	Time to Stop Gas Flow (min.)	Time for One Circulation (min.)	Time Less than One Circulation Yes/No	Surface Pressure when Influx Ceased (psia)	Maximum Pump Pressure (psi)	Successful Kill? Yes/No
KP #2	83	9.4 ppg $CaCl_2$	10	No	-	28	-	3,130	3,145	No
			11	Yes	47	25	No	4,048	4,063	No
			12	Yes	30	23	No	5,013	5,028	No
		12 ppg	6	No	-	46	-	340	1,550	No
			7	Yes	73	39	No	1,432	1,550	No
			8	Yes	38	35	Yes	2,475	2,490	No
			9	Yes	27	31	Yes	3,629	3,644	Yes
		15 ppg	4	No	-	69	-	Vacuum	1,550	No
			5	Yes	164	55	No	Vacuum	1,550	No
			6	Yes	45	46	Yes	Vacuum	1,550	Yes

Table 6: Dynamic Kill Fluid Density and Pump Rate Sensitivity Results for KP #3

Alternative Kill Methods Results Summary										
Initial Conditions										
Key Point	Gas Rate (MMscf/D	Kill Fluid	Kill Rate (bpm)	Gas Flow Stopped? Yes/No	Time to Stop Gas Flow (min.)	Time for One Circulation (min.)	Time Less than One Circulation Yes/No	Surface Pressure when Influx Ceased (psia)	Maximum Pump Pressure (psi)	Successful Kill? Yes/No
KP #3	81	9.4 ppg $CaCl_2$	9	No	-	31	-	2,132	2,147	No
			10	Yes	101	28	No	3,100	3,115	No
			11	Yes	42	25	No	3,994	4,009	No
			12	Yes	28	23	No	4,974	4,989	No
			13	Yes	22	21	No	6,021	6,036	Yes
		12 ppg	6	No	-	46	-	305	1,521	No
			7	Yes	63	39	No	1,373	1,521	No
			8	Yes	35	35	Yes	2,416	2,431	Yes
		15 ppg	4	No	-	69	-	Vacuum	1,521	No
			5	Yes	110	55	No	Vacuum	1,521	No
			6	Yes	43	46	Yes	Vacuum	1,521	Yes

Table 7: Dynamic Kill Fluid Density and Pump Rate Sensitivity Results for KP #4

Alternative Kill Methods Results Summary										
Initial Conditions										
Key Point	Gas Rate (MMscf/D	Kill Fluid	Kill Rate (bpm)	Gas Flow Stopped? Yes/No	Time to Stop Gas Flow (min.)	Time for One Circulation (min.)	Time Less than One Circulation Yes/No	Surface Pressure when Influx Ceased (psia)	Maximum Pump Pressure (psi)	Successful Kill? Yes/No
KP #4	81	9.4 ppg $CaCl_2$	9	No	-	31	-	2,112	2,127	No
			10	Yes	84	28	No	3,071	3,086	No
			11	Yes	40	25	No	3,973	3,988	No
			12	Yes	27	23	No	4,936	4,951	No
			13	Yes	22	21	No	5,998	6,013	No
		12 ppg	6	No	-	46	-	314	1,502	No
			7	Yes	59	39	No	1,345	1,502	No
			8	Yes	35	35	Yes	2,395	2,410	Yes
		15 ppg	4	No	-	69	-	Vacuum	1,502	No
			5	Yes	98	55	No	Vacuum	1,502	No
			6	Yes	42	46	Yes	Vacuum	1,502	Yes

Table 8: Dynamic Kill Fluid Density and Pump Rate Sensitivity Results for KP #5

Alternative Kill Methods Results Summary										
Initial Conditions										
Key Point	Gas Rate (MMscf/D	Kill Fluid	Kill Rate (bpm)	Gas Flow Stopped? Yes/No	Time to Stop Gas Flow (min.)	Time for One Circulation (min.)	Time Less than One Circulation Yes/No	Pump Pressure when Influx Ceased (psia)	Maximum Pump Pressure (psi)	Successful Kill? Yes/No
KP #5	78	Fresh Water	10	No	-	28	-	2,795	2,810	No
			11	Yes	154	25	No	3,709	3,724	No
			12	Yes	45	23	No	4,609	4,624	No
			13	Yes	29	21	No	5,541	5,556	No
		12 ppg	6	No	-	46	-	250	1,464	No
			7	Yes	49	39	No	1,270	1,464	No
			8	Yes	32	35	Yes	2,314	2,329	Yes
		15 ppg	4	No	-	69	-	Vacuum	1,464	No
			5	Yes	75	55	No	Vacuum	1,464	No
			6	Yes	38	46	Yes	Vacuum	1,464	Yes

Table 9: Dynamic Kill Fluid Density and Pump Rate Sensitivity Results for KP #6

Alternative Kill Methods Results Summary										
Initial Conditions										
Key Point	Gas Rate (MMscf/D	Kill Fluid	Kill Rate (bpm)	Gas Flow Stopped? Yes/No	Time to Stop Gas Flow (min.)	Time for One Circulation (min.)	Time Less than One Circulation Yes/No	Pump Pressure when Influx Ceased (psia)	Maximum Pump Pressure (psi)	Successful Kill? Yes/No
KP #6	78	Fresh Water	10	No	-	28	-	2,759	2,774	No
			11	Yes	126	25	No	3,698	3,713	No
			12	Yes	44	23	No	4,565	4,580	No
			13	Yes	39	21	No	5,498	5,513	No
		12 ppg	6	No	-	46	-	232	1,459	No
			7	Yes	49	39	No	1,261	1,459	No
			8	Yes	32	35	Yes	2,303	2,318	Yes
		15 ppg	4	No	-	69	-	Vacuum	1,459	No
			5	Yes	73	55	No	Vacuum	1,459	No
			6	Yes	38	46	Yes	Vacuum	1,459	Yes

Table 10: Dynamic Kill Fluid Density and Pump Rate Sensitivity Results for KP #7

Alternative Kill Methods Results Summary										
Initial Conditions										
Key Point	Gas Rate (MMscf/D	Kill Fluid	Kill Rate (bpm)	Gas Flow Stopped? Yes/No	Time to Stop Gas Flow (min.)	Time for One Circulation (min.)	Time Less than One Circulation Yes/No	Surface Pressure when Influx Ceased (psia)	Maximum Pump Pressure (psi)	Successful Kill? Yes/No
KP #7	60	Fresh Water	7	No	-	39	-	246	1,151	No
			8	Yes	63	35	No	939	1,151	No
			9	Yes	35	31	No	1,586	1,601	No
			10	Yes	25	28	Yes	2,309	2,324	Yes
		12 ppg	4	No	-	69	-	Vacuum	1,151	No
			5	Yes	56	55	No	Vacuum	1,151	No
			6	Yes	34	46	Yes	Vacuum	1,151	Yes
		15 ppg	3	No	-	92	-	Vacuum	1,151	No
			4	Yes	94	69	No	Vacuum	1,151	No
			5	Yes	33	55	Yes	Vacuum	1,151	Yes

5 Dynamic Kill with Hypothetical Low Gas Flow Rate

This section presents the results for dynamic kill simulations from a scenario that assumes a hypothetical low gas flow rate representing the reservoir conditions presumably assumed for the kill attempts. These conditions were achieved by implementing a Forchheimer influx model with a reservoir pressure of 2,400 psia and an absolute open flow of 30 MMscf/D (Figure 10).

It should be noted that this scenario is considered physically inadmissible, and is, therefore, hypothetical—the pressure conditions (THP and CHP) at the time of the kill attempts could not have existed given the assumed physical system being modeled. For these hypothetical reservoir conditions and with the assumed physical system, the THP and CHP at the KPs would have been significantly lower.

When applied to KPs #1 and #2, a resulting gas flow rate of 28 MMscf/D (referred to as approximately 30 MMscf/D or AOF 30 MMscf/D throughout this report) was calculated, rather than the most likely rates of 93 MMscf/D and 83 MMscf/D, which are presumed to be the actual flow rates at KPs #1 and #2, respectively.

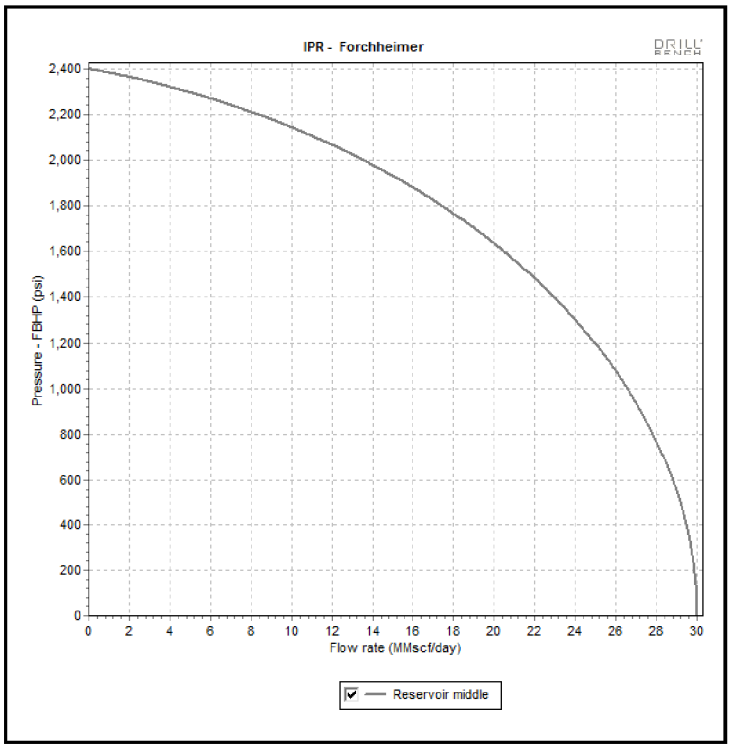

Figure 10: Forchheimer IPR Curve Used to Represent a Hypothetical Low Gas Flow Rate Scenario

Figure 11 shows the kill simulation results for the hypothetical low gas rate case; the FBHP does not approach the reservoir pressure, indicating that the kill attempt would have been unsuccessful even at the low gas rate.

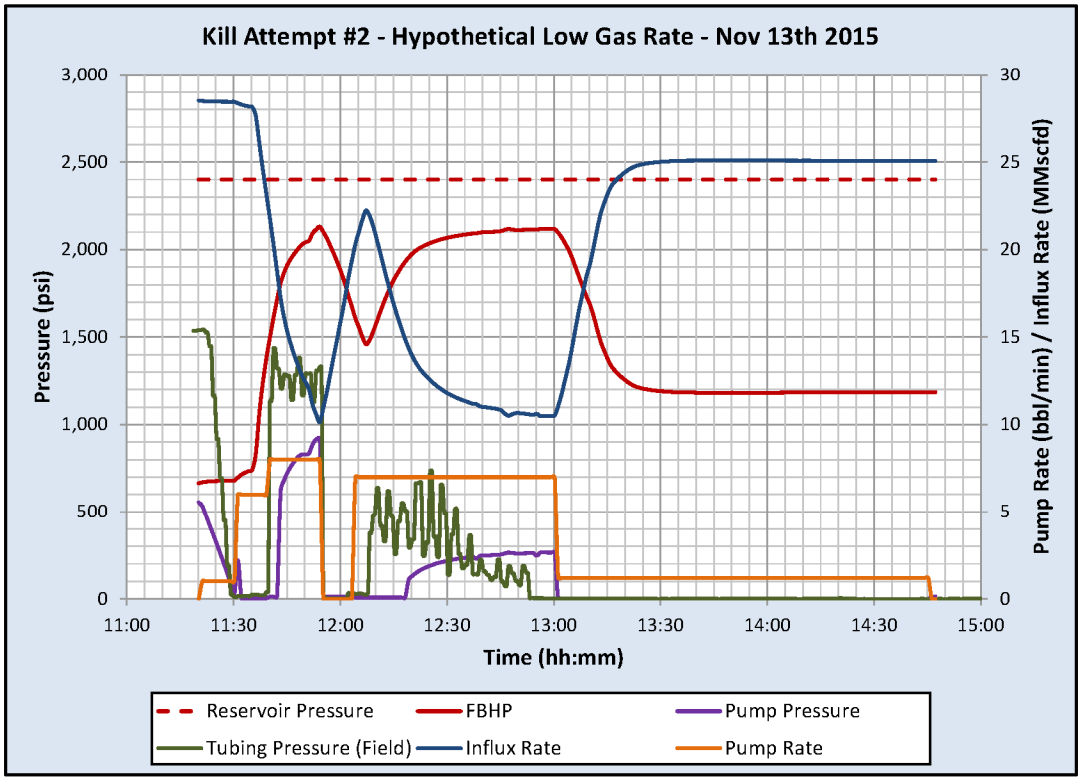

Figure 11: Simulation Results for Kill Attempt #2 Pumping Schedule Applied to the Hypothetical Low Gas Rate Scenario

Sensitivity studies based on varying kill fluid densities and pump rates were performed to show a range of pump rates for each fluid density. The range of pump rates presented extends up to the minimum rate needed to achieve a successful kill, or if a successful kill cannot be achieved, the range of pump rates extends up to the rate at which the surface equipment pressure limit of 5,000 psi is exceeded.

Table 11 and Table 12 show the results for dynamic kill sensitivity studies where the hypothetical low gas rate scenario is assumed for KPs #1 and #2, respectively. Successful kills are theoretically possible as indicated by the highlighted rows in the tables. The background of the table is shaded to differentiate the hypothetical low gas flow rate results from the tables in Section 4 that show results for kill simulations with the expected gas flow rates.

As expected, this scenario represents conditions that make killing the well easier. An observation from these results is that a successful kill is shown to be possible for the low-density fluids considered (similar to the fluids used in Kill Attempts #1 and #2).

Table 11: Dynamic Kill Results for KP #1 with a Hypothetical Low Gas Flow Rate

Alternative Kill Methods Results Summary									
Initial Conditions									
Key Point	Gas Rate (MMscf/D	Kill Fluid	Kill Rate (bpm)	Gas Flow Stopped? Yes/No	Time to Stop Gas Flow (min.)	Time for One Circulation (min.)	Time Less than One Circulation Yes/No	Surface Pressure When Influx Ceased (psia)	Successful Kill? Yes/No
Low Gas Rate KP #1	AOF 30	10 ppg	6	No	-	46	-	92	No
			7	Yes	50	39	No	995	No
			8	Yes	33	35	Yes	1,741	Yes

Table 12: Dynamic Kill Results for KP #2 with a Hypothetical Low Gas Flow Rate

Alternative Kill Methods Results Summary									
Initial Conditions									
Key Point	Gas Rate (MMscf/D	Kill Fluid	Kill Rate (bpm)	Gas Flow Stopped? Yes/No	Time to Stop Gas Flow (min.)	Time for One Circulation (min.)	Time Less than One Circulation Yes/No	Pump Pressure when Influx Ceased (psia)	Successful Kill? Yes/No
Low Gas Rate KP #2	AOF 30	9.4 ppg $CaCl_2$	7	No	-	39	-	265	No
			8	Yes	57	35	No	1,140	No
			9	Yes	35	31	No	1,879	No
			10	Yes	26	28	Yes	2,703	Yes
		12 ppg	4	No	-	69	-	Vacuum	No
			5	Yes	106	55	No	Vacuum	No
			6	Yes	46	46	Yes	42	Yes
		15 ppg	3	No	-	92	-	Vacuum	No
			4	Yes	81	69	No	Vacuum	No
			5	Yes	41	55	Yes	Vacuum	Yes

6 Dynamic Kill with a Leak Depth of 440 ft

This section shows the simulation results for an assumed leak depth of 440 ft as hypothesized in a report released by the Department of Energy [2]. The well conditions were adjusted for the change in leak depth for the Kill Attempt #4 conditions assumed for this analysis.

Figure 12 shows the model results for a leak at 440 ft. The results for a leak at 440 ft reveal slightly higher FBHP than for a leak at 892 ft because of the longer column of fluid in the well. However, at the assumed pump rate of 9 bpm, the FBHP never reaches the reservoir pressure, and therefore, the kill is not successful for a leak depth of 440 ft.

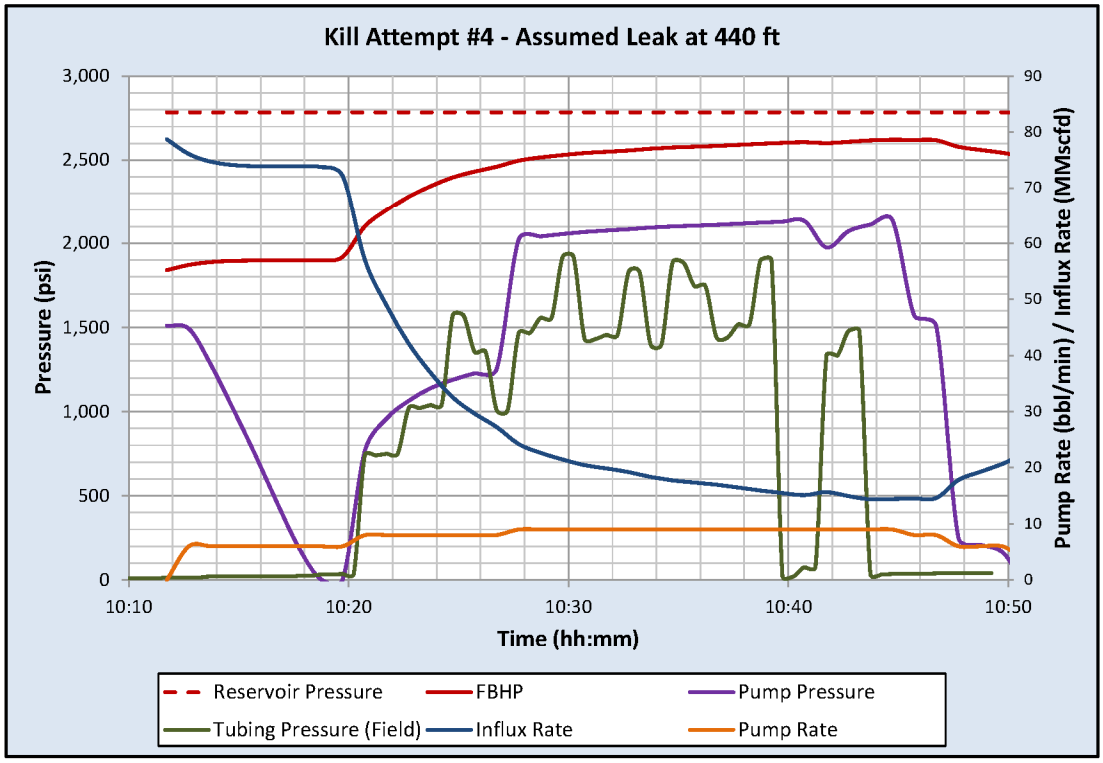

Figure 12: Simulation Results for Kill Attempt #4 at a Leak at 440 ft

6.1 Kill Attempt #4 for a Leak at 440 ft

The following are the assumed fluids and pump rate:

- 230 bbl of 9.4 ppg $CaCl_2$
- 35 bbl of 18 ppg barite pill
- 50 bbl of 9.4 ppg $CaCl_2$
- Maximum pump rate 9 bpm

6.2 Dynamic Kill with Leak at 440 ft

Table 13 show the results for dynamic kill sensitivity with an assumed leak depth at 440 ft. Successful kills were theoretically possible as indicated by the highlighted rows in the table. The background of the table is shaded to differentiate the assumed case results from the tables in Section 4 that show results for kill simulations with the expected gas flow rates. The results are very similar to the kill results shown in Table 7 for the same well conditions at a leak depth of 892 ft.

Table 13: Dynamic Kill Results for KP #4 with a Leak Depth at 440 ft

Alternative Kill Methods Results Summary									
Initial Conditions		Kill Fluid	Kill Rate (bpm)	Gas Flow Stopped? Yes/No	Time to Stop Gas Flow (min.)	Time for One Circulation (min.)	Time Less than One Circulation Yes/No	Pump Pressure when Influx Ceased (psia)	Successful Kill? Yes/No
Key Point	Gas Rate (MMscf/D								
KP #4 with Leak Depth of 440 ft	78.7	9.4 ppg $CaCl_2$	9	No	-	31	-	2,197	No
			10	Yes	44	28	No	3,078	No
			11	Yes	30	25	No	3,968	No
			12	Yes	23	23	Yes	4,946	Yes
			13	Yes	19	21	Yes	6,003	No
		12 ppg	6	No	-	46	-	360	No
			7	Yes	44	39	No	1,354	No
			8	Yes	31	35	Yes	2,398	Yes
		15 ppg	4	No	-	69	-	Vacuum	No
			5	Yes	74	55	No	Vacuum	No
			6	Yes	37	46	Yes	Vacuum	Yes

7 Discussion of the Kill Attempts

This section discusses the individual kill attempts with a focus on the design and execution of each attempt. We reviewed the available daily reports[v] to understand the field operations and the results for each kill attempt. Multiple reports by different writers for the same operations can result in minor discrepancies among the reports. Blade made an effort to ignore the minor discrepancies and focus on the bigger picture to understand what was done and what could have been done better. Based on the operations, we tried to draw conclusions as to what the results were and what was learned. The experience acquired from each attempt should have led to modifications and improvements for subsequent attempts.

7.1 General Comments

According to the daily reports for Kill Attempt #1, SoCalGas and Halliburton pumped down the tubing, which plugged, and then pumped down the 7 in. x 2 7/8 in. annulus. A well-control company was contracted to lead future well control operations following this kill attempt.

From reviewing the records, it is not clear what gas flow rate was used by the well-control company and SoCalGas in the planning of the kill operations for SS-25. SoCalGas responded to a DOGGR District Information Request, which asked for information related to the kill attempt modeling, by sending an IPR curve for approximately 30 MMscf/D [14]. The information request implied that Lawrence Berkley National Laboratories (LNBL) was modeling the kill attempts for DOGGR, and DOGGR wanted LNBL to use the same data that Halliburton was using. However, analyses by Add Energy [12] and then by Blade [1] estimate that the initial flow rate for SS-25 was in the range of 80 to 93 MMscf/D, respectively. The difference in the gas flow rate from 30 to 80 MMscf/D is significant when planning a well kill operation. SoCalGas provided SS-25 Flow Test Data to Blade showing historical well flow rates in excess of 80 MMscf/D [15]. The cause for this flow rate discrepancy is unclear; however, knowing the gas flow rate is crucial for kill planning.

Field experience shows that friction limits the pump rates to a sustained 12–14 bpm through 2 7/8 in. tubing, regardless of fluid density or other properties. This rate can be higher when filling the tubing and annulus during the early part of a kill attempt because of the lack of friction pressure in the gas filled pipe.

A well kill best practice is to maximize the use of the pump capacity, mud density, and fluid loss control possible at the first opportunity without resorting to exotic materials or methods given the severity of the surface leak (approximately 93 MMscf/D) and impact to the environment. Doing everything possible on the first attempt is better than doing *just enough* to kill a well. It is understood that at the time of the first kill attempts, there were many unknowns with respect to the depth of the leak and the condition of the tubing and casing.

No records of well kill modeling have been located for Kill Attempts #2–6. Blade received modeling results apparently for Kill Attempt #7 that used 25 MMscf/D as the gas flow rate [16]. An email attachment states the influx stopped after pumping 300 bbl of 15 ppg fluid [17]. Blade had estimated that the gas flow rate was 57 MMscf/D on December 22, 2015. The results of Blade's modeling indicate that a successful well kill

[v] Available reports included SoCalGas' daily reports [21], DOGGR's daily reports [30], and the well-control company daily reports documented in the Add Energy simulation report [12].

could have been achieved with 15 ppg fluid at 5 bpm. It is not clear if the modeling included a fluid density and pump rate safety factor to allow for uncertainty in the gas flow assumption.

Blade also received documents that appear to be modeling results, which are not dated. One document shows a flow rate of 24 MMscf/D and a statement:

> "The influx stops after pumping 300 bbl of 15.0 ppg fluid or at the end of pumping Diaseal." [18]

The second document shows a gas flow rate of 15 MMscf/D, AOF of 25 MMscf/D and a statement:

> "Snapshot of pumping 15.0 ppg WBM at the rate of 3 bpm." [19]

Modeling shows that a gas flow of 30 MMscf/D could not have been killed by pumping low-density clear fluids at the modest displacement rates of 8–9 bpm used in the kill attempts. Modeling goes on to show that the well could have been killed with 15 ppg mud at 7 bpm at a flow rate of 93 MMscf/D.

The use of clear solids-free kill fluids (brine and fresh water) after Kill Attempt #2 is questionable because fluids with low viscosity are poor for reducing gas migration. The results of Kill Attempt #2 indicated a shallow leak when gas broached the surface. Perhaps there was concern that high density and high viscosity kill mud would damage the formation. There are no records or information available that address the reasons for the decisions made.

At that point, the focus should have been on analyzing which materials, i.e., the best formation damaging material available, should be used to successfully kill the well and stop the gas leak at surface. High density drilling fluid (mud) had the best chance to stop the gas flow—mud's high viscosity minimizes gas migration to keep the well dead until it can be permanently sealed.

7.1.1 Summary of the SS-25 Kill Events

Table 14 shows a tabular summary of the SS-25 Kill Events.

Table 14: SS-25 Summary of Kill Events

Date	Event Description from the Reference	Reference
10/23/2015	Normal operation CP 2,700 psi. TP 2,700 psi. SCP should be 0 psi. Normal operates on casing injection and casing WD. It may be operated on dual flow. Well on injection - heard noise in wellhead.	[20]
10/23/15 4:00 PM	CP 270 psi. TP 1,700 psi. SCP 140 psi. Ops noticed leaking annulus on well. They responded by closing 2 in. surface annulus valve and noticed 140 psi on gauge. When Ops closed injection header valve, the WKM SSV on casing closed almost immediately by low pressure pilot (setpoint is 270–300 psi). It was at that time Ops noticed sound of gas flow in wellhead.	[20]
10/23/15 4:10 PM	CP 270 psi. TP 1,700 psi. SCP 140 psi. Well shut in by Ops. We initially suspected an up/down wellhead seal leak between the 7 in. casing and the 11 3/4 in. surface casing. Called Cameron.	[20]
10/24/15 6:00 AM	CP 270 psi. TP 1,700 psi. SCP 140 psi. Cameron began repairing wellhead seals. Cameron initially tested both seals to 1,200 psi, both bled down to 600 psi. They then pumped 14 tubes of plastic into primary seal cavity.	[20]

Date	Event Description from the Reference	Reference
10/24/15 12:27 PM	CP 290 psi. TP 1,700 psi. SCP 140 psi. Kill Attempt 1 Halliburton circulated down tubing. Pumped 11.8 bbl of 10 ppg polymer brine. Pressure tubing rose to 3,500 psi. Shut down. 7 in. casing pressure remained at 290 psi. Surface casing pressure remained at 140 psi. Monitored tubing pressure for 20 minutes. Tubing pressure bled to 2,700 psi.	[20]
10/24/15 1:20 PM	Shut well in with 2,700 psi TP.	[20]
10/24/15 1:30 PM	TP 50 psi. Put well on tubing flow to frac tank for few minutes and bled tubing down to 50 psi.	[20]
10/24/15 2:00 PM	CP 290 psi. TP 2,700 psi. Decided to pump and bleed down 7 in. casing to fill casing using 8.6 ppg lease water.	[20]
10/24/15 2:07 PM	CP 290 psi. TP 50 psi. SCP 140 psi. Halliburton began pumping 8.6 ppg lease water down 7 in. casing. Started pumping 8.6 ppg lease water at 1.5 bpm. At 20 bbl increased rate to 2.5 bpm, at 33 bbl increased to 3.5 bpm. Began monitoring location for gas. Inspected wellhead, noticed noise and vibration had subsided. Continued pumping. At 89 bbl, gas broke through surface at location and surrounding location. Continued monitoring.	[20]
10/24/15 2:30 PM	CP 400 psi. When we shut down after 89 bbl and gas came to surface, the 7 in. CP increased to 400 psi.	[20]
11/13/2015	Kill Attempt 2 not successful	[21]
11/15/2015	Kill Attempt 3 not successful	[21]
11/18/2015	Kill Attempt 4 not successful	[21]
11/24/2015	Kill Attempt 5 not successful	[21]
11/25/2015	Kill Attempt 6 not successful	[21]
12/22/2015	Kill Attempt 7 not successful	[21]
02/11/2016	Relief well Porter 39A successful kill. SS-25 sealed.	[22]

7.2 Kill Attempt #1 October 24, 2015

The first attempt to bring the well under control was performed by SoCalGas using Halliburton's pumping equipment.

Two Halliburton Services pump trucks with total pump capacity of 1,300 hydraulic horsepower (HHP) arrived on the location and rigged up to pump 10 ppg xanthan gum (XC) polymer fluid down the tubing. After pumping 11.8 bbl at a low rate, the injection pressure rose rapidly to 3,034 psi. It was later determined that the fluid formed a plug inside the 2 7/8 in. production tubing. After the plug was removed, a temperature survey shows a minimum temperature of <18°F around 450 ft [23]. The cause of

the low-temperature condition is discussed in a separate report *Analysis of the Post-Failure Gas Pathways and Temperature Anomalies at the SS-25 Site* [24].

Since injection down the production tubing was no longer possible, lease water was pumped into the 7 in. x 2 7/8 in. annulus—an attempted Pump and Bleed operation. After pumping 89 bbl into the annulus, gas broke through at surface from cracks in the ground. Pumping was shut down.

This kill attempt was a reasonable response because the extent of the failure on SS-25 was unknown. Similar well kill operations had been carried out in the past on wells with casing leaks, namely Frew 3 in 1984 and Fernando Fee (FF) 34A in 1990. The two wells were killed successfully by pumping fluid down the tubing. Later analysis of the SS-25 casing failure and gas flow rates showed that there were significant differences in the SS-25's conditions when compared to Frew 3 and FF-34A's conditions. Additional details are available in another document [25].

Gas broaching to surface from cracks in the ground following Kill Attempt #1 indicate that SS-25 had serious problems and that a shallow casing leak was likely to exist.

After Kill Attempt #1 had failed, the well-control company was contracted to provide technical and operational support for well kill operations. Before attempting the next kill attempt, the well-control company assessed the surface condition of the well and then:

1. Rearranged the surface lines and plumbing and tested the tubing hanger.
2. Performed diagnostics with slick line by attempting to determine the nature of the bridge in the tubing. The plug was tagged at 456 ft; the following day it was tagged at 36 ft.
3. Mobilized a continuous coiled tubing unit and washed out the plug near surface to around 482 ft.
4. Attempted to relieve some surface pressures by flowing the well.
5. Ran a slick-line gauge ring to locate the seating nipple at 8,425 ft.
6. Ran a memory log with a spinner survey and temperature, pressure, and gamma ray (GR) sensors to 8,425 ft.
7. Ran an electric line noise and temperature tool to 8,435 ft and attempted to run a gyro survey that was not successful.
8. Set an EZSV (easy drill sliding valve) bridge plug at 8,393 ft.
9. Perforated four holes at 8,387–8,391 ft in the tubing.

After our review of the reports, it is not clear to us why a bridge plug was set. The bridge plug and perforations added a downhole restriction in the tubing that interfered with the flow path of the kill fluid and added to the pumping friction pressure. The tubing was perforated just above the plug to re-open the flow path for kill fluids. Section 7.9 includes a discussion about the bridge plug.

7.3 Kill Attempt #2 November 13, 2015

Kill Attempt #2 consisted of pumping 9.4 ppg fluid at rates up to 8 bpm down the production tubing, followed by pumping several junk shots consisting of golf balls and other material with 9.4 ppg brine down the 7 in. x 2 7/8 in. annulus. Section 3.1 includes the details of the fluids pumped.

The reports show no indications that this attempt resulted in a near-kill. The surface annulus pressure at the end of the attempt was within approximately 50 psi of initial pressure (192 psi vs. 253 psi).

A Drillbench analysis shows that Kill Attempt #2 would not have killed 30 MMscf/D and certainly not 83 MMscf/D, the estimated gas rate. The engineering parameters used to design the effort are unclear.

Sufficient pumping capacity of 1,600 HHP was available on site and 295 HHP (18%) were used for the pumping operations. As Table 5 shows, a 12 ppg fluid at a pump rate of 9 bpm should have killed the well. The maximum pump pressure was 1,526 psi. Such a kill attempt, perhaps with a bit higher density and a bit higher flow rate, could have killed this well.

Kill Attempt #3 was virtually the same as Kill Attempt #2.

7.4 Kill Attempt #3 November 15, 2015

This kill attempt consisted of 170 bbl of 9.4 ppg brine followed by 19 bbl of 18.0 ppg barite pill. These fluids were all pumped at up to 8 bpm and displaced with 9.4 ppg fluid but failed to kill the well. The details of the fluids pumped are included in Section 3.2.

Sufficient pumping capacity of 1,600 HHP was available on site, and 320 HHP (20%) were used for the pumping operations.

The use of a barite pill is questionable. The purpose of a barite pill is to settle and create a solid plug of barite. Barite cannot settle if the well is flowing. A barite pill can be effective if gas flow has been stopped for some time, around two to five hours, while the barite settles to form a solid plug [26]. However, the use of a small barite pill here, in this case 19 bbl, was useless, unless the well flow was killed by injecting the 9.4 ppg brine. Brine injection at 8 bpm could not kill the gas flow—this was proven by Kill Attempt #2.

The estimated flow rate on November 15, 2015, was 81 MMscf/D. The surface pressure limitation would not allow sufficient injection rate with 9.4 ppg brine. This is shown in Table 6 along with modeling results for various fluid densities and pump rates that would have killed the well while flowing at 81 MMscf/D.

However, for the current conditions, the modeling shows that the well could have been killed with 15.0 ppg mud at 6 bpm or with 12.0 ppg mud at 8 bpm. The well could have been killed without exceeding the safe surface pressure limitations if either 12.0 ppg or 15.0 ppg mud had been used.

There is little indication that Kill Attempt #3 was effective. When the 7 in. x 2 7/8 in. annulus pressure dropped from 217 psi to 107 psi, there was a brief respite from the flow in the crater, but the annulus pressure returned to 205 psi in an hour, and the flow in the crater resumed.

7.5 Kill Attempt #4 November 18, 2015

This kill attempt was similar to Kill Attempt #3. The job consisted of pumping 9.4 ppg brine, 35 bbl of an 18.0 ppg barite pill, followed by additional 9.4 ppg brine. The maximum reported pressure while pumping was 1,975 psi. Section 3.3 includes the details of the fluids pumped.

Much like the previous two kill attempts, this attempt produced no indications that the well was being brought under control. A barite pill was used again, but its purpose is unclear because there was no indication that the well flow ever ceased; therefore, the pill had no opportunity to settle.

Sufficient pumping capacity of 1,600 HHP was available on site, and 435 HHP (27%) were used for the pumping operations.

An additional volume of 9.4 ppg brine and a larger barite pill were used for this attempt, but there is no indication that the flow from bottom was significantly reduced. Reports indicate that the barite pill was blown to surface; therefore, its use was clearly not part of the solution. The use of low-density clear fluids continues to be an issue. At the time of this attempt, the Drillbench model shows the well would have been killed with 12 ppg fluid pumped at 8 bpm or 15 ppg mud pumped at 6 bpm (Table 7).

7.6 Kill Attempt #5 November 24, 2015

A 50 bbl LCM (lost circulation material) pill weighing 9.4 ppg was pumped ahead of 950 bbl of 8.34 ppg fresh water, followed by 35 bbl of an 18.0 barite pill, followed by 56 bbl of 9.4 ppg brine. The displacement rate was increased up to 13 bpm with a reported maximum injection pressure of 4,167 psi. Based on one interpretation, this attempt may have nearly killed the well, as pressure on the 7 in. x 2 7/8 in. annulus dropped from 160 psi to 8 psi for a brief time. Reports show that 700 bbl of injection fluid were recovered at surface.

The use of LCM seems reasonable, but following the LCM pill with a large volume of fresh water cannot be justified.

Sufficient pumping capacity of 1,600 HHP was available on site and 1,330 HHP (82%) were used for the pumping operations.

Blade analysis indicates that at the time of this kill attempt, the well was flowing at 78 MMscf/D. The Drillbench model shows that a sustained pump rate of 13 bpm with fresh water could have stopped the gas flow, but the equipment's pressure limits would have been exceeded, and fluid leak-off into the permeable reservoir would have prevented maintaining a stable fluid column in the annulus of sufficient height to keep the well static.

Table 8 shows that 12.0 ppg mud pumped at 8 bpm or 15.0 ppg mud at 6 bpm would have also stopped the gas flow. The mud would have tended to maintain a stable fluid column because of the damage to the reservoir permeability, while clear water or clear brine would not remain stable because of fluid loss into the permeable reservoir.

The 7 in. x 2 7/8 in. annulus pressure was essentially killed, and a reported amount of 700 bbl of injected fluid returned to surface. Fluid loss into the permeable rock allowed the hydrostatic column to drop, which allowed the reservoir to resume flowing. It is apparent that a clear kill fluid was unacceptable.

7.7 Kill Attempt #6 November 25, 2015

This attempt was a near repeat of Kill Attempt #5, except that the 35 bbl barite pill was replaced with a 100 bbl 9.4 ppg LCM pill, and higher pump rate was applied to the kill attempt. The maximum displacement rate was 13 bpm at 4,173 psi. After signs of a positive kill (7 in. x 2 7/8 in. annulus pressure dropped to 0 psi), the displacement rate was dropped to 2 bpm and further dropped to 1 bpm. However, at least two surface connections failed because pipes broke off; consequently, the pumping was suspended. Section 3.5 shows details of the fluids pumped.

At this point, the wellhead and surface casing were structurally unstable. Gas and fluid flow around the surface location removed enough soil and formation to allow considerable oscillation of the wellhead.

This kill attempt could be termed as a *near kill*. It seems to have almost worked, but the vibration at the surface, probably due to the increased cratering around the wellhead, prevented the continuation of the operations that would have led to a successful conclusion.

Sufficient pumping capacity of 1,600 HHP was available on site and 1,330 HHP (82%) were used for the pumping operations; this was the first attempt that showed signs of being successful.

Kill attempt #6 used a large LCM pill and a high pump rate. It appeared to have killed the well, but fluid loss into the formation kept the annular fluid column from stabilizing. It is probable that continued pumping from the surface might have kept up with the fluid loss, but surface plumbing failures prevented the well from being kept filled. The use of fresh water and clear brine contributed to the attempt's failure because of fluid loss into the formation and loss of hydrostatic pressure, which allowed the well to start flowing after the kill attempt.

7.8 Kill Attempt #7 December 22, 2015

After installing guy wires to reduce wellhead oscillations, the pump job for this kill attempt consisted of injecting 15.1 ppg WBM, with a varying LCM content, at a rate of 5 bpm. (Reports are inconsistent—the actual rate may have been 5.8 bpm.) After pumping 300 bbl, the injection rate was reduced to 0.5 bpm for 15 minutes. Pumping was terminated due to rocking of the wellhead and a subsequent failure of the injection connection. The reports are vague regarding the reported pressure, but it seems that the flow from the crater slowed considerably for a while.

Figure 13 is a photograph of Site SS-25 after the final kill attempt. Because surface conditions had deteriorated, no additional surface interventions were attempted.

This was the first attempt to utilize an engineered approach—some documents indicate that well kill modeling had been attempted prior to the job. As discussed in Section 7.1, the well gas flow rate may have been underestimated. (A total of 332 bbl of 15.1 ppg was pumped.) It appears that the well was essentially dead when the surface equipment failed. The inability to continuously fill the well allowed the production zone to resume flowing after some (undetermined) time.

The 11 3/4 in. x 7 in. annulus valve on the wellhead backed out during this kill attempt, which created an unrestricted gas flow path to surface. The gas flow out the 2 in. threaded outlet contributed to crater enlargement on the south side. It is likely that the crater, unsupported lines and valves, wellhead movement, and vibration contributed to the valve backing out, which made the overall surface situation worse.

By December 22, 2015, more than 4,000 bbl of various fluids had been pumped into the well—most fluids returned to surface under high velocity. Additionally, a large volume of gas had escaped through the surface fissures and crater. The surface conditions had deteriorated to a point that it became unsafe for personnel to work near the wellhead. The relief well started being drilled on December 4, 2015, and was successful in killing SS-25 on February 11, 2016.

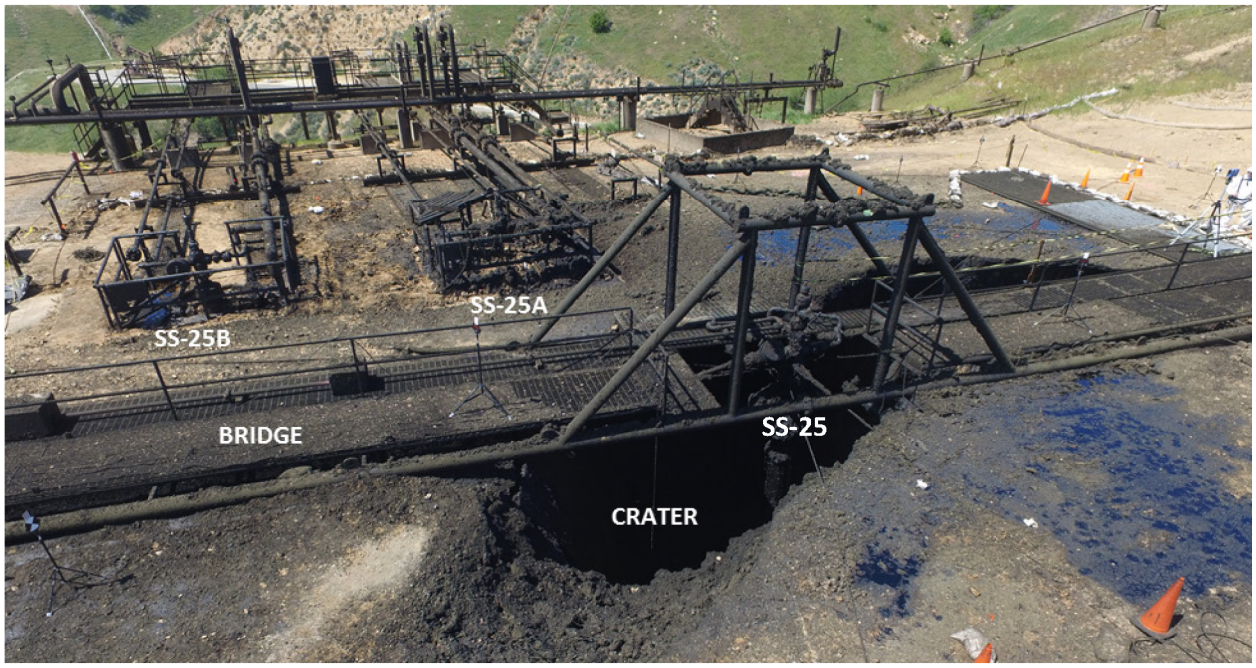

Figure 13: Site SS-25 after the Kill Attempts; SS-25 Wellhead Under the Bridge Frame

7.9 Installation of the EZSV Bridge Plug in the Tubing String

The EZSV bridge plug created potential problems for later well kill operations. Several discussions in this report emphasize the need for high-rate pumping and the use of high density fluids as aids in killing the well. The TFA (total flow area) of the production tubing was 4.7 in^2. Perforations were necessary and were made after setting the EZSV, before pumping into the well. The TFA of the perforations was 0.44 in^2. This major reduction in the TFA had several adverse effects on subsequent operations:

- The sustained pump rate with any fluid was severely hampered due to the increased circulating pressure.
- The maximum size of any particulate material (LCM) was greatly reduced as each perforation was only 3/8 in. diameter. Plugging of the perforations was possible with an LCM size of 1/2 to 1/6 of the perforation diameter.
- The probability of accidently plugging the perforations with debris sharply increased.
- The momentum vector was changed in an adverse way by directing the fluid flow from the tubing from vertical to horizontal.

It is not clear why the bridge plug was set. It entailed shipping the equipment from Texas to California, having the setting tools modified by a local machine shop, and using an electric line logging unit to set the plug. The plug was set on November 12, 2015, and the tubing was punched on November 13. No pressure test or tubing integrity test was reported. Again, the reason for setting the plug is unclear. Setting the plug complicated later kill attempts.

8 Background Data and Assumptions

This section summarizes other data and assumptions considered for this analysis, including the data discussed in Section 2.

8.1 Geothermal Temperature Profile

Given that thermal behavior was given far more scrutiny in the Well Nodal Analysis report [1] performed by Blade and that the Drillbench Blowout Control software is more limited in its thermal analysis capability, the original geothermal gradient was modified based on input from the Well Nodal Analysis report [1]. This modification is intended to provide more accurate reservoir fluid temperatures entering the wellbore.

Since the high gas flow rates considered are shown to induce significant temperature reduction due to the Joule Thompson effect prior to entering the wellbore, the modified geothermal gradient considered for this analysis had the formation temperature at reservoir depth reduced to 120 °F to include this effect. Figure 14 shows both the original and the modified geothermal gradients considered for this analysis [27].

8.2 Wellbore Trajectory

The SS-25 wellbore is assumed to be nearly vertical. The wellbore survey goes to 8,378 ft MD (8,368 ft TVD), and it is assumed that the final trajectory was maintained to TD of 8,749 ft MD (8,733 ft TVD). The gyro survey run on January 16, 2016 was used in the model [28].

8.3 Relief Conduit Trajectory

The relief conduit, acting as a proxy for flow from the leak in the 7 in. casing to surface via the formation, is 20 ft long[vi], horizontal, and assumed to intercept the main well at 892 ft.

8.4 Reservoir Properties

The reservoir pressure should have reduced throughout the period when the kills were attempted. The values assumed, based on SS-5's reservoir pressures, are shown in Table 1 (Section 2.6).

Other assumed reservoir properties are:

- Reservoir fluid—Methane
- Gas Productivity Index, PI 0.083 MMscf/D/psi—base case (93 MMscf/D)
- Water Gas Ratio—0.35 STB/MMscf
- Condensate Gas Ratio—0.01 STB /MMscf

[vi] This length was chosen as equal to two times the minimal grid size of the model and has no relation to actual flow distance to surface from the assumed leak at 892 ft.

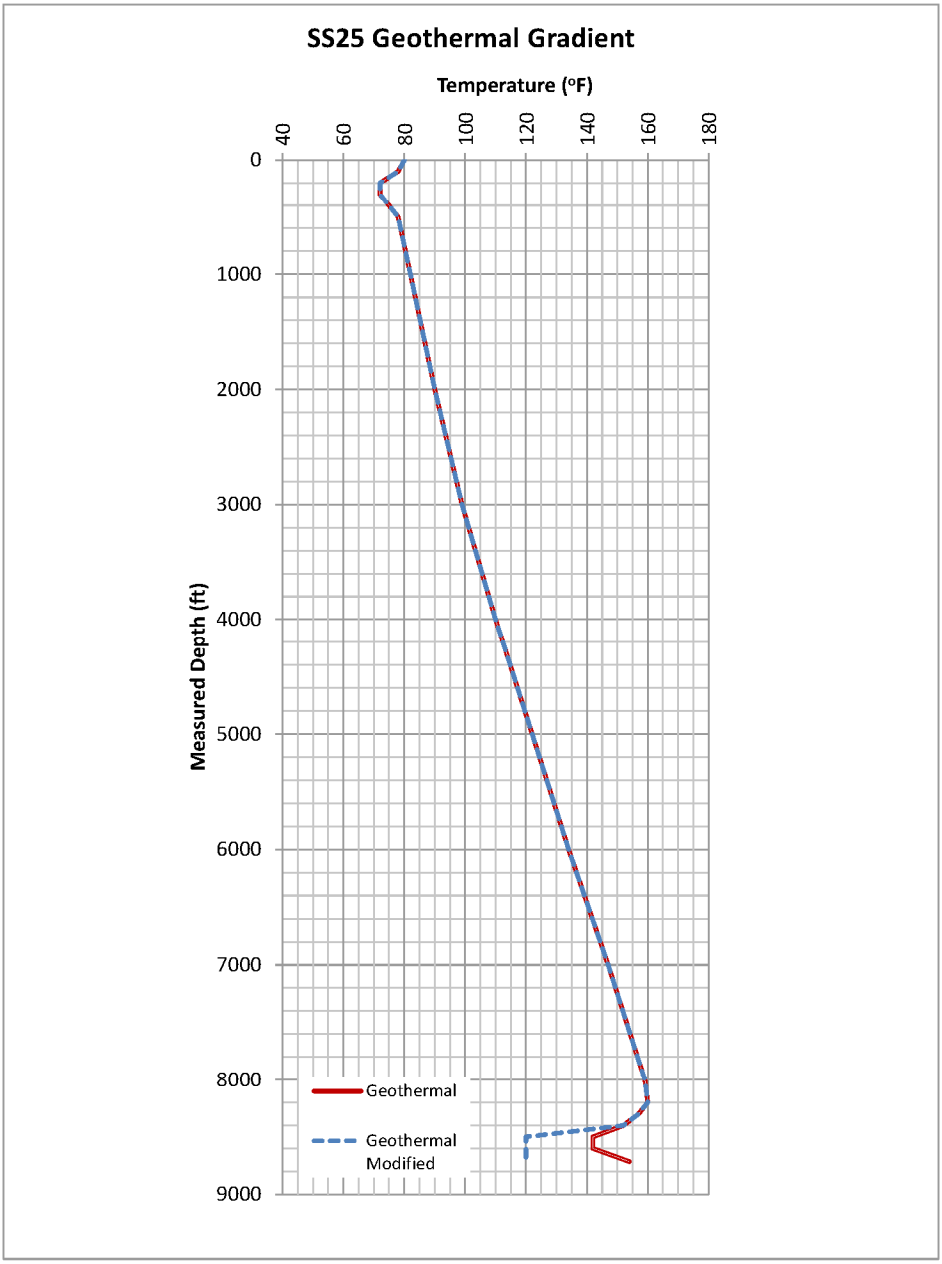

Figure 14: Geothermal Temperature Gradient

8.5 Kill Fluid Properties

All kill fluids were assumed to be water-based.

8.5.1 Freshwater

The viscosity at the temperatures in the tubing and 7 in. x 2 7/8 in. annulus of 68 °F to 104 °F was assumed to be 0.825 cP (average of 1.00 cP and 0.653 cP) [29].

Density was assumed to be 8.34 ppg.

8.5.2 $CaCl_2$

The viscosity of $CaCl_2$ was assumed to be 1.33 cP based on the approximate pump pressure match between simulation and field data throughout Kill Attempt #2 to Kill Attempt #4, where $CaCl_2$ was the primary kill fluid.

Numerous sensitivities were performed to assess the impact of changing the $CaCl_2$ viscosity on the *killability* of the well. In general, the impact was found to be relatively minor and, therefore, results are not shown.

The $CaCl_2$ density was assumed to be 9.40 ppg.

8.5.3 Other Kill Fluids

Table 15 shows the viscosity is assumed to be 20 cP for all fluids considered. Sensitivity studies were performed to assess the impact of changing kill fluid viscosities. Similar to $CaCl_2$, changes in well kill results are minor.

Table 15: Kill Fluid Density and Viscosity Assumptions

Kill Fluid	Density (ppg)	Viscosity (cp)
Polymer Pill	9.4	20
Barite Pill	18.0	20
GEO Zan Pill[a]	9.4	20
10 ppg Mud	10.0	20
15 ppg Mud	15.0	20
15 ppg Mud with LCM	15.0	20
[a] GEO Drilling Fluids, Inc. 9.4 ppg brine with xanthan gum viscosifier		

8.6 Surface Roughness

Surface roughness within the tubing and 7 in. x 2 7/8 in. annulus was assumed to be 0.001 in. and 0.0072 in., respectively.

Surface roughness within the open hole section was assumed to be 0.1 in.

9 Conclusions

The main points of the analysis are summarized here:

- The lack of kill modeling for Kill Attempts #2–6 is a possible explanation for the failed attempts. Kill Attempt #2 showed that 9.4 ppg clear fluid pumped at 8 bpm was not successful in killing the well. The results from Kill Attempt #2 indicated a serious well control problem; gas broached to surface from an apparent shallow casing leak. However, the design for Kill Attempt #3 consisted of a smaller volume of 9.4 ppg brine and a small volume of 18 ppg barite pill. The results of Kill Attempt #3 were similar to Kill Attempt #2. Kill Attempts #4, #5, and #6 were somewhat repeats of the previous kill attempts, i.e., pumping of low-density-clear fluids and small volumes of barite and LCM pills. The pump rates for Kill Attempts #5 and #6 were increased to 13 bpm, but the clear fluids pumped leaked off into the formation, which allowed the well to flow after *near kills* were observed.
- The prolonged uncontrolled flow from October 23, 2015, to February 11, 2016, did not cause additional damage to the casing, other than flow caused erosion to the faces of the parted casing and edges of the casing rupture. Examination of the failed casing showed featureless areas where the fracture surfaces were eroded to a smooth surface.
- The apparent underestimation of the gas flow rate was a deficiency in planning the kill attempts. An IPR curve showing 30 MMscf/D was sent to DOGGR via an information request. Add Energy and Blade have estimated the gas flow rate to be 80 and 93 MMscf/D, respectively, when Kill Attempt #1 was pumped. There is evidence that modeling was done prior to the kill attempt in December 2015. However, it appears that a gas flow rate of 25 MMscf/D was used at the time. Blade's estimate is that a gas flow rate of 57 MMscf/D should have been used.
- The lack of kill modeling early in the process and the underestimation of the gas flow rate required a number of kill attempts and resulted in the formation of a large crater around the well, which caused the wellhead and exposed casing to become unstable. The crater became a safety hazard, and the well continued to leak gas to the atmosphere until the well was killed in February 2016. The unsupported wellhead and the multiple unsuccessful kill attempts caused the 11 3/4 in. x 7 in. annulus valve to back out, which allowed unrestricted gas flow to surface to enlarge the crater and make the surface situation worse.
- The Blade modeling showed it was highly improbable to achieve a successful kill with either fresh water or 10 ppg fluid for Kill Attempt #1. On October 24, 2015, when Kill Attempt #1 was performed, the gas flow rate was approximately 93 MMscf/D and the reservoir pressure was 3,195 psia.
- The likelihood of a successful kill for Kill Attempts #2–6 was low according to modeling results. Kill Attempts #6 and 7 appeared to be close to killing the well, but the attempts were terminated because of undesirable movement of the wellhead and pump lines that broke during the job. Kill attempts were suspended after Kill Attempt #7.
- The simulations showed a successful kill could have been achieved for all seven kill attempts if 12 ppg or higher density mud had been used in a dynamic kill. Modeling showed that pumping a higher density fluid at a reasonable rate would have provided a good chance of killing the well at gas rates of 93 and 83 MMscf/D, which were the estimated rates for Kill Attempt #1 and #2, respectively. A successful design for Kill Attempt #1 was 12 ppg fluid at 10 bpm or 15 ppg fluid at 7 bpm based on modeling results. For Kill Attempt #2, the design was 12 ppg at 9 bpm or 15 ppg at 6 bpm. Lower pump rates are acceptable for subsequent kill attempts because of the reduced BHP and gas rates.

- The sensitivity analyses in which the gas flow rate was hypothetically reduced to approximately 30 MMscf/D by decreasing the formation IPR shows that Kill Attempt #1 could have been successful with 10 ppg fluid at 8 bpm with acceptable pump pressure and Kill Attempt #2 could have been successful with 9.4 ppg fluid at 10 bpm with acceptable pump pressure. However, it should be noted that these scenarios are considered physically inadmissible because the gas flow rate was severely underestimated. The reason for considering these scenarios is that 30 MMscf/D may have been the gas flow rate assumed when planning the early kill attempts.
- The modeling results for kill simulations with an assumed leak depth at 440 ft showed minimal changes when compared to the results for a leak at 892 ft. A leak at a shallow depth is slightly easier to kill because of a longer column of fluid from the reservoir to the leak depth.

10 References

[1] Blade, "SS-25 Well Nodal Analysis with Uncontrolled Leak Estimation," 2019.

[2] Federal Task Force, "Ensuring Safe and Reliable Underground Natural Gas Storage, Final Report of the Interagency Task Force on Natural Gas Storage Safety," October 2015.

[3] O. B. Rygg, P. Smestad and J. W. Wright, "SPE 24578, Dynamic Two-Phase Flow Simulator: A Powerful Tool for Blowout and Relief Well Kill Analysis," in *67th Annual Technical Conference and Exhibition of the Society of Petroleum Engineers*, Washington DC, 1992.

[4] K. Bendiksen, D. Malnes, R. Moe and S. Nuland, "SPE 19451, The Dynamic Two-Flow Model OLGA: Theory and Application," *SPE Production Engineering,* May 1991.

[5] Halliburton, "Kill Attempt 1 Job Report, AC_BLD_0041890-AC_BLD_0041899, October 24, 2015 (Halliburton Kill Attempt 1 AC_BLD_0041890.pdf)".

[6] Halliburton, "Kill Attempt 2 Job Report, AC_BLD_0041900-AC_BLD_0041911, November 14, 2019 (Halliburton Kill Attempt 2 AC_BLD_0041900.pdf)".

[7] Halliburton, "Kill Attempt 3 Job Report, AC_BLD_004912-AC_BLD_0041921, November 15, 2015 (Halliburton Kill Attempt 3 AC_BLD_0041912.pdf)".

[8] Halliburton, "Kill Attempt 4 Job Report, AC_BLD_41922-AC_BLD_930, November 18, 2015 (Halliburton Kill Attempt 4 AC_BLD_0041922.pdf)".

[9] Halliburton, "Kill Attempt 5 Job Report, AC_BLD_0041931-AC_BLD_0041944, November 24, 2015 (Halliburton Kill Attempt 5 AC_BLD_0041931.pdf)".

[10] Halliburton, "Kill Attempt 6 Job Report, AC_BLD_0079371, November 25, 2015 (AC_BLD_0079371.docx)".

[11] Halliburton, "Kill Attempt 7 Job Report, AC_BLD_0041945-AC_BLD_0041963, December 22, 2015 (Halliburton Kill Attempt 7 AC_BLD_0041945.pdf)".

[12] Add Energy, "Dynamic Simulations Aliso Canyon SS25, AC_BLD_003304-AC_BLD_0031422, February 16, 2016 (C042 AC_BLD_0031304 Optimized Add Energy.pdf)".

[13] Halliburton, "Kill Attempt 6 Job Data, AC_BLD_0019060, November 25, 2015 (Halliburton Kill Attempt 6 11-25-2015_AC_BLD_0019060.xlsx)".

[14] SoCalGas, "Email, 28 Dec 2015, SoCalGas to DOGGR, Subject: Supplemental SoCalGas Response to Information Request - 12-23, (Information Request - 12-23 Calculations Email.docx, DOGGR -1_Supp Response Q2_ 122815.docx, Input Data for Flow Analysis.docx)".

[15] SoCalGas, "SS-25 Flow Test Data Since 1978, AC_BLD_009734 (SS-25 Flow Test Data Since 1978 AC_BLD_009734.pdf)".

[16] SoCalGas, "Email SoCalGas to DOC, Subject: FW: 25 MMscfd.pptx, AC_BLD_0082977-AC_BLD_0082978, December 18, 2015 (AC_BLD_0082977.pdf)".

[17] Unknown, "Email Attachment, Modeling Results, AC_BLD_0082979 (AC_BLD_0082979.pdf)".

[18] Unknown, "Kill Attempt Modeling, AC_BLD_0075832, (no date) (AC_BLD_0075832.pdf)".

[19] Unknown, "Kill Attempt Modeling, AC_BLD_0075853, (no date) (AC_BLD_0075853.pdf)".

[20] SoCalGas, *SS25 Well Pressures, AC_CPUC_0000100 (SS-25 Well Documentation (from SoCalGas)_N.pdf, page 78).*

[21] SoCalGas, "History of Oil or Gas Well (SS-25 03700776 Data_03-19-08 (2).pdf, Pages 49-59)".

[22] Department of Conservation, *State Regulators Confirm Aliso Canyon Natural Gas Well is Permanently Sealed (State officials confirm Aliso Canyon gas leak has been halted 2016-02-18.pdf, pages 1-2).*

[23] SoCalGas, "Completion Profiler Analysis, AC_BLD_0018125-AC_BLD_0018136, November 8, 2015 (SS-25 Completion Profiler Pages.pdf)".

[24] Blade, "Analysis of the Post-Failure Gas Pathways and Temperature Anomalies at the SS-25 Site," 2019.

[25] Blade, "Analysis of Aliso Canyon Gas Storage Wells with Casing Failures," 2019.

[26] R. D. Grace, Advanced Blowout and Well Control, Houston: Gulf Publishing Company, 1994.

[27] Blade, "Geothermal Gradients, (SS-25 Geothermal Gradients Rev 2.xlsx)," 2016.

[28] SDI, "Gyroscopic Survey, SS-25, AC_BLD_0020032, January 16, 2016 (SS-25 Directional Survey_ 1-16-2016 (20032).xlsx)".

[29] P. Anton, "Viscosity of Water," [Online]. Available: https://wiki.anton-paar.com/en/water/. [Accessed 23 February 2019].

[30] Department of Oil, Gas, and Geothermal Resources, "SS-25 Chronology Summary (STANDARD SESNON 25 Chronology Summary-1 from DOGGR.docx)".